HUMBOLDT-UNIVERSITÄT ZU BERLIN

Adaptive Discontinuous Petrov-Galerkin Finite-Element-Methods

Dissertation
zur Erlangung des akademischen Grades
doctor rerum naturalium (Dr. rer. nat.)
im Fach Mathematik,
eingereicht an der
Mathematisch-Naturwissenschaftliche Fakultät
der Humboldt-Universität zu Berlin
von

M. Sc. Friederike Hellwig

Präsidentin der Humboldt-Universität zu Berlin
Prof. Dr. Sabine Kunst

Dekan der Mathematisch-Naturwissenschaftlichen Fakultät
Prof. Dr. Elmar Kulke

Gutachter:
1. Prof. Dr. Carsten Carstensen (Humboldt-Universität zu Berlin)
2. Prof. Dr. Rob Stevenson (University of Amsterdam)
3. Prof. Dr. Norbert Heuer (Pontificia Universidad Católica de Chile)

Tag der mündlichen Prüfung: 22.11.2018

Abstract

The thesis »Adaptive Discontinuous Petrov-Galerkin Finite-Element-Methods« proves optimal convergence rates for four lowest-order discontinuous Petrov-Galerkin methods for the Poisson model problem for a sufficiently small initial mesh-size in two different ways by equivalences to two other non-standard classes of finite element methods, the reduced mixed and the weighted Least-Squares method. The first is a mixed system of equations with first-order conforming Courant and nonconforming Crouzeix-Raviart functions. The second is a generalized Least-Squares formulation with a midpoint quadrature rule and weight functions. The thesis generalizes a result on the primal discontinuous Petrov-Galerkin method from [Carstensen, Bringmann, Hellwig, Wriggers 2018] and characterizes all four discontinuous Petrov-Galerkin methods simultaneously as particular instances of these methods. It establishes alternative reliable and efficient error estimators for both methods. A main accomplishment of this thesis is the proof of optimal convergence rates of the adaptive schemes in the axiomatic framework [Carstensen, Feischl, Page, Praetorius 2014]. The optimal convergence rates of the four discontinuous Petrov-Galerkin methods then follow as special cases from this rate-optimality. Numerical experiments verify the optimal convergence rates of both types of methods for different choices of parameters. Moreover, they complement the theory by a thorough comparison of both methods among each other and with their equivalent discontinuous Petrov-Galerkin schemes.

Zusammenfassung

Die vorliegende Arbeit »Adaptive Discontinuous Petrov-Galerkin Finite-Element-Methods« beweist optimale Konvergenzraten für vier diskontinuierliche Petrov-Galerkin (dPG) Finite-Elemente-Methoden für das Poisson-Modell-Problem für genügend feine Anfangstriangulierung. Sie zeigt dazu die Äquivalenz dieser vier Methoden zu zwei anderen Klassen von Methoden, den reduzierten gemischten Methoden und den verallgemeinerten Least-Squares-Methoden. Die erste Klasse benutzt ein gemischtes System aus konformen Courant- und nichtkonformen Crouzeix-Raviart-Finite-Elemente-Funktionen. Die zweite Klasse verallgemeinert die Standard-Least-Squares-Methoden durch eine Mittelpunktsquadratur und Gewichtsfunktionen. Diese Arbeit verallgemeinert ein Resultat aus [Carstensen, Bringmann, Hellwig, Wriggers 2018], indem die vier dPG-Methoden simultan als Spezialfälle dieser zwei Klassen charakterisiert werden. Sie entwickelt alternative Fehlerschätzer für beide Methoden und beweist deren Zuverlässigkeit und Effizienz. Ein Hauptresultat der Arbeit ist der Beweis optimaler Konvergenzraten der adaptiven Methoden durch Beweis der Axiome aus [Carstensen, Feischl, Page, Praetorius 2014]. Daraus folgen dann insbesondere die optimalen Konvergenzraten der vier dPG-Methoden. Numerische Experimente bestätigen diese optimalen Konvergenzraten für beide Klassen von Methoden. Außerdem ergänzen sie die Theorie durch ausführliche Vergleiche beider Methoden untereinander und mit den äquivalenten dPG-Methoden.

Contents

1. Introduction

This thesis analyses and proves optimal convergence rates for four lowest-order adaptive discontinuous Petrov-Galerkin (dPG) finite element methods in any space dimension for the Poisson model problem. The first part of this introduction gives a motivation and historical overview of dPG and adaptive finite element methods. The remainder of the introduction describes the discrete primal dPG method and special cases of two equivalent discrete schemes analysed in this thesis, as well as the corresponding adaptive algorithms, and elaborates on the main results of this thesis.

Motivation

Partial differential equations are a powerful tool in the description of a variety of phenomena in engineering, physics, and stochastics. A powerful tool for their numerical solution is the plethora of finite element methods with a multitude of applications ranging from automotive design to bio-engineering.

A recent asset to this family is the discontinuous Petrov-Galerkin finite element methodology introduced by L. Demkowicz and J. Gopalakrishnan [DG10; DG11a; DGN12; ZMDG+11]. Originally motivated by the construction of optimal test functions from a fixed space of trial functions [DG11b], they are characterized as a minimal residual method with a discontinuous test space. Based on an analysis of inf-sup conditions, the dPG methodology may circumvent the cumbersome construction of balanced discrete trial and test spaces and instead provide well-posedness of the discrete problem by the choice of a sufficiently large discrete test space. Additional advantages of these methods, such as flexible mesh design, improved stability properties and a built-in error estimate [CDG14], have lead to various applications. Among the linear problems, there are publications on the Poisson model problem [DG11b; DG13; CGHW14], linear elasticity [BDGQ12; CH16; KFD16; FKDL17], the Stokes equations [RBD14; CP18], and the Kirchhoff-Love plate model [FHK18]. A number of papers study the convection-diffusion-reaction equations with or without singular pertubation [DG10; DGN12; DH13; CEQ14; CHBD14; BS14; BS15; FH17; HK17a; MZ17; BDS18; Füh18]. Other applications include Maxwell's equations [DL13; CDG16], wave propagation [DGMZ12; GMO14; PD17], the Schrödinger equation [DGNS17], the fractional Laplacian [ABH18] and fractional advection-diffusion [EFHK17], the heat equation [FHS17a], transmission problems [HK15; FHK17; FHKR17] and a hypersingular integral equation [HP14; HK17b]. The dPG methodology has also been applied to nonlinear model problems [CBHW18], to a contact problem [FHS17b], in nonlinear fluid mechanics [CDM14; RDM15] and viscoelasticity [KKRE+17; FDW17].

In most of these applications, the discrete test space employs a theoretically verified [HKS14] polynomial degree of $p+n$ for the space dimension n and the polynomial degree p of the discrete trial space. In contrast to that, [BGH14; CGHW14; CH16; CBHW18; CP18] and this

thesis analyse a lowest-order version with $p = 0$ in the discrete trial space and degree $p + 1$ in the discrete test space.

Several of the mentioned publications utilize the built-in error estimator [CDG14] to drive adaptive algorithms and present numerical experiments with h- and hp-adaptive refinement. The multitude of valuable applications of the dPG methods and their prevalent use of adaptivity make an analysis of adaptive dPG schemes desirable. However, the paper [CH18b] presented also as part of this thesis is the first to analyse convergence and optimal rates of an h-adaptive dPG finite element method theoretically.

The need for adaptive refinement strategies arises for solutions with singularities, e.g., caused by re-entrant corners of non-convex domains or boundary conditions. The resulting reduced regularity of the exact solution [Gri11] leads to a suboptimal convergence rate for uniform refinement of the coarse initial triangulation. Whereas the possible remedy of graded meshes needs a priori knowledge of the solution, the design of adaptive refinement strategies aims at the automatic detection of those singularities and local refinement in convenient parts of the domain. Figure 1 shows an adaptively refined triangulation of an L-shaped domain with constant right-hand side $f \equiv 1$ in the Poisson model problem calculated with the primal dPG method and its built-in error estimator.

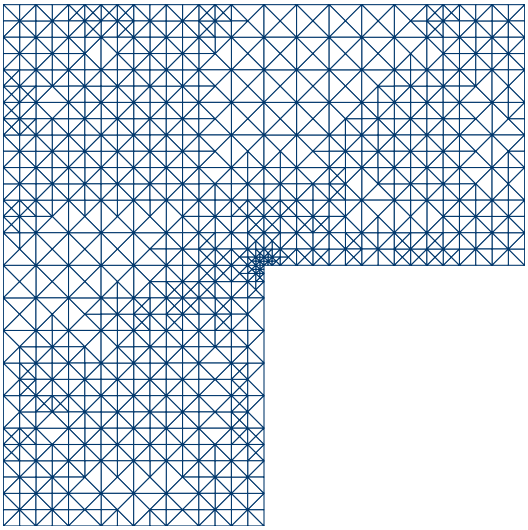

Figure 1: Adaptively refined triangulation of L-shaped domain with singularity at the re-entrant corner.

The adaptive algorithm introduced in [Dör96] relies on the construction of a computable error estimator that is utilized for marking and then refining certain elements. However, the analysis of convergence of those adaptive algorithms is not trivial compared to that of uniform refinement strategies, since convergence of the latter is based on estimates in terms of the maximal mesh-size, which may not converge to 0 in case of adaptive refinement. In fact, while the early works on construction of error estimators with application to adaptive refinement strategies trace back to [BR78; BR81; BV84], a proof of convergence of an adaptive

algorithm in $2d$ was not until [Dör96; MNS00]. However, next to plain convergence of the adaptive algorithm, the main question of interest is that of rate-optimality. [BDD04] were the first with a proof of optimal convergence rates, but they needed an additional coarsening step. The paper [Ste07] features the first proof of optimal convergence rates without coarsening and utilizes the concept of nonlinear aproximation classes. The recent contributions [CFPP14; CR17] provide an abstract axiomatic framework on the analysis of adaptive mesh-refinement able to cover various finite element methods and problems, among those the dPG methods analysed in this thesis.

For the dPG methods, the built-in a posteriori error estimate from [CDG14] provides an error estimator which is efficient and reliable up to data approximation terms and can be utilized in adaptive refinement strategies. Unfortunately, the aforementioned axiomatic approach cannot be applied to this estimator immediately due to the lack of a factor of the mesh-size h in the estimator, which leads to severe difficulties in the proof of estimator reduction. This problem is known from the least-squares (LS) methods, where [CP15] were the first to prove rate-optimality for adaptive methods for the Poisson model problem by use of an alternative error estimator. The strategy of constructing an equivalent error estimator and proving of the axioms of adaptivity for it is also employed in this thesis twice. Four lowest-order dPG methods for the Poisson model problem are shown to be equivalent to a mixed system with Crouzeix-Raviart and Courant finite element spaces, and additionally, to a generalized LS method. Both approaches lead to alternative error estimators for the four dPG methods for which the axiomatic framework of [CR17] is applicable and proves optimal convergence rates.

Problem Setting and Discrete Schemes

Let $\Omega \subset \mathbb{R}^n$ be a bounded Lipschitz domain with polyhedral boundary $\partial\Omega$. Given a right-hand side function $f \in L^2(\Omega)$, consider the Poisson model problem as a second-order partial differential equation that seeks $u \in H^1(\Omega)$ with

$$-\Delta u = f \text{ in } \Omega \quad \text{and} \quad u = 0 \text{ on } \partial\Omega, \tag{1.1}$$

or as a first-order system of equations that seeks $u \in H^1(\Omega)$ and $\sigma \in H(\mathrm{div}, \Omega)$ with

$$-\mathrm{div}\,\sigma = f \text{ in } \Omega \quad \text{and} \quad \sigma = \nabla u \text{ in } \Omega \quad \text{and} \quad u = 0 \text{ on } \partial\Omega. \tag{1.2}$$

The standard weak formulation [BBF13, p. 7] departs from (1.1) with multiplication of a test function in the Sobolev space $H^1_0(\Omega)$ and and integration by parts on the domain Ω and seeks $u \in H^1_0(\Omega)$ with

$$\int_\Omega \nabla u \cdot \nabla v \,\mathrm{d}x = \int_\Omega f v \,\mathrm{d}x \quad \text{for all } v \in H^1_0(\Omega). \tag{1.3}$$

The variational formulation beneath the *primal dPG formulation* [DG13] bases on a regular triangulation $\mathcal{T}$ of Ω and an integration by parts of (1.1) on each finite element domain

$T \in \mathcal{T}$, which yields $\int_T \nabla u \cdot \nabla v \,\mathrm{d}x - \int_{\partial T} v \nabla u \cdot \nu_T \,\mathrm{d}s = \int_T f v \,\mathrm{d}x$ for any $v \in H^1(\mathcal{T}) := \{v \in L^2(\Omega) \,|\, \forall T \in \mathcal{T}, v|_T \in H^1(T)\}$ and outer unit normal ν_T along ∂T. The sum over all $T \in \mathcal{T}$ and the introduction of the trace variable $t := (t_T)_{T\in\mathcal{T}}$ with $t_T := \nabla u \cdot \nu_T \in H^{-1/2}(\partial T)$ lead to

$$b((u,t),v) := \sum_{T\in\mathcal{T}} \Big(\int_T \nabla u \cdot \nabla v \,\mathrm{d}x - \int_{\partial T} v\, t_T \,\mathrm{d}s \Big) = \int_\Omega f v \,\mathrm{d}x =: F(v) \quad \text{for all } v \in H^1(\mathcal{T}). \tag{1.4}$$

A lowest-order discretization [BGH14] employs discrete spaces $P_1(\mathcal{T})$ of piecewise affine functions, $S^1_0(\mathcal{T}) := P_1(\mathcal{T}) \cap H^1_0(\mathcal{T})$ of piecewise affine, globally continuous functions with homogeneous boundary conditions and piecewise constant functions $P_0(\mathcal{E})$ on the sides $\mathcal{E}$ of the triangulation. For any $v_1, w_1 \in P_1(\mathcal{T})$, define the piecewise gradient by $(\nabla_{NC} v_1)|_T := \nabla(v_1|_T)$ for any $T \in \mathcal{T}$, the scalar product $(v_1, w_1)_{H^1(\mathcal{T})} := (v_1, w_1)_{L^2(\Omega)} + (\nabla_{NC} v_1, \nabla_{NC} w_1)_{L^2(\Omega)}$, and the norm $\|v_1\|_{H^1(\mathcal{T})} := (v_1, v_1)^{1/2}_{H^1(\mathcal{T})}$. Then one characterization of the discrete dPG method is the minimization of the residual in the discrete dual norm in $S^1_0(\mathcal{T}) \times P_0(\mathcal{E})$,

$$\begin{aligned} (u_C, t_0) = \operatorname*{argmin}_{(w_C,s_0)\in S^1_0(\mathcal{T})\times P_0(\mathcal{E})} \|F - b((w_C,s_0),\bullet)\|_{P_1(\mathcal{T})^*}, \quad \text{where} \\ \|F - b((w_C,s_0),\bullet)\|_{P_1(\mathcal{T})^*} := \sup_{w_1\in P_1(\mathcal{T})\setminus\{0\}} \frac{|F(w_1) - b((w_C,s_0),w_1)|}{\|w_1\|_{H^1(\mathcal{T})}}. \end{aligned} \tag{1.5}$$

An equivalent characterization of this discrete dPG solution is the mixed system [CDW12] that seeks $(u_C, t_0, v_1) \in S^1_0(\mathcal{T}) \times P_0(\mathcal{E}) \times P_1(\mathcal{T})$ with

$$\begin{aligned} (v_1, w_1)_{H^1(\mathcal{T})} + b((u_C,t_0),w_1) &= F(w_1) && \text{for all } w_1 \in P_1(\mathcal{T}), \\ b((w_C,s_0),v_1) &= 0 && \text{for all } (w_C,s_0) \in S^1_0(\mathcal{T}) \times P_0(\mathcal{E}). \end{aligned} \tag{1.6}$$

Whereas $u_C \in S^1_0(\mathcal{T})$ is an approximation of the exact solution $u \in H^1_0(\mathcal{T})$ and $t_0 \in P_0(\mathcal{E})$ an approximation of $(\nabla u \cdot \nu_T)_{T\in\mathcal{T}}$, the variable $v_1 \in P_1(\mathcal{T})$ is the Riesz representation of the residual $F - b((u_C,t_0),\bullet)$ in $P_1(\mathcal{T})$ and an approximation of the exact residual 0.

These two different notions (1.5) and (1.6) of the discrete dPG method are the starting point for the two equivalent discrete schemes introduced first for a nonlinear model problem generalizing the Poisson model problem in [CBHW18] and utilized in this thesis for the proof of optimal convergence rates.

The so-called *reduced mixed system* employs the piecewise affine, globally continuous functions $S^1_0(\mathcal{T})$ as well as the Crouzeix-Raviart finite element space $CR^1_0(\mathcal{T})$ of piecewise affine functions that are continuous in the midpoints of inner sides and vanish on midpoints of boundary sides. Then a reasoned elimination of the element boundary terms in the approach of the dPG scheme as the mixed system of equations (1.6) leads to the equivalent reduced mixed method that seeks $(v_{CR}, u_C) \in CR^1_0(\mathcal{T}) \times S^1_0(\mathcal{T})$ with

$$\begin{aligned} (\nabla_{NC} v_{CR} + \nabla u_C, \nabla_{NC} w_{CR})_{L^2(\Omega)} + (v_{CR}, w_{CR})_{L^2(\Omega)} &= (f, w_{CR})_{L^2(\Omega)} \text{ for all } w_{CR} \in CR^1_0(\mathcal{T}), \\ (\nabla w_C, \nabla_{NC} v_{CR})_{L^2(\Omega)} &= 0 \qquad \text{for all } w_C \in S^1_0(\mathcal{T}). \end{aligned} \tag{1.7}$$

The solution to this system consists of an approximation $u_C \in S^1_0(\mathcal{T})$ of the exact solution $u \in H^1_0(\Omega)$ to the weak formulation (1.3) and of an approximation $v_{CR} \in CR^1_0(\mathcal{T})$ to the exact residual 0.

The other nonstandard discrete scheme for the Poisson model problem analysed in this thesis, the *weighted LS method*, departs from the point of view of the primal dPG method as a minimal residual method (1.5) and generalizes standard LS finite element schemes. It considers mesh-dependent piecewise constant weight functions $S(\mathcal{T}) \in P_0(\mathcal{T};\mathbb{R}^{n\times n})$ and the space of Raviart-Thomas finite element functions $RT_0(\mathcal{T})$ consisting of certain $H(\mathrm{div})$-conforming functions in the space of piecewise affine vector fields. Then a direct calculation of the discrete dual norm $\|F - b((w_C, s_0), \bullet)\|_{P_1(\mathcal{T})^*}$ with an extension of the trace variable s_0 to a unique $q_{RT} \in RT_0(\mathcal{T})$ leads to an equivalent weighted LS method that seeks the minimizer

$$
\begin{aligned}
(p_{LS}, u_{LS}) = \operatorname*{arg\,min}_{(q_{RT}, w_C)\in RT_0(\mathcal{T})\times S^1_0(\mathcal{T})} \Big(& \|\Pi_0 f + \operatorname{div} q_{RT}\|^2_{L^2(\Omega)} + \\
& + \big\| (I_{n\times n} + S(\mathcal{T}))^{-1/2} \big(\Pi_0 q_{RT} - \nabla v_C + \Pi_0 (f(\mathrm{id} - \mathrm{mid}(\mathcal{T})))\big) \big\|^2_{L^2(\Omega)} \Big).
\end{aligned}
\tag{1.8}
$$

Here, $u_{LS} \in S^1_0(\mathcal{T})$ approximates the exact solution $u \in H^1_0(\Omega)$ and $p_{LS} \in RT_0(\mathcal{T})$ approximates $\nabla u \in H(\mathrm{div}, \Omega)$.

Figures 2-4 display the parts of the discrete solutions of the primal dPG method (1.6), the reduced mixed method (1.7), and of the weighted LS method (1.8) and illustrate their equivalence on a uniform triangulation of an L-shaped domain with 384 triangles for a constant right-hand side $f \equiv 1$.

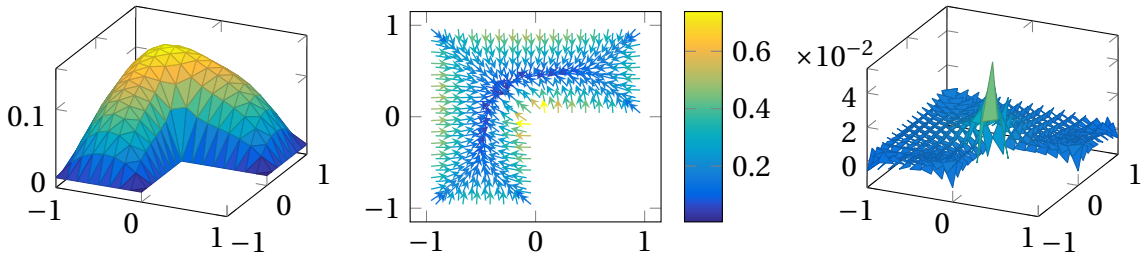

$u_C \in S^1_0(\mathcal{T})$ $\quad t_0 \in P_0(\mathcal{E})$ $\quad v_1 \in P_1(\mathcal{T})$

Figure 2: Solution plots of primal dPG scheme (1.6) with 1921 degrees of freedom, where $t_0 \in P_0(\mathcal{E})$ is visualized by a quiver plot of its unique extension $p_{RT} \in RT_0(\mathcal{T})$.

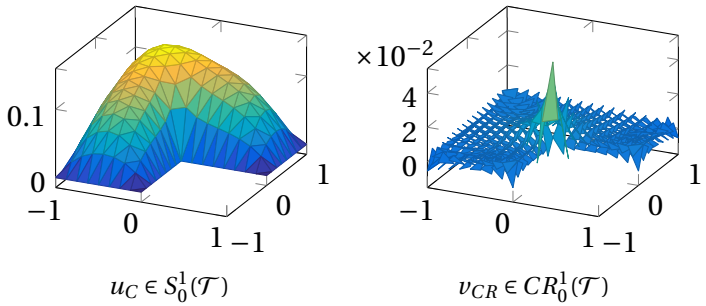

$u_C \in S^1_0(\mathcal{T})$ $v_{CR} \in CR^1_0(\mathcal{T})$

Figure 3: Solution plots of reduced mixed scheme (1.7) with 705 degrees of freedom.

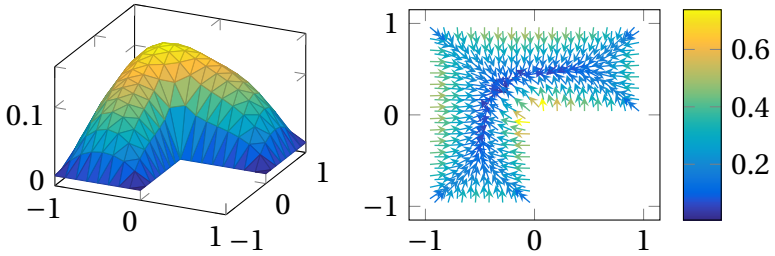

$u_{LS} \in S^1_0(\mathcal{T})$ $p_{LS} \in RT_0(\mathcal{T})$

Figure 4: Solution plots of weighted LS scheme (1.8) with 769 degrees of freedom.

The primal dPG method and the reduced mixed method utilize the standard adaptive finite element loop visualized in Figure 5.

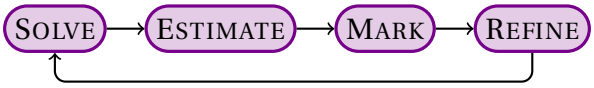

Figure 5: Standard adaptive loop for collective marking.

This means that after the discrete solution on a triangulation $\mathcal{T}$, the step `estimate` computes an error estimator $\eta(\mathcal{T}, T) \geq 0$ for any simplex $T \in \mathcal{T}$ and $\eta(\mathcal{T}) := (\sum_{T\in\mathcal{T}} \eta(\mathcal{T}, T)^2)^{1/2}$. Based on this refinement indicator, the standard adaptive algorithm employs collective marking, also called Doerfler marking [Dör96], to select simplices which are then refined in the last step of the loop.

The adaptive algorithm with separate marking is needed for the weighted LS method, since its a posteriori error estimate contains an additional data approximation term $\mu(\mathcal{T}) \geq 0$. If the estimator $\eta(\mathcal{T}, T)$ dominates $\mu(\mathcal{T})$, the loop utilizes collective marking as before. In the other case, a data approximation algorithm leads to a new triangulation with a reduced $\mu(\mathcal{T})$. Figure 6 illustrates the adaptive finite element loop with separate marking.

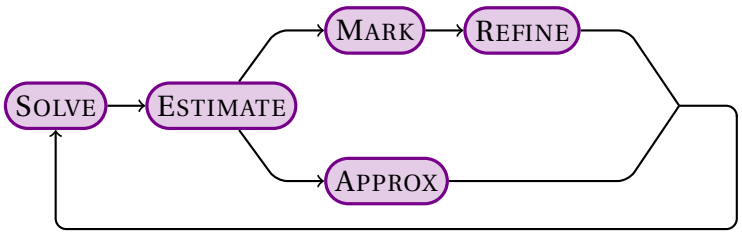

Figure 6: Adaptive loop for separate marking.

The analysis of convergence and rate-optimality of these adaptive algorithms is possible through a framework [CFPP14; CR17] consisting of axioms (A1), (A2), (A3), (A4), and (QM) that concern the error estimators and some distance function. A proof of these axioms implies optimal convergence rates of the estimator in terms of the degrees of freedom for the output $(\mathcal{T}_\ell)_{\ell\in\mathbb{N}_0}$ of the adaptive algorithm, i.e., that any $s>0$ satisfies

$$\sup_{\ell\in\mathbb{N}_0}(1+|\mathcal{T}_\ell|-|\mathcal{T}_0|)^s\eta(\mathcal{T}_\ell)\approx\sup_{N\in\mathbb{N}_0}(1+N)^s\min\{\eta(\mathcal{T})\,|\,\mathcal{T}\in\mathbb{T}\text{ with }|\mathcal{T}|-|\mathcal{T}_0|\le N\}. \tag{1.9}$$

Figure 7 illustrates this notion of rate-optimality with a convergence history plot of an adaptive primal lowest-order dPG method for the Poisson model problem on the non-convex slit domain for a constant right-hand side $f\equiv 1$. It shows that whereas the re-entrant corner of the domain leads to the suboptimal convergence rate 0.3 for uniform refinement, the convergence rate s of the adaptive scheme is 0.5, which is the optimal rate for approximation with this polynomial degree. The crosses symbolize the (not computed) optimal triangulations in terms of the error estimators with respect to the number of degrees of freedom of the right-hand side of (1.9).

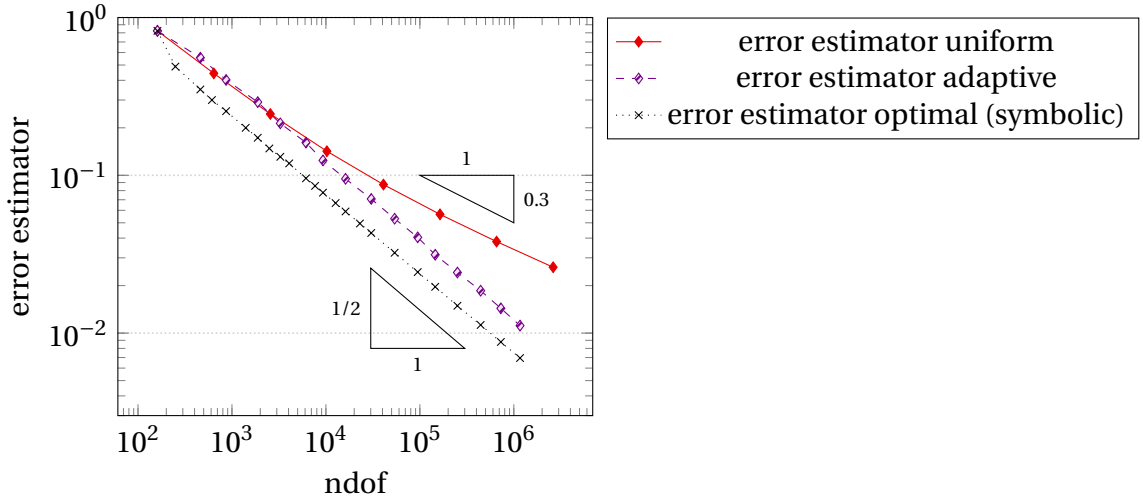

Figure 7: Convergence history plot of error estimators for primal dPG method on slit domain with right-hand side $f\equiv 1$.

Main Results

This thesis proves optimal convergence rates for four lowest-order dPG methods for the Poisson model problem for a sufficiently small initial mesh-size in two different ways by equivalences to two other types of methods, the reduced mixed and the weighted LS methods.

A main step to prove rate-optimality is the characterization of all four dPG methods as particular instances of these two methods. This is a major generalization of the equivalence developed in [CBHW18] only for the primal dPG method. In order to treat all four dPG methods simultaneously, the reduced mixed and the weighted LS method from [CBHW18] described in this introduction are equipped with more general parameters and weights, including but not restricted to those that lead to the four different dPG methods. Assumptions on these parameters and weights were derived as general as possible to include as many as possible different methods, but still guaranteeing well-posedness and eventually also rate-optimality of the adaptive alogorithm.

Since this shows that all properties, e.g., optimal convergence rates, of the four dPG methods follow as special cases from the respective properties of the reduced mixed or the weighted least-squares methods, this thesis then focuses on the analysis of these two methods for general parameters and weights.

The first important result in the analysis of the adaptive reduced mixed and weighted LS methods is the derivation of reliable and efficient computable error estimators. Both estimators utilize residual error estimators with volume terms and jump terms along the sides, both weighted with factors of the mesh-size h. An important tool in the construction of both estimators is the equivalence

$$\|\nabla_{NC} w_{CR}\|^2_{L^2(\Omega)} \approx \sum_{E\in\mathcal{E}(\Omega)} |E|^{1/(n-1)} \|[\nabla_{NC} w_{CR}]_E\|^2_{L^2(E)}$$

developed in this thesis for Crouzeix-Raviart functions $w_{CR} \in CR^1_0(\mathcal{T})$ that satisfy the L^2 orthogonality $\nabla_{NC} w_{CR} \perp \nabla S^1_0(\mathcal{T})$. The error estimator for the weighted LS method has an additional data approximation error term $\|(1-\Pi_0) f\|_{L^2(\Omega)}$, which causes the need for separate instead of collective marking in the adaptive algorithm for this method.

Whereas the proofs of the axioms of stability (A1) and reduction (A2) for both methods follow standard arguments, the proofs of discrete reliability (A3) and quasi-orthogonality (A4) are essential achievements of this thesis.

The proof of discrete reliablity for the reduced mixed method subtly combines tools of the discrete reliability for the Crouzeix-Raviart method, in particular, a discrete quasi-interpolation operator from [CGS13] and introduces some nonconforming energies as auxiliary variables. The quasi-orthogonality (A4) is proved in form of some quasi-orthogonality with a small parameter ε, which leads to (A4) for a sufficiently fine initial triangulation. This condition is needed for the proof of quasi-monotonicity (QM) as well and finally leads to the statement of optimal convergence rates for the reduced mixed methods.

In contrast to the reduced mixed methods, the axiom of quasi-monotonicity (QM) for the weighted LS methods does not need the condition of a sufficiently small initial mesh-size. The analysis of discrete reliablity (A3) for the weighted LS methods follows the strategy prescribed for the standard LS method in [CP15], but with some extra technical difficulties caused by the weight functions that differ from triangulation to triangulation. A central lemma for overcoming this problem estimates the error of differently weighted vector fields by a difference of the eigenvalues of the matrix-valued weights. Furthermore, an insight gained from the connection of these weighted LS methods to the reduced mixed methods enabled the proof of discrete reliability without a discrete Helmholtz decomposition, which therefore holds in any space dimension as compared to only $n = 2$ in [CP15]. The proof of quasi-orthogonality with a parameter ε also relies on the estimation of the weights. This leads to the main result of optimal convergence rates with the separate marking adaptive algorithm for the weighted LS methods.

All proofs gather explicit constants in the spirit of [CH18a], sometimes subsumed within the proofs for the sake of readability. Table 1 gives an overview of constants employed in the proofs with references.

The numerical experiments of this thesis verify the optimal convergence rates of both types of methods for different choices of parameters. Moreover, they complement the theory by a thorough comparison of both methods among each other and with their equivalent dPG schemes.

Outline of this thesis

The remainder of this thesis is organized as follows. Section 2 gives a detailed introduction into the notation and tools employed in this thesis. It starts with a recapitulation on function spaces, triangulations, refinements and the set of admissible triangulations. It then introduces the adaptive algorithms and the axioms of adaptivity. Afterwards, it summarizes the existing literature on the abstract framework of dPG methods and the trace operators essential to them. The section concludes with a collection of important tools, inequalities and interpolation operators utilized in this thesis.

The main part of this thesis consists of Sections 3-8, which is basically divided into two parts of analogous structure. The first part analyses the reduced mixed method and is a more detailed exposition of [CH18b], whereas the second part contains the analysis of the weighted LS method, which is yet unpublished. Section 3 introduces the reduced mixed method, proves well-posedness thereof, derives an efficient and reliable error estimator and states a number of abstract assumptions on the parameters of the method. Section 4 inserts the four lowest-order dPG methods into this framework by proving equivalence to the reduced mixed scheme for different choices of parameters. Finally, Section 5 proves the axioms of adaptivity (A1)-(A4) and all intermediate steps needed for them and deduces the statement of quasi-monotonicity (QM) and therefore, rate-optimality in a summarising theorem.

Constant		Reference
c_{sr}	shape regularity	Definition 2.14 on p. 17
$c_{\mathrm{dF}}, c_{\mathrm{F}}$	(discrete) Friedrichs inequality	Theorems 2.28, 2.29 on p. 23
$c_{\mathrm{dP}}, c_{\mathrm{P}}$	(discrete) Poincaré inequality	Theorem 2.30 on p. 24
c_{inv}	inverse inequality	Theorem 2.31 on p. 24
$c_{\mathrm{dtr}}, c_{\mathrm{tr}}$	(discrete) trace inequality	Lemma 2.33, Remark 2.34 on p. 24
κ_{NC}	nonconforming interpolation operator	Theorem 2.36 on p. 25
$c_{\mathrm{apx}}(J_k)$	conforming companion operator	Theorem 2.37 on p. 25
c_{dQI}	discrete quasi interpolation	Theorem 2.38 on p. 26
c_{dCR}	discrete quasi interpolation for CR	Theorem 2.39 on p. 26
c_{jc}	discrete jump control	[CR17, Lem. 5.2]
c_{Q}	approximation property of Q	Assumption (3.5) on p. 30
$c_{\mathrm{rel}}, c_{\mathrm{eff}}$	reliability and efficiency for reduced mixed method	Corollary 3.3 on p. 30
c_{LS}	standard LS equivalence	(6.3) on p. 53
$\underline{\lambda}, \overline{\lambda}$	uniform boundedness of M_0	Assumption (6.6) on p. 54
κ_1	boundedness of F_0	Assumption (6.7) on p. 54
$c_{\mathrm{rel}}, c_{\mathrm{eff}}$	reliability and efficiency for weighted LS method	Lemma 6.7 on p. 58
Λ_1	Stability (A1)	Subsection 2.4, Thm. 5.1 on p. 42, and Thm. 8.2 on p. 68
Λ_2, ϱ_2	Reduction (A2)	Subsection 2.4, Thm. 5.2 on p. 42, and Thm. 8.3 on p. 69
$\Lambda_3, \widehat{\Lambda}_3$	Discrete reliability (A3)	Subsection 2.4, Thm. 5.5 on p. 45, and Thm. 8.10 on p. 73
Λ_4	Quasiorthogonality (A4)	Subsection 2.4, Thm. 5.8 on p. 49, and Thm. 8.13 on p. 78
Λ_{QM}	Quasiomonotonicity (QM)	Subsection 2.4 and Thm. 8.1 on p. 67

Table 1: Overview of constants in this thesis

The structure of Sections 6-8 for the weighted LS method is similar. The introduction of the method and its error estimator, its stability, and the general assumptions on the weights are contained in Section 6. It is followed by Section 7 with proofs of equivalence of the four dPG methods to the weighted LS method for certain choices of the weights. Section 8 proves the axioms of adaptivity (QM) and (A1)-(A4) and gives the resulting statement of optimal convergence rates. Sections 3, 5, 6, and 8 treat the analysis of the reduced mixed method and the weighted LS method and can be read independently of previous knowledge of dPG methods.

Section 9 presents numerical experiments on five benchmark examples, four of which have known exact solutions. It includes a variety of convergence history plots, solution plots, triangulations and tables examining optimal convergence rates and illustrating equivalence of the methods. A special focus is on the examination of the computational differences between the theoretically equivalent methods, including a study of computation times.

The thesis closes with a conclusion of the achieved results and an outlook of future research in Section 10.

Appendix A comments on the software attached to this thesis and utilized for the numerical experiments.

Acknowledgements

As the writing of a PhD thesis involves more than just one person, I want to take the opportunity to appreciate the help and support of several people. First of all, there is my supervisor Prof. Carstensen, who has accompanied my scientific development for several years by now. I am very grateful to him for teaching me so much about numerical analysis and mathematical writing, and for supporting my career. Next to that, I want to thank my working group and my colleagues all across the world, for all the great experiences at various scientific events and all the knowledge they shared with me. Furthermore, thank you to the The Berlin Mathematical School and the Deutsche Forschungsgemeinschaft in the Priority Program 1748 “Reliable simulation techniques in solid mechanics. Development of non-standard discretization methods, mechanical and mathematical analysis” (CA 151/22-1) for their financial support.

What is more, I want to express my gratitude to my friends and family for always being there, for always listening to me, having my back and also for taking my mind off work if necessary. My friend and colleague Philipp occupies a special place in the intersection of different areas of my life. I cannot thank you enough for your highly appreciated thoughts on mathematics and everything else, for your diverse help, and for being such a good company over the years of our friendship and as colleagues. Last but not least – Nino and Stevie. You are invaluable to me, each of you in their individual way, and I am beyond grateful for having you in my life. Your love and support keep me going.

Space		Reference
$C^k(\Omega)$	k times continuously differentiable functions	[Alt16, p. 43]
$C^\infty(\Omega)$	$:= \bigcap_{k\in\mathbb{N}_0} C^k(\Omega)$	[Alt16, p. 45]
$C_c^\infty(\Omega)$	$:= \{f \in C^\infty(\Omega) \mid \operatorname{supp}(f) \subseteq \Omega \text{ compact}\}$	[Eva10, p. 242]
$L^p(\Omega)$	Lebesgue functions	Definition 2.1
$H^1(\Omega)$	Sobolev space of functions with weak derivative	Definition 2.3
$H_0^1(\Omega)$	Sobolev space with zero boundary condition	Definition 2.3
$H(\operatorname{div},\Omega)$	functions with weak divergence	Definition 2.4
$H^{1/2}(\partial\mathcal{T})$	traces of Sobolev functions on skeleton	Definition 2.20
$H^{-1/2}(\partial\mathcal{T})$	normal traces of $H(\operatorname{div})$ functions on skeleton	Definition 2.20
$H^1(\mathcal{T})$	piecewise Sobolev functions	Definition 2.5
$H^1_{NC}(\mathcal{T})$	piecewise Sobolev functions with jump condition	Definition 2.7

Table 2: Overview of continuous function spaces, all discrete spaces in Subsection 2.2

2. Notation and Preliminaries

Throughout this thesis, consider a polyhedral, bounded Lipschitz domain [Gri11, p. 5-7] $\Omega \subset \mathbb{R}^n$ with boundary $\partial\Omega$ for $n = 2,3$. Denote the Euclidean scalar product $a \cdot b$ and the tensor product $a \otimes b := ab^\top \in \mathbb{R}^{\ell\times\ell}$ of two vectors $a, b \in \mathbb{R}^\ell$, $\ell \in \mathbb{N}$ and the symmetric matrices $\mathbb{S} \subset \mathbb{R}^{\ell\times\ell}$. The measure $|\bullet|$ is context-sensitive and refers to the modulus $(a \cdot a)^{1/2}$ of a scalar or vector $a \in \mathbb{R}^\ell$, the number of elements of some finite set or the Lebesgue measure $|\omega|$ of a Lebesgue measurable set $\omega \subset \mathbb{R}^n$. Denote the identity mapping $\bullet = \mathrm{id}$ and the identity matrix $I_{n\times n} \in \mathbb{S}$.

2.1. Function Spaces

This section recalls the standard notation on Lebesgue and Sobolev spaces summarized in Table 2.

Definition 2.1 (Lebesgue spaces [Alt16, pp. 50 ff.]) For $1 \le p \le \infty$, $L^p(\Omega)$ denotes the space of Lebesgue functions Ω with norm $\|f\|_{L^p(\Omega)} = (\int_\Omega |f|^p \,\mathrm{d}x)^{1/p}$ for $1 \le p < \infty$ and $\|f(x)\|_{L^\infty(\Omega)} = \operatorname{esssup}_{x\in\Omega} |f(x)|$. For sets $U \subseteq \mathbb{R}$, $U \subseteq \mathbb{R}^\ell$, or $U \subseteq \mathbb{R}^{\ell\times m}$, $\ell, m \in \mathbb{N}$, $L^p(\Omega;U)$ denotes the Lebesgue functions on Ω with values in U. For functions $f, g \in L^2(\Omega;U)$, $U \subseteq \mathbb{R}^\ell$, $\ell \in \mathbb{N}$, the L^2 scalar product reads $(f,g)_{L^2(\Omega)} := \int_\Omega f \cdot g \,\mathrm{d}x$.

Remark 2.2 For ease of notation, most of the definitions in the remainder of this chapter focus on scalar valued functions. However, the definitions of operators apply componentwise to vector- or matrixvalued functions as well and are denoted with the same variable. In case of function spaces, the "$;U$" in the name of the space like in Definition 2.1 above or in the discrete spaces of Definition 2.6 below indicates the range $U \subseteq \mathbb{R}, \mathbb{R}^\ell, \mathbb{R}^{\ell\times m}$, $\ell, m \in \mathbb{N}$, of the functions.

Definition 2.3 (Weak derivative, Sobolev space [Eva10, p. 245]) For any $j \in \{1,\dots,n\}$ and a function $v \in L^2(\Omega)$, the j^{th} weak partial derivative $\partial v/\partial x_j$ of v is a function $w : \Omega \to \mathbb{R}$ that satisfies $\int_\Omega v\,\partial\varphi/\partial x_j \,\mathrm{d}x = -\int_\Omega w\varphi \,\mathrm{d}x$ for any $\varphi \in C_c^\infty(\Omega)$ [Eva10, p. 245]. The gradient of v is the column vector $\nabla v = (\partial v/\partial x_1,\dots,\partial v/\partial x_n)^\top$. The Sobolev space

$$H^1(\Omega) := \{v \in L^2(\Omega) \mid \nabla v \text{ exists in a weak sense and } \nabla v \in L^2(\Omega;\mathbb{R}^n)\}$$

employs the norm $\|v\|^2_{H^1(\Omega)} := \|v\|^2_{L^2(\Omega)} + \|\nabla v\|^2_{L^2(\Omega)}$ for any $v \in H^1(\Omega)$. In the sense of traces defined in Theorem 2.18 in Subsection 2.5 below, define the space

$$H^1_0(\Omega) := \{v \in H^1(\Omega) \mid v = 0 \text{ almost everywhere along } \partial\Omega\}$$

with norm $|||v||| := \|\nabla v\|_{L^2(\Omega)}$ for any $v \in H^1_0(\Omega)$.

Next to functions with weak derivative, this thesis employs functions with weak divergence.

Definition 2.4 (H(div) space [BBF13, p. 49]) For any $q \in L^2(\Omega;\mathbb{R}^n)$, the weak divergence $\operatorname{div} q$ of q is a function $w : \Omega \to \mathbb{R}$ that satisfies $\int_\Omega u \cdot \nabla\varphi \,\mathrm{d}x = -\int_\Omega w\varphi \,\mathrm{d}x$ for any $\varphi \in C_c^\infty(\Omega)$. Define

$$H(\operatorname{div},\Omega) := \{q \in L^2(\Omega;\mathbb{R}^n) \mid \operatorname{div} q \text{ exists in a weak sense and } \operatorname{div} q \in L^2(\Omega)\}$$

with norm $\|q\|^2_{H(\operatorname{div})} := \|q\|^2_{L^2(\Omega)} + \|\operatorname{div} q\|^2_{L^2(\Omega)}$ for any $q \in H(\operatorname{div},\Omega)$.

Definition 2.5 (Piecewise Sobolev and H(div) space) Given a triangulation $\mathcal{T}$ of the domain Ω, define the piecewise H^1 and $H(\operatorname{div})$ spaces by

$$\begin{aligned} H^1(\mathcal{T}) &:= \{v_\mathcal{T} \in L^2(\Omega) \mid \forall T \in \mathcal{T}, v_\mathcal{T}|_T \in H^1(T)\},\\ H(\operatorname{div},\mathcal{T}) &:= \{q_\mathcal{T} \in L^2(\Omega;\mathbb{R}^n) \mid \forall T \in \mathcal{T}, q_\mathcal{T}|_T \in H(\operatorname{div},T)\}. \end{aligned}$$

Furthermore, define the piecewise weak gradient ∇_{NC} for any $v_\mathcal{T} \in H^1(\mathcal{T})$ and $T \in \mathcal{T}$ by $(\nabla_{NC} v_\mathcal{T})|_T := \nabla(v_\mathcal{T}|_T)$ and the piecewise weak divergence div_{NC} by $(\operatorname{div}_{NC} q_\mathcal{T})|_T := \operatorname{div}(q_\mathcal{T}|_T)$ for any $q_\mathcal{T} \in H^1(\mathcal{T})$. With $|||\cdot|||_{NC} := \|\nabla_{NC}\cdot\|^2_{L^2(\Omega)}$ on $H^1(\mathcal{T})$, the norms on these spaces read

$$\begin{aligned} \|v_\mathcal{T}\|^2_{H^1(\mathcal{T})} &:= \|v_\mathcal{T}\|^2_{L^2(\Omega)} + |||v_\mathcal{T}|||^2_{NC} && \text{for any } v_\mathcal{T} \in H^1(\mathcal{T}),\\ \|q_\mathcal{T}\|^2_{H(\operatorname{div},NC)} &:= \|q_\mathcal{T}\|^2_{L^2(\Omega)} + \|\operatorname{div}_{NC} q_\mathcal{T}\|^2_{L^2(\Omega)} && \text{for any } q_\mathcal{T} \in H(\operatorname{div},\mathcal{T}). \end{aligned}$$

Define the bilinear form $a_{NC}(v_\mathcal{T}, w_\mathcal{T}) := (\nabla_{NC} v_\mathcal{T}, \nabla_{NC} w_\mathcal{T})_{L^2(\Omega)}$ for any $v_\mathcal{T}, w_\mathcal{T} \in H^1(\mathcal{T})$.

2.2. Triangulation and Discrete Spaces

For any n-simplex $T = \operatorname{conv}\{z_1,\dots,z_{n+1}\} \subseteq \mathbb{R}^n$, $\mathcal{N}(T) = \{z_1,\dots,z_{n+1}\}$ denotes its nodes and $\mathcal{E}(T)$ its sides. Similarly, for a regular triangulation $\mathcal{T}$ of the domain Ω into simplices [Cia02, p. 38], let $\mathcal{N} = \bigcup_{T\in\mathcal{T}} \mathcal{N}(T)$ (resp. $\mathcal{N}(\Omega)$ resp. $\mathcal{N}(\partial\Omega)$) the set of all nodes (resp.

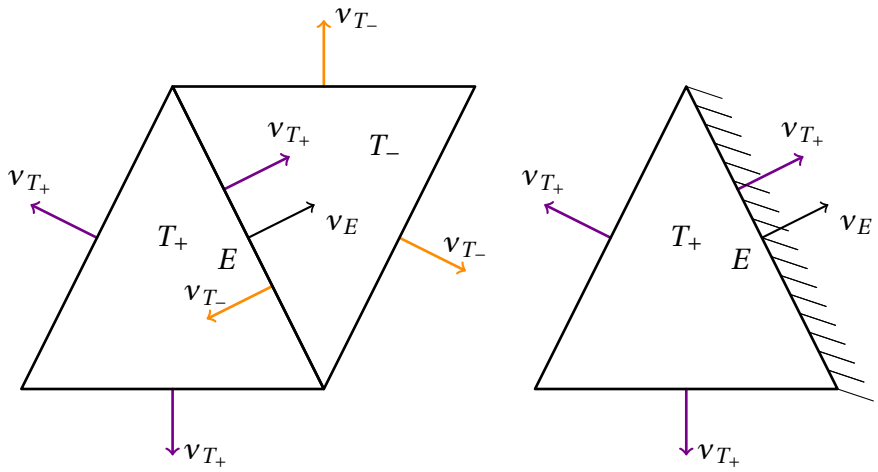

Figure 8: Side patch ω_E and normal vectors for an inner side and a boundary side in $2d$

inner nodes resp. boundary nodes) and $\mathcal{E} = \bigcup_{T\in\mathcal{T}} \mathcal{E}(T)$ (resp. $\mathcal{E}(\Omega)$ resp. $\mathcal{E}(\partial\Omega)$) the set of all sides (resp. inner sides resp. boundary sides). For any simplex $T \in \mathcal{T}$, denote the patch $\omega_T = \bigcup_{K\in\mathcal{T}, \mathcal{N}(T)\cap\mathcal{N}(K)\neq\emptyset} K$. Furthermore, define the skeleton of a triangulation by $\partial\mathcal{T} := \bigcup_{T\in\mathcal{T}} \bigcup_{E\in\mathcal{E}(T)} E$.

Let ν_T the outer unit normal vector along the boundary ∂T of a simplex T. For any inner side $E = \partial T_+ \cap \partial T_- \in \mathcal{E}(\Omega)$ as in Figure 8, denote the side patch $\omega_E = \operatorname{int}(\overline{T_+} \cup \overline{T_-})$ and fix one of the two possible directions of the unit normal vector ν_E of the side and thus, the notation of the neighboring elements T_+ and T_- via $\nu_{T_+}|_E = \nu_E$. For a boundary edge $E \in \mathcal{E}(\partial\Omega)$ with $E = \partial T \cap \partial\Omega$, let $\omega_E = T$ and the unit normal vector ν_E of the side point outwards.

Define the jump of $v \in H^1(\mathcal{T})$ by $[v]_E := v|_{T_+} - v|_{T_-} \in L^2(E)$ on any inner side $E \in \mathcal{E}(\Omega)$ and by $[v]_E := v \in L^2(E)$ on any boundary side $E \in \mathcal{E}(\partial\Omega)$. For any $v \in L^2(E)$, define the integral mean $\fint_E v \,\mathrm{d}s := \int_E v \,\mathrm{d}s/|E|$ along the side. The side normals $\nu_E = \pm\nu_{T_\pm}$ from above generate jumps in that any $v \in H^1(\mathcal{T})$ satisfies

$$\sum_{T\in\mathcal{T}} \int_{\partial T} v\nu_T \,\mathrm{d}s = \sum_{E\in\mathcal{E}} \int_E [v]_E \nu_E \,\mathrm{d}s. \tag{2.1}$$

Consider the midpoint $\operatorname{mid}(T) := 1/(n+1)\sum_{z\in\mathcal{N}(T)} z$, diameter $h_T := \sup_{x,y\in T}|x-y|$, and the Lebesgue measure $H_T := |T|^{1/n}$ of any simplex T and the corresponding piecewise constant functions $\operatorname{mid}(\mathcal{T})$, $h_\mathcal{T}$, and $H_\mathcal{T}$ defined by $\operatorname{mid}(\mathcal{T})|_T := \operatorname{mid}(T)$, $h_\mathcal{T}|_T := h_T$, and $H_\mathcal{T}|_T := H_T$ for any $T \in \mathcal{T}$. These satisfy the pointwise estimate $|\bullet - \operatorname{mid}(\mathcal{T})| \leq n h_\mathcal{T}/(n+1)$.

Definition 2.6 (Piecewise polynomials) The piecewise polynomials of degree $k \in \mathbb{N}_0$ read

$$\begin{aligned}
P_k(T) &:= \{v_k \in L^\infty(T) \mid v_k \text{ algebraic polynomial on } T \text{ of total degree } \leq k\},\\
P_k(\mathcal{T}) &:= \{v_k \in L^\infty(\Omega) \mid \forall T \in \mathcal{T},\, v_k|_T \in P_k(T)\},\\
P_k(T;U) &:= \{q_k \in L^\infty(T;U) \mid \text{each component of } q_k \text{ is in } P_k(T)\}, \text{ for } U \subseteq \mathbb{R}, \mathbb{R}^\ell, \text{ or } \mathbb{R}^{\ell\times m},\\
P_k(\mathcal{T};U) &:= \{q_k \in L^\infty(\Omega;U) \mid \forall T \in \mathcal{T},\, v_k|_T \in P_k(T;U)\}.
\end{aligned}$$

Analogously, define piecewise polynomials on edges,

$$P_k(E) := \{v_k \in L^\infty(E) \mid v_k \text{ algebraic polynomial on } E \text{ of total degree } \le k\},$$
$$P_k(\mathcal{E}) := \{v_k \in L^\infty(\mathcal{E}) \mid \forall E \in \mathcal{E},\ v_k|_E \in P_k(E)\}.$$

The following classical finite element spaces trace back to [Cou43; CR73; RT77] and employ piecewise polynomials with some additional continuity and boundary conditions.

Definition 2.7 (Finite element spaces) For any $k \in \mathbb{N}_0$, define the conforming spaces

$$S_0^k(\mathcal{T}) := P_k(\mathcal{T}) \cap H_0^1(\Omega) \subseteq S^k(\mathcal{T}) := P_k(\mathcal{T}) \cap H^1(\Omega).$$

The Crouzeix-Raviart functions form a subspace of $H^1_{NC}(\mathcal{T})$, where

$$H^1_{NC}(\mathcal{T}) := \{v_\mathcal{T} \in H^1(\mathcal{T}) | \forall E \in \mathcal{E}(\Omega), \fint_E [v_\mathcal{T}]_E \,\mathrm{d}s = 0\},$$
$$CR^1(\mathcal{T}) := \{v_{CR} \in P_1(\mathcal{T}) \mid \forall E \in \mathcal{E}(\Omega),\ v_{CR} \text{ continuous at } \mathrm{mid}(E)\} \subseteq H^1_{NC}(\mathcal{T}),$$
$$CR^1_0(\mathcal{T}) := \{v_{CR} \in CR^1(\mathcal{T}) \mid \forall E \in \mathcal{E}(\partial\Omega),\ v_{CR}(\mathrm{mid}(E)) = 0\}.$$

The (piecewise) lowest-order Raviart-Thomas functions read

$$RT_0^{NC}(\mathcal{T}) := \{q_1 \in L^\infty(\Omega;\mathbb{R}^n) \mid \exists A \in P_0(\mathcal{T};\mathbb{R}^n), b \in P_0(\mathcal{T}), q_1 = A + b(\bullet - \mathrm{mid}(\mathcal{T}))\},$$
$$RT_0(\mathcal{T}) := RT_0^{NC}(\mathcal{T}) \cap H(\mathrm{div},\Omega).$$

Definition 2.8 (Galerkin projection) Define the linear and bounded operator $G : H^1(\mathcal{T}) \to S^1_0(\mathcal{T})$ by $Gv_\mathcal{T} := v_C$ for any $v_\mathcal{T} \in H^1(\mathcal{T})$ and the unique $v_C \in S^1_0(\mathcal{T})$ that satisfies

$$\int_\Omega \nabla v_C \cdot \nabla w_C \,\mathrm{d}x = \int_\Omega \nabla_{NC} v_\mathcal{T} \cdot \nabla w_C \,\mathrm{d}x \quad \text{for all } w_C \in S^1_0(\mathcal{T}).$$

For properties of the subsequently defined L^2 projection Π_k see Lemma 2.24 below.

Definition 2.9 (L^2 projection and oscillations) For any $k \in \mathbb{N}_0$, define the L^2 projection $\Pi_k : L^2(\Omega) \to P_k(\mathcal{T})$ uniquely for any $v \in L^2(\Omega)$ via $((1-\Pi_k)v, v_k)_{L^2(\Omega)} = 0$ for any $v_k \in P_k(\mathcal{T})$. Furthermore, define the oscillation $\mathrm{osc}(f,\mathcal{T}) := \|h_\mathcal{T}(f - \Pi_0 f)\|_{L^2(\Omega)}$.

The following piecewise constant functions are weights of the dPG methods in the context of the weighted least-squares formulation from Section 6.

Definition 2.10 (Weights) Define the piecewise constant mappings $S(\mathcal{T}) \in P_0(\mathcal{T};\mathbb{S})$, $s(\mathcal{T}) \in P_0(\mathcal{T})$ and the operator $H_0 : L^2(\Omega) \to P_0(\mathcal{T};\mathbb{R}^n)$ by

$$S(\mathcal{T}) := \Pi_0((\bullet - \mathrm{mid}(\mathcal{T})) \otimes (\bullet - \mathrm{mid}(\mathcal{T}))),$$
$$s(\mathcal{T}) := \mathrm{tr}\, S(\mathcal{T}) = \Pi_0 |\bullet - \mathrm{mid}(\mathcal{T})|^2,$$
$$H_0 f := \Pi_0(f(\bullet - \mathrm{mid}(\mathcal{T}))) \quad \text{for any } f \in L^2(\Omega).$$

Remark 2.11 ($P_1(\mathcal{T})$ and $RT_0^{NC}(\mathcal{T})$) Any $v_1 \in P_1(\mathcal{T})$ and $q_1 \in RT_0^{NC}(\mathcal{T})$ satisfy

$$v_1 = \Pi_0 v_1 + \nabla_{NC} v_1 \cdot (\bullet - \operatorname{mid}(\mathcal{T})) \quad \text{and} \quad q_1 = \Pi_0 q_1 + \operatorname{div}_{NC} q_1 (\bullet - \operatorname{mid}(\mathcal{T}))/n.$$

This and the orthogonality of $\operatorname{id} - \operatorname{mid}(\mathcal{T}) = (1 - \Pi_0)\operatorname{id}$ onto $P_0(\mathcal{T})$ lead to an alternative representation of norms

$$\begin{aligned} \|v_1\|^2_{H^1(\mathcal{T})} &= \|\Pi_0 v_1\|^2_{L^2(\Omega)} + \|(1 + S(\mathcal{T}))^{1/2} \nabla_{NC} v_1\|^2_{L^2(\Omega)}, \\ \|q_1\|^2_{H(\operatorname{div},NC)} &= \|\Pi_0 q_1\|^2_{L^2(\Omega)} + \|(1 + s(\mathcal{T})/n^2)^{1/2} \operatorname{div}_{NC} q_1\|^2_{L^2(\Omega)}. \end{aligned}$$

2.3. Refinement

Any n-simplex $T = \operatorname{conv}\{P_1, \dots, P_{n+1}\}$ is identified with the $(n+1)$-tuple $(P_1, \dots, P_{n+1})$. Its refinement edge is $\overline{P_1 P_{n+1}}$ and $\operatorname{bisec}(T) := \{T_1, T_2\}$ is defined with $T_1 := \operatorname{conv}\{P_1, (P_1 + P_{n+1})/2, P_2, \dots, P_n\}$ and $T_2 := \operatorname{conv}\{P_{n+1}, (P_1 + P_{n+1})/2, P_2, \dots, P_n\}$. The ordering of the nodes in the $(n+1)$-tuples corresponding to T_1 and T_2 and thus, the refinement edges, for the new simplices T_1 and T_2 are fixed and for $n = 3$ additionally depend on the type of the (tagged) n-simplex [Tra97; Ste08].

For any triangulation $\mathcal{T}$, a refinement $\widehat{\mathcal{T}}$ is defined as a regular triangulation such that, for any $T \in \widehat{\mathcal{T}}$, there exists $K \in \mathcal{T}$ such that $T \subseteq K$. The notation $\mathcal{T} \cap \widehat{\mathcal{T}}$ refers to simplices that are both in $\mathcal{T}$ and in $\widehat{\mathcal{T}}$, i.e., that have not been refined. In a similar manner, $\mathcal{T} \setminus \widehat{\mathcal{T}}$ denotes simplices in the coarse triangulation $\mathcal{T}$ that are refined, i.e., simplices before the refinement. Denote $\widehat{\mathcal{T}} \setminus \mathcal{T}$ the simplices in the fine triangulation $\widehat{\mathcal{T}}$ that have been refined, i.e., simplices after the refinement. Given some $\mathcal{T}$ and a refinement $\widehat{\mathcal{T}}$, this thesis often utilizes properties or quantities x and $\widehat{x}$ to symbolyze the respective relation to these two generic triangulations.

Given a regular triangulation $\mathcal{T}$ and an arbitrary set $\mathcal{M} \subseteq \mathcal{T}$ of marked simplices, the *newest vertex bisection* algorithm [Mit89; Ste08] bases on a successive bisection of simplices and generates a minimal refinement $\widehat{\mathcal{T}}$ of $\mathcal{T}$ such that the marked simplices are refined, i.e., $\mathcal{M} \subseteq \mathcal{T} \setminus \widehat{\mathcal{T}}$. Strictly speaking, the newest vertex bisection requires a tagged simplex and the initialization requires an initial condition [Ste08, §4] suppressed here for simplicity of notation.

Definition 2.12 Given a regular initial triangulation $\mathcal{T}_0$, define the *admissible triangulations*

$$\mathbb{T} := \{\mathcal{T} \mid \mathcal{T} \text{ is refinement of } \mathcal{T}_0 \text{ by a sequence of newest vertex bisections}\}.$$

Furthermore, given $\mathcal{T} \in \mathbb{T}$, define the set of admissible refinements of $\mathcal{T}$ by

$$\mathbb{T}(\mathcal{T}) := \{\widehat{\mathcal{T}} \mid \widehat{\mathcal{T}} \text{ is refinement of } \mathcal{T} \text{ by a sequence of newest vertex bisections}\}.$$

The set of admissible simplices reads $\bigcup \mathbb{T} = \bigcup_{\mathcal{T} \in \mathbb{T}} \mathcal{T}$. For any $K \in \mathcal{T} \in \mathbb{T}$ and a refinement $\widehat{\mathcal{T}} \in \mathbb{T}(\mathcal{T})$, define $\widehat{\mathcal{T}}(K) := \{T \in \widehat{\mathcal{T}} \mid T \subseteq K\}$. Furthermore, for $\delta > 0$, denote $\mathbb{T}(\delta) = \{\mathcal{T} \in \mathbb{T} \mid h_{\mathcal{T}} \leq \delta \text{ a.e. in } \Omega\}$. The maximal mesh size $h_{\max} := \max_{\mathcal{T} \in \mathbb{T}} \max_{T \in \mathcal{T}} h_T$ is bounded by $h_0 := \max_{T \in \mathcal{T}_0} h_T \leq \operatorname{diam}(\Omega)$.

Definition 2.13 (Tilde notation) The inequality $A \lesssim B$ abbreviates the relation $A \leq CB$ with a generic constant $0 < C$ independent of the underlying triangulation, but solely dependent on the initial triangulation $\mathcal{T}_0$. In other words, C may depend on $\Omega, \mathcal{T}_0, h_0$, and the minimal interior angle. $A \approx B$ abbreviates $A \lesssim B \lesssim A$.

The newest vertex bisection results in a shape regular set of admissible triangulations $\mathbb{T}$ [Tra97, p. 128].

Definition 2.14 (Shape regularity) A family $\mathbb{T}$ of triangulations is called shape regular if for the radius $\varrho(T) := \max\{r > 0 | T \text{ contains ball of radius } r\}$ of the incircle of a simplex $T \in \mathcal{T} \in \mathbb{T}$, it holds $\sup_{\mathcal{T} \in \mathbb{T}} \max_{T \in \mathcal{T}} h_T / \varrho(T) < \infty$.

In particular, there exists $c_{\mathrm{sr}} \approx 1$ such that any $T \in \mathcal{T} \in \mathbb{T}$ and $E \in \mathcal{E}(T)$ satisfy $n|T| \leq h_T^n \leq c_{\mathrm{sr}}|T|$, $(n-1)|E| \leq h_T^{n-1} \leq c_{\mathrm{sr}}|E|$, $|E|^{n/(n-1)} \leq c_{\mathrm{sr}}|T|$, and $|T| \leq c_{\mathrm{sr}}|E|^{n/(n-1)}$, in short $|T|^{1/n} \approx h_T \approx |E|^{1/(n-1)}$.

For any $T \in \mathcal{T}$, let α_T the minimal angle between any two hypersurfaces in $\mathcal{E}(T)$, then the minimal angle condition $0 < \omega_0 := \min\{\alpha_T \,|\, T \in \mathcal{T}\}$ is equivalent [Tra97, p. 116] to shape regularity. For $n = 2$, [CH18a] states an explicit dependence of $c_{\mathrm{sr}} \approx 1$ in terms of ω_0.

2.4. Adaptivity

Unlike uniform refinement, adaptive refinement strategies rely on a local refinement depending on the discrete solution. A main task is the design of a refinement indicator $\eta(\mathcal{T}, T) \geq 0$ for any triangulation $\mathcal{T}$ and simplex $T \in \mathcal{T}$. For any subset $\mathcal{M} \subseteq \mathcal{T}$, abbreviate $\eta(\mathcal{T}, \mathcal{M}) := (\sum_{T \in \mathcal{M}} \eta^2(\mathcal{T}, T))^{1/2}$ and $\eta(\mathcal{T}) := \eta(\mathcal{T}, \mathcal{T})$ with $\eta^2(\bullet) := \eta(\bullet)^2$.

Algorithm 1 utilizes this refinement indicator in collective marking, also called Doerfler marking [Dör96] and follows the standard adaptive loop with notation $\eta_\ell(T) := \eta(\mathcal{T}_\ell, T)$ for any $T \in \mathcal{T}_\ell$ and $\ell \in \mathbb{N}_0$. The adaptive algorithm with collective marking will be applied to the reduced mixed method.

Algorithm 1 AFEM

Input: regular triangulation $\mathcal{T}_0$ and parameter $0 < \theta \leq 1$
  for $\ell = 0, 1, 2, \ldots$ **do**
    Solve discrete problem for x_ℓ on $\mathcal{T}_\ell$.
    Compute $\eta_\ell(T)$ for any $T \in \mathcal{T}_\ell$.
    Mark (almost) minimal subset $\mathcal{M}_\ell \subseteq \mathcal{T}_\ell$ with $\theta \sum_{T \in \mathcal{T}_\ell} \eta_\ell^2(T) \leq \sum_{T \in \mathcal{M}_\ell} \eta_\ell^2(T)$.
    Refine $\mathcal{T}_\ell$ with newest vertex bisection to compute $\mathcal{T}_{\ell+1}$ with $\mathcal{M}_\ell \subseteq \mathcal{T}_\ell \setminus \mathcal{T}_{\ell+1}$.
  end for
Output: sequence of triangulations $(\mathcal{T}_\ell)_{\ell \in \mathbb{N}_0}$ with $(x_\ell)_{\ell \in \mathbb{N}_0}$ and $(\eta_\ell)_{\ell \in \mathbb{N}_0}$.

In the marking step of the algorithm, understand *(almost) minimal subset* $\mathcal{M}_\ell \subseteq \mathcal{T}_\ell$ as $|\mathcal{M}_\ell| \lesssim |\mathcal{M}_{\ell,\min}|$, where $\mathcal{M}_{\ell,\min} \subseteq \mathcal{T}_\ell$ is a set of minimal cardinality from all sets that satisfy $\theta \sum_{T\in\mathcal{T}_\ell} \eta_\ell^2(T) \leq \sum_{T\in\mathcal{M}_{\ell,\min}} \eta_\ell^2(T)$.

In contrast to Algorithm 1 with collective marking utilized for the reduced mixed method, the weighted LS method analysed in this thesis employs an adaptive algorithm with separate marking from [CR17] that utilizes Dörfler marking and a data approximation algorithm `approx`, for details and possible choices, see [CR17, §3.3]. For two triangulations $\mathcal{T}, \widetilde{\mathcal{T}} \in \mathbb{T}$, $\mathcal{T} \oplus \widetilde{\mathcal{T}}$ denotes the overlay, i.e., the coarsest common refinement [CKNS08, §3.3]. The algorithm relies on two refinement indicators $\eta(\mathcal{T}, T), \mu(T) \geq 0$ and $\sigma(\mathcal{T}, T) := (\sigma^2(\mathcal{T}, T))^{1/2} := (\eta^2(\mathcal{T}, T) + \mu^2(T))^{1/2}$ for any triangulation $\mathcal{T}$ and simplex $T \in \mathcal{T}$ and with $\mu^2(\bullet) := \mu(\bullet)^2$. With abbreviations $\eta_\ell(T) := \eta(\mathcal{T}_\ell, T)$, $\sigma_\ell(T) := \sigma(\mathcal{T}_\ell, T)$ for any $T \in \mathcal{T}_\ell$, and $\mu_\ell^2 := \sum_{T\in\mathcal{T}_\ell} \mu^2(T)$ for any $\ell \in \mathbb{N}_0$, it reads as follows.

Algorithm 2 SAFEM

Input: regular triangulation $\mathcal{T}_0$ and parameters $0 < \theta \leq 1$, $0 < \varrho < 1$, $0 < \kappa$
  for $\ell = 0, 1, 2, \ldots$ **do**
    Solve discrete problem for x_ℓ on $\mathcal{T}_\ell$.
    Compute $\eta_\ell^2(T)$, $\mu^2(T)$ for any $T \in \mathcal{T}_\ell$.
    if $\mu_\ell^2 \leq \kappa \eta_\ell^2$ **then**
      Mark (almost) minimal subset $\mathcal{M}_\ell \subseteq \mathcal{T}_\ell$ with $\theta \sum_{T\in\mathcal{T}_\ell} \eta_\ell^2(T) \leq \sum_{T\in\mathcal{M}_\ell} \eta_\ell^2(T)$.
      Refine $\mathcal{T}_\ell$ with newest vertex bisection to compute $\mathcal{T}_{\ell+1}$ with $\mathcal{M}_\ell \subseteq \mathcal{T}_\ell \setminus \mathcal{T}_{\ell+1}$.
    else
      $\mathcal{T}_{\ell+1} = \mathcal{T}_\ell \oplus \mathtt{approx}(\varrho\mu_\ell^2, \mu(T) : T \in \mathcal{T}_0)$.
    end if
  end for
Output: sequence of triangulations $(\mathcal{T}_\ell)_{\ell\in\mathbb{N}_0}$ with $(x_\ell)_{\ell\in\mathbb{N}_0}$ and $(\eta_\ell)_{\ell\in\mathbb{N}_0}$, $(\mu_\ell)_{\ell\in\mathbb{N}_0}$, $(\sigma_\ell)_{\ell\in\mathbb{N}_0}$.

In order to analyse convergence and optimal rates of these algorithms, the papers [CFPP14; CR17] propose an axiomatic framework. It assumes the following properties of the refinement indicators $\eta(\mathcal{T}, T)$, $\mu(\mathcal{T})$, and $\sigma(\mathcal{T}, T)$ and some distance $\delta(\mathcal{T}, \widehat{\mathcal{T}}) \geq 0$ for any $\mathcal{T} \in \mathbb{T}$ and refinement $\widehat{\mathcal{T}} \in \mathbb{T}(\mathcal{T})$.

(A1) Stability. There exists $\Lambda_1 \approx 1$ such that any $\mathcal{T} \in \mathbb{T}$, $\widehat{\mathcal{T}} \in \mathbb{T}(\mathcal{T})$ satisfy

$$\big|\eta(\mathcal{T}, \mathcal{T} \cap \widehat{\mathcal{T}}) - \eta(\widehat{\mathcal{T}}, \mathcal{T} \cap \widehat{\mathcal{T}})\big| \leq \Lambda_1 \delta(\mathcal{T}, \widehat{\mathcal{T}}).$$

(A2) Reduction. There exists $\Lambda_2 \approx 1$ and $\varrho_2 < 1$ such that any $\mathcal{T} \in \mathbb{T}$, $\widehat{\mathcal{T}} \in \mathbb{T}(\mathcal{T})$ satisfy

$$\eta(\widehat{\mathcal{T}}, \widehat{\mathcal{T}} \setminus \mathcal{T}) \leq \varrho_2 \eta(\mathcal{T}, \mathcal{T} \setminus \widehat{\mathcal{T}}) + \Lambda_2 \delta(\mathcal{T}, \widehat{\mathcal{T}}).$$

(A3) Discrete reliability. There exist $\Lambda_3, \widehat{\Lambda}_3, \Lambda_{\mathrm{ref}} \approx 1$ such that for any $\mathcal{T} \in \mathbb{T}$, $\widehat{\mathcal{T}} \in \mathbb{T}(\mathcal{T})$, there exists $\mathcal{T} \setminus \widehat{\mathcal{T}} \subseteq \mathcal{R} \subseteq \mathcal{T}$ with $|\mathcal{R}| \leq \Lambda_{\mathrm{ref}} |\mathcal{T} \setminus \widehat{\mathcal{T}}|$ such that

$$\delta^2(\mathcal{T}, \widehat{\mathcal{T}}) \leq \Lambda_3 (\eta^2(\mathcal{T}, \mathcal{R}) + \mu^2(\mathcal{T})) + \widehat{\Lambda}_3 \eta^2(\widehat{\mathcal{T}}).$$

(A4) Quasiorthogonality. There exists $\Lambda_4 \approx 1$ such that any $\ell, m \in \mathbb{N}_0$, and the output $(\mathcal{T}_k)_{k\in\mathbb{N}_0}$ of the Algorithm 2 satisfy

$$\sum_{k=\ell}^{\ell+m} \delta^2(\mathcal{T}_k, \mathcal{T}_{k+1}) \leq \Lambda_4 \sigma^2(\mathcal{T}_\ell).$$

(B1) Rate s data approximation. There exists $\Lambda_5 \approx 1$ and $s > 0$ such that any $\mathrm{Tol} > 0$, $\mathcal{T}_{\mathrm{Tol}} := \texttt{approx}(\mathrm{Tol}, \mu(K) : K \in \mathcal{T}_0)$ satisfy

$$|\mathcal{T}_{\mathrm{Tol}}| - |\mathcal{T}_0| \leq \Lambda_5 \,\mathrm{Tol}^{-1/(2s)} \quad \text{and} \quad \mu^2(\mathcal{T}_{\mathrm{Tol}}) \leq \mathrm{Tol}.$$

(B2) Quasimonotonicity of μ. There exists $\Lambda_6 \approx 1$ such that any $\mathcal{T} \in \mathbb{T}$, $\widehat{\mathcal{T}} \in \mathbb{T}(\mathcal{T})$ satisfy

$$\mu(\widehat{\mathcal{T}}) \leq \Lambda_6 \mu(\mathcal{T}).$$

(QM) Quasimonotonicity of σ. There exists $\Lambda_{QM} \approx 1$ such that any $\mathcal{T} \in \mathbb{T}$, $\widehat{\mathcal{T}} \in \mathbb{T}(\mathcal{T})$ satisfy

$$\sigma(\widehat{\mathcal{T}}) \leq \Lambda_{QM} \sigma(\mathcal{T}).$$

These axioms imply optimal convergence rates of Algorithm 2, specified in more detail for the two classes of methods analysed in this paper in Subsections 5.4 and 8.5. Since Algorithm 1 is contained in Algorithm 2 as the special case $\mu = 0$ (hence, (B1) and (B2) are satisfied automatically), it suffices to prove (A1)-(A4) and (QM) in this case.

2.5. Discontinuous Petrov-Galerkin Methods

This subsection gives a brief outline of the dPG methodology, which was developed by L. Demkowicz and J. Gopalakrishnan [DG11b; DG13] and originally motivated by the search for optimal test functions [DG11a]. The following will focus on the characterizations of dPG as minimization of a residual in the dual space and as a mixed system of equations.

The dPG methodology considers, even in the continuous setting, a triangulation $\mathcal{T}$, local Banach spaces $X(T)$ and local Hilbert spaces $Y(T)$ for each $T \in \mathcal{T}$. The global *trial space* $X \subseteq \prod_{T\in\mathcal{T}} X(T)$ with norm $\|\bullet\|_X$ is a Banach space which may include constraints, such as continuity properties, whereas the global *test space* $Y = \prod_{T\in\mathcal{T}} Y(T)$ with scalar product $\langle \bullet, \bullet \rangle_Y$ and induced norm $\|\bullet\|_Y$ is discontinuous. The continuous problem employs a bilinear form $b : X \times Y \to \mathbb{R}$ and a linear form $F \in Y^*$ and seeks $x \in X$ such that

$$b(x, y) = F(y) \quad \text{for all } y \in Y. \tag{2.2}$$

An equivalent formulation of this variational formulation is the minimization of $\|F - b(\xi, \bullet)\|_{Y^*} = \sup_{y\in Y, \|y\|_Y=1} |F(y) - b(\xi, y)|$ with respect to $\xi \in X$. With finite-dimensional subspaces $X_h \subseteq X$ and $Y_h \subseteq Y$ and the discrete dual norm $\|F - b(\xi, \bullet)\|_{Y_h^*} = \sup_{y_h\in Y_h, \|y_h\|_Y=1} |F(y_h) -$

$b(\xi, y_h)|$ for any $\xi \in X$, this motivates the discrete formulation (so-called practical dPG method [GQ14]) that minimizes

$$x_h = \operatorname*{arg\,min}_{\xi_h \in X_h} \|F - b(\xi_h, \bullet)\|_{Y_h^*}. \tag{minRes}$$

An equivalent mixed system of equations [CDW12] utilizes the Riesz representation $y_h \in Y_h$ of $F - b(x_h, \bullet)$ in Y_h and seeks $(x_h, y_h) \in X_h \times Y_h$ with

$$\begin{aligned} \langle y_h, \eta_h \rangle_Y + b(x_h, \eta_h) &= F(\eta_h) && \text{for all } \eta_h \in Y_h, \\ b(\xi_h, y_h) &= 0 && \text{for all } \xi_h \in X_h. \end{aligned} \tag{M}$$

The well-posedness of the continuous and discrete problem follows from a continuous and a discrete inf-sup condition [CDG14] as shown below.

Theorem 2.15 (A priori error estimate [GQ14]) If the bilinear form satisfies the discrete inf-sup condition $1 \lesssim \inf_{x_h \in X_h, \|x_h\|_X = 1} \sup_{y_h \in Y_h, \|y_h\|_Y = 1} b(x_h, y_h)$, the discrete problem (minRes) has a unique solution $x_h \in X_h$, and satisfies the quasi best-approximation

$$\|x - x_h\|_X \lesssim \min_{\xi_h \in X_h} \|x - \xi_h\|_X. \qquad \square$$

Provided a continuous inf-sup condition $1 \lesssim \inf_{x \in X, \|x\|_X = 1} \sup_{y \in Y, \|y\|_Y = 1} b(x, y)$, the discrete inf-sup condition is equivalent [CH16] to the existence of a linear and bounded Fortin operator $\Pi : Y \to Y_h$ that satisfies $b(x_h, (1 - \Pi) y) = 0$ for any $x_h \in X_h$ and $y \in Y$. This operator appears in the following a posteriori error estimate.

Theorem 2.16 (Built-in a posteriori error control [CDG14]) If the bilinear form satisfies the continuous inf-sup condition and there exists a Fortin operator $\Pi : Y \to Y_h$ as above, the exact solution $x \in X$ to (2.2) and any discrete $\xi_h \in X_h$ satisfy

$$\|x - \xi_h\|_X \approx \|F - b(\xi_h, \bullet)\|_{Y_h^*} + \|F \circ (1 - \Pi)\|_{Y^*}.$$

In particular, the discrete solution $(x_h, y_h) \in X_h \times Y_h$ to (M) satisfies

$$\|x - x_h\|_X \approx \|y_h\|_{Y_h} + \|F \circ (1 - \Pi)\|_{Y^*}. \qquad \square$$

Remark 2.17 For several applications in [CDG14], the data approximation term $\|F \circ (1 - \Pi)\|_{Y^*}$ is of higher order. However, for the lowest-order methods analysed in this thesis, this is not the case. For example, for the primal dPG method from Section 4.1, $\Pi = I_{NC}$ and the interpolation error estimate (2.5) below proves $\|F \circ (1 - \Pi)\|_{Y^*} \lesssim \|h_{\mathcal{T}} f\|_{L^2(\Omega)}$, whereas for the ultraweak dPG method from Section 4.4, it holds $\|F \circ (1 - \Pi)\|_{Y^*} \lesssim h_{\max} \|f\|_{L^2(\Omega)}$ as shown for linear elasticity in [CH16].

In applications of this abstract framework, piecewise integration by parts with the above-mentioned discontinuous test spaces leads to trace terms. The notation of traces, trace spaces and norms is introduced below.

The following two trace operators [Eva10, p. 272; Tem77, pp. 7 ff.] extend the point evaluation operators for smooth functions to more general function spaces and enable a general integration by parts formula.

Theorem 2.18 (Trace operator in H^1) For any bounded Lipschitz domain $\omega \subset \mathbb{R}^n$, there exists a unique bounded, linear operator $\gamma_0 : H^1(\omega) \to L^2(\partial\omega)$ with

$$\gamma_0 w = w|_{\partial\omega} \quad \text{for any } w \in H^1(\omega) \cap C^0(\overline{\omega}). \qquad \square$$

The range of this operator is denoted by $H^{1/2}(\partial\omega) := \gamma_0(H^1(\omega))$ and its dual by $H^{-1/2}(\partial\omega) = (H^{1/2}(\partial\omega))^*$ with the duality pairing $\langle \bullet, \bullet \rangle_{\partial\omega} : H^{-1/2}(\partial\omega) \times H^{1/2}(\partial\omega) \to \mathbb{R}$.

Theorem 2.19 (Normal trace operator in $H(\mathrm{div})$) For any bounded Lipschitz domain $\omega \subset \mathbb{R}^n$, there exists a unique bounded, linear operator $\gamma_\nu : H(\mathrm{div}, \omega) \to H^{-1/2}(\partial\omega)$ with

$$\gamma_\nu q = q|_{\partial\omega} \cdot \nu \quad \text{for any } q \in C^1(\overline{\omega}).$$

Any $q \in H(\mathrm{div}, \omega)$ and $w \in H^1(\omega)$ satisfy

$$\langle \gamma_\nu q, \gamma_0 w \rangle_{\partial\omega} = (q, \nabla w)_{L^2(\omega)} + (\mathrm{div}\, q, w)_{L^2(\omega)}. \qquad \square$$

The application of these trace operators on the finite element domains of a triangulation yields the trace operators and trace spaces on skeletons for the dPG method.

Definition 2.20 (Traces on skeleton) Given a triangulation $\mathcal{T}$, define the operators $\gamma_0^{\mathcal{T}} : H^1(\mathcal{T}) \to \prod_{T\in\mathcal{T}} H^{1/2}(\partial T)$ and $\gamma_\nu^{\mathcal{T}} : H(\mathrm{div}, \mathcal{T}) \to \prod_{T\in\mathcal{T}} H^{-1/2}(\partial T)$ by

$$\begin{aligned} \gamma_0^{\mathcal{T}} w &:= (s_T)_{T\in\mathcal{T}} \quad \text{with } s_T := \gamma_0(w|_T) \quad \text{for any } T \in \mathcal{T}, w \in H^1(\mathcal{T}), \\ \gamma_\nu^{\mathcal{T}} q &:= (t_T)_{T\in\mathcal{T}} \quad \text{with } t_T := \gamma_\nu(q|_T) \quad \text{for any } T \in \mathcal{T}, q \in H(\mathrm{div}, \mathcal{T}). \end{aligned}$$

Define the trace spaces and discrete spaces

$$\begin{aligned} H^{1/2}(\partial\mathcal{T}) &:= \gamma_0^{\mathcal{T}}(H_0^1(\Omega)), \\ H^{-1/2}(\partial\mathcal{T}) &:= \gamma_\nu^{\mathcal{T}}(H(\mathrm{div}, \Omega)), \\ S_0^k(\mathcal{E}) &:= \gamma_0^{\mathcal{T}}(S_0^k(\mathcal{T})) \end{aligned}$$

with minimal extension norms defined for any $s \in H^{1/2}(\partial\mathcal{T})$ and $t \in H^{-1/2}(\partial\mathcal{T})$ by

$$\begin{aligned} \|s\|_{H^{1/2}(\partial\mathcal{T})} &:= \min\{|||w||| \mid w \in H_0^1(\Omega), \gamma_0^{\mathcal{T}} w = s\}, \\ \|t\|_{H^{-1/2}(\partial\mathcal{T})} &:= \min\{\|q\|_{H(\mathrm{div})} \mid q \in H(\mathrm{div}, \Omega), \gamma_\nu^{\mathcal{T}} q = t\}. \end{aligned}$$

Furthermore, for any $t \in \prod_{T\in\mathcal{T}} H^{-1/2}(\partial T)$ and $s \in \prod_{T\in\mathcal{T}} H^{1/2}(\partial T)$, consider

$$\langle t, s \rangle_{\partial\mathcal{T}} := \langle (t_T)_{T\in\mathcal{T}}, (s_T)_{T\in\mathcal{T}} \rangle_{\partial\mathcal{T}} := \sum_{T\in\mathcal{T}} \langle t_T, s_T \rangle_{\partial T}.$$

Remark 2.21 ($RT_0(\mathcal{T})$ and $P_0(\mathcal{E})$ are isomorphic) Any $q_{RT} \in RT_0(\mathcal{T})$ and $E \in \mathcal{E}$ satisfy $q_{RT}|_E \cdot \nu_E \in P_0(E)$. Conversely, for any $t_0 \in P_0(\mathcal{E})$ there exists a unique $q_{RT} \in RT_0(\mathcal{T})$ with $q_{RT}|_E \cdot \nu_E = t_0|_E$ on any $E \in \mathcal{E}$. In this sense, $RT_0(\mathcal{T}) \subseteq H(\mathrm{div}, \Omega)$ motivates the notation $\|t_0\|_{H^{-1/2}(\partial\mathcal{T})} := \|\gamma_\nu^{\mathcal{T}}(q_{RT})\|_{H^{-1/2}(\partial\mathcal{T})}$ for any $t_0 \in P_0(\mathcal{E})$ and the unique $q_{RT} \in RT_0(\mathcal{T})$ from above and [CGHW14, Lem. 3.2] proves $\|t_0\|_{H^{-1/2}(\partial\mathcal{T})} \approx \|q_{RT}\|_{H(\mathrm{div})}$. This isomorphy defines an embedding $P_0(\mathcal{E}) \hookrightarrow H^{-1/2}(\partial\mathcal{T})$, $t_0 \mapsto \gamma_\nu^{\mathcal{T}}(q_{RT})$ which justifies the notation $P_0(\mathcal{E}) \subset H^{-1/2}(\partial\mathcal{T})$.

Remark 2.22 (Short notation) For $v \in H^1(\mathcal{T})$ and $q \in H(\mathrm{div}, \mathcal{T})$, this thesis employs the short notation $\langle q \cdot \nu, v \rangle_{\partial\mathcal{T}} := \langle \gamma_\nu^{\mathcal{T}} q, \gamma_0^{\mathcal{T}} v \rangle_{\partial\mathcal{T}}$.

Remark 2.23 (Integration by parts) The local integration by parts from Theorem 2.19 proves that any $q_{\mathcal{T}} \in H(\mathrm{div}, \mathcal{T})$ and $v_{\mathcal{T}} \in H^1(\mathcal{T})$ satisfy

$$\langle q_{\mathcal{T}} \cdot \nu, v_{\mathcal{T}} \rangle_{\partial\mathcal{T}} = (\mathrm{div}_{NC}\, q_{\mathcal{T}}, v_{\mathcal{T}})_{L^2(\Omega)} + (q_{\mathcal{T}}, \nabla_{NC}\, v_{\mathcal{T}})_{L^2(\Omega)}. \tag{2.3}$$

2.6. Preliminaries and Tools

The following lemma contains standard properties of the L^2 projection from Definition 2.9. They follow directly from the defining property of Π_k and the nestedness of polynomial spaces, but are explicitly collected here without proof for consistency in display, because a more general operator in the context of reduced mixed methods in Subsection 3.3 assumes these properties.

Lemma 2.24 For any triangulation $\mathcal{T}$, refinement $\widehat{\mathcal{T}} \in \mathbb{T}(\mathcal{T})$, and $k \in \mathbb{N}_0$, the operators $\Pi_k : L^2(\Omega) \to P_k(\mathcal{T})$ and $\widehat{\Pi}_k : L^2(\Omega) \to P_k(\widehat{\mathcal{T}})$ from Definition 2.9 satisfy $\Pi_k = \Pi_k \circ \widehat{\Pi}_k = \widehat{\Pi}_k \circ \Pi_k$.□

It is well-known that Raviart-Thomas and Crouzeix-Raviart functions integrate by parts without boundary or interface terms.

Lemma 2.25 (Integration by parts of RT and CR) *Let $p_1 \in RT_0^{NC}(\mathcal{T})$, then $p_1 \in RT_0(\mathcal{T})$ if and only if*

$$(\Pi_0 p_1, \nabla_{NC}\, w_{CR})_{L^2(\Omega)} + (\mathrm{div}_{NC}\, p_1, \Pi_0 w_{CR})_{L^2(\Omega)} = 0 \quad \textit{for all } w_{CR} \in CR_0^1(\mathcal{T}).$$

Proof: The orthogonality of $1 - \Pi_0$ onto $P_0(\mathcal{T})$ in $L^2(\Omega)$, a piecewise integration by parts, and (2.1) on p. 14 imply that any $w_{CR} \in CR_0^1(\mathcal{T})$ satisfies

$$\begin{aligned}(\Pi_0 p_1, \nabla_{NC}\, w_{CR})_{L^2(\Omega)} + (\mathrm{div}_{NC}\, p_1, \Pi_0 w_{CR})_{L^2(\Omega)} &= (p_1, \nabla_{NC}\, w_{CR})_{L^2(\Omega)} + (\mathrm{div}_{NC}\, p_1, w_{CR})_{L^2(\Omega)} \\ &= \sum_{T \in \mathcal{T}} \int_{\partial T} w_{CR} p_1 \cdot \nu_T \,\mathrm{d}s = \sum_{E \in \mathcal{E}} \int_E [w_{CR} p_1]_E \cdot \nu_E \,\mathrm{d}s.\end{aligned}$$

The definition of the jump implies $[w_{CR} p_1]_E \cdot \nu_E = w_{CR}|_{T_+} [p_1]_E \cdot \nu_E + [w_{CR}]_E p_1|_{T_-} \cdot \nu_E$. The structure of the functions in $RT_0^{NC}(\mathcal{T})$ implies that $[p_1]_E \cdot \nu_E$ and $p_1|_{T_-} \cdot \nu_E$ are constant along $E \in \mathcal{E}$. Hence $\int_E [w_{CR}]_E \,\mathrm{d}s = 0$ implies

$$\sum_{E \in \mathcal{E}} \int_E [w_{CR} p_1]_E \cdot \nu_E \,\mathrm{d}s = \sum_{E \in \mathcal{E}} [p_1]_E \cdot \nu_E \int_E w_{CR}|_{T_+} \,\mathrm{d}s.$$

The equivalence of $p_1 \in H(\mathrm{div},\Omega)$ and $[p_1]_E \cdot \nu_E = 0$ [BBF13, p. 57] along $E \in \mathcal{E}$ concludes the proof. □

Lemma 2.26 (Invertibility of traces) *Given any $\Lambda \in P_1(\mathcal{T})^*$ with $CR_0^1(\mathcal{T}) \subseteq \ker \Lambda$, there exists a unique $t_0 \in P_0(\mathcal{E})$ such that $\langle t_0, \bullet \rangle_{\partial\mathcal{T}} = \Lambda$ in $P_1(\mathcal{T})$.*

Proof: Any $t_0 \in P_0(\mathcal{E})$ with unique extension $p_{RT} \in RT_0(\mathcal{T})$, $\gamma_\nu^{\mathcal{T}} p_{RT} = t_0$ from Remark 2.21 and $v_1 \in P_1(\mathcal{T})$ with $\Pi_0 v_1 = \mathrm{div}\, p_{RT}$ and $\nabla_{NC} v_1 = \Pi_0 p_{RT}$ satisfy

$$\begin{aligned}\|t_0\|_{H^{-1/2}(\partial\mathcal{T})} \le \|p_{RT}\|_{H(\mathrm{div})} &\approx (\|\Pi_0 p_{RT}\|_{L^2(\Omega)}^2 + \|\mathrm{div}\, p_{RT}\|_{L^2(\Omega)}^2)^{1/2} \\ &= \frac{(p_{RT}, \nabla_{NC} v_1)_{L^2(\Omega)} + (\mathrm{div}\, p_{RT}, v_1)_{L^2(\Omega)}}{(\|\Pi_0 v_1\|_{L^2(\Omega)}^2 + \|\nabla_{NC} v_1\|_{L^2(\Omega)}^2)^{1/2}}.\end{aligned}$$

The integration by parts (2.3) proves that the numerator equals $\langle t_0, v_1 \rangle_{\partial\mathcal{T}}$. Hence the continuous bilinear form $\langle \bullet, \bullet \rangle_{\partial\mathcal{T}} : P_0(\mathcal{E}) \times P_1(\mathcal{T}) \to \mathbb{R}$ satisfies an inf-sup condition

$$\|t_0\|_{H^{-1/2}(\partial\mathcal{T})} \lesssim \sup_{v_1 \in P_1(\mathcal{T}), v_1 \neq 0} \frac{\langle t_0, v_1 \rangle_{\partial\mathcal{T}}}{\|v_1\|_{H^1(\mathcal{T})}}.$$

Since $\{v_1 \in P_1(\mathcal{T}) | \langle s_0, v_1 \rangle_{\partial\mathcal{T}} = 0 \text{ for any } s_0 \in P_0(\mathcal{E})\} = CR_0^1(\mathcal{T})$, the application of the Lax-Milgram lemma [Bra07, Thm 3.6, p. 125] concludes the proof. □

2.7. Inequalities

This thesis utilizes several inequalities summarized in this subsection.

Theorem 2.27 (Cauchy inequality [BS08, (1.1.5)]) Any $f, g \in L^2(\Omega)$ satisfy

$$(f, g)_{L^2(\Omega)} \le \|f\|_{L^2(\Omega)} \|g\|_{L^2(\Omega)}.$$ □

Theorem 2.28 (Friedrichs inequality [Bra07, p. 31]) Any $v \in H_0^1(\Omega)$ and $c_{\mathrm{F}} = \mathrm{diam}(\Omega)/\pi$ satisfy

$$\|v\|_{L^2(\Omega)} \le c_{\mathrm{F}} \|\nabla v\|_{L^2(\Omega)}.$$ □

The discrete Friedrichs inequality [BS08, p. 301] is proven in [CH18a] with explicit constant that depends on a constant $c_{\mathrm{apx}}(J_1)$ introduced in Theorem 2.37 below.

Theorem 2.29 (Discrete Friedrichs inequality) Any $v_{CR} \in CR_0^1(\mathcal{T})$ and $c_{\mathrm{dF}} = h_{\max} c_{\mathrm{apx}}(J_1) + c_{\mathrm{F}}(1 + c_{\mathrm{inv}} c_{\mathrm{apx}}(J_1))$ satisfy

$$\|v_{CR}\|_{L^2(\Omega)} \le c_{\mathrm{dF}} \|\nabla_{NC} v_{CR}\|_{L^2(\Omega)}.$$ □

The following discrete Poincaré inequality from [CH18a] holds for the general nonconforming space $H^1_{NC}(\mathcal{T})$ with application to $CR^1_0(\mathcal{T}) \subseteq H^1_{NC}(\mathcal{T})$. In the case of a conforming function $v \in H^1(\Omega)$, the Poincaré constant in the subsequent theorem simplifies to $c_{\mathrm{dP}} = c_{\mathrm{P}} = 6^{-1/2}$ or for $n = 2$, to the optimal constant $c_{\mathrm{P}} = 1/j_{1,1}$ [LS10] with the first positive root $j_{1,1}$ of the Bessel function of the first kind.

Theorem 2.30 (Discrete Poincaré inequality) Any $\mathcal{T}$ and any refinement $\widehat{\mathcal{T}} \in \mathbb{T}(\mathcal{T})$, $K \in \mathcal{T}$, $v_{\widehat{\mathcal{T}}} \in H^1_{NC}(\widehat{\mathcal{T}}(K))$ and $c_{\mathrm{dP}} = (3/8)^{1/2}$ for $n = 2$, $c_{\mathrm{dP}} = 5^{1/2}/3$ for $n = 3$ satisfy

$$\|h_{\mathcal{T}}^{-1}(v_{\widehat{\mathcal{T}}} - \Pi_0 v_{\widehat{\mathcal{T}}})\|_{L^2(K)} \le c_{\mathrm{dP}} \|\nabla_{NC} v_{\widehat{\mathcal{T}}}\|_{L^2(K)}. \qquad \square$$

The inverse inequality is proven in [CH18a] with explicit constant $c_{\mathrm{inv}} = 24\cot(\omega_0)(2\cot(\omega_0) - \cot(2\omega_0) + ((2\cot(\omega_0) - \cot(2\omega_0))^2 - 3)^{1/2})$ for $k = 1$, $n = 2$, and the minimal interior angle ω_0 of the family of triangulations. It also holds for more general cases by a similar analysis of the eigenvalues of local mass and stiffness matrices.

Theorem 2.31 (Inverse inequality) *For any $k \in \mathbb{N}_0$ there exists $c_{\mathrm{inv}} = c_{\mathrm{inv}}(k) \approx 1$ such that any $v_k \in P_k(\mathcal{T})$ satisfies*

$$\|\nabla_{NC} v_k\|_{L^2(K)} \le c_{\mathrm{inv}} \|h_{\mathcal{T}}^{-1} v_k\|_{L^2(K)} \quad \text{for any } K \in \mathcal{T}.$$

A binomial formula proves the Young inequality.

Theorem 2.32 (Young inequality [Alt16, p. 53]) Any $a, b, \lambda > 0$ satisfy

$$ab \le \frac{1}{2\lambda} a^2 + \frac{\lambda}{2} b^2. \qquad \square$$

The following trace inequalities are well-known [DE12, p. 27-28] but are proven here for explicit gathering of constants in the spirit of [CH18a].

Lemma 2.33 (Trace inequality) *Let $T = \mathrm{conv}\{E, P\} \in \mathcal{T}$ an n-simplex with side $E \in \mathcal{E}(T)$ and opposite vertex $P \in \mathcal{N}(T)$. Then any $v_{\mathcal{T}} \in H_1(\mathcal{T})$ and $c_{\mathrm{tr}} := c_{\mathrm{sr}}^{1/2+1/(n-1)}$ satisfy*

$$\Big|\int_E v_{\mathcal{T}}|_T \,\mathrm{d}x\Big| \le c_{\mathrm{tr}} |E|^{n/(2n-2)} (\|h_{\mathcal{T}}^{-1} v_{\mathcal{T}}\|_{L^2(\omega_E)} + \|\nabla_{NC} v_{\mathcal{T}}\|_{L^2(\omega_E)}).$$

Proof: The trace identity [CH18a] proves

$$\int_E v_{\mathcal{T}}|_T \,\mathrm{d}x = |E|/|T| \Big(\int_T v_{\mathcal{T}} \,\mathrm{d}x + \frac{1}{n} \int_T (x - P) \cdot \nabla v_{\mathcal{T}} \,\mathrm{d}x \Big).$$

The Cauchy inequality plus $\|1\|_{L^2(T)} = |T|^{1/2}$, $\|\bullet - P\|_{L^2(T)} \le (n/(n+2))^{1/2} h_T |T|^{1/2}$ imply

$$\begin{aligned}\Big|\int_E v_{\mathcal{T}}|_T \,\mathrm{d}x\Big| &\le |E|/|T| (|T|^{1/2} \|v_{\mathcal{T}}\|_{L^2(T)} + |T|^{1/2} h_T \|\nabla v_{\mathcal{T}}\|_{L^2(T)} (n(n+2))^{-1/2}) \\ &\le |E|/|T|^{1/2} h_T (\|h_T^{-1} v_{\mathcal{T}}\|_{L^2(T)} + \|\nabla v_{\mathcal{T}}\|_{L^2(T)}).\end{aligned}$$

The shape regularity implies $|T|^{-1/2} \le c_{\mathrm{sr}}^{1/2} |E|^{-n/(2n-2)}$ and therefore

$$|E|/|T|^{1/2} h_T \le c_{\mathrm{sr}}^{1/2+1/(n-1)} |E|^{-n/(2n-2)} |E| |E|^{1/(n-1)}.$$

Since $-n/(2n-2) + 1 + 1/(n-1) = n/(2n-2)$, this concludes the proof. $\square$

Remark 2.34 (Discrete trace inequality) If $v \in P_k(\mathcal{T})$, an application of the inverse inequality in the proof of Lemma 2.33 leads to a discrete trace inequality with $c_{\mathrm{dtr}} := c_{\mathrm{sr}}^{1/2+1/(n-1)}(1 + c_{\mathrm{inv}}(n(n+2))^{-1/2})$ in

$$|\int_E v_k|_T \,\mathrm{d}x| \leq c_{\mathrm{dtr}}|E|^{n/(2n-2)}\|h_{\mathcal{T}}^{-1} v_k\|_{L^2(\omega_E)} \text{ for any } T \in \mathcal{T}, E \in \mathcal{E}(T). \qquad \square$$

2.8. Interpolation Operators

This subsection collects several interpolation operators and their properties from the literature. Given a triangulation $\mathcal{T}$ and its refinement $\widehat{\mathcal{T}} \in \mathbb{T}(\mathcal{T})$, the definition of $H^1_{NC}(\widehat{\mathcal{T}})$ from Def. 2.7 on p. 15 implies $\int_E [v_{\widehat{\mathcal{T}}}]_E \,\mathrm{d}s = 0$ along any coarse edge $E \in \mathcal{E}$. Hence, the subsequent interpolation operator, that generalizes nonconforming interpolation for conforming functions, is well-defined.

Definition 2.35 For $\mathcal{T}$ and its refinement $\widehat{\mathcal{T}} \in \mathbb{T}(\mathcal{T})$, define the nonconforming interpolation operator $I_{NC} : H^1_{NC}(\widehat{\mathcal{T}}) \to CR^1(\mathcal{T})$ for $v_{\widehat{\mathcal{T}}} \in H^1_{NC}(\widehat{\mathcal{T}})$ by

$$(I_{NC} v_{\widehat{\mathcal{T}}})(\mathrm{mid}(E)) = \fint_E v_{\widehat{\mathcal{T}}} \,\mathrm{d}s \quad \text{for any } E \in \mathcal{E}.$$

The following error estimate for the nonconforming interpolation operator is proven in [CH18a] on $CR^1_0(\widehat{\mathcal{T}})$, but the proofs for estimate and integral mean property hold verbatim for $H^1_{NC}(\widehat{\mathcal{T}})$.

Theorem 2.36 (Discrete nonconforming interpolation) Any $\mathcal{T}$ and any refinement $\widehat{\mathcal{T}} \in \mathbb{T}(\mathcal{T})$, $v_{\widehat{\mathcal{T}}} \in H^1_{NC}(\widehat{\mathcal{T}})$, and $\kappa^2_{NC} := c^2_{\mathrm{dP}} + (n+1)^{-1}(n+2)^{-1}n^{-2}$ satisfies

$$\Pi_0 \nabla_{NC} v_{\widehat{\mathcal{T}}} = \nabla_{NC} I_{NC} v_{\widehat{\mathcal{T}}} \quad \text{and} \tag{2.4}$$

$$\|h_{\mathcal{T}}^{-1}(v_{\widehat{\mathcal{T}}} - I_{NC} v_{\widehat{\mathcal{T}}})\|_{L^2(K)} \leq \kappa_{NC}\|\nabla_{NC}(v_{\widehat{\mathcal{T}}} - I_{NC} v_{\widehat{\mathcal{T}}})\|_{L^2(K)} \quad \text{for any } K \in \mathcal{T}. \tag{2.5}$$

Furthermore, (2.4) implies $\|\nabla_{NC}(v_{\widehat{\mathcal{T}}} - I_{NC} v_{\widehat{\mathcal{T}}})\|_{L^2(K)} \leq \min_{p_0 \in P_0(\mathcal{T};\mathbb{R}^n)} \|\nabla_{NC} v_{\widehat{\mathcal{T}}} - p_0\|_{L^2(K)}$ and the boundedness of I_{NC} in $|||\bullet|||_{NC}$ with constant 1. $\square$

[Gal14, Prop. 5.4] and its proof introduce conforming companion operators with integral mean and approximation properties. For $n = 2$, [CH18a, Thm. 4.5, Rem. 4.7, Lem. 4.8] calculates the constant $c_{\mathrm{apx}}(J_1)$ explicitly in terms of the minimal interior angle ω_0.

Theorem 2.37 (Conforming companions) For $k = 1, n, n+1$, there exist linear and bounded operators $J_k : CR^1_0(\mathcal{T}) \to S^k_0(\mathcal{T})$ and constants $c_{\mathrm{apx}}(J_k) \approx 1$ such that any $v_{CR} \in CR^1_0(\mathcal{T})$ satisfies

$$\nabla_{NC} v_{CR} = \Pi_0 \nabla J_k v_{CR},$$

$$\|h_{\mathcal{T}}^{-1}(v_{CR} - J_k v_{CR})\|_{L^2(\Omega)} + |||v_{CR} - J_k v_{CR}|||_{NC} \leq c_{\mathrm{apx}}(J_k) \min_{v \in H^1_0(\Omega)} |||v_{CR} - v|||_{NC}.$$

Furthermore, $v_{CR} = I_{NC} J_k v_{CR}$ for $k = n, n+1$, and $v_{CR} - J_{n+1} v_{CR}$ is orthogonal to $P_0(\mathcal{T})$ in $L^2(\Omega)$. $\square$

An explicit constant for an operator with the properties of the Scott-Zhang quasi-interpolator below in case $n = 2$ can be found in [CH18a, Rem. 5.2].

Theorem 2.38 (Discrete quasi-interpolation) For $\mathcal{T}$ and refinement $\widehat{\mathcal{T}} \in \mathbb{T}(\mathcal{T})$, there exists $J_{\mathrm{dQI}} : S^1_0(\widehat{\mathcal{T}}) \to S^1_0(\mathcal{T})$ such that any $\widehat{v}_C \in S^1_0(\widehat{\mathcal{T}})$ and $c_{\mathrm{dQI}} = (1+c_{\mathrm{inv}})(\kappa^2_{NC}+c_{\mathrm{apx}}(J_1)^2)^{1/2}$ satisfies

$$\begin{aligned}
\widehat{v}_C - J_{\mathrm{dQI}}\widehat{v}_C &= 0 \quad \text{on } \mathcal{T} \cap \widehat{\mathcal{T}},\\
\|h_{\mathcal{T}}^{-1}(\widehat{v}_C - J_{\mathrm{dQI}}\widehat{v}_C)\|_{L^2(T)} + \|\nabla(\widehat{v}_C - J_{\mathrm{dQI}}\widehat{v}_C)\|_{L^2(T)} &\le c_{\mathrm{dQI}}\|\nabla \widehat{v}_C\|_{L^2(\omega_T)} \quad \text{for any } T \in \mathcal{T},\\
\|h_{\mathcal{T}}^{-1}(\widehat{v}_C - J_{\mathrm{dQI}}\widehat{v}_C)\|_{L^2(\Omega)} + \|\nabla(\widehat{v}_C - J_{\mathrm{dQI}}\widehat{v}_C)\|_{L^2(\Omega)} &\le c_{\mathrm{dQI}}\|\nabla \widehat{v}_C\|_{L^2(\Omega)}.
\end{aligned}$$

□

The operator from [CGS13, Thm. 3.2] and its error estimate followed by a side-wise Poincaré inequality as pointed out in [CBJ02, (5.3)] and the equivalence $\operatorname{diam}(E) \approx |T|^{1/n}$ for any $T \in \mathcal{T}$ and $E \in \mathcal{E}(T)$ prove the following result needed for discrete reliability.

Theorem 2.39 (Discrete quasi-interpolation for CR) For $\mathcal{T}$ and refinement $\widehat{\mathcal{T}} \in \mathbb{T}(\mathcal{T})$, there exists $J_{\mathrm{dCR}} : CR^1_0(\mathcal{T}) \to CR^1_0(\widehat{\mathcal{T}})$ and $c_{\mathrm{dCR}} \approx 1$ such that any $v_{CR} \in CR^1_0(\mathcal{T})$ satisfies

$$\begin{aligned}
v_{CR} - J_{\mathrm{dCR}} v_{CR} &= 0 \quad \text{on } \mathcal{T} \cap \widehat{\mathcal{T}},\\
\|\nabla(v_{CR} - J_{\mathrm{dCR}} v_{CR})\|^2_{L^2(\Omega)} &\le c^2_{\mathrm{dCR}} \sum_{T \in \mathcal{T}\setminus\widehat{\mathcal{T}}} |T|^{1/n} \sum_{E \in \mathcal{E}(T)} \|[\nabla_{NC} v_{CR}]_E\|^2_{L^2(E)}.
\end{aligned}$$

□

3. A Priori Analysis of Reduced Mixed Methods

This section is devoted to a general error analysis of the reduced mixed methods introduced and analysed in [CH18b].

For a (local) orthogonal projection $Q : L^2(\Omega) \to L^2(\Omega)$ with properties as described in Subsection 3.3 below and a global parameter $0 \le \alpha \le 1$, the *reduced mixed system* for nonconforming and conforming P_1 finite element functions based on a triangulation $\mathcal{T}$ with the solution $(v_{CR}, u_C) \in CR^1_0(\mathcal{T}) \times S^1_0(\mathcal{T})$ reads

$$\begin{aligned} a_{NC}(v_{CR}+u_C, w_{CR}) + \alpha(Qv_{CR}, w_{CR})_{L^2(\Omega)} &= (f, Qw_{CR})_{L^2(\Omega)} \text{ for all } w_{CR} \in CR^1_0(\mathcal{T}), \\ a_{NC}(w_C, v_{CR}) &= 0 \qquad\qquad \text{for all } w_C \in S^1_0(\mathcal{T}). \end{aligned} \tag{R}$$

The suitable adaptive algorithm for this reduced mixed method is Algorithm 1 with collective marking and an error estimator, which is motivated in Subsection 3.2 below and reads, for $K \in \mathcal{T}$ and the solution $(v_{CR}, u_C) \in CR^1_0(\mathcal{T}) \times S^1_0(\mathcal{T})$ to (R), as

$$\eta^2(K) := |K|^{2/n} \|f - \alpha Q v_{CR}\|^2_{L^2(K)} + |K|^{1/n} \sum_{E \in \mathcal{E}(K)} \|[\nabla_{NC} v_{CR}]_E\|^2_{L^2(E)}. \tag{3.1}$$

3.1. A Priori Error Analysis

Let $Q : L^2(\Omega) \to L^2(\Omega)$ a bounded orthogonal projection.

Theorem 3.1 (A priori error estimate) *There exists a unique discrete solution* (v_{CR}, u_C) *to* (R). *This discrete and the exact solution* $u \in H^1_0(\Omega)$ *to* (1.3) *satisfy*

$$|||v_{CR}|||_{NC} + |||u - u_C||| \lesssim |||u - I_{NC}u|||_{NC} + \operatorname{osc}(f, \mathcal{T}) + \sup_{\substack{\psi_{CR} \in CR^1_0(\mathcal{T}) \\ |||\psi_{CR}|||_{NC}=1}} (f - Qf, \psi_{CR})_{L^2(\Omega)}.$$

Proof: The proof merely utilizes the boundedness of Q and is based on companion operators introduced in Theorem 2.37. The Brezzi splitting lemma [BBF13, Thm. 4.2.1; Bra07, pp.131–132] applied to elliptic bilinear forms $a_{NC} : S^1_0(\mathcal{T}) \times CR^1_0(\mathcal{T}) \to \mathbb{R}$ and $a_{NC} + \alpha(Q\bullet, \bullet)_{L^2(\Omega)} : CR^1_0(\mathcal{T}) \times CR^1_0(\mathcal{T}) \to \mathbb{R}$ shows that the composite bilinear form $B : X(\mathcal{T}) \times X(\mathcal{T}) \to \mathbb{R}$, defined for $(\varphi_{CR}, \varphi_C), (\psi_{CR}, \psi_C) \in X(\mathcal{T}) := CR^1_0(\mathcal{T}) \times S^1_0(\mathcal{T})$ by

$$B((\varphi_{CR}, \varphi_C), (\psi_{CR}, \psi_C)) := a_{NC}(\varphi_{CR} + \varphi_C, \psi_{CR}) + a_{NC}(\psi_C, \varphi_{CR}) + \alpha(Q\varphi_{CR}, \psi_{CR})_{L^2(\Omega)},$$

satisfies an inf-sup condition

$$1 \lesssim \beta \le \inf_{\substack{(\varphi_{CR}, \varphi_C) \in X(\mathcal{T}) \\ |||\varphi_{CR}|||^2_{NC} + |||\varphi_C|||^2 = 1}} \sup_{\substack{(\psi_{CR}, \psi_C) \in X(\mathcal{T}) \\ |||\psi_{CR}|||^2_{NC} + |||\psi_C|||^2 = 1}} B((\varphi_{CR}, \varphi_C), (\psi_{CR}, \psi_C)).$$

In particular, the reduced system (R) has a unique solution $(v_{CR}, u_C) \in X(\mathcal{T})$. In order to prove the claimed estimate, consider the best-approximation $Gu \in S^1_0(\mathcal{T})$ to u from Definition 2.8 and $(\varphi_{CR}, \varphi_C) := (I_{NC}u - Gu - v_{CR}, Gu - u_C) \in X(\mathcal{T})$. The inf-sup condition for B leads to some $(\psi_{CR}, \psi_C) \in X(\mathcal{T})$ with $|||\psi_{CR}|||^2_{NC} + |||\psi_C|||^2 = 1$ and

$$\begin{aligned}\beta(|||I_{NC}u - Gu - v_{CR}|||^2_{NC} + |||Gu - u_C|||^2)^{1/2} \\ \leq B((I_{NC}u - Gu - v_{CR}, Gu - u_C), (\psi_{CR}, \psi_C)).\end{aligned} \tag{3.2}$$

System (R), $\Pi_0 \nabla u = \nabla_{NC} I_{NC} u$ from Theorem 2.36, and the definition of G show that the right-hand side equals

$$\begin{aligned}&a_{NC}(I_{NC}u - v_{CR} - u_C, \psi_{CR}) + a_{NC}(\psi_C, I_{NC}u - Gu - v_{CR}) \\ &\qquad + \alpha(Q(I_{NC}u - Gu - v_{CR}), \psi_{CR})_{L^2(\Omega)} \\ &= a_{NC}(I_{NC}u, \psi_{CR}) + a_{NC}(\psi_C, I_{NC}u - Gu) \\ &\qquad + \alpha(Q(I_{NC}u - Gu), \psi_{CR})_{L^2(\Omega)} - (Qf, \psi_{CR})_{L^2(\Omega)} \\ &= a_{NC}(u, \psi_{CR}) - (f, \psi_{CR})_{L^2(\Omega)} + \alpha(Q(I_{NC}u - Gu), \psi_{CR})_{L^2(\Omega)} \\ &\qquad + (f - Qf, \psi_{CR})_{L^2(\Omega)}.\end{aligned} \tag{3.3}$$

Recall J_{n+1} from Theorem 2.37 and observe that $I_{NC}J_{n+1}\psi_{CR} = \psi_{CR}$ and $\Pi_0 \nabla u = \nabla_{NC} I_{NC} u$ imply $a_{NC}(u, \psi_{CR}) = a_{NC}(u, I_{NC}J_{n+1}\psi_{CR}) = a_{NC}(I_{NC}u, J_{n+1}\psi_{CR})$. This, the weak formulation (1.3) for u with test function $J_{n+1}\psi_{CR}$, and $a_{NC}(u - I_{NC}u, \psi_{CR}) = 0$ prove

$$a_{NC}(u - I_{NC}u, \psi_{CR} - J_{n+1}\psi_{CR}) + (f, J_{n+1}\psi_{CR})_{L^2(\Omega)} = a_{NC}(u, \psi_{CR}).$$

Hence, $(\Pi_0 f, J_{n+1}\psi_{CR} - \psi_{CR})_{L^2(\Omega)} = 0$ and the stability of J_{n+1} from Theorem 2.37 imply

$$\begin{aligned}a_{NC}(u, \psi_{CR}) - (f, \psi_{CR})_{L^2(\Omega)} &= a_{NC}(u - I_{NC}u, (1 - J_{n+1})\psi_{CR}) - ((1 - \Pi_0)f, (1 - J_{n+1})\psi_{CR})_{L^2(\Omega)} \\ &\lesssim |||u - I_{NC}u|||_{NC} + \operatorname{osc}(f, \mathcal{T}).\end{aligned} \tag{3.4}$$

The discrete Friedrichs inequality from Theorem 2.29, $\alpha \leq 1$, the boundedness of Q in L^2, and $|||\psi_{CR}|||^2_{NC} \leq 1$ prove $\alpha(Q(I_{NC}u - Gu), \psi_{CR})_{L^2(\Omega)} \lesssim |||I_{NC}u - Gu|||_{NC}$. This, a triangle inequality, and the combination of (3.2)-(3.4) prove

$$\begin{aligned}|||v_{CR}|||_{NC} + |||u - u_C||| &\leq |||I_{NC}u - Gu - v_{CR}|||_{NC} + |||Gu - u_C||| + |||I_{NC}u - Gu|||_{NC} \\ &\qquad + |||u - Gu||| \\ &\lesssim |||u - I_{NC}u|||_{NC} + |||I_{NC}u - Gu|||_{NC} + |||u - Gu||| \\ &\qquad + \operatorname{osc}(f, \mathcal{T}) + (f - Qf, \psi_{CR})_{L^2(\Omega)}.\end{aligned}$$

For $J_1 I_{NC}$ with the operator J_1 from Theorem 2.37, Pythagoras' theorem shows $|||I_{NC}u - J_1 I_{NC}u|||^2_{NC} = |||I_{NC}u - Gu|||^2_{NC} + |||Gu - J_1 I_{NC}u|||^2_{NC}$ and therefore

$$|||I_{NC}u - Gu|||_{NC} \leq |||(1 - J_1)I_{NC}u|||_{NC} \lesssim \min_{v \in H^1_0(\Omega)} |||I_{NC}u - v|||_{NC} \leq |||u - I_{NC}u|||_{NC}.$$

The combination of the previous two displayed estimates and a triangle inequality concludes the proof. □

3.2. Global Error Control of the Residual

The following equivalence holds on a global level and is the main ingredient for the reliability of the alternative error estimators for both the reduced methods of this section in Corollary 3.3 as well as for the weighted least-squares methods in Lemma 6.7 of Section 6. Although this estimate holds for both the normal and the tangential components of the jumps separately, the proof of discrete reliability in Theorem 5.5 below needs both components, which is also observed for least-squares methods in [CP15, Thm. 3.1, Thm. 5.1]

Lemma 3.2 *Any $w_{CR} \in CR^1_0(\mathcal{T})$ with the L^2 orthogonality $\nabla_{NC} w_{CR} \perp \nabla S^1_0(\mathcal{T})$ satisfies*

$$\begin{aligned}|||w_{CR}|||^2_{NC} &\approx \sum_{T\in\mathcal{T}} |T|^{1/n} \sum_{E\in\mathcal{E}(T)} \|[\nabla_{NC} w_{CR}]_E \cdot \nu_E\|^2_{L^2(E)} \\ &\approx \sum_{T\in\mathcal{T}} |T|^{1/n} \sum_{E\in\mathcal{E}(T)} \|[\nabla_{NC} w_{CR}]_E \cdot \tau_E\|^2_{L^2(E)}.\end{aligned}$$

Proof: The assumed orthogonality, a piecewise integration by parts, and (2.1) on p. 14 prove that any $w_C \in S^1_0(\mathcal{T})$ satisfies

$$|||w_{CR}|||^2_{NC} = \int_\Omega \nabla_{NC} w_{CR} \cdot \nabla_{NC}(w_{CR} - w_C)\,\mathrm{d}x = \sum_{E\in\mathcal{E}} \int_E [\nabla_{NC} w_{CR}(w_{CR} - w_C)]_E \cdot \nu_E \,\mathrm{d}s.$$

For $w_{CR} \in CR^1_0(\mathcal{T})$ and side $E \in \mathcal{E}(\Omega)$, $\fint_E [w_{CR} - w_C]_E \,\mathrm{d}s = 0$ implies that the integral mean $\fint_E (w_{CR} - w_C)\,\mathrm{d}s$ along E is unique. This and a calculation with the jumps as in the proof of Lemma 2.25 prove

$$|||w_{CR}|||^2_{NC} = \sum_{E\in\mathcal{E}} [\nabla_{NC} w_{CR}]_E \cdot \nu_E \int_E (w_{CR} - w_C)\,\mathrm{d}s.$$

The discrete trace inequality from Remark 2.34 on $E \in \mathcal{E}(\Omega)$ proves

$$\Big|\int_E (w_{CR} - w_C)\,\mathrm{d}s\Big| \le c_{\mathrm{dtr}} |E|^{n/(2n-2)} \|h_{\mathcal{T}}^{-1}(w_{CR} - w_C)\|_{L^2(\omega_E)}.$$

The sum of all such terms for E over $\mathcal{E}(\Omega)$, the Cauchy inequality in $\mathbb{R}^{|\mathcal{E}(\Omega)|}$, and the finite overlap of $(\omega_E)_{E\in\mathcal{E}(\Omega)}$ leads to

$$|||w_{CR}|||^2_{NC} \le (n+1)^{1/2} c_{\mathrm{tr}} \Big(\sum_{E\in\mathcal{E}(\Omega)} |E|^{1/(n-1)} \|[\nabla_{NC} w_{CR}]_E \cdot \nu_E\|^2_{L^2(E)} \Big)^{1/2} \|h_{\mathcal{T}}^{-1}(w_{CR} - w_C)\|_{L^2(\Omega)}.$$

The choice $w_C = J_1 w_{CR}$ as a conforming companion from Theorem 2.37 leads to the estimate $\|h_{\mathcal{T}}^{-1}(w_{CR} - w_C)\|_{L^2(\Omega)} \le c_{\mathrm{apx}}(J_1)|||w_{CR}|||_{NC}$. This and the shape regularity $|E|^{1/(n-1)} \le c_{\mathrm{sr}}^{1/n} |T|^{1/n}$ for any $T \in \mathcal{T}$ and $E \in \mathcal{E}(T)$ conclude the proof of the first inequality $\lesssim$ in the lemma.

The Cauchy inequality with $|\nu_E| = 1$ and the discrete jump control of [CR17, Lem. 5.2] with constant $c_{\mathrm{jc}} \approx 1$ result in the reverse estimate

$$\sum_{T\in\mathcal{T}} |T|^{1/n} \sum_{E\in\mathcal{E}(T)} \|[\nabla_{NC} w_{CR}]_E \cdot \nu_E\|^2_{L^2(E)} \le c_{\mathrm{jc}}^2 |||w_{CR}|||^2_{NC}.$$

The second equivalence utilizes $|||w_{CR}|||_{NC} = \min_{w_C \in S^1_0(\mathcal{T})} |||w_{CR} - w_C|||_{NC}$ as a consequence of the assumed orthogonality. This and the shape regularity conclude the proof together with the equivalence in [CEHL12, Thm. 5.1] (and an analogous statement for $n > 2$), which reads

$$\min_{w_C \in S^1_0(\mathcal{T})} |||w_{CR} - w_C|||^2_{NC} \approx \sum_{E \in \mathcal{E}} |E|^{1/(n-1)} \|[\nabla_{NC} w_{CR}]_E \cdot \tau_E\|^2_{L^2(E)}. \qquad \square$$

The subsequent consequence of Lemma 3.2 follows from the second equation of (R) and is required below.

Corollary 3.3 There exist $c_{\mathrm{rel}}, c_{\mathrm{eff}} \approx 1$ such that the solution $(v_{CR}, u_C) \in CR^1_0(\mathcal{T}) \times S^1_0(\mathcal{T})$ to (R) satisfies

$$c^{-1}_{\mathrm{rel}} |||v_{CR}|||^2_{NC} \leq \sum_{T \in \mathcal{T}} |T|^{1/n} \sum_{E \in \mathcal{E}(T)} \|[\nabla_{NC} v_{CR}]_E\|^2_{L^2(E)} \leq c_{\mathrm{eff}} |||v_{CR}|||^2_{NC}. \qquad \square$$

3.3. Conditions on Q

The projection operator $Q := Q_{\mathcal{T}}$ in (R) is defined abstractly through local projections with two additional assumptions on the nestedness with respect to refinement and an approximation estimate. These assumptions on Q are designed as general as possible with regard to the proof of optimal convergence rates of the reduced method. They allow for the specific examples $Q = \mathrm{id}$ and $Q = \Pi_0$ from the dPG methods of Section 4 below. Recall the set of all admissible simplices $\bigcup \mathbb{T}$, i.e., $K \in \bigcup \mathbb{T}$ iff $K \in \mathcal{T}$ for some $\mathcal{T} \in \mathbb{T}$, and $\widehat{\mathcal{T}}(K)$ for $K \in \mathcal{T}$ and $\widehat{\mathcal{T}} \in \mathbb{T}(\mathcal{T})$ from Def. 2.12 on p. 16.

Local projections. For each $K \in \bigcup \mathbb{T}$, let $Q_K : L^2(K) \to L^2(K)$ be an orthogonal projection, i.e., Q_K is linear and bounded and any $v, w \in L^2(K)$ satisfy $((1 - Q_K)v, Q_K w)_{L^2(K)} = 0$. Then given any $\mathcal{T} \in \mathbb{T}$, construct $Q := Q_{\mathcal{T}} : L^2(\Omega) \to L^2(\Omega)$ on $K \in \mathcal{T}$ by

$$(Q_{\mathcal{T}} v)|_K := Q_K(v|_K) \quad \text{a.e. in } K \text{ for all } v \in L^2(\Omega).$$

Nestedness. Suppose that the family of operators $(Q_T \mid T \in \bigcup \mathbb{T})$ is nested as defined in the following. Given any $\mathcal{T} \in \mathbb{T}$ and any refinement $\widehat{\mathcal{T}} \in \mathbb{T}(\mathcal{T})$, suppose that $Q_{\widehat{\mathcal{T}}} Q_{\mathcal{T}} = Q_{\mathcal{T}}$ in the sense that for any $K \in \mathcal{T}$ and $T \in \widehat{\mathcal{T}}(K)$, it holds

$$Q_T((Q_K v)|_T) = Q_K v \quad \text{a.e. in } T \text{ for all } v \in L^2(K).$$

Approximation. Suppose that there exists $c_{\mathrm{Q}} \approx 1$ such that given $\mathcal{T} \in \mathbb{T}$, a refinement $\widehat{\mathcal{T}} \in \mathbb{T}(\mathcal{T})$, and $K \in \mathcal{T}$, any $\widehat{w}_{CR} \in CR^1(\widehat{\mathcal{T}}(K))$ satisfies

$$\|(1 - Q_{\mathcal{T}})\widehat{w}_{CR}\|_{L^2(K)} \leq c_{\mathrm{Q}} h_K \|\nabla_{NC} \widehat{w}_{CR}\|_{L^2(K)}. \tag{3.5}$$

Example 3.4 The aforementioned assumptions permit to write and analyse all the cases of Q and α for the dPG methods from Table 4 on p. 36 simultaneously. For several of these examples, $Q_{\mathcal{T}} = \mathrm{id}$ and the above assumptions are trivial with $c_{\mathrm{Q}} = 0$. For the other examples, $Q = \Pi_0$ (understood with respect to $\mathcal{T} \in \mathbb{T}$) and the local projection and nestedness properties follows from Definition 2.9 and Lemma 2.24. The discrete Poincaré inequality from Theorem 2.30 leads to (3.5) with $c_{\mathrm{Q}} = c_{\mathrm{dP}}$ in this notation.

Although not utilized for the dPG methods, $Q = \Pi_k$ also satisfies the assumptions above.

The analysis below frequently employs a few properties guaranteed by the aforementioned assumptions.

Lemma 3.5 (Properties of Q) *The operators $Q := Q_{\mathcal{T}}$ and $\widehat{Q} := Q_{\widehat{\mathcal{T}}}$ for $\mathcal{T} \in \mathbb{T}$ and $\widehat{\mathcal{T}} \in \mathbb{T}(\mathcal{T})$ with $\Omega' := \operatorname{int}\big(\bigcup(\mathcal{T} \setminus \widehat{\mathcal{T}})\big)$ satisfy, for any $v, w \in L^2(\Omega)$ and $K \in \mathcal{T}$*

$$\|Qv\|_{L^2(\Omega)} \leq \|v\|_{L^2(\Omega)}, \tag{3.6}$$

$$(Qv, w)_{L^2(K)} = (Qv, Qw)_{L^2(K)} = (v, Qw)_{L^2(K)}, \tag{3.7}$$

$$(Qv, (1-Q)w)_{L^2(K)} = (Qv, (1-\widehat{Q})w)_{L^2(K)} = (Qv, (Q-\widehat{Q})w)_{L^2(K)} = 0, \tag{3.8}$$

$$(\widehat{Q} - Q)v = 0 \text{ on any } T \in \mathcal{T} \cap \widehat{\mathcal{T}}, \tag{3.9}$$

$$\|(1-Q)v\|^2_{L^2(K)} + \|Q(v-w)\|^2_{L^2(K)} = \|v - Qw\|^2_{L^2(K)}, \tag{3.10}$$

$$\|(1-\widehat{Q})v\|^2_{L^2(K)} + \|\widehat{Q}v - Qw\|^2_{L^2(K)} = \|v - Qw\|^2_{L^2(K)}, \tag{3.11}$$

$$\|(\widehat{Q}-Q)v\|^2_{L^2(K)} + \|Q(v-w)\|^2_{L^2(K)} = \|\widehat{Q}v - Qw\|^2_{L^2(K)}. \tag{3.12}$$

Furthermore, any $\widehat{w}_{CR} \in CR^1(\widehat{\mathcal{T}}(K))$ satisfies

$$\|(\widehat{Q}-Q)\widehat{w}_{CR}\|_{L^2(K)} \leq c_{\mathrm{Q}} h_K \|\nabla_{NC}\widehat{w}_{CR}\|_{L^2(K)}. \tag{3.13}$$

Proof: The projection property $((1-Q)v, Qw)_{L^2(K)} = 0$ shows (3.6)-(3.7). The nestedness of $\widehat{Q}$, Q, and (3.7) prove $(Qv, \widehat{Q}w)_{L^2(K)} = (v, Q\widehat{Q}w)_{L^2(K)} = (Qv, Qw)_{L^2(K)}$ and therefore the orthogonalities (3.8). The local definition of Q and $\widehat{Q}$ implies (3.9) and the Pythagoras theorem with the orthogonalities (3.8) prove (3.10)-(3.12). The choice $v = w = \widehat{w}_{CR}$ in (3.11) leads to $\|(\widehat{Q}-Q)\widehat{w}_{CR}\|_{L^2(K)} \leq \|(1-Q)\widehat{w}_{CR}\|_{L^2(K)}$ and therefore, (3.5) concludes the proof of (3.13). □

The above properties of the local nested projection Q provide the following lemma.

Lemma 3.6 *Any sequence of successive refinements $(\mathcal{T}_k)_{k\in\mathbb{N}}$, i.e., $\mathcal{T}_{k+1} \in \mathbb{T}(\mathcal{T}_k)$ for $k \in \mathbb{N}$, any $\ell, m \in \mathbb{N}$, $K \in \mathcal{T}_\ell$, and $f \in L^2(K)$ satisfy*

$$\sum_{k=\ell}^{\ell+m} \|H_{\mathcal{T}_k}(Q_{\mathcal{T}_{k+1}}f - Q_{\mathcal{T}_k}f)\|^2_{L^2(K)} \leq \|H_{\mathcal{T}_\ell}(f - Q_{\mathcal{T}_\ell}f)\|^2_{L^2(K)}.$$

Proof: The Pythagoras theorem (3.11) for $v = w = H_{\mathcal{T}_k} f$, the local linearity of $Q_{\mathcal{T}_k}, Q_{\mathcal{T}_{k+1}}$, and the pointwise estimate $H_{\mathcal{T}_{k+1}} \le H_{\mathcal{T}_k}$ in K prove

$$\begin{aligned}\|H_{\mathcal{T}_k}(Q_{\mathcal{T}_{k+1}} f - Q_{\mathcal{T}_k} f)\|^2_{L^2(K)} &= \|H_{\mathcal{T}_k}(f - Q_{\mathcal{T}_k} f)\|^2_{L^2(K)} - \|H_{\mathcal{T}_k}(f - Q_{\mathcal{T}_{k+1}} f)\|^2_{L^2(K)} \\ &\le \|H_{\mathcal{T}_k}(f - Q_{\mathcal{T}_k} f)\|^2_{L^2(K)} - \|H_{\mathcal{T}_{k+1}}(f - Q_{\mathcal{T}_{k+1}} f)\|^2_{L^2(K)}.\end{aligned}$$

Hence, a telescoping sum shows

$$\sum_{k=\ell}^{\ell+m} \|H_{\mathcal{T}_k}(Q_{\mathcal{T}_{k+1}} f - Q_{\mathcal{T}_k} f)\|^2_{L^2(K)} \le \|H_{\mathcal{T}_\ell}(f - Q_{\mathcal{T}_\ell} f)\|^2_{L^2(K)} - \|H_{\mathcal{T}_{\ell+m+1}}(f - Q_{\mathcal{T}_{\ell+m+1}} f)\|^2_{L^2(K)}. \quad \square$$

3.4. Total Error

Throughout this section, consider the notation of Table 3, i.e., a triangulation $\mathcal{T} \in \mathbb{T}$ and a refinement $\widehat{\mathcal{T}} \in \mathbb{T}(\mathcal{T})$, $Q := Q_{\mathcal{T}}$ and $\widehat{Q} := Q_{\widehat{\mathcal{T}}}$, and discrete solutions $(v_{CR}, u_C) \in CR^1_0(\mathcal{T}) \times S^1_0(\mathcal{T})$ to (R) with respect to $\mathcal{T}$ and $(\widehat{v}_{CR}, \widehat{u}_C) \in CR^1_0(\widehat{\mathcal{T}}) \times S^1_0(\widehat{\mathcal{T}})$ to (R̂) with respect to $\widehat{\mathcal{T}}$,

$$\begin{aligned} a_{NC}(\widehat{v}_{CR} + \widehat{u}_C, \widehat{w}_{CR}) + \alpha(\widehat{Q}\widehat{v}_{CR}, \widehat{w}_{CR})_{L^2(\Omega)} &= (f, \widehat{Q}\widehat{w}_{CR})_{L^2(\Omega)} \text{ for all } \widehat{w}_{CR} \in CR^1_0(\widehat{\mathcal{T}}), \\ a_{NC}(\widehat{w}_C, \widehat{v}_{CR}) &= 0 \qquad\qquad\quad \text{for all } \widehat{w}_C \in S^1_0(\widehat{\mathcal{T}}). \end{aligned} \tag{R̂}$$

Recall the unrefined simplices $\mathcal{T} \setminus \widehat{\mathcal{T}}$, the domain of unrefined simplices $\Omega' = \operatorname{int}\big(\bigcup(\mathcal{T} \setminus \widehat{\mathcal{T}})\big)$ and the neighborhood $\mathcal{R} := \{K \in \mathcal{T} : \exists T \in \mathcal{T} \setminus \widehat{\mathcal{T}}, \operatorname{dist}(K, T) = 0\}$, which consists of $\mathcal{T} \setminus \widehat{\mathcal{T}}$ and one neighboring layer, i.e., all simplices that share at least one node with a simplex in $\mathcal{T} \setminus \widehat{\mathcal{T}}$. In particular, $|\mathcal{R}| \lesssim |\mathcal{T} \setminus \widehat{\mathcal{T}}|$ in terms of the counting measure $|\bullet|$, i.e., the cardinality of the finite sets.

The distance function $\delta := \delta(\mathcal{T}, \widehat{\mathcal{T}})$ is defined as the square root of

$$\delta^2 := \delta^2(\mathcal{T}, \widehat{\mathcal{T}}) := (\delta(\mathcal{T}, \widehat{\mathcal{T}}))^2 = |||\widehat{v}_{CR} - v_{CR}|||^2_{NC} + \alpha\|\widehat{Q}\widehat{v}_{CR} - Qv_{CR}\|^2_{L^2(\Omega)}. \tag{3.14}$$

Neither the error estimator η nor the distance function $\delta = \delta(\mathcal{T}, \widehat{\mathcal{T}})$ include the conforming component $u_C \in S^1_0(\mathcal{T})$ of the solution (v_{CR}, u_C) to (R). Nevertheless, the error estimator η is eventually reliable for the total error $\delta + |||\widehat{u}_C - u_C|||$.

The proof of the error estimate of this section is based on the subsequent observation, which relies on a standard argument of a posteriori error control [NSV09].

Lemma 3.7 *It holds* $a_{NC}(v_{CR}, \widehat{u}_C) \lesssim \eta(\mathcal{R})|||\widehat{u}_C - u_C|||$.

$\mathcal{T}$	$\widehat{\mathcal{T}} \in \mathbb{T}(\mathcal{T})$
(v_{CR}, u_C) solves (R)	$(\widehat{v}_{CR}, \widehat{u}_C)$ solves (R̂)
$Q := Q_{\mathcal{T}}$	$\widehat{Q} := Q_{\widehat{\mathcal{T}}}$
$\eta(K) := \eta(\mathcal{T}, K), K \in \mathcal{T}$ from (3.1)	$\widehat{\eta}(T) := \eta(\widehat{\mathcal{T}}, T), T \in \widehat{\mathcal{T}}$
$h_{\mathcal{T}}, H_{\mathcal{T}}$ mesh-size	$h_{\widehat{\mathcal{T}}}, H_{\widehat{\mathcal{T}}}$ mesh-size
$\delta^2 := \delta^2(\mathcal{T}, \widehat{\mathcal{T}}) := \|\|\|\widehat{v}_{CR} - v_{CR}\|\|\|_{NC}^2 + \alpha \|\widehat{Q}\widehat{v}_{CR} - Q v_{CR}\|_{L^2(\Omega)}^2$ from (3.14)	
$\mathcal{R} := \{K \in \mathcal{T} : \exists T \in \mathcal{T} \setminus \widehat{\mathcal{T}}, \operatorname{dist}(K, T) = 0\}$	
$\Omega' := \operatorname{int}\big(\bigcup(\mathcal{T} \setminus \widehat{\mathcal{T}})\big)$	

Table 3: Standard notation for $\mathcal{T}$ and its refinement $\widehat{\mathcal{T}} \in \mathbb{T}(\mathcal{T})$ for reduced mixed method

Proof: Consider the Scott-Zhang quasi-interpolation $J_{\mathrm{dQI}}\widehat{v}_C \in S^1_0(\mathcal{T})$ of $\widehat{v}_C \in S^1_0(\widehat{\mathcal{T}})$ from Theorem 2.38 and observe that the second equation of (R) implies $a_{NC}(v_{CR}, J_{\mathrm{dQI}}\widehat{u}_C) = 0$. Hence, a piecewise integration by parts and $\widehat{u}_C - J_{\mathrm{dQI}}\widehat{u}_C = 0$ on $T \in \mathcal{T} \cap \widehat{\mathcal{T}}$ lead to

$$a_{NC}(v_{CR}, \widehat{u}_C) = a_{NC}(v_{CR}, \widehat{u}_C - J_{\mathrm{dQI}}\widehat{u}_C) = \sum_{T \in \mathcal{T} \setminus \widehat{\mathcal{T}}} \int_{\partial T} (\widehat{u}_C - J_{\mathrm{dQI}}\widehat{u}_C) \nabla_{NC} v_{CR} \cdot \nu_T \, \mathrm{d}s.$$

Since $\widehat{u}_C - J_{\mathrm{dQI}}\widehat{u}_C = 0$ along any $E = \partial T_+ \cap \partial T_- \in \mathcal{E}(\Omega)$ with $T_+ \in \mathcal{T} \cap \widehat{\mathcal{T}}$ or $T_- \in \mathcal{T} \cap \widehat{\mathcal{T}}$, i.e., $\widehat{u}_C - J_{\mathrm{dQI}}\widehat{u}_C = 0$ on $\partial\Omega'$, the argumentation (2.1) on p. 14 on $\mathcal{E}(\mathcal{T} \setminus \widehat{\mathcal{T}}) = \bigcup_{T \in \mathcal{T} \setminus \widehat{\mathcal{T}}} \mathcal{E}(T)$ implies

$$a_{NC}(v_{CR}, \widehat{u}_C) = \sum_{E \in \mathcal{E}(\mathcal{T} \setminus \widehat{\mathcal{T}})} \int_E (\widehat{u}_C - J_{\mathrm{dQI}}\widehat{u}_C) [\nabla_{NC} v_{CR}]_E \cdot \nu_E \, \mathrm{d}s.$$

Similar to the proof of Lemma 3.2, the discrete trace inequality, the estimate $|E|^{1/(n-1)} \leq c_{\mathrm{sr}}^{1/n} |T|^{1/n}$ for any $T \in \mathcal{T}$ and $E \in \mathcal{E}(T)$, and the finite overlap of $(\omega_E)_{E \in \mathcal{E}(\mathcal{T} \setminus \widehat{\mathcal{T}})}$ prove that

$$a_{NC}(v_{CR}, \widehat{u}_C) \leq (n+1)^{1/2} c_{\mathrm{dtr}} c_{\mathrm{sr}}^{1/n} \eta(\mathcal{T} \setminus \widehat{\mathcal{T}}) \| h_{\mathcal{T}}^{-1} (\widehat{u}_C - J_{\mathrm{dQI}}\widehat{u}_C) \|_{L^2(\Omega)}.$$

Since $u_C = J_{\mathrm{dQI}} u_C$ on Ω, the approximation property from Theorem 2.38 in $\| h_{\mathcal{T}}^{-1} (\widehat{u}_C - J_{\mathrm{dQI}}\widehat{u}_C) \|_{L^2(\Omega)} = \| h_{\mathcal{T}}^{-1} ((\widehat{u}_C - u_C) - J_{\mathrm{dQI}}(\widehat{u}_C - u_C)) \|_{L^2(\Omega)} \leq c_{\mathrm{dQI}} |\|\widehat{u}_C - u_C\|\|$ concludes the proof.□

Proposition 3.8 *It holds* $|\|\widehat{u}_C - u_C\|\| \lesssim \delta + \eta(\mathcal{R})$.

Proof: For $w_{CR} := u_C - I_{NC}\widehat{u}_C \in CR^1_0(\mathcal{T})$, the second equation of the discrete problem (R) shows $a_{NC}(v_{CR}, w_{CR}) = -a_{NC}(v_{CR}, I_{NC}\widehat{u}_C)$. Consequently, (2.4) in Theorem 2.36 proves $a_{NC}(v_{CR} + u_C, w_{CR}) = -a_{NC}(v_{CR}, \widehat{u}_C) + a_{NC}(u_C, u_C - \widehat{u}_C)$. This, the projection property (3.7) of Q, and the first equality of (R) with test function $w_{CR} \in CR^1_0(\mathcal{T})$ prove

$$a_{NC}(u_C, u_C - \widehat{u}_C) = (Q(f - \alpha v_{CR}), w_{CR})_{L^2(\Omega)} + a_{NC}(v_{CR}, \widehat{u}_C).$$

The discrete problem (R̂) with the test function $\widehat{u}_C - u_C \in S^1_0(\widehat{\mathcal{T}}) \subset CR^1_0(\widehat{\mathcal{T}})$ in both equations leads to

$$a_{NC}(\widehat{u}_C, \widehat{u}_C - u_C) = (\widehat{Q}f, \widehat{u}_C - u_C)_{L^2(\Omega)} - \alpha(\widehat{Q}\widehat{v}_{CR}, \widehat{u}_C - u_C)_{L^2(\Omega)}.$$

With $\widehat{u}_C - I_{NC}\widehat{u}_C = 0$ on $\Omega \setminus \Omega'$, the sum of these two identities is equal to

$$\begin{aligned}
|||\widehat{u}_C - u_C|||^2 &= (Q(f - \alpha v_{CR}), \widehat{u}_C - I_{NC}\widehat{u}_C)_{L^2(\Omega)} - (Q(f - \alpha v_{CR}), \widehat{u}_C - u_C)_{L^2(\Omega)} \\
&\quad + a_{NC}(v_{CR}, \widehat{u}_C) + (\widehat{Q}f, \widehat{u}_C - u_C)_{L^2(\Omega)} - \alpha(\widehat{Q}\widehat{v}_{CR}, \widehat{u}_C - u_C)_{L^2(\Omega)} \\
&= (Q(f - \alpha v_{CR}), \widehat{u}_C - I_{NC}\widehat{u}_C)_{L^2(\Omega')} + ((\widehat{Q} - Q)f, \widehat{u}_C - u_C)_{L^2(\Omega)} \\
&\quad + a_{NC}(v_{CR}, \widehat{u}_C) - \alpha(\widehat{Q}\widehat{v}_{CR} - Qv_{CR}, \widehat{u}_C - u_C)_{L^2(\Omega)}. \qquad (3.15)
\end{aligned}$$

Since Theorem 2.36 shows $|||\widehat{u}_C - I_{NC}\widehat{u}_C|||_{NC} \le |||\widehat{u}_C - u_C|||$, the Cauchy and the inverse inequality result in an estimate of the first two terms,

$$\begin{aligned}
&(Q(f - \alpha v_{CR}), \widehat{u}_C - I_{NC}\widehat{u}_C)_{L^2(\Omega')} + ((\widehat{Q} - Q)f, \widehat{u}_C - u_C)_{L^2(\Omega)} \\
&\qquad \le c_{\mathrm{inv}}(\|h_{\mathcal{T}} Q(f - \alpha v_{CR})\|_{L^2(\Omega')} + \|h_{\mathcal{T}}(\widehat{Q} - Q)f\|_{L^2(\Omega)})|||\widehat{u}_C - u_C|||.
\end{aligned}$$

The Pythagoras theorems (3.12) and (3.11) with $v = h_{\mathcal{T}} f, w = \alpha h_{\mathcal{T}} v_{CR}$ and (3.9) on $\Omega \setminus \Omega'$ lead to

$$\begin{aligned}
&\|h_{\mathcal{T}}(\widehat{Q} - Q)f\|^2_{L^2(\Omega)} + \|h_{\mathcal{T}} Q(f - \alpha v_{CR})\|^2_{L^2(\Omega')} = \|h_{\mathcal{T}}(\widehat{Q}f - \alpha Q v_{CR})\|^2_{L^2(\Omega')} \text{ and} \\
&\|h_{\mathcal{T}}(1 - \widehat{Q})f\|^2_{L^2(\Omega')} + \|h_{\mathcal{T}}(\widehat{Q}f - \alpha Q v_{CR})\|_{L^2(\Omega')} = \|h_{\mathcal{T}}(f - \alpha Q v_{CR})\|_{L^2(\Omega')}
\end{aligned}$$

Hence $h_{\mathcal{T}} \le c_{\mathrm{sr}}^{1/n} H_{\mathcal{T}}$ proves

$$\|h_{\mathcal{T}}(\widehat{Q}f - \alpha Q v_{CR})\|_{L^2(\Omega')} \le \|h_{\mathcal{T}}(f - \alpha Q v_{CR})\|_{L^2(\Omega')} \le c_{\mathrm{sr}}^{1/n}\eta(\mathcal{R}).$$

This results in

$$(Q(f - \alpha v_{CR}), \widehat{u}_C - I_{NC}\widehat{u}_C)_{L^2(\Omega)} + ((\widehat{Q} - Q)f, \widehat{u}_C - u_C)_{L^2(\Omega)} \le c_{\mathrm{inv}} 2^{1/2} c_{\mathrm{sr}}^{1/n}\eta(\mathcal{R})|||\widehat{u}_C - u_C|||.$$

Lemma 3.7 controls the third term of (3.15). The Cauchy and the Friedrichs inequality from Theorem 2.28 plus $\alpha \le 1$ bound the last term in (3.15). Consequently,

$$|||\widehat{u}_C - u_C|||^2 \lesssim (\eta(\mathcal{R}) + \|\widehat{Q}\widehat{v}_{CR} - Qv_{CR}\|_{L^2(\Omega)})|||\widehat{u}_C - u_C|||. \qquad \square$$

3.5. Reliability and Efficiency

This section proves reliability and efficiency of the total error.

Theorem 3.9 (Reliability) *It holds* $|||v_{CR}|||^2_{NC} + |||u - u_C|||^2 \lesssim \eta^2(\mathcal{T})$.

Proof: Corollary 3.3 implies the reliability of $|||v_{CR}|||^2_{NC} \le c_{\mathrm{rel}}\eta^2(\mathcal{T})$. For any $k \in \mathbb{N}$, consider the triangulations from k uniform bisections, i.e., $\mathcal{T}_k := \mathrm{bisec}^{(k)}(\mathcal{T}) := \mathrm{bisec}(\mathrm{bisec}(\ldots(\mathcal{T})))$ with solutions $(v_k, u_k) \in CR^1_0(\mathcal{T}_k) \times S^1_0(\mathcal{T}_k)$ to (R) on $\mathcal{T}_k$. Then $\mathcal{T} \setminus \mathcal{T}_k = \mathcal{T}$ and $h_{\mathcal{T}_k} \to 0$ for $k \to \infty$ pointwise. Theorem 3.1 with the integral mean property (2.4) for the nonconforming

interpolation operator and $\Pi_0^{(k)} : L^2(\Omega;\mathbb{R}^n) \to P_0(\mathcal{T}_k;\mathbb{R}^n)$ in the first term and (3.7) and the approximation property (3.5) in the last term results in

$$|||v_k|||_{NC} + |||u - u_k||| \lesssim \|(1 - \Pi_0^{(k)})\nabla u\|_{L^2(\Omega)} + \operatorname{osc}(f, \mathcal{T}_k) + \|h_{\mathcal{T}_k} f\|_{L^2(\Omega)}.$$

The density of $C_c^\infty(\Omega)$ in $L^2(\Omega)$ [Alt16] and the Poincaré inequality in Theorem 2.30 prove that the right-hand side converges to zero, hence $v_k \to 0$ and $u_k \to u$ in $|||\bullet|||_{NC}$ for $k \to \infty$. The error control from Proposition 3.8 is employed for $\mathcal{T}$ and $\widehat{\mathcal{T}} = \mathcal{T}_k$ and reads $|||u_C - u_k||| \lesssim |||v_{CR} - v_k|||_{NC} + \|Q_{\mathcal{T}} v_{CR} - Q_{\mathcal{T}_k} v_k\|_{L^2(\Omega)} + \eta(\mathcal{T})$. The limit of this for $k \to \infty$, the boundedness (3.6) of Q, and the discrete Friedrichs inequality prove $|||u - u_C||| \lesssim |||v_{CR}|||_{NC} + \eta(\mathcal{T})$ and conclude the proof. □

Theorem 3.10 (Efficiency) *It holds* $\eta^2(\mathcal{T}) \lesssim |||v_{CR}|||_{NC}^2 + |||u - u_C|||^2 + \operatorname{osc}^2(f, \mathcal{T})$.

Proof: Corollary 3.3 results in the global efficiency of the jump terms. The pointwise estimate $H_{\mathcal{T}} \lesssim h_{\mathcal{T}} \lesssim 1$ and $\alpha \le 1$ prove that the volume contributions $\|H_{\mathcal{T}}(f - \alpha Q v_{CR})\|_{L^2(\Omega)}$ are bounded up to a multiplicative constant by $\|h_{\mathcal{T}} f\|_{L^2(\Omega)} + \|Q v_{CR}\|_{L^2(\Omega)}$. The first term is well-established from the beginning of the a posteriori error control. Although [Ver96, p. 15] only treats the solution to the standard discrete weak formulation in $S_0^1(\mathcal{T})$, a careful inspection of the proof reveals that the efficiency statement of $h_T \|f\|_{L^2(\Omega)}$ holds in fact for any function in $P_1(\mathcal{T})$, in particular, $u_C \in S_0^1(\mathcal{T}) \subseteq P_1(\mathcal{T})$ satisfies

$$\|h_{\mathcal{T}} f\|_{L^2(\Omega)} \lesssim \|\nabla u - \nabla u_C\|_{L^2(\Omega)} + \operatorname{osc}(f, \mathcal{T}).$$

The boundedness (3.6) of Q and the discrete Friedrichs inequality from Theorem 2.29 show $\|Q v_{CR}\|_{L^2(\Omega)} \le \|v_{CR}\|_{L^2(\Omega)} \le c_{\mathrm{dF}} |||v_{CR}|||_{NC}$ and conclude the proof. □

	Q	α
Primal dPG	id	1
Dual dPG	Π_0	1
Primal Mixed dPG	id	1/2
Ultraweak dPG	id	1/2
Nonconforming	id	0
Mixed	Π_0	0

Table 4: Projection Q and parameter α

4. dPG as a Reduced Mixed Method

This section establishes the equivalence of four dPG methods as well as the standard nonconforming and mixed methods to the reduced mixed system (R) with Q and α of Table 4. These equivalences rely on the mixed system of equations (M) for dPG on p. 20.

4.1. Primal dPG Formulation

The primal dPG formulation of the Poisson model problem [DG13] utilizes the spaces and discrete subspaces

$$X := H^1_0(\mathcal{T}) \times H^{-1/2}(\partial\mathcal{T}) \text{ and } Y := H^1(\mathcal{T}),$$
$$X_h := S^1_0(\mathcal{T}) \times P_0(\mathcal{E}) \subset X \text{ and } Y_h := P_1(\mathcal{T}) \subset Y$$

with norms $\|(u,t)\|^2_X := |||u|||^2 + \|t\|^2_{H^{-1/2}(\partial\mathcal{T})}$, $\|v\|^2_Y := \|v\|^2_{H^1(\mathcal{T})}$, and bilinear and linear forms with $b(u,t;v) := a_{NC}(u,v) - \langle t, v\rangle_{\partial\mathcal{T}}$ and $F(v) := (f,v)_{L^2(\Omega)}$ for $(u,t) \in X$ and $v \in Y$.

The recent paper [CBHW18] contains the following proof of equivalence of this primal dPG method to the reduced mixed scheme for the special case $\phi \equiv 1$ of a more general nonlinear model problem.

Theorem 4.1 ((R)$\Leftrightarrow$(M)) *If $(u_C, t_0; v_1) \in X_h \times Y_h$ solves* (M)*, then $v_1 \in CR^1_0(\mathcal{T})$ and $(v_1, u_C) \in CR^1_0(\mathcal{T}) \times S^1_0(\mathcal{T})$ solves* (R) *with $Q = \mathrm{id}$ and $\alpha = 1$. Conversely, for any solution (v_{CR}, u_C) to* (R) *with $Q = \mathrm{id}$ and $\alpha = 1$, there exists a unique $t_0 \in P_0(\mathcal{E})$ such that $(u_C, t_0; v_{CR})$ solves* (M)*.*

Proof: For the solution $(u_C, t_0; v_1) \in X_h \times Y_h$ to (M) and any $s_0 \in P_0(\mathcal{E})$, (M) leads to $0 = -b(0, s_0; v_1) = \langle s_0, v_1\rangle_{\partial\mathcal{T}}$. This implies $\int_E [v_1]_E = 0$ for any $E \in \mathcal{E}(\Omega)$, hence $v_1 \in CR^1_0(\mathcal{T})$. Both equations of (R) for $Q = \mathrm{id}$ and $\alpha = 1$ then directly follow with test function $(w_C, 0; w_{CR}) \in X_h \times Y_h$ in (M).

If, conversely, $(v_1, u_C) \in CR^1_0(\mathcal{T}) \times S^1_0(\mathcal{T})$ solves (R) with $Q = \mathrm{id}$ and $\alpha = 1$, the first equation of (R) makes Lemma 2.26 applicable for $\Lambda := a_{NC}(u_C + v_1, \bullet) + (v_1, \bullet)_{L^2(\Omega)} - (f, \bullet)_{L^2(\Omega)} \in$

$P_1(\mathcal{T})^*$. This leads to a unique $t_0 \in P_0(\mathcal{E})$ with $\langle t_0, \bullet\rangle_{\partial\mathcal{T}} = \Lambda$, in other words, $(u_C, t_0; v_1) \in X_h \times Y_h$ satisfies the first equation of (M). The second equation of (M) follows from the second equation of (R) and $v_1 \in CR_0^1(\mathcal{T})$, thus, $\langle s_0, v_1\rangle_{\partial\mathcal{T}} = 0$ for any $s_0 \in P_0(\mathcal{E})$. □

4.2. Dual dPG Formulation

The dual dPG [CDG16] bases on a piecewise integration by parts in the second equation of the first-order system (1.2) on p. 3 and utilizes the spaces and discrete subspaces

$$X := H(\mathrm{div},\Omega) \times L^2(\Omega) \times H^{1/2}(\partial\mathcal{T}) \text{ and } Y := H(\mathrm{div},\mathcal{T}) \times L^2(\Omega),$$
$$X_h := RT_0(\mathcal{T}) \times P_0(\mathcal{T}) \times S_0^1(\mathcal{E}) \subset X \text{ and } Y_h := RT_0^{NC}(\mathcal{T}) \times P_0(\mathcal{T}) \subset Y$$

with norms $\|(p,w,s)\|_X^2 := \|p\|_{H(\mathrm{div})}^2 + \|w\|_{L^2(\Omega)}^2 + \|s\|_{H^{1/2}(\partial\mathcal{T})}^2$, $\|(q,v)\|_Y^2 := \|q\|_{H(\mathrm{div},NC)}^2 + \|v\|_{L^2(\Omega)}^2$, and bilinear and linear forms

$$b(p,w,s;q,v) := (p,q)_{L^2(\Omega)} + (w,\mathrm{div}_{NC}\, q)_{L^2(\Omega)} - (\mathrm{div}\, p, v)_{L^2(\Omega)} - \langle q\cdot\nu, s\rangle_{\partial\mathcal{T}},$$
$$F(q,v) := (f,v)_{L^2(\Omega)} \quad \text{for } (p,w,s) \in X \text{ and } (q,v) \in Y.$$

Theorem 4.2 *(a) If $(p_{RT}, w_0, s_C; q_1, v_0) \in X_h \times Y_h$ solves* (M)*, there exists a unique $v_{CR} \in CR_0^1(\mathcal{T})$ with $\nabla_{NC} v_{CR} = -\Pi_0 q_1$ and $\Pi_0 v_{CR} = v_0$ such that $(v_{CR}, u_C) \in CR_0^1(\mathcal{T}) \times S_0^1(\mathcal{T})$ with $\gamma_0^{\mathcal{T}}\, u_C = s_C$ solves* (R) *with $Q = \Pi_0$ and $\alpha = 1$.*

(b) Conversely, for any solution (v_{CR}, u_C) to (R) *with $Q = \Pi_0$ and $\alpha = 1$, there exists a unique $(p_{RT}, w_0, q_1, v_0) \in RT_0(\mathcal{T}) \times P_0(\mathcal{T}) \times RT_0^{NC}(\mathcal{T}) \times P_0(\mathcal{T})$ such that $(p_{RT}, w_0, \gamma_0^{\mathcal{T}}\, u_C; q_1, v_0) \in X_h \times Y_h$ solves* (M)*.*

Proof: (a) For the test function $(0,u_0,0) \in X_h$, (M) implies $\mathrm{div}_{NC}\, q_1 = 0$. Consider the solution $v_{CR} \in CR_0^1(\mathcal{T})$ to $a_{NC}(v_{CR}, w_{CR}) = -(\Pi_0 q_1, \nabla_{NC} w_{CR})_{L^2(\Omega)}$ for all $w_{CR} \in CR_0^1(\mathcal{T})$. Lemma 2.25 shows $\Pi_0 q_1 + \nabla_{NC} v_{CR} \in RT_0(\mathcal{T})$ with $\mathrm{div}(\Pi_0 q_1 + \nabla_{NC} v_{CR}) = 0$. The test function $(\Pi_0 q_1 + \nabla_{NC} v_{CR}, 0, 0) \in X_h$ in (M) then proves

$$0 = (\Pi_0 q_1 + \nabla_{NC} v_{CR}, \Pi_0 q_1)_{L^2(\Omega)} = \|\Pi_0 q_1 + \nabla_{NC} v_{CR}\|_{L^2(\Omega)}.$$

This implies $-\nabla_{NC} v_{CR} = \Pi_0 q_1 = q_1$ and therefore $(q_{RT}, q_1)_{L^2(\Omega)} = -(\mathrm{div}\, q_{RT}, \Pi_0 v_{CR})_{L^2(\Omega)}$ for any $q_{RT} \in RT_0(\mathcal{T})$. Since (M) with $(q_{RT}, 0, 0) \in X_h$ proves $(q_{RT}, q_1)_{L^2(\Omega)} = -(\mathrm{div}\, q_{RT}, v_0)_{L^2(\Omega)}$, it follows $\Pi_0 v_{CR} = v_0$. An integration by parts in (M) with the test function $(0, 0, \gamma_0^{\mathcal{T}}\, w_C) \in X_h$ for any $w_C \in S_0^1(\mathcal{T})$ results in the second equation of (R). Another integration by parts in (M) with $u_C \in S_0^1(\mathcal{T})$, $\gamma_0^{\mathcal{T}}\, u_C = s_C$ and Lemma 2.25 for $p_{RT} \in RT_0(\mathcal{T})$ shows that any $w_{CR} \in CR_0^1(\mathcal{T})$ with the test function $(-\nabla_{NC} w_{CR}, \Pi_0 w_{CR}) \in Y_h$ satisfies

$$\begin{aligned}(f, \Pi_0 w_{CR})_{L^2(\Omega)} &= -(q_1, \nabla_{NC} w_{CR})_{L^2(\Omega)} + (v_0, \Pi_0 w_{CR})_{L^2(\Omega)} \\ &\quad - (p_{RT}, \nabla_{NC} w_{CR})_{L^2(\Omega)} - (\mathrm{div}\, p_{RT}, \Pi_0 w_{CR})_{L^2(\Omega)} + (\nabla_{NC} w_{CR}, \nabla u_C)_{L^2(\Omega)} \\ &= (\nabla_{NC} v_{CR}, \nabla_{NC} w_{CR})_{L^2(\Omega)} + (\Pi_0 v_{CR}, \Pi_0 w_{CR})_{L^2(\Omega)} + (\nabla_{NC} w_{CR}, \nabla u_C)_{L^2(\Omega)}.\end{aligned}$$

(b) The second equation of (R) plus $v_0 \coloneqq \Pi_0 v_{CR} \in P_0(\mathcal{T})$ and $q_1 \coloneqq -\nabla_{NC} v_{CR} \in RT_0^{NC}(\mathcal{T})$ imply the second equation of (M). The first equation of (R) and Lemma 2.25 prove that $p_{RT} \coloneqq \nabla u_C + \nabla_{NC} v_{CR} + (\Pi_0 v_{CR} - \Pi_0 f)(\bullet - \mathrm{mid}(\mathcal{T}))/n \in RT_0(\mathcal{T})$. Hence, $(p_{RT}, w_0, \gamma_0^{\mathcal{T}} u_C) \in X_h$ for $w_0 \coloneqq \Pi_0 u_C - \Pi_0(p_{RT}(\bullet - \mathrm{mid}(\mathcal{T})))/n$ and any $(\widetilde{q}_1, \widetilde{v}_0) \in Y_h$ satisfy

$$\begin{aligned}
&\langle q_1, v_0; \widetilde{q}_1, \widetilde{v}_0\rangle_Y + b(p_{RT}, w_0, \gamma_0^{\mathcal{T}} u_C; \widetilde{q}_1, \widetilde{v}_0)\\
&\quad = (q_1, \widetilde{q}_1)_{L^2(\Omega)} + (v_0, \widetilde{v}_0)_{L^2(\Omega)} + (p_{RT}, \widetilde{q}_1)_{L^2(\Omega)} + (w_0, \mathrm{div}_{NC}\, \widetilde{q}_1)_{L^2(\Omega)}\\
&\qquad - (\mathrm{div}\, p_{RT}, \widetilde{v}_0)_{L^2(\Omega)} - (\mathrm{div}_{NC}\, \widetilde{q}_1, u_C)_{L^2(\Omega)} - (\widetilde{q}_1, \nabla u_C)_{L^2(\Omega)}\\
&\quad = (p_{RT} - \nabla_{NC} v_{CR} - \nabla u_C, \widetilde{q}_1)_{L^2(\Omega)} + (\Pi_0 v_{CR}, \widetilde{v}_0)_{L^2(\Omega)}\\
&\qquad - (p_{RT}(\bullet - \mathrm{mid}(\mathcal{T}))/n, \mathrm{div}_{NC}\, \widetilde{q}_1)_{L^2(\Omega)} - (\Pi_0 v_{CR} - \Pi_0 f, \widetilde{v}_0)_{L^2(\Omega)}\\
&\quad = (p_{RT} - \nabla_{NC} v_{CR} - \nabla u_C, \widetilde{q}_1)_{L^2(\Omega)} - (p_{RT}, \mathrm{div}_{NC}\, \widetilde{q}_1(\bullet - \mathrm{mid}(\mathcal{T}))/n)_{L^2(\Omega)}\\
&\qquad + (\Pi_0 f, \widetilde{v}_0)_{L^2(\Omega)}.
\end{aligned}$$

The split $\widetilde{q}_1 = \Pi_0 \widetilde{q}_1 + \mathrm{div}_{NC}\, \widetilde{q}_1(\bullet - \mathrm{mid}(\mathcal{T}))/n$ shows

$$\begin{aligned}
&(p_{RT} - \nabla_{NC}(v_{CR} + u_C), \widetilde{q}_1)_{L^2(\Omega)} - (p_{RT}, \mathrm{div}_{NC}\, \widetilde{q}_1(\bullet - \mathrm{mid}(\mathcal{T}))/n)_{L^2(\Omega)}\\
&\qquad\qquad = (\Pi_0 p_{RT} - \nabla_{NC}(v_{CR} + u_C), \Pi_0 \widetilde{q}_1)_{L^2(\Omega)} = 0.
\end{aligned}$$

This concludes the proof of the first equation in (M). □

4.3. Primal Mixed dPG Formulation

The primal mixed dPG formulation [CDG16] departs from a piecewise integration by parts of the first equation of (1.2) on p. 3 and employs the spaces and discrete subspaces

$$\begin{aligned}
&X \coloneqq L^2(\Omega;\mathbb{R}^n) \times H_0^1(\Omega) \times H^{-1/2}(\partial\mathcal{T}) \text{ and } Y \coloneqq L^2(\Omega;\mathbb{R}^n) \times H^1(\mathcal{T}),\\
&X_h \coloneqq P_0(\mathcal{T};\mathbb{R}^n) \times S_0^1(\mathcal{T}) \times P_0(\mathcal{E}) \subset X \text{ and } Y_h \coloneqq P_0(\mathcal{T};\mathbb{R}^n) \times P_1(\mathcal{T}) \subset Y
\end{aligned}$$

with norms $\|(r,u,t)\|_X^2 \coloneqq \|r\|_{L^2(\Omega)}^2 + |||u|||^2 + \|t\|_{H^{-1/2}(\partial\mathcal{T})}^2$, $\|(q,v)\|_Y^2 \coloneqq \|q\|_{L^2(\Omega)}^2 + \|v\|_{H^1(\mathcal{T})}^2$, and bilinear and linear forms

$$\begin{aligned}
b(r,u,t;q,v) &\coloneqq (r - \nabla u, q)_{L^2(\Omega)} + (r, \nabla_{NC} v)_{L^2(\Omega)} - \langle t, v\rangle_{\partial\mathcal{T}},\\
F(q,v) &\coloneqq (f,v)_{L^2(\Omega)} \quad \text{for } (r,u,t) \in X \text{ and } (q,v) \in Y.
\end{aligned}$$

Theorem 4.3 *(a) If* $(r_0, u_C, t_0; q_0, v_1) \in X_h \times Y_h$ *solves* (M), $v_1 \in CR_0^1(\mathcal{T})$ *and* $(2v_1, u_C) \in CR_0^1(\mathcal{T}) \times S_0^1(\mathcal{T})$ *solves* (R) *with* $Q = \mathrm{id}$ *and* $\alpha = 1/2$.

(b) Conversely, for any solution (v_{CR}, u_C) *to* (R) *with* $Q = \mathrm{id}$ *and* $\alpha = 1/2$, *there exists a unique* $(r_0, t_0, q_0) \in P_0(\mathcal{T};\mathbb{R}^n) \times P_0(\mathcal{E}) \times P_0(\mathcal{T};\mathbb{R}^n)$ *such that* $(r_0, u_C, t_0; q_0, v_{CR}/2)$ *solves* (M).

Proof: (a) For any $s_0 \in P_0(\mathcal{E})$, (M) implies $0 = -b(0,0,s_0;q_0,v_1) = \langle s_0, v_1\rangle_{\partial\mathcal{T}}$. This proves $v_1 \in CR_0^1(\mathcal{T})$. Furthermore, $0 = b(r_0,0,0;q_0,v_1)$ and $0 = b(0,w_C,0;q_0,v_1)$ for any $r_0 \in P_0(\mathcal{T};\mathbb{R}^n)$ and $w_C \in S_0^1(\mathcal{T})$ lead to $q_0 + \nabla_{NC} v_1 = 0$ and $(q_0, \nabla w_C)_{L^2(\Omega)} = 0$, and thus, and the second equation of (R). Any $w_{CR} \in CR_0^1(\mathcal{T})$ and test function $(-\nabla_{NC} w_{CR}, w_{CR}) \in Y_h$ in (M) satisfy

$$\begin{aligned}(f, w_{CR})_{L^2(\Omega)} &= -(q_0, \nabla_{NC} w_{CR})_{L^2(\Omega)} + (v_1, w_{CR})_{L^2(\Omega)} + (\nabla_{NC} v_1, \nabla_{NC} w_{CR})_{L^2(\Omega)} \\ &\qquad + (\nabla u_C - r_0, \nabla_{NC} w_{CR})_{L^2(\Omega)} + (r_0, \nabla_{NC} w_{CR})_{L^2(\Omega)} \\ &= 2(\nabla_{NC} v_1, \nabla_{NC} w_{CR})_{L^2(\Omega)} + (v_1, w_{CR})_{L^2(\Omega)} + (\nabla u_C, \nabla_{NC} w_{CR})_{L^2(\Omega)}.\end{aligned}$$

This is (R) for $v_{CR} = 2v_1$, $\alpha = 1/2$ and $Q = \mathrm{id}$.

(b) The choices $v_1 := v_{CR}/2$ and $q_0 := -\nabla_{NC} v_1$ and the second equation of (R) lead to the second equation of (M). The existence of a unique $t_0 \in P_0(\mathcal{E})$ such that $\langle t_0, \bullet\rangle_{\partial\mathcal{T}} = \Lambda := a_{NC}(u_C, \bullet) + 2a_{NC}(v_1, \bullet) + (v_1, \bullet)_{L^2(\Omega)} - (f, \bullet)_{L^2(\Omega)} \in P_1(\mathcal{T})^*$ follows from Lemma 2.26 because (R) shows that $CR_0^1(\mathcal{T}) \subseteq \ker\Lambda$. Hence, for $r_0 := \nabla_{NC} v_1 + \nabla u_C \in P_0(\mathcal{T};\mathbb{R}^n)$, any $(\widetilde{q}_0, \widetilde{v}_1) \in P_0(\mathcal{T};\mathbb{R}^n) \times P_1(\mathcal{T})$ satisfies

$$\begin{aligned}&\langle q_0, v_1; \widetilde{q}_0, \widetilde{v}_1\rangle_Y + b(r_0, u_C, t_0; \widetilde{q}_0, \widetilde{v}_1) \\ &\quad = (q_0, \widetilde{q}_0)_{L^2(\Omega)} + (v_1, \widetilde{v}_1)_{L^2(\Omega)} + (\nabla_{NC} v_1, \nabla_{NC} \widetilde{v}_1)_{L^2(\Omega)} \\ &\qquad + (r_0 - \nabla u_C, \widetilde{q}_0)_{L^2(\Omega)} + (r_0, \nabla_{NC} \widetilde{v}_1)_{L^2(\Omega)} - \langle t_0, \widetilde{v}_1\rangle_{\partial\mathcal{T}} \\ &\quad = (v_1, \widetilde{v}_1)_{L^2(\Omega)} + 2(\nabla_{NC} v_1, \nabla_{NC} \widetilde{v}_1)_{L^2(\Omega)} + (\nabla u_C, \nabla_{NC} \widetilde{v}_1)_{L^2(\Omega)} - \langle t_0, \widetilde{v}_1\rangle_{\partial\mathcal{T}} \\ &\quad = (f, \widetilde{v}_1)_{L^2(\Omega)}.\end{aligned}$$

This is the first equation of (M) and concludes the proof. □

4.4. Ultraweak dPG Formulation

The ultraweak dPG formulation [DG11b] integrates both equations of the first-order system (1.2) on p. 3 by parts and utilizes the spaces and discrete subspaces [CGHW14]

$$\begin{aligned}X &:= L^2(\Omega;\mathbb{R}^n) \times L^2(\Omega) \times H^{-1/2}(\partial\mathcal{T}) \times H^{-1/2}(\partial\mathcal{T}) \text{ and } Y := H(\mathrm{div},\mathcal{T}) \times H^1(\mathcal{T}), \\ X_h &:= P_0(\mathcal{T};\mathbb{R}^n) \times P_0(\mathcal{T}) \times P_0(\mathcal{E}) \times S_0^1(\mathcal{E}) \subset X \qquad \text{and } Y_h := RT_0^{NC}(\mathcal{T}) \times P_1(\mathcal{T}) \subset Y\end{aligned}$$

with the norms $\|(r,w,t,s)\|_X^2 := \|r\|_{L^2(\Omega)}^2 + \|w\|_{L^2(\Omega)}^2 + \|t\|_{H^{-1/2}(\partial\mathcal{T})}^2 + \|s\|_{H^{1/2}(\partial\mathcal{T})}^2$ and $\|(q,v)\|_Y^2 := \|q\|_{H(\mathrm{div},NC)}^2 + \|v\|_{H^1(\mathcal{T})}^2$, and bilinear and linear form

$$\begin{aligned}b(r,w,t,s;q,v) &:= (r,q)_{L^2(\Omega)} + (r, \nabla_{NC} v)_{L^2(\Omega)} + (w, \mathrm{div}_{NC}\, q)_{L^2(\Omega)} \\ &\qquad - \langle q\cdot\nu, s\rangle_{\partial\mathcal{T}} - \langle t, v\rangle_{\partial\mathcal{T}}, \\ F(q,v) &:= (f,v)_{L^2(\Omega)} \quad \text{for } (r,w,t,s) \in X \text{ and } (q,v) \in Y.\end{aligned}$$

Theorem 4.4 *(a) If $(r_0, w_0, t_0, s_C; q_1, v_1) \in X_h \times Y_h$ solves* (M)*, $v_1 \in CR_0^1(\mathcal{T})$ and $(2v_1, u_C) \in CR_0^1(\mathcal{T}) \times S_0^1(\mathcal{T})$ with $\gamma_0^{\mathcal{T}} u_C = s_C$ solves* (R) *with $Q = \mathrm{id}$ and $\alpha = 1/2$.*

(b) Conversely, for any solution (v_{CR}, u_C) to (R) *with $Q = \mathrm{id}$ and $\alpha = 1/2$, there exists a unique $(r_0, w_0, t_0, q_1) \in P_0(\mathcal{T};\mathbb{R}^n) \times P_0(\mathcal{T}) \times P_0(\mathcal{E}) \times RT_0^{NC}(\mathcal{T})$ such that $(r_0, w_0, t_0, \gamma_0^{\mathcal{T}} u_C; q_1, v_{CR}/2)$ solves* (M)*.*

Proof: (a) Since $(p_0, u_0, s_0, 0) \in X_h$ is arbitrary in the second equation of (M), it follows $v_1 \in CR_0^1(\mathcal{T})$, $\operatorname{div}_{NC} q_1 = 0$, and $q_1 + \nabla_{NC} v_1 = 0$. This and an integration by parts with any $w_C \in S_0^1(\mathcal{T})$ in (M) shows the second equation of (R) for $v_{CR} = 2v_1$. With test functions $(-\nabla_{NC} w_{CR}, w_{CR}) \in Y_h$ for any $w_{CR} \in CR_0^1(\mathcal{T})$ and $v_{CR} := 2v_1$, (M) and an integration by parts with $u_C \in S_0^1(\mathcal{T})$ imply

$$\begin{aligned}(f, w_{CR})_{L^2(\Omega)} &= -(q_1, \nabla_{NC} w_{CR})_{L^2(\Omega)} + (v_1, w_{CR})_{L^2(\Omega)} + (\nabla_{NC} v_1, \nabla_{NC} w_{CR})_{L^2(\Omega)} \\ &\qquad - (r_0, \nabla_{NC} w_{CR})_{L^2(\Omega)} + (r_0, \nabla_{NC} w_{CR})_{L^2(\Omega)} + (\nabla_{NC} w_{CR}, \nabla u_C)_{L^2(\Omega)} \\ &= 2(\nabla_{NC} v_1, \nabla_{NC} w_{CR})_{L^2(\Omega)} + (v_1, w_{CR})_{L^2(\Omega)} + (\nabla_{NC} w_{CR}, \nabla u_C)_{L^2(\Omega)} \\ &= (\nabla_{NC} v_{CR}, \nabla_{NC} w_{CR})_{L^2(\Omega)} + (v_{CR}, w_{CR})_{L^2(\Omega)}/2 + (\nabla_{NC} w_{CR}, \nabla u_C)_{L^2(\Omega)}.\end{aligned}$$

This is the first equation of (R) for $\alpha = 1/2$ and $Q = \mathrm{id}$.

(b) With $v_1 := v_{CR}/2$ and $q_1 := -\nabla_{NC} v_1$, (R) and an integration by parts prove the second equation of (M) for $(q_1, v_1) \in Y_h$. The first equation of (R) and Lemma 2.26 prove unique existence of $t_0 \in P_0(\mathcal{E})$ such that $\langle t_0, \bullet \rangle_{\partial\mathcal{T}} = a_{NC}(u_C, \bullet) + 2a_{NC}(v_1, \bullet) + (v_1, \bullet)_{L^2(\Omega)} - (f, \bullet)_{L^2(\Omega)}$ in $P_1(\mathcal{T})$. This, an integration by parts with $u_C \in S_0^1(\mathcal{T})$, and the choices $r_0 := \nabla_{NC} v_1 + \nabla u_C$, $w_0 := \Pi_0 u_C$ prove that any $(\widetilde{q}_1, \widetilde{v}_1) \in RT_0^{NC}(\mathcal{T}) \times P_1(\mathcal{T})$ satisfies

$$\begin{aligned}&\langle q_1, v_1; \widetilde{q}_1, \widetilde{v}_1 \rangle_Y + b(r_0, w_0, t_0, \gamma_0^{\mathcal{T}} u_C; \widetilde{q}_1, \widetilde{v}_1) \\ &\quad = (q_1, \widetilde{q}_1)_{L^2(\Omega)} + (v_1, \widetilde{v}_1)_{L^2(\Omega)} + (\nabla_{NC} v_1, \nabla_{NC} \widetilde{v}_1)_{L^2(\Omega)} + (r_0, \widetilde{q}_1 + \nabla_{NC} \widetilde{v}_1)_{L^2(\Omega)} \\ &\qquad + (w_0, \operatorname{div}_{NC} \widetilde{q}_1)_{L^2(\Omega)} - (\nabla u_C, \widetilde{q}_1)_{L^2(\Omega)} - (u_C, \operatorname{div}_{NC} \widetilde{q}_1)_{L^2(\Omega)} - \langle t_0, \widetilde{v}_1 \rangle_{\partial\mathcal{T}} \\ &\quad = (v_1, \widetilde{v}_1)_{L^2(\Omega)} + 2(\nabla_{NC} v_1, \nabla_{NC} \widetilde{v}_1)_{L^2(\Omega)} + (\nabla u_C, \nabla_{NC} \widetilde{v}_1)_{L^2(\Omega)} - \langle t_0, \widetilde{v}_1 \rangle_{\partial\mathcal{T}} \\ &\quad = (f, \widetilde{v}_1)_{L^2(\Omega)}.\end{aligned}$$

This proves the first equation of (M). □

4.5. Nonconforming and Mixed Methods

Table 4 on p. 36 also includes the nonconforming Crouzeix-Raviart and the Raviart-Thomas mixed finite element method.

For $Q = \mathrm{id}$ and $\alpha = 0$, the first equation of (R) is equivalent to $u_{CR} := v_{CR} + u_C \in CR_0^1(\mathcal{T})$ solving the nonconforming problem $a_{NC}(u_{CR}, w_{CR}) = (f, w_{CR})_{L^2(\Omega)}$ for all $w_{CR} \in CR_0^1(\mathcal{T})$. Furthermore, the second equation of (R) implies that $u_C \in S_0^1(\mathcal{T})$ solves the conforming P_1 finite element method, i.e., $a(u_C, w_C) = (f, w_C)_{L^2(\Omega)}$ for all $w_C \in S_0^1(\mathcal{T})$. Conversely, for the nonconforming solution $u_{CR} \in CR_0^1(\mathcal{T})$, the Galerkin projection $u_C = G u_{CR} \in S_0^1(\mathcal{T})$ and $v_{CR} := u_{CR} - u_C \in CR_0^1(\mathcal{T})$ solve (R) with $Q = \mathrm{id}$ and $\alpha = 0$.

The equivalence of the mixed method and and (R) relies on this observation for the nonconforming method. For $Q = \Pi_0$ and $\alpha = 0$, $u_{CR} := v_{CR} + u_C \in CR_0^1(\mathcal{T})$ is the solution to the nonconforming problem with right-hand side $\Pi_0 f$. Marini's identity [Mar85, (1.3), (2.16)] then proves that $p_{RT} := \nabla_{NC}(v_{CR} + u_C) + \Pi_0 f(\bullet - \mathrm{mid}(\mathcal{T}))/n \in RT_0(\mathcal{T})$ and $u_0 :=$

$\Pi_0(v_{CR}+u_C)-s(\mathcal{T})\Pi_0 f/n^2\in P_0(\mathcal{T})$ with $s(\mathcal{T})$ from Definition 2.10 solve the mixed formulation,

$$\begin{aligned}(p_{RT},q_{RT})_{L^2(\Omega)}+(u_0,\operatorname{div}q_{RT})_{L^2(\Omega)}&=0 && \text{for all } q_{RT}\in RT_0(\mathcal{T}),\\ (v_0,\operatorname{div}p_{RT})_{L^2(\Omega)}&=(f,v_0)_{L^2(\Omega)} && \text{for all } v_0\in P_0(\mathcal{T}).\end{aligned}$$

Conversely, given the solution $(p_{RT},u_0)\in RT_0(\mathcal{T})\times P_0(\mathcal{T})$ to this mixed formulation, $u_{CR}\coloneqq u_0+s(\mathcal{T})\Pi_0 f/n^2+\Pi_0 p_{RT}\cdot(\bullet-\operatorname{mid}(\mathcal{T}))\in CR_0^1(\mathcal{T})$ solves the nonconforming problem with right-hand side $\Pi_0 f$. Then as argued for the nonconforming method above, the solution $u_C\in S_0^1(\mathcal{T})$ to $(\nabla u_C,\nabla w_C)_{L^2(\Omega)}=(\Pi_0 p_{RT},\nabla w_C)_{L^2(\Omega)}$ for all $w_C\in S_0^1(\mathcal{T})$ and $v_{CR}\coloneqq u_{CR}-u_C\in CR_0^1(\mathcal{T})$ solve (R) with $Q=\Pi_0$ and $\alpha=0$.

5. Optimal Convergence Rates of Reduced Mixed Methods

The following subsections establish the axioms of adaptivity (A1)–(A4) from Subsection 2.4 with $\Lambda_1, \dots, \Lambda_4 \approx 1$.

5.1. Stability and Reduction

The notation of Table 3 on p. 33 applies throughout this subsection for a triangulation $\mathcal{T} \in \mathbb{T}$ and a refinement $\widehat{\mathcal{T}} \in \mathbb{T}(\mathcal{T})$.

Theorem 5.1 (Stability) *There exists* $\Lambda_1 \approx 1$ *with*

$$\big|\eta(\mathcal{T} \cap \widehat{\mathcal{T}}) - \widehat{\eta}(\mathcal{T} \cap \widehat{\mathcal{T}})\big| \le \Lambda_1 \delta(\mathcal{T}, \widehat{\mathcal{T}}). \tag{A1}$$

Proof: Consider some vector $v \in \mathbb{R}^m$, $m := (n+2)|\mathcal{T} \cap \widehat{\mathcal{T}}|$, with, for any $T \in \mathcal{T} \cap \widehat{\mathcal{T}}$, the $(n+2)$ entries $|T|^{1/n}\|f - \alpha Q v_{CR}\|_{L^2(T)}$ and $|T|^{1/(2n)}\|[\nabla_{NC} v_{CR}]_E\|_{L^2(E)}$ for $E \in \mathcal{E}(T)$. Then $\eta(\mathcal{T} \cap \widehat{\mathcal{T}}) = |v|$ for the Euklidean norm $|v|$ of v. In an analogous way with respect to $\widehat{\mathcal{T}}$, $\widehat{\eta}(\mathcal{T} \cap \widehat{\mathcal{T}}) = |\widehat{v}|$ for some $\widehat{v} \in \mathbb{R}^m$. The reverse triangle inequality in $\mathbb{R}^m$ proves that

$$\begin{aligned}
|\eta(\mathcal{T} \cap \widehat{\mathcal{T}}) - \widehat{\eta}(\mathcal{T} \cap \widehat{\mathcal{T}})|^2 &= \big||v| - |\widehat{v}|\big|^2 \le |v - \widehat{v}|^2 \\
&= \sum_{T \in \mathcal{T} \cap \widehat{\mathcal{T}}} \Big(|T|^{1/n} \sum_{E \in \mathcal{E}(T)} \big(\|[\nabla_{NC} v_{CR}]_E\|_{L^2(E)} - \|[\nabla_{NC} \widehat{v}_{CR}]_E\|_{L^2(E)}\big)^2 \\
&\qquad + |T|^{2/n} \big(\|f - \alpha Q v_{CR}\|_{L^2(T)} - \|f - \alpha \widehat{Q} \widehat{v}_{CR}\|_{L^2(T)}\big)^2 \Big).
\end{aligned}$$

The reverse triangle inequality in $L^2(T)$, $n^{1/n}|T|^{1/n} \le h_{\max}$ on $T \in \mathcal{T} \cap \widehat{\mathcal{T}}$, and $\alpha \le 1$ imply

$$|T|^{2/n} \big(\|f - \alpha Q v_{CR}\|_{L^2(T)} - \|f - \alpha \widehat{Q} \widehat{v}_{CR}\|_{L^2(T)}\big)^2 \le \alpha h_{\max}^2 \|Q v_{CR} - \widehat{Q} \widehat{v}_{CR}\|_{L^2(T)}^2 / n^{2/n}.$$

Moreover, the reverse triangle inequality in $L^2(E)$ with $e := \nabla_{NC} v_{CR} - \nabla_{NC} \widehat{v}_{CR} \in P_0(\widehat{\mathcal{T}}; \mathbb{R}^n)$ and the discrete jump control of [CR17, Lem. 5.2] with constant $c_{\mathrm{jc}} \approx 1$ lead to

$$\begin{aligned}
&\sum_{T \in \mathcal{T} \cap \widehat{\mathcal{T}}} |T|^{1/n} \sum_{E \in \mathcal{E}(T)} \big(\|[\nabla_{NC} v_{CR}]_E\|_{L^2(E)} - \|[\nabla_{NC} \widehat{v}_{CR}]_E\|_{L^2(E)}\big)^2 \\
&\qquad \le \sum_{T \in \mathcal{T} \cap \widehat{\mathcal{T}}} |T|^{1/n} \sum_{E \in \mathcal{E}(T)} \|[e]_E\|_{L^2(E)}^2 \le c_{\mathrm{jc}}^2 \|e\|_{L^2(\Omega)}^2.
\end{aligned}$$

This and $\Lambda_1^2 = \max\{h_{\max}^2 / n^{2/n}, c_{\mathrm{jc}}^2\}$ conclude the proof. □

Theorem 5.2 (Reduction) *The constant* $\Lambda_2 = \Lambda_1 \approx 1$ *satisfies*

$$\widehat{\eta}(\widehat{\mathcal{T}} \setminus \mathcal{T}) - 2^{-1/(2n)} \eta(\mathcal{T} \setminus \widehat{\mathcal{T}}) \le \Lambda_2 \delta(\mathcal{T}, \widehat{\mathcal{T}}). \tag{A2}$$

Proof: Similar to the proof of Theorem 5.1, consider some vector $\widehat{v} \in \mathbb{R}^m$, $m := (n+2)|\widehat{\mathcal{T}} \setminus \mathcal{T}|$, with, for any $T \in \widehat{\mathcal{T}} \setminus \mathcal{T}$, the $(n+2)$ entries $|T|^{1/n}\|f - \alpha\widehat{Q}\widehat{v}_{CR}\|_{L^2(T)}$ and $|T|^{1/(2n)}\|[\nabla_{NC}\widehat{v}_{CR}]_E\|_{L^2(E)}$ for $E \in \mathcal{E}(T)$. Furthermore, consider the vector $v \in \mathbb{R}^m$ with entries $|T|^{1/n}\|f - \alpha Q v_{CR}\|_{L^2(T)}$ and $|T|^{1/(2n)}\|[\nabla_{NC} v_{CR}]_E\|_{L^2(E)}$ for any $T \in \widehat{\mathcal{T}} \setminus \mathcal{T}$ and $E \in \mathcal{E}(T)$. Then the triangle inequality in $\mathbb{R}^m$ shows

$$\widehat{\eta}(\widehat{\mathcal{T}} \setminus \mathcal{T}) = |\widehat{v}| \le |\widehat{v} - v| + |v|. \tag{5.1}$$

For any $K \in \mathcal{T} \setminus \widehat{\mathcal{T}}$, $\nabla_{NC} v_{CR} \in P_0(\mathcal{T})$ implies $[\nabla_{NC} v_{CR}]_{\widehat{E}} \equiv 0$ along any $\widehat{E} \in \bigcup_{T \in \widehat{\mathcal{T}}(K)} \mathcal{E}(T)$ with $\widehat{E} \not\subseteq \partial K$. Hence, $|T| \le |K|/2$ for $T \in \widehat{\mathcal{T}}(K)$ proves

$$\begin{aligned}
|v|^2 &= \sum_{K \in \mathcal{T} \setminus \widehat{\mathcal{T}}} \sum_{T \in \widehat{\mathcal{T}}(K)} \Big(|T|^{2/n} \|f - \alpha Q v_{CR}\|^2_{L^2(T)} + |T|^{1/n} \sum_{\widehat{E} \in \mathcal{E}(T)} \|[\nabla_{NC} v_{CR}]_{\widehat{E}}\|^2_{L^2(\widehat{E})} \Big) \\
&\le \sum_{K \in \mathcal{T} \setminus \widehat{\mathcal{T}}} \Big(|K|^{2/n} 2^{-2/n} \|f - \alpha Q v_{CR}\|^2_{L^2(K)} + |K|^{1/n} 2^{-1/n} \sum_{E \in \mathcal{E}(K)} \|[\nabla_{NC} v_{CR}]_E\|^2_{L^2(E)} \Big) \\
&\le 2^{-1/n} \eta^2(\mathcal{T} \setminus \widehat{\mathcal{T}}).
\end{aligned}$$

Analogeously to the proof of Stability (A1) above, reverse triangle inequalities in $L^2(T)$ and $L^2(E)$, the estimate $|T|^{2/n} \le n^{-2/n} h_T^2 \le n^{-2/n} h_{\max}^2$ for any $T \in \widehat{\mathcal{T}} \setminus \mathcal{T}$, and $\alpha \le 1$ lead to

$$\begin{aligned}
|\widehat{v} - v|^2 &= \sum_{T \in \widehat{\mathcal{T}} \setminus \mathcal{T}} \Big(|T|^{2/n} (\|f - \alpha Q v_{CR}\|_{L^2(T)} - \|f - \alpha \widehat{Q}\widehat{v}_{CR}\|_{L^2(T)})^2 \\
&\qquad + |T|^{1/n} \sum_{\widehat{E} \in \mathcal{E}(T)} (\|[\nabla_{NC} v_{CR}]_{\widehat{E}}\|_{L^2(\widehat{E})} - \|[\nabla_{NC} \widehat{v}_{CR}]_{\widehat{E}}\|_{L^2(\widehat{E})})^2 \Big) \\
&\le \sum_{T \in \widehat{\mathcal{T}} \setminus \mathcal{T}} \Big(h_{\max}^2 n^{-2/n} \alpha \|\widehat{Q}\widehat{v}_{CR} - Q v_{CR}\|^2_{L^2(T)} \\
&\qquad + |T|^{1/n} \sum_{\widehat{E} \in \mathcal{E}(T)} \|[\nabla_{NC} \widehat{v}_{CR} - \nabla_{NC} v_{CR}]_{\widehat{E}}\|^2_{L^2(\widehat{E})} \Big).
\end{aligned}$$

The discrete jump control of [CR17, Lem. 5.2] on $\widehat{\mathcal{T}}$ proves

$$\sum_{T \in \widehat{\mathcal{T}} \setminus \mathcal{T}} |T|^{1/n} \sum_{\widehat{E} \in \mathcal{E}(T)} \|[\nabla_{NC} \widehat{v}_{CR} - \nabla_{NC} v_{CR}]_{\widehat{E}}\|^2_{L^2(\widehat{E})} \le c_{\mathrm{jc}}^2 \|\nabla_{NC} \widehat{v}_{CR} - \nabla_{NC} v_{CR}\|_{L^2(\Omega)}.$$

Hence, $|\widehat{v} - v| \le \Lambda_1 \delta(\mathcal{T}, \widehat{\mathcal{T}})$ with $\Lambda_1 = \max\{h_{\max}/n^{1/n}, c_{\mathrm{jc}}\}$ and (5.1) conclude the proof. □

5.2. Discrete Reliability

This subsection is devoted to the proof of discrete reliability (A3) and requires an estimate of the energies $\widehat{E} - E$, where

$$E := -\frac{1}{2}(f, Q v_{CR})_{L^2(\Omega)} \quad \text{and} \quad \widehat{E} := -\frac{1}{2}(f, \widehat{Q}\widehat{v}_{CR})_{L^2(\Omega)}, \tag{5.2}$$

for $\mathcal{T} \in \mathbb{T}$ and its refinement $\widehat{\mathcal{T}} \in \mathbb{T}(\mathcal{T})$ with the notation of Table 3 on p. 33. The reduced problems (R) and ($\hat{\text{R}}$) lead to the alternative representations

$$E := -\frac{1}{2}|||v_{CR}|||_{NC}^2 - \frac{\alpha}{2}\|Qv_{CR}\|_{L^2(\Omega)}^2 \quad \text{and} \quad \widehat{E} := -\frac{1}{2}|||\widehat{v}_{CR}|||_{NC}^2 - \frac{\alpha}{2}\|\widehat{Q}\widehat{v}_{CR}\|_{L^2(\Omega)}^2. \tag{5.3}$$

The proof of discrete reliability utilizes the subsequent identity for the energy differences.

Lemma 5.3 *It holds*

$$\frac{1}{2}\delta^2 + E - \widehat{E} = (f - \alpha Qv_{CR}, \widehat{Q}\widehat{v}_{CR} - QI_{NC}\widehat{v}_{CR})_{L^2(\Omega)}.$$

Proof: Elementary algebra with (5.3) leads to

$$\begin{aligned}\frac{1}{2}\delta^2 - E + \widehat{E} &= \frac{1}{2}(|||\widehat{v}_{CR} - v_{CR}|||_{NC}^2 + |||v_{CR}|||_{NC}^2 - |||\widehat{v}_{CR}|||_{NC}^2) \\ &\quad + \frac{\alpha}{2}(\|\widehat{Q}\widehat{v}_{CR} - Qv_{CR}\|_{L^2(\Omega)}^2 + \|Qv_{CR}\|_{L^2(\Omega)}^2 - \|\widehat{Q}\widehat{v}_{CR}\|_{L^2(\Omega)}^2) \\ &= a_{NC}(v_{CR}, v_{CR} - \widehat{v}_{CR}) + \alpha(Qv_{CR}, Qv_{CR} - \widehat{Q}\widehat{v}_{CR})_{L^2(\Omega)}. \end{aligned} \tag{5.4}$$

The integration property of the nonconforming interpolation operator of Theorem 2.36 implies $a_{NC}(v_{CR}, \widehat{v}_{CR}) = a_{NC}(v_{CR}, I_{NC}\widehat{v}_{CR})$. The same argument with $u_C \in S^1_0(\mathcal{T}) \subset S^1_0(\widehat{\mathcal{T}})$ in the second equations of (R) and ($\hat{\text{R}}$) shows $a_{NC}(u_C, v_{CR}) = 0$ and $a_{NC}(u_C, I_{NC}\widehat{v}_{CR}) = a_{NC}(u_C, \widehat{v}_{CR}) = 0$. This and the first equation of (R) for $w_{CR} := v_{CR} - I_{NC}\widehat{v}_{CR} \in CR^1_0(\mathcal{T})$ results in

$$a_{NC}(v_{CR}, v_{CR} - \widehat{v}_{CR}) = a_{NC}(v_{CR}, w_{CR}) = (f, Qw_{CR})_{L^2(\Omega)} - \alpha(Qv_{CR}, w_{CR}).$$

This and $\alpha(Qv_{CR}, w_{CR})_{L^2(\Omega)} = \alpha(Qv_{CR}, Qv_{CR} - QI_{NC}\widehat{v}_{CR})_{L^2(\Omega)}$ from (3.7) lead in (5.4) to

$$\frac{1}{2}\delta^2 - E + \widehat{E} = (f, Q(v_{CR} - I_{NC}\widehat{v}_{CR}))_{L^2(\Omega)} - \alpha(Qv_{CR}, \widehat{Q}\widehat{v}_{CR} - QI_{NC}\widehat{v}_{CR})_{L^2(\Omega)}.$$

The sum of this and $2E - 2\widehat{E} = (f, \widehat{Q}\widehat{v}_{CR} - Qv_{CR})_{L^2(\Omega)}$ from (5.2) concludes the proof. □

The discrete reliability additionally requires some novel approximation.

Lemma 5.4 *Given $v_{CR} \in CR^1_0(\mathcal{T})$ there exists some $v^*_{CR} \in CR^1_0(\widehat{\mathcal{T}})$ with $v_{CR} = I_{NC}v^*_{CR}$ and $|||v_{CR} - v^*_{CR}|||_{NC} \lesssim \eta(\mathcal{R})$.*

Proof: The operator $J_{\mathrm{dCR}} : CR^1_0(\mathcal{T}) \to CR^1_0(\widehat{\mathcal{T}})$ from Theorem 2.39 defines $J_{\mathrm{dCR}}v_{CR} \in CR^1_0(\widehat{\mathcal{T}})$ with $|||v_{CR} - J_{\mathrm{dCR}}v_{CR}|||_{NC} \le c_{\mathrm{dCR}}\eta(\mathcal{R})$, i.e., the above properties except $I_{NC}J_{\mathrm{dCR}}v_{CR} - v_{CR} = 0$. Define $u_{CR} := I_{NC}(v_{CR} - J_{\mathrm{dCR}}v_{CR}) \in CR^1_0(\mathcal{T})$ and consider the conforming companion $J_n u_{CR} \in S^n_0(\mathcal{T})$ from Theorem 2.37 that satisfies $I_{NC}J_n u_{CR} = u_{CR}$ and $|||(1 - J_n)u_{CR}||| \le c_{\mathrm{apx}}(J_n)|||u_{CR}|||_{NC}$, hence $|||J_n u_{CR}||| \le |||u_{CR}|||_{NC} + |||(1 - J_n)u_{CR}||| \le (1 + c_{\mathrm{apx}}(J_n))|||u_{CR}|||_{NC}$. The boundedness of I_{NC} from Theorem 2.36 with constant 1 proves $|||u_{CR}|||_{NC} \le |||v_{CR} -$

$J_{\mathrm{dCR}} v_{CR}|||_{NC} \le c_{\mathrm{dCR}}\eta(\mathcal{R})$. Hence, the triangle inequality and the boundedness of $\widehat{I}_{NC} : H^1_0(\Omega) \to CR^1_0(\widehat{\mathcal{T}})$ prove that $v^*_{CR} := \widehat{I}_{NC} J_n u_{CR} + J_{\mathrm{dCR}} v_{CR} \in CR^1_0(\widehat{\mathcal{T}})$ satisfies

$$|||v^*_{CR} - v_{CR}|||_{NC} \le |||\widehat{I}_{NC} J_n u_{CR}|||_{NC} + |||J_{\mathrm{dCR}} v_{CR} - v_{CR}|||_{NC} \le (2 + c_{\mathrm{apx}}(J_n)) c_{\mathrm{dCR}} \eta(\mathcal{R}).$$

Since Definition 2.35 of the nonconforming interpolation operator proves $I_{NC}\widehat{I}_{NC} J_n u_{CR} = I_{NC} J_n u_{CR} = u_{CR}$, the definition of u_{CR} implies

$$I_{NC} v^*_{CR} = u_{CR} + I_{NC} J_{\mathrm{dCR}} v_{CR} = v_{CR}. \qquad \square$$

This enables the proof of discrete reliability (A3) with $\widehat{\Lambda}_3 = \Lambda_3 c_{\mathrm{rel}} h^2_{\max}$.

Theorem 5.5 (Discrete reliability) *There exists $\Lambda_3 \approx 1$ such that any $\mathcal{T}$ with admissible refinement $\widehat{\mathcal{T}}$ satisfies*

$$\delta^2(\mathcal{T}, \widehat{\mathcal{T}}) \le \Lambda_3 \big(\eta^2(\mathcal{R}) + \alpha h^2_{\max} \eta^2(\widehat{\mathcal{T}})\big). \tag{A3}$$

Proof: The first substep of this proof deduces a split of δ^2 into four terms. Steps two to five then derive estimates of those terms. The final step condenses these estimates to the proof of the claimed discrete reliability.

Step 1. Rearrangement of the left-hand side. The first equation of (R̂) with test function $v^*_{CR} \in CR^1_0(\widehat{\mathcal{T}})$ from Lemma 5.4 for the solution $v_{CR} \in CR^1_0(\mathcal{T})$ shows

$$0 = a_{NC}(v^*_{CR}, \widehat{v}_{CR}) + a_{NC}(\widehat{u}_C, v^*_{CR}) + \alpha(\widehat{Q}\widehat{v}_{CR}, \widehat{Q} v^*_{CR})_{L^2(\Omega)} - (f, \widehat{Q} v^*_{CR})_{L^2(\Omega)}.$$

The test function $v_{CR} \in CR^1_0(\mathcal{T})$ in (R), $a_{NC}(v_{CR}, v_{CR}) = a_{NC}(I_{NC} v^*_{CR}, v_{CR}) = a_{NC}(v^*_{CR}, v_{CR})$, and algebra for the last term result in

$$\begin{aligned} 0 &= -a_{NC}(v^*_{CR}, v_{CR}) + (f, Q v_{CR})_{L^2(\Omega)} - \alpha(Q v_{CR}, Q v_{CR})_{L^2(\Omega)} \\ &= -a_{NC}(v^*_{CR}, v_{CR}) + (f, Q v_{CR})_{L^2(\Omega)} - \alpha(Q v_{CR}, Q v_{CR} - \widehat{Q} v^*_{CR})_{L^2(\Omega)} \\ &\quad - \alpha(Q v_{CR} - \widehat{Q}\widehat{v}_{CR}, \widehat{Q} v^*_{CR})_{L^2(\Omega)} - \alpha(\widehat{Q}\widehat{v}_{CR}, \widehat{Q} v^*_{CR})_{L^2(\Omega)}. \end{aligned}$$

The sum of these two identities and (5.4) from the proof of Lemma 5.3 proves

$$\begin{aligned} \frac{1}{2}\delta^2 - E + \widehat{E} &= a_{NC}(v_{CR} - v^*_{CR}, v_{CR} - \widehat{v}_{CR}) + a_{NC}(\widehat{u}_C, v^*_{CR}) \\ &\quad + (f - \alpha Q v_{CR}, Q v_{CR} - \widehat{Q} v^*_{CR})_{L^2(\Omega)} + \alpha(Q v_{CR} - \widehat{Q}\widehat{v}_{CR}, Q v_{CR} - \widehat{Q} v^*_{CR})_{L^2(\Omega)}. \end{aligned}$$

The sum of this and the identity of Lemma 5.3 reads

$$\begin{aligned} \delta^2 &= a_{NC}(v_{CR} - v^*_{CR}, v_{CR} - \widehat{v}_{CR}) + a_{NC}(\widehat{u}_C, v^*_{CR}) \\ &\quad + (f - \alpha Q v_{CR}, \widehat{Q}(\widehat{v}_{CR} - v^*_{CR}) + Q(v_{CR} - I_{NC}\widehat{v}_{CR}))_{L^2(\Omega)} \\ &\quad + \alpha(Q v_{CR} - \widehat{Q}\widehat{v}_{CR}, Q v_{CR} - \widehat{Q} v^*_{CR})_{L^2(\Omega)}. \end{aligned} \tag{5.5}$$

The remaining steps estimate the four terms on the right-hand side of this identity.

Step 2. Estimate of the first term. The Cauchy and the Young inequality with $\lambda = 4$ plus the estimate for v_{CR}^* from Lemma 5.4 with constant $C_1 \approx 1$ result in

$$a_{NC}(v_{CR} - v_{CR}^*, v_{CR} - \widehat{v}_{CR}) \le 2|||v_{CR} - v_{CR}^*|||_{NC}^2 + \frac{1}{8}|||v_{CR} - \widehat{v}_{CR}|||_{NC}^2 \le C_1\eta^2(\mathcal{R}) + \frac{1}{8}\delta^2.$$

Step 3. Estimate of the second term. Since $v_{CR} = I_{NC}v_{CR}^*$ in Lemma 5.4, property (2.4) of Theorem 2.36 and (R) prove $0 = a_{NC}(u_C, v_{CR}) = a_{NC}(u_C, I_{NC}v_{CR}^*) = a_{NC}(u_C, v_{CR}^*)$. Hence,

$$a_{NC}(\widehat{u}_C, v_{CR}^*) = a_{NC}(\widehat{u}_C - u_C, v_{CR}^* - v_{CR}) + a_{NC}(\widehat{u}_C, v_{CR}).$$

The Cauchy inequality, Lemma 5.4, and Lemma 3.7 imply

$$a_{NC}(\widehat{u}_C, v_{CR}^*) \lesssim \eta(\mathcal{R})|||\widehat{u}_C - u_C|||.$$

Proposition 3.8 and the Young inequality $\eta(\mathcal{R})\delta \le \eta^2(\mathcal{R}) + \delta^2/4$ result in $C_2 \approx 1$ with

$$a_{NC}(\widehat{u}_C, v_{CR}^*) \le C_2\eta^2(\mathcal{R}) + \delta^2/4.$$

Step 4. Estimate of the third term. The orthogonality (3.8) and $v_{CR} = I_{NC}v_{CR}^*$ prove the split

$$\begin{aligned}(f - \alpha Q v_{CR}, \widehat{Q}(\widehat{v}_{CR} - v_{CR}^*) + Q(v_{CR} - I_{NC}\widehat{v}_{CR}))_{L^2(\Omega)} \\ = (\widehat{Q}f - \alpha Q v_{CR}, (\widehat{Q} - Q)(\widehat{v}_{CR} - v_{CR}^*) + Q(1 - I_{NC})(\widehat{v}_{CR} - v_{CR}^*))_{L^2(\Omega)}.\end{aligned}$$

The orthogonalities $((1 - \widehat{Q})f, (\widehat{Q} - Q)(\widehat{v}_{CR} - v_{CR}^*))_{L^2(\Omega)} = 0$ and $(Q(f - \alpha v_{CR}), (\widehat{Q} - Q)(\widehat{v}_{CR} - v_{CR}^*))_{L^2(\Omega)} = 0$ from (3.8), $(\widehat{Q} - Q)(\widehat{v}_{CR} - v_{CR}^*) = 0$ on $\Omega \setminus \Omega'$ in (3.9) and the piecewise approximation property (3.13) show

$$\begin{aligned}(\widehat{Q}f - \alpha Q v_{CR}, (\widehat{Q} - Q)(\widehat{v}_{CR} - v_{CR}^*))_{L^2(\Omega)} &= ((1 - Q)f, (\widehat{Q} - Q)(\widehat{v}_{CR} - v_{CR}^*))_{L^2(\Omega')} \\ &\le c_Q\|h_{\mathcal{T}}(1 - Q)f\|_{L^2(\Omega')}|||\widehat{v}_{CR} - v_{CR}^*|||_{NC}.\end{aligned}$$

The nestedness $Q\widehat{Q}f = Qf$, $(1 - I_{NC})(\widehat{v}_{CR} - v_{CR}^*)$ on $\bigcup(\mathcal{T} \cap \widehat{\mathcal{T}}) = \Omega \setminus \Omega'$, and the interpolation error estimate (2.5) from Theorem 2.36 lead to

$$\begin{aligned}(\widehat{Q}f - \alpha Q v_{CR}, Q(1 - I_{NC})(\widehat{v}_{CR} - v_{CR}^*))_{L^2(\Omega)} &= (Q(f - \alpha v_{CR}), (1 - I_{NC})(\widehat{v}_{CR} - v_{CR}^*))_{L^2(\Omega')} \\ &\le \kappa_{NC}\|h_{\mathcal{T}}Q(f - \alpha v_{CR})\|_{L^2(\Omega')}|||\widehat{v}_{CR} - v_{CR}^*|||_{NC}.\end{aligned}$$

The Cauchy inequality in $\mathbb{R}^2$ and the orthogonality (3.10) with $v = h_{\mathcal{T}}f$, $w = \alpha h_{\mathcal{T}}v_{CR}$ proves

$$c_Q\|h_{\mathcal{T}}(1 - Q)f\|_{L^2(\Omega')} + \kappa_{NC}\|h_{\mathcal{T}}Q(f - \alpha v_{CR})\|_{L^2(\Omega')} = (c_Q^2 + \kappa_{NC}^2)\|h_{\mathcal{T}}(f - \alpha Q v_{CR})\|_{L^2(\Omega')}.$$

The previous four displayed inequalities and $h_{\mathcal{T}} \le c_{\mathrm{sr}}^{1/n}H_{\mathcal{T}}$ lead to

$$\begin{aligned}(f - \alpha Q v_{CR}, \widehat{Q}(\widehat{v}_{CR} - v_{CR}^*) + Q(v_{CR} - I_{NC}\widehat{v}_{CR}))_{L^2(\Omega)} \\ \lesssim \|h_{\mathcal{T}}(f - \alpha Q v_{CR})\|_{L^2(\Omega')}|||\widehat{v}_{CR} - v_{CR}^*|||_{NC} \lesssim \eta(\mathcal{R})|||\widehat{v}_{CR} - v_{CR}^*|||_{NC}.\end{aligned}$$

The triangle inequality and Lemma 5.4 prove

$$|||\widehat{v}_{CR} - v^*_{CR}|||_{NC} \le |||\widehat{v}_{CR} - v_{CR}|||_{NC} + |||v_{CR} - v^*_{CR}|||_{NC} \lesssim \delta + \eta(\mathcal{R}).$$

Consequently, the Young inequality $\eta(\mathcal{R})\delta \le \eta^2(\mathcal{R}) + \delta^2/4$ leads to a final estimate of the third term in the right-hand side of Step 1, with $C_3 \approx 1$ that satisfies

$$(f - \alpha Q v_{CR}, \widehat{Q}(\widehat{v}_{CR} - v^*_{CR}) + Q(v_{CR} - I_{NC}\widehat{v}_{CR}))_{L^2(\Omega)} \le C_3\eta^2(\mathcal{R}) + \delta^2/4.$$

Step 5. Estimate of the fourth term. The split $Qv_{CR} - \widehat{Q}v^*_{CR} = -\widehat{Q}(1 - I_{NC})v^*_{CR} + (Q - \widehat{Q})v_{CR}$, the Cauchy and Young inequality for $\lambda = 2$ in the first term, and the orthogonality $(Qv_{CR} - Q\widehat{v}_{CR}, (Q - \widehat{Q})v_{CR})_{L^2(\Omega)} = 0$ from (3.8) in the second term prove

$$\begin{aligned}\alpha(Qv_{CR} - \widehat{Q}\widehat{v}_{CR}, Qv_{CR} - \widehat{Q}v^*_{CR})_{L^2(\Omega)} &= \frac{\alpha}{4}\|Qv_{CR} - \widehat{Q}\widehat{v}_{CR}\|^2_{L^2(\Omega)} + \alpha\|\widehat{Q}(1 - I_{NC})v^*_{CR}\|^2_{L^2(\Omega)} \\ &\quad + \alpha((Q - \widehat{Q})\widehat{v}_{CR}, (Q - \widehat{Q})v_{CR})_{L^2(\Omega)}. \qquad (5.6)\end{aligned}$$

The boundedness of $\widehat{Q}$ from (3.6), the interpolation error estimate from Theorem 2.36 and $(1 - I_{NC})v^*_{CR} = v^*_{CR} - v_{CR}$ in the estimate of Lemma 5.4 prove

$$\alpha\|\widehat{Q}(1 - I_{NC})v^*_{CR}\|^2_{L^2(\Omega)} \le \kappa^2_{NC}\alpha h^2_{\max}|||(1 - I_{NC})v^*_{CR}|||^2_{NC} \lesssim \alpha h^2_{\max}\eta^2(\mathcal{R}). \qquad (5.7)$$

The Cauchy inequality, the discrete approximation inequality (3.13), $|||v_{CR}|||_{NC} \le |||\widehat{v}_{CR} - v_{CR}|||_{NC} + |||\widehat{v}_{CR}|||_{NC}$, and the Young inequality with $\lambda = 2$ prove

$$\begin{aligned}\alpha((\widehat{Q} - Q)\widehat{v}_{CR}, (\widehat{Q} - Q)v_{CR})_{L^2(\Omega)} &\le \alpha\|(\widehat{Q} - Q)\widehat{v}_{CR}\|_{L^2(\Omega)}\|(\widehat{Q} - Q)v_{CR}\|_{L^2(\Omega)} \\ &\le \alpha c^2_{\mathrm{Q}} h^2_{\max}|||\widehat{v}_{CR}|||_{NC}|||v_{CR}|||_{NC} \\ &\le (\alpha c^2_{\mathrm{Q}} h^2_{\max} + \alpha^2 c^4_{\mathrm{Q}} h^4_{\max})|||\widehat{v}_{CR}|||^2_{NC} + \frac{1}{4}|||\widehat{v}_{CR} - v_{CR}|||^2_{NC}. \qquad (5.8)\end{aligned}$$

The combination of (5.6)-(5.8) with $|||\widehat{v}_{CR}|||_{NC} \le c_{\mathrm{rel}}\widehat{\eta}$ from Corollary 3.3 leads to $C_4 \approx 1$ with

$$\alpha(Qv_{CR} - \widehat{Q}\widehat{v}_{CR}, Qv_{CR} - \widehat{Q}v^*_{CR})_{L^2(\Omega)} \le \frac{1}{4}\delta^2 + C_4\eta^2(\mathcal{R}) + C_4\alpha h^2_{\max}\widehat{\eta}^2.$$

Step 6. Finish of the proof. The identity from Step 1 and the estimates from Steps 2–5 condense to

$$\delta^2 \le (C_1 + C_2 + C_3 + C_4)\eta^2(\mathcal{R}) + \frac{7}{8}\delta^2 + C_4\alpha h^2_{\max}\widehat{\eta}^2.$$

The absorption of $7\delta^2/8$ into the left-hand side concludes the proof with $\Lambda_3 = 8(C_1 + C_2 + C_3 + C_4)$. □

5.3. Quasiorthogonality

This section is devoted to the proof of a weaker form of quasiorthogonality with some parameter $\varepsilon > 0$ that implies (A4) for ε sufficiently small in Subsection 5.4. Its proof relies on the two subsequent lemmas that employ the notation of Table 3 on p. 33 for a triangulation $\mathcal{T}$ and a refinement $\widehat{\mathcal{T}} \in \mathbb{T}(\mathcal{T})$. They contain estimates for δ and the energies based on the identity from Lemma 5.3 and an estimate for the volume error estimator terms.

Lemma 5.6 *With constants $\kappa_{NC} \approx 1 \approx c_{\mathrm{Q}}$ from Theorem 2.36 and* (3.5)*, any $\varrho > 0$ satisfies*

$$\frac{1}{4}\delta^2 + E - \widehat{E} \leq \kappa_{NC}^2 c_{\mathrm{sr}}^{2/n} \|H_{\mathcal{T}}(\widehat{Q}f - \alpha Q v_{CR})\|_{L^2(\Omega')}^2 + \frac{c_{\mathrm{Q}}^2 c_{\mathrm{sr}}^{2/n}}{2\varrho} \|H_{\mathcal{T}}(\widehat{Q} - Q)f\|_{L^2(\Omega)}^2 + \frac{\varrho}{2} |||\widehat{v}_{CR}|||_{NC}^2.$$

Proof: The local definition of I_{NC} implies $\widehat{v}_{CR} = I_{NC}\widehat{v}_{CR}$ a.e. in $\Omega \setminus \Omega'$. With this and

$$(Q(f - \alpha v_{CR}), (\widehat{Q} - Q)\widehat{v}_{CR})_{L^2(\Omega)} = 0 = ((1 - \widehat{Q})f, Q(\widehat{v}_{CR} - I_{NC}\widehat{v}_{CR}))_{L^2(\Omega)}$$

from (3.8), the right-hand side in Lemma 5.3 reads

$$\begin{aligned}&(f - \alpha Q v_{CR}, (\widehat{Q} - Q)\widehat{v}_{CR})_{L^2(\Omega)} + (f - \alpha Q v_{CR}, Q(\widehat{v}_{CR} - I_{NC}\widehat{v}_{CR}))_{L^2(\Omega)} \\ &\quad = ((\widehat{Q} - Q)f, (\widehat{Q} - Q)\widehat{v}_{CR})_{L^2(\Omega)} + (\widehat{Q}f - \alpha Q v_{CR}, Q(\widehat{v}_{CR} - I_{NC}\widehat{v}_{CR}))_{L^2(\Omega')}.\end{aligned}$$

Hence, Lemma 5.3, the Cauchy inequality, the discrete approximation property (3.13), the boundedness and linearity of Q in $\|h_{\mathcal{T}}^{-1} Q(\widehat{v}_{CR} - I_{NC}\widehat{v}_{CR})\|_{L^2(\Omega')} \leq \|h_{\mathcal{T}}^{-1}(\widehat{v}_{CR} - I_{NC}\widehat{v}_{CR})\|_{L^2(\Omega)}$, and the nonconforming interpolation error estimate (2.5) from Theorem 2.36 prove

$$\begin{aligned}\frac{1}{2}\delta^2 + E - \widehat{E} &\leq c_{\mathrm{Q}} \|h_{\mathcal{T}}(\widehat{Q} - Q)f\|_{L^2(\Omega)} |||\widehat{v}_{CR}|||_{NC} \\ &\qquad + \kappa_{NC} \|h_{\mathcal{T}}(\widehat{Q}f - \alpha Q v_{CR})\|_{L^2(\Omega')} |||\widehat{v}_{CR} - I_{NC}\widehat{v}_{CR}|||_{NC}.\end{aligned}$$

Theorem 2.36 implies $|||\widehat{v}_{CR} - I_{NC}\widehat{v}_{CR}|||_{NC} \leq |||\widehat{v}_{CR} - v_{CR}|||_{NC} \leq \delta$. Hence, the Young inequality with $\lambda = 2$ and the absorption of $\delta^2/4$ into the left-hand side result in

$$\frac{1}{4}\delta^2 + E - \widehat{E} \leq c_{\mathrm{Q}} \|h_{\mathcal{T}}(\widehat{Q} - Q)f\|_{L^2(\Omega)} |||\widehat{v}_{CR}|||_{NC} + \kappa_{NC}^2 \|h_{\mathcal{T}}(\widehat{Q}f - \alpha Q v_{CR})\|_{L^2(\Omega')}^2.$$

The application of the Young inequality with $\lambda = \varrho$ on the term $c_{\mathrm{Q}} \|h_{\mathcal{T}}(\widehat{Q} - Q)f\|_{L^2(\Omega)} |||\widehat{v}_{CR}|||_{NC}$ and the pointwise estimate $h_{\mathcal{T}}^2 \leq c_{\mathrm{sr}}^{2/n} H_{\mathcal{T}}^2$ conclude the proof. □

Lemma 5.7 *Any $0 < \lambda \leq 2$ satisfies*

$$\begin{aligned}&\|H_{\mathcal{T}}(\widehat{Q}f - \alpha Q v_{CR})\|_{L^2(\Omega')}^2/4 + \|H_{\widehat{\mathcal{T}}}\widehat{Q}(f - \alpha\widehat{v}_{CR})\|_{L^2(\Omega)}^2 \\ &\qquad \leq (1 + \lambda)\|H_{\mathcal{T}}(\widehat{Q} - Q)f\|_{L^2(\Omega)}^2 + (1 + \lambda)\|H_{\mathcal{T}} Q(f - \alpha v_{CR})\|_{L^2(\Omega)}^2 \\ &\qquad\quad + (1 + \lambda^{-1}) h_{\max}^2 \alpha^2 n^{-2/n} \|\widehat{Q}\widehat{v}_{CR} - Q v_{CR}\|_{L^2(\Omega)}^2.\end{aligned}$$

Proof: Let $g := \widehat{Q}f - \alpha Q v_{CR}$ and $\widehat{g} := \widehat{Q}f - \alpha\widehat{Q}\widehat{v}_{CR}$. Since $2H^2_{\widehat{\mathcal{T}}} \le H^2_{\mathcal{T}}$ a.e. in Ω', $H^2_{\mathcal{T}}/4 \le H^2_{\mathcal{T}} - 3H^2_{\widehat{\mathcal{T}}}/2$ a.e. in Ω'. Consequently,

$$\|H_{\mathcal{T}} g\|^2_{L^2(\Omega')}/4 \le \|H_{\mathcal{T}} g\|^2_{L^2(\Omega')} - 3\|H_{\widehat{\mathcal{T}}} g\|^2_{L^2(\Omega')}/2. \tag{5.9}$$

The triangle and Young inequality show that any $\lambda > 0$ satisfies

$$\|H_{\widehat{\mathcal{T}}}\widehat{g}\|^2_{L^2(\Omega')} \le (1+\lambda)\|H_{\widehat{\mathcal{T}}} g\|^2_{L^2(\Omega')} + (1+\lambda^{-1})\|H_{\widehat{\mathcal{T}}}(\widehat{g}-g)\|^2_{L^2(\Omega')}. \tag{5.10}$$

For $\lambda = 1/2$, the combination of (5.9)-(5.10) proves

$$\|H_{\mathcal{T}} g\|^2_{L^2(\Omega')}/4 + \|H_{\widehat{\mathcal{T}}}\widehat{g}\|^2_{L^2(\Omega')} \le \|H_{\mathcal{T}} g\|^2_{L^2(\Omega')} + 3\|H_{\widehat{\mathcal{T}}}(\widehat{g}-g)\|^2_{L^2(\Omega')}.$$

This and the pointwise estimate $2H^2_{\widehat{\mathcal{T}}} \le H^2_{\mathcal{T}} \le h^2_{\max} n^{-2/n}$ a.e. in Ω' lead to

$$\|H_{\mathcal{T}} g\|^2_{L^2(\Omega')}/4 + \|H_{\widehat{\mathcal{T}}}\widehat{g}\|^2_{L^2(\Omega')} \le \|H_{\mathcal{T}} g\|^2_{L^2(\Omega')} + 3h^2_{\max} n^{-2/n}\alpha^2\|\widehat{Q}\widehat{v}_{CR} - Q v_{CR}\|^2_{L^2(\Omega')}/2. \tag{5.11}$$

The Young inequality and $H_{\mathcal{T}} = H_{\widehat{\mathcal{T}}}$ a.e. in $\Omega'' := \Omega \setminus \Omega'$ show

$$\|H_{\widehat{\mathcal{T}}}\widehat{g}\|^2_{L^2(\Omega'')} \le (1+\lambda)\|H_{\mathcal{T}} g\|^2_{L^2(\Omega'')} + (1+\lambda^{-1})h^2_{\max}\alpha^2 n^{-2/n}\|\widehat{Q}\widehat{v}_{CR} - Q v_{CR}\|_{L^2(\Omega'')}.$$

Since $\lambda \le 2$ implies $3/2 \le 1 + \lambda^{-1}$, the sum of this with (5.11) leads to

$$\begin{aligned}\|H_{\mathcal{T}}(\widehat{Q}f - \alpha Q v_{CR})\|^2_{L^2(\Omega')}/4 &+ \|H_{\widehat{\mathcal{T}}}\widehat{Q}(f - \alpha\widehat{v}_{CR})\|^2_{L^2(\Omega)} \\ &\le (1+\lambda)\|H_{\mathcal{T}}(\widehat{Q}f - \alpha Q v_{CR})\|^2_{L^2(\Omega)} + (1+\lambda^{-1})h^2_{\max}\alpha^2 n^{-2/n}\|\widehat{Q}\widehat{v}_{CR} - Q v_{CR}\|^2_{L^2(\Omega)}.\end{aligned}$$

The orthogonality $\|H_{\mathcal{T}}(\widehat{Q}f - \alpha Q v_{CR})\|^2_{L^2(\Omega)} = \|H_{\mathcal{T}}(\widehat{Q} - Q)f\|^2_{L^2(\Omega)} + \|H_{\mathcal{T}} Q(f - \alpha v_{CR})\|^2_{L^2(\Omega)}$ in (3.12) concludes the proof. □

The proof of quasiorthogonality with ε utilizes constants $c_{\mathrm{dF}}, \kappa_{NC}, c_{\mathrm{Q}}, c_{\mathrm{rel}} \approx 1$ from Theorems 2.29 and 2.36, the approximation property (3.5) and Corollary 3.3.

Theorem 5.8 (Quasiorthogonality with $\varepsilon > 0$) *For any $\varepsilon > 0$, there exist $\Lambda_4(\varepsilon), c(\varepsilon) \approx 1$ such that for $\alpha h_{\max} \le c(\varepsilon)$ (i.e., $\alpha = 0$ or $\mathcal{T}_0 \in \mathbb{T}(c(\varepsilon)/\alpha)$), any $\ell, m \in \mathbb{N}_0$, and the output $(\mathcal{T}_k)_{k\in\mathbb{N}_0}$ of Algorithm 1 satisfy*

$$\sum_{k=\ell}^{\ell+m} \delta^2(\mathcal{T}_k, \mathcal{T}_{k+1}) \le \Lambda_4 \eta^2(\mathcal{T}_\ell) + \varepsilon \sum_{k=\ell}^{\ell+m} \eta^2(\mathcal{T}_k). \tag{A4$_\varepsilon$}$$

Proof: Consider the solutions $(v_k, u_k) \in CR^1_0(\mathcal{T}_k) \times S^1_0(\mathcal{T}_k)$ to (R) on $\mathcal{T}_k$ and denote the corresponding energies E_k from Definition (5.2), $\Omega_k := \mathrm{int}(\bigcup(\mathcal{T}_k \setminus \mathcal{T}_{k+1}))$, $Q_k := Q_{\mathcal{T}_k}$, $h_k := h_{\mathcal{T}_k}$, $H_k := H_{\mathcal{T}_k}$, $\eta_k := \eta(\mathcal{T}_k)$. In this notation, for any $0 < \varrho \le 1$, Lemma 5.6 reads

$$\begin{aligned}\frac{1}{4}\delta^2(\mathcal{T}_k, \mathcal{T}_{k+1}) \le E_{k+1} - E_k &+ \kappa^2_{NC} c^{2/n}_{\mathrm{sr}} \|H_k(Q_{k+1}f - \alpha Q_k v_k)\|^2_{L^2(\Omega_k)} \\ &+ c^2_{\mathrm{Q}} c^{2/n}_{\mathrm{sr}}/(2\varrho)\|H_k(Q_{k+1} - Q_k)f\|^2_{L^2(\Omega)} + \varrho|||v_{k+1}|||^2_{NC}/2.\end{aligned}$$

The sum of this over all levels from ℓ to $\ell+m$ employs a telescoping sum for E_k, the estimates $\varrho|||v_{\ell+m+1}|||^2_{NC}/2 + E_{\ell+m+1} \le 0$, $-E_\ell \le (1+\alpha c_{\mathrm{dF}})|||v_\ell|||^2_{NC}/2$ from (5.3), and the discrete Friedrichs inequality and proves

$$\begin{aligned}\frac{1}{4}\sum_{k=\ell}^{\ell+m}\delta^2(\mathcal{T}_k,\mathcal{T}_{k+1}) &\le E_{\ell+m+1} - E_\ell + \kappa_{NC}^2 c_{\mathrm{sr}}^{2/n}\sum_{k=\ell}^{\ell+m}\|H_k(Q_{k+1}f - \alpha Q_k v_k)\|^2_{L^2(\Omega_k)}\\ &\quad + c_{\mathrm{Q}}^2 c_{\mathrm{sr}}^{2/n}/(2\varrho)\sum_{k=\ell}^{\ell+m}\|H_k(Q_{k+1}-Q_k)f\|^2_{L^2(\Omega)} + \varrho\sum_{k=\ell}^{\ell+m}|||v_{k+1}|||^2_{NC}/2\\ &\le (1+\alpha c_{\mathrm{dF}})|||v_\ell|||^2_{NC}/2 + \kappa_{NC}^2 c_{\mathrm{sr}}^{2/n}\sum_{k=\ell}^{\ell+m}\|H_k(Q_{k+1}f - \alpha Q_k v_k)\|^2_{L^2(\Omega_k)}\\ &\quad + c_{\mathrm{Q}}^2 c_{\mathrm{sr}}^{2/n}/(2\varrho)\sum_{k=\ell}^{\ell+m}\|H_k(Q_{k+1}-Q_k)f\|^2_{L^2(\Omega)} + \varrho\sum_{k=\ell+1}^{\ell+m}|||v_k|||^2_{NC}/2. \qquad (5.12)\end{aligned}$$

The first sum on the right-hand side is treated with Lemma 5.7, which reads

$$\begin{aligned}\|H_k(Q_{k+1}f - \alpha Q_k v_k)\|^2_{L^2(\Omega_k)} &\le -4\|H_{k+1}Q_{k+1}(f-\alpha v_{k+1})\|^2_{L^2(\Omega)}\\ &\quad + 4(1+\lambda)\|H_k(Q_{k+1}-Q_k)f\|^2_{L^2(\Omega)} + 4(1+\lambda)\|H_kQ_k(f-\alpha v_k)\|^2_{L^2(\Omega)}\\ &\quad + 4(1+\lambda^{-1})h_{\max}^2\alpha^2 n^{-2/n}\|Q_{k+1}v_{k+1} - Q_k v_k\|^2_{L^2(\Omega)}.\end{aligned}$$

A telescoping sum for the terms $\|H_kQ_k(f-\alpha v_k)\|^2_{L^2(\Omega)}$ leads to the factor 4λ in

$$\begin{aligned}\sum_{k=\ell}^{\ell+m}\|H_k(Q_{k+1}f - \alpha Q_k v_k)\|^2_{L^2(\Omega_k)} &\le 4\|H_\ell Q_\ell(f-\alpha v_\ell)\|^2_{L^2(\Omega)}\\ &\quad + 4(1+\lambda)\sum_{k=\ell}^{\ell+m}\|H_k(Q_{k+1}-Q_k)f\|^2_{L^2(\Omega)} + 4\lambda\sum_{k=\ell}^{\ell+m}\|H_kQ_k(f-\alpha v_k)\|^2_{L^2(\Omega)}\\ &\quad + 4(1+\lambda^{-1})h_{\max}^2\alpha^2 n^{-2/n}\sum_{k=\ell}^{\ell+m}\|Q_{k+1}v_{k+1} - Q_k v_k\|^2_{L^2(\Omega)}.\end{aligned}$$

This estimate in (5.12) leads to

$$\begin{aligned}\frac{1}{4}\sum_{k=\ell}^{\ell+m}\delta^2(\mathcal{T}_k,\mathcal{T}_{k+1}) &\le (1+\alpha c_{\mathrm{dF}})|||v_\ell|||^2_{NC}/2 + 4\kappa_{NC}^2 c_{\mathrm{sr}}^{2/n}\|H_\ell Q_\ell(f-\alpha v_\ell)\|^2_{L^2(\Omega)}\\ &\quad + (4\kappa_{NC}^2 c_{\mathrm{sr}}^{2/n}(1+\lambda) + c_{\mathrm{Q}}^2 c_{\mathrm{sr}}^{2/n}/(2\varrho))\sum_{k=\ell}^{\ell+m}\|H_k(Q_{k+1}-Q_k)f\|^2_{L^2(\Omega)}\\ &\quad + 4\kappa_{NC}^2 c_{\mathrm{sr}}^{2/n}\lambda\sum_{k=\ell}^{\ell+m}\|H_kQ_k(f-\alpha v_k)\|^2_{L^2(\Omega)} + \varrho\sum_{k=\ell+1}^{\ell+m}|||v_k|||^2_{NC}/2\\ &\quad + 4\kappa_{NC}^2 c_{\mathrm{sr}}^{2/n}(1+\lambda^{-1})h_{\max}^2\alpha^2 n^{-2/n}\sum_{k=\ell}^{\ell+m}\|Q_{k+1}v_{k+1} - Q_k v_k\|^2_{L^2(\Omega)}.\end{aligned}$$

Recall that $\|Q_{k+1}v_{k+1} - Q_k v_k\|_{L^2(\Omega)} \le \delta_{k,k+1}$ so that, provided the initial mesh-size $h_{\max}$ is so small that $4\kappa_{NC}^2 c_{\mathrm{sr}}^{2/n}(1+\lambda^{-1})h_{\max}^2\alpha^2 n^{-2/n} \le 1/8$, the absorption of this into the left-hand

side shows

$$\begin{aligned}\frac{1}{8}\sum_{k=\ell}^{\ell+m}\delta^2(\mathcal{T}_k,\mathcal{T}_{k+1}) &\le (1+\alpha c_{\mathrm{dF}})|||v_\ell|||_{NC}^2/2 + 4\kappa_{NC}^2 c_{\mathrm{sr}}^{2/n}\|H_\ell Q_\ell(f-\alpha v_\ell)\|_{L^2(\Omega)}^2\\ &\quad + (4\kappa_{NC}^2 c_{\mathrm{sr}}^{2/n}(1+\lambda) + c_{\mathrm{Q}}^2 c_{\mathrm{sr}}^{2/n}/(2\varrho))\sum_{k=\ell}^{\ell+m}\|H_k(Q_{k+1}-Q_k)f\|_{L^2(\Omega)}^2\\ &\quad + 4\kappa_{NC}^2 c_{\mathrm{sr}}^{2/n}\lambda\sum_{k=\ell}^{\ell+m}\|H_kQ_k(f-\alpha v_k)\|_{L^2(\Omega)}^2 + \varrho\sum_{k=\ell+1}^{\ell+m}|||v_k|||_{NC}^2/2. \qquad (5.13)\end{aligned}$$

The orthogonality (3.10) in $\|H_kQ_k(f-\alpha v_k)\|_{L^2(\Omega)}^2 = \|H_k(f-\alpha Q_k v_k)\|_{L^2(\Omega)}^2 - \|H_k(f-Q_kf)\|_{L^2(\Omega)}^2$ plus $c_{\mathrm{rel}}^{-1}|||v_k|||_{NC}^2 + \|H_k(f-\alpha Q_k v_k)\|_{L^2(\Omega)}^2 \le \eta_k^2$ from Corollary 3.3 and $h_k^2 \le c_{\mathrm{sr}}^{2/n}H_k^2$ imply

$$\begin{aligned}&4\kappa_{NC}^2 c_{\mathrm{sr}}^{2/n}\lambda\sum_{k=\ell}^{\ell+m}\|H_kQ_k(f-\alpha v_k)\|_{L^2(\Omega)}^2 + \varrho\sum_{k=\ell+1}^{\ell+m}|||v_k|||_{NC}^2/2\\ &\quad\le \max\{4\kappa_{NC}^2 c_{\mathrm{sr}}^{2/n}\lambda, c_{\mathrm{rel}}\varrho/2\}\sum_{k=\ell}^{\ell+m}\eta_k^2 - 4\kappa_{NC}^2 c_{\mathrm{sr}}^{2/n}\lambda\sum_{k=\ell}^{\ell+m}\|H_k(f-Q_kf)\|_{L^2(\Omega)}^2. \qquad (5.14)\end{aligned}$$

Moreover, (3.11) implies $\|H_k(Q_{k+1}-Q_k)f\|_{L^2(\Omega)}^2 \le \|H_k(f-Q_kf)\|_{L^2(\Omega)}^2$ and Lemma 3.6 proves

$$\begin{aligned}&(4\kappa_{NC}^2 c_{\mathrm{sr}}^{2/n}(1+\lambda) + c_{\mathrm{Q}}^2 c_{\mathrm{sr}}^{2/n}/(2\varrho))\sum_{k=\ell}^{\ell+m}\|H_k(Q_{k+1}-Q_k)f\|_{L^2(\Omega)}^2\\ &\qquad - 4\kappa_{NC}^2 c_{\mathrm{sr}}^{2/n}\lambda\sum_{k=\ell}^{\ell+m}\|H_k(f-Q_kf)\|_{L^2(\Omega)}^2\\ &\qquad\le (4\kappa_{NC}^2 c_{\mathrm{sr}}^{2/n} + c_{\mathrm{Q}}^2 c_{\mathrm{sr}}^{2/n}/(2\varrho))\sum_{k=\ell}^{\ell+m}\|H_k(Q_{k+1}-Q_k)f\|_{L^2(\Omega)}^2\\ &\qquad\le (4\kappa_{NC}^2 c_{\mathrm{sr}}^{2/n} + c_{\mathrm{Q}}^2 c_{\mathrm{sr}}^{2/n}/(2\varrho))\|H_\ell(f-Q_\ell f)\|_{L^2(\Omega)}^2. \qquad (5.15)\end{aligned}$$

The combination of (5.13)-(5.15) and the orthogonality $\|H_\ell Q_\ell(f-\alpha v_\ell)\|_{L^2(\Omega)}^2 + \|H_\ell(f-Q_\ell f)\|_{L^2(\Omega)}^2 = \|H_\ell(f-\alpha Q_\ell v_\ell)\|_{L^2(\Omega)}^2$ in (3.10) show

$$\begin{aligned}\frac{1}{8}\sum_{k=\ell}^{\ell+m}\delta^2(\mathcal{T}_k,\mathcal{T}_{k+1}) &\le (1+\alpha c_{\mathrm{dF}})|||v_\ell|||_{NC}^2/2 + (4\kappa_{NC}^2 c_{\mathrm{sr}}^{2/n} + c_{\mathrm{Q}}^2 c_{\mathrm{sr}}^{2/n}/(2\varrho))\|H_\ell(f-\alpha Q_\ell v_\ell)\|_{L^2(\Omega)}^2\\ &\quad + \max\{4\kappa_{NC}^2 c_{\mathrm{sr}}^{2/n}\lambda, c_{\mathrm{rel}}\varrho/2\}\sum_{k=\ell}^{\ell+m}\eta_k^2.\end{aligned}$$

The reliability from Corollary 3.3 and the choice of $0<\lambda=\lambda(\varepsilon)$, $\varrho=\varrho(\varepsilon)\le 1$ such that $4\max\{8\kappa_{NC}^2 c_{\mathrm{sr}}^{2/n}\lambda, 4c_{\mathrm{rel}}\varrho\}\le\varepsilon$ concludes the proof with $c(\varepsilon) := (32\kappa_{NC}^2 c_{\mathrm{sr}}^{2/n}(1+\lambda^{-1})n^{-2/n})^{-1/2}$ and $\Lambda_4(\varepsilon) := 4\max\{(1+\alpha c_{\mathrm{dF}})c_{\mathrm{rel}}, c_{\mathrm{sr}}^{2/n}(8\kappa_{NC}^2 + c_{\mathrm{Q}}^2/\varrho)\}$. □

5.4. Optimal Convergence Rates

This subsection recapitulates the optimal convergence rates of [CR17, Thm. 2.1]. The proof also shows that the condition of a sufficiently small initial mesh-size is not necessary for $\alpha = 0$.

Theorem 5.9 (Optimal rates) *There exists $c > 0$ such that for $\alpha h_{\max} \le c$, i.e., $\alpha = 0$ or $\mathcal{T}_0 \in \mathbb{T}(c/\alpha)$, and sufficiently small bulk parameter θ, the output $(\mathcal{T}_k)_{k=1,2,\dots}$ of the AFEM algorithm with corresponding quantities $\eta_k := \eta(\mathcal{T}_k)$ and any $s > 0$ satisfy*

$$\sup_{\ell\in\mathbb{N}_0} (1 + |\mathcal{T}_\ell| - |\mathcal{T}_0|)^s \eta_\ell \approx \sup_{N\in\mathbb{N}_0} (1+N)^s \min\{\eta(\mathcal{T}) \,|\, \mathcal{T} \in \mathbb{T} \text{ with } |\mathcal{T}| - |\mathcal{T}_0| \le N\}.$$

Proof: Theorems 5.1, 5.2, and 5.5 imply (A1)–(A3) from [CR17]. Consider $\varepsilon_0 := (1-\varrho_{12})/\Lambda_{12}$ from [CR17, Thm 3.1] with ϱ_{12}, Λ_{12} depending on the bulk-parameter $\theta < \theta_0 := (1+\Lambda_1^2\Lambda_3)^{-1}$, Λ_1, Λ_2, and $\varrho_2 := 2^{-1/(2n)}$. Choose ε small enough such that $\varepsilon < \varepsilon_0$ and $h_{\max} < 1$ with $\alpha h_{\max} \le c := \min\{c(\varepsilon), (\Lambda_1^2+\Lambda_2^2)^{-1}\Lambda_3^{-1}\}$ for $c(\varepsilon)$ from Theorem 5.8. This choice leads to $(\Lambda_1^2+\Lambda_2^2)\Lambda_3\alpha h_{\max}^2 < 1$ and so [CR17, Thm 3.2] implies quasimonotonicity (QM). Furthermore, since $\varepsilon < \varepsilon_0$ in Theorem 5.8, [CR17, Thm 3.1] proves (A4):=(A4)$_0$. In conclusion, [CR17, Thm 2.1] applies to collective marking (this is a particular case $\mu \equiv 0$ in that paper) and provides optimal convergence rates as displayed in the assertion. □

Theorem 5.9 provides optimal convergence rates in terms of the error estimator. The equivalence of the error estimator and the total error of Subsection 3.5 and Theorem 5.9 imply optimal convergence rates with respect to the concept of nonlinear approximation classes [BDD04; CFPP14; Ste07; CKNS08].

6. A Priori Analysis of Weighted Least-Squares Methods

Given $M_0 \in P_0(\mathcal{T};\mathbb{S})$ piecewise symmetric and positive definite (SPD) and $F_0 \in P_0(\mathcal{T};\mathbb{R}^n)$, the generalized or *weighted least-squares formulation* of this thesis computes the minimizer $(p_{LS}, u_{LS}) \in RT_0(\mathcal{T}) \times S^1_0(\mathcal{T})$ of the functional

$$LS(f,\mathcal{T};q_{RT},v_C) := \|M_0^{-1/2}(\Pi_0 q_{RT} - \nabla v_C + F_0)\|^2_{L^2(\Omega)} + \|\Pi_0 f + \operatorname{div} q_{RT}\|^2_{L^2(\Omega)} \tag{6.1}$$

amongst $(q_{RT}, v_C) \in RT_0(\mathcal{T}) \times S^1_0(\mathcal{T})$.

The standard div-LS FEM [BG09] is based on the functional

$$LS(f;q_{RT},v_C) = \|q_{RT} - \nabla v_C\|^2_{L^2(\Omega)} + \|f + \operatorname{div} q_{RT}\|^2_{L^2(\Omega)}. \tag{6.2}$$

The well-known equivalence for this standard least-squares functional (6.2) with constant from [CS18] states that any $(q_{RT}, v_C) \in RT_0(\mathcal{T}) \times S^1_0(\mathcal{T})$ satisfies

$$c_{\mathrm{LS}}^{-1}(\|q_{RT}\|^2_{H(\mathrm{div})} + |||v_C|||^2) \le LS(0;q_{RT},v_C) \le c_{\mathrm{LS}}(\|q_{RT}\|^2_{H(\mathrm{div})} + |||v_C|||^2). \tag{6.3}$$

Similar to the standard least-squares methods [CP15], the presence of an extra data approximation term μ in the a posteriori error estimate below requires the separate marking strategy from Algorithm 2 for the weighted least-squares method. The respective error estimator η and data approximation μ read, for $K \in \mathcal{T}$ and the solution $(p_{LS}, u_{LS}) \in RT_0(\mathcal{T}) \times S^1_0(\mathcal{T})$ to (6.1), as

$$\eta^2(K) := |K|^{2/n}\|\operatorname{div} p_{LS}\|^2_{L^2(K)} + |K|^{1/n}\sum_{E\in\mathcal{E}(K)}\|[M_0^{-1}(\Pi_0 p_{LS} - \nabla u_{LS} + F_0)]_E\|^2_{L^2(E)}, \tag{6.4}$$

$$\mu^2(K) := \|(1-\Pi_0)f\|^2_{L^2(K)}, \quad \sigma^2(K) := \eta^2(K) + \mu^2(K). \tag{6.5}$$

6.1. Well-Posedness

The minimization of (6.1) is equivalent to the discrete Euler-Lagrange equations that seek $(p_{LS}, u_{LS}) \in RT_0(\mathcal{T}) \times S^1_0(\mathcal{T})$ such that any $(q_{RT}, v_C) \in RT_0(\mathcal{T}) \times S^1_0(\mathcal{T})$ satisfies

$$0 = (M_0^{-1}(\Pi_0 p_{LS} - \nabla u_{LS} + F_0), \Pi_0 q_{RT} - \nabla v_C)_{L^2(\Omega)} + (\Pi_0 f + \operatorname{div} p_{LS}, \operatorname{div} q_{RT})_{L^2(\Omega)}. \tag{LS}$$

Lemma 6.1 *There exists a unique solution* $(p_{LS}, u_{LS}) \in RT_0(\mathcal{T}) \times S^1_0(\mathcal{T})$ *to the discrete Euler-Lagrange equations* (LS).

Proof: It suffices to show that the seminorm $(\|\operatorname{div} q_{RT}\|^2_{L^2(\Omega)} + \|M_0^{-1/2}(\Pi_0 q_{RT} - \nabla v_C)\|^2_{L^2(\Omega)})^{1/2}$ on $RT_0(\mathcal{T}) \times S^1_0(\mathcal{T})$ is positive definite. Let $(q_{RT}, v_C) \in RT_0(\mathcal{T}) \times S^1_0(\mathcal{T})$ with $0 = \|\operatorname{div} q_{RT}\|^2_{L^2(\Omega)} + \|M_0^{-1/2}(\Pi_0 q_{RT} - \nabla v_C)\|^2_{L^2(\Omega)}$, then $\operatorname{div} q_{RT} = 0$ and the piecewise positive definiteness of

M_0, hence, invertibility of $M_0^{-1/2}$ proves $\nabla v_C = \Pi_0 q_{RT}$. Furthermore, Remark 2.11 shows $q_{RT} = \Pi_0 q_{RT}$. The equivalence (6.3) for the standard least-squares functional shows

$$\begin{aligned} c_{\mathrm{LS}}^{-1}(\|q_{RT}\|_{H(\mathrm{div})}^2 + |||v_C|||^2) &\le \|\operatorname{div} q_{RT}\|_{L^2(\Omega)}^2 + \|q_{RT} - \nabla v_C\|_{L^2(\Omega)}^2 \\ &= \|\operatorname{div} q_{RT}\|_{L^2(\Omega)}^2 + \|(1-\Pi_0) q_{RT}\|_{L^2(\Omega)}^2 = 0. \end{aligned}$$

Since this implies $q_{RT} = 0$ and $v_C = 0$, the bounded bilinear form $(M_0^{-1}(\Pi_0 \bullet - \nabla \bullet), \Pi_0 \bullet - \nabla \bullet)_{L^2(\Omega)} + (\operatorname{div} \bullet, \operatorname{div} \bullet)_{L^2(\Omega)}$ of the discrete Euler-Lagrange equations (LS) is positive definite and the application of the Lax-Milgram lemma [Bra07, Thm 2.5, p. 38] concludes the proof.□

6.2. Conditions on Weights

This subsection contains some conditions on the weight functions $M_0 \in P_0(\mathcal{T}; \mathbb{S})$ and $F_0 \in P_0(\mathcal{T}; \mathbb{R}^n)$ presented as general as possible for the proof of the axioms of adaptivity in Section 8 and including the weights for the dPG methods of Section 7. For any $A \in \mathbb{R}^{\ell \times \ell}$, recall the spectral radius $\varrho(A) := \max\{|\lambda| \,|\, \lambda \text{ eigenvalue of } A\}$. For symmetric matrices, the spectral radius coincides with the spectral norm [Mey00, p. 281] and is therefore submultiplicative with respect to the Euklidean norm, i.e., any $A \in \mathbb{S}$ and $v \in \mathbb{R}^\ell$ satisfy $|Av| \le \varrho(A)|v|$.

Positive definiteness. Suppose that given any $\mathcal{T} \in \mathbb{T}$, there exists $M_0 := M_0^{(\mathcal{T})} \in P_0(\mathcal{T}; \mathbb{S})$ that is piecewise SPD so that $M_0|_T \in \mathbb{S}$ has the eigenvalues $0 < \lambda_1(T) \le \cdots \le \lambda_n(T)$ and

$$0 < \underline{\lambda}(\mathcal{T}) := \min_{T \in \mathcal{T}} \lambda_1(T) \le \max_{T \in \mathcal{T}} \lambda_n(T) =: \overline{\lambda}(\mathcal{T}) < \infty.$$

Uniform boundedness. Suppose that there exist uniform upper and lower bounds $\underline{\lambda}, \overline{\lambda} \approx 1$ for the eigenvalues of $M_0 \in P_0(\mathcal{T}; \mathbb{S})$,

$$0 < \underline{\lambda} \le \min_{\mathcal{T} \in \mathbb{T}} \underline{\lambda}(\mathcal{T}) \le \max_{\mathcal{T} \in \mathbb{T}} \overline{\lambda}(\mathcal{T}) \le \overline{\lambda} < \infty. \tag{6.6}$$

Assume that there exist $F_0 := F_0^{(\mathcal{T})} \in P_0(\mathcal{T}; \mathbb{R}^n)$, $\kappa_1(\mathcal{T})$, and $\kappa_1 \lesssim 1$ with

$$\|F_0\|_{L^2(\Omega)} \le \kappa_1(\mathcal{T}) \|(1-\Pi_0) f\|_{L^2(\Omega)} \le \kappa_1 \|(1-\Pi_0) f\|_{L^2(\Omega)}. \tag{6.7}$$

Convergence at refinement. Suppose that for any $\varepsilon > 0$, there exists $\delta > 0$ such that any $\mathcal{T} \in \mathbb{T}(\delta) = \{\mathcal{T} \in \mathbb{T} \,|\, h_{\mathcal{T}} \le \delta \text{ a.e. in } \Omega\}$ and any refinement $\widehat{\mathcal{T}} \in \mathbb{T}(\mathcal{T})$ with corresponding $M_0 \in P_0(\mathcal{T}; \mathbb{S})$ and $\widehat{M}_0 \in P_0(\widehat{\mathcal{T}}; \mathbb{S})$ satisfy

$$\varrho(\widehat{M}_0^{-1/2}, M_0^{-1/2}) := \big\| \varrho\big(\widehat{M}_0^{-1/2} - M_0^{-1/2}\big) \big\|_{L^\infty(\Omega)} < \varepsilon \quad \text{and } \kappa_1(\mathcal{T}) < \varepsilon. \tag{6.8}$$

Remark 6.2 (Eigenvalues of powers of M_0) The condition of uniform boundedness above states that all eigenvalues of M_0 lie in $[\underline{\lambda}, \overline{\lambda}]$ for any triangulation. Hence, the eigenvalues of $M_0^{1/2}$ belong to $[\underline{\lambda}^{1/2}, \overline{\lambda}^{1/2}]$, the eigenvalues of M_0^{-1} belong to $[\overline{\lambda}^{-1}, \underline{\lambda}^{-1}]$, and the eigenvalues of $M_0^{-1/2}$ belong to $[\overline{\lambda}^{-1/2}, \underline{\lambda}^{-1/2}]$. This is utilized throughout this thesis in estimates of the form $\|A_0 g\|_{L^2(\Omega)} \le \max_{T \in \mathcal{T}} \varrho(A_0|_T) \|g\|_{L^2(\Omega)}$ for any $g \in L^2(\Omega; \mathbb{R}^n)$, $A_0 \in P_0(\mathcal{T}; \mathbb{S})$ piecewise SPD.

The subsequent lemma proves the above assumptions for the special cases of M_0 and F_0 from Table 5 on p. 60 employed in the dPG methods of Subsection 7. Recall $S(\mathcal{T}) = \Pi_0((\bullet - \mathrm{mid}(\mathcal{T})) \otimes (\bullet - \mathrm{mid}(\mathcal{T}))) \in P_0(\mathcal{T};\mathbb{S})$ and $H_0 f = \Pi_0(f(\bullet - \mathrm{mid}(\mathcal{T}))) \in P_0(\mathcal{T};\mathbb{R}^n)$ for $f \in L^2(\Omega)$ from Definition 2.10 on p. 15.

Lemma 6.3 (Examples for M_0, F_0) *Consider fixed parameters $\delta_1 \geq 1$, $\delta_2 \geq 0$, $\delta_3 \geq 0$. Then $M_0 := \delta_1 I_{n\times n} + \delta_2 S(\mathcal{T}) \in P_0(\mathcal{T};\mathbb{S})$ and $F_0 := \delta_3 H_0 f \in P_0(\mathcal{T};\mathbb{R}^n)$ satisfy the three above properties with $\underline{\lambda} = \delta_1$, $\overline{\lambda} = \delta_1 + \delta_2 h_{\max}^2$, $\kappa_1 = \delta_3 h_{\max} \lesssim 1$ and $\varrho(\widehat{M}_0^{-1/2}, M_0^{-1/2}) \leq 2\delta_2^{-1/2} h_{\max}$.*

Proof: The properties (6.7) and (6.8) for F_0 directly follow from $\Pi_0(f(\bullet - \mathrm{mid}(\mathcal{T}))) = \Pi_0((f - \Pi_0 f)(\bullet - \mathrm{mid}(\mathcal{T})))$, the Cauchy inequality, and the estimate $\|\bullet - \mathrm{mid}(\mathcal{T})\|_{L^2(\Omega)} \leq h_{\max} H_{\mathcal{T}}^{n/2}$. Let $T \in \mathcal{T}$ and abbreviate $S_T = S(\mathcal{T})|_T \in \mathbb{S}$. Since the matrix valued function $(\bullet - \mathrm{mid}(T)) \otimes (\bullet - \mathrm{mid}(T))$ is positive semi-definite a.e. in Ω, its integral mean S_T is positive semi-definite as well. The invariance of the trace of a matrix under similarity transformations [Mey00, p. 256] implies that the eigenvalues $0 \leq \lambda_1, \dots, \lambda_n$ of S_T satisfy

$$\max\{\lambda_1, \dots, \lambda_n\} \leq \lambda_1 + \cdots + \lambda_n = \mathrm{tr}(S_T) = |T|^{-1} \int_T |x - \mathrm{mid}(T)|^2 \,\mathrm{d}x \leq n h_T^2/(n+1) \leq h_{\max}^2.$$

Since the matrices $\delta_1 I_{n\times n}$ and $\delta_2 S_T$ commute, they are simultaneously diagonizable [Mey00, p. 522] and hence, their eigenvalues add up. Consequently, $M_0|_T = \delta_1 I_{n\times n} + \delta_2 S_T$ has eigenvalues in $[\delta_1, \delta_1 + \delta_2 h_{\max}^2]$ and is piecewise SPD.

Given any $\mathcal{T} \in \mathbb{T}$ and any refinement $\widehat{\mathcal{T}} \in \mathbb{T}(\mathcal{T})$, Remark 6.2 shows that the eigenspectra of $M_0^{-1/2}$ and $\widehat{M}_0^{-1/2}$ are contained in $[(\delta_1 + \delta_2 h_{\max}^2)^{-1/2}, \delta_1^{-1/2}]$. In particular, $\delta_1^{-1/2} I_{n\times n} - M_0^{-1/2}$ is piecewise positive semi-definite with $\|\varrho(\delta_1^{-1/2} I_{n\times n} - M_0^{-1/2})\|_{L^\infty(\Omega)} \leq \delta_1^{-1/2} - (\delta_1 + \delta_2 h_{\max}^2)^{-1/2}$. For any $a \geq 1$ and $b > 0$, it holds $1 \leq a^{1/2}(a+b)^{1/2}$. This and the triangle inequality $(a+b)^{1/2} \leq a^{1/2} + b^{1/2}$ imply

$$0 \leq a^{-1/2} - (a+b)^{-1/2} \leq \frac{a^{-1/2} - (a+b)^{-1/2}}{a^{-1/2}(a+b)^{-1/2}} = (a+b)^{1/2} - a^{1/2} \leq b^{1/2}.$$

Hence, $\delta_1^{-1/2} - (\delta_1 + \delta_2 h_{\max}^2)^{-1/2} \leq \delta_2^{-1/2} h_{\max}$. An analogous estimate for the eigenspectrum of $\delta_1^{-1/2} I_{n\times n} - \widehat{M}_0^{-1/2}$ and a triangle inequality for the spectral norm leads to

$$\begin{aligned}\big\|\varrho\big(\widehat{M}_0^{-1/2} - M_0^{-1/2}\big)\big\|_{L^\infty(\Omega)} &\leq \big\|\varrho\big(\widehat{M}_0^{-1/2} - \delta_1^{-1/2} I_{n\times n}\big)\big\|_{L^\infty(\Omega)} + \big\|\varrho\big(\widehat{\delta}_1^{-1/2} I_{n\times n} - M_0^{-1/2}\big)\big\|_{L^\infty(\Omega)} \\ &\leq 2\delta_2^{-1/2} h_{\max}.\end{aligned}$$

Hence, $h_{\max} \to 0$ implies $\varrho(\widehat{M}_0^{-1/2}, M_0^{-1/2}) \to 0$. This concludes the proof of (6.8). □

6.3. Norm Equivalence

Theorem 6.4 *The exact solution $u \in H_0^1(\Omega)$ to the Poisson model problem (1.3) with $p = \nabla u \in H(\mathrm{div},\Omega)$ and any discrete $(q_{RT}, v_C) \in RT_0(\mathcal{T}) \times S_0^1(\mathcal{T})$ satisfy the equivalence*

$$\|p - q_{RT}\|_{H(\mathrm{div},\Omega)}^2 + |||u - v_C|||^2 \approx LS(f, \mathcal{T}; q_{RT}, v_C) + \|(1-\Pi_0) f\|_{L^2(\Omega)}^2 + \|(1-\Pi_0) q_{RT}\|_{L^2(\Omega)}^2.$$

Proof: The equivalence (6.3) for the standard least-squares functional and the L^2-orthogonality of $(1-\Pi_0)q_{RT}$ and $(1-\Pi_0)f$ onto piecewise constants implies

$$\begin{aligned}
c_{\mathrm{LS}}^{-1}(\|p-q_{RT}\|_{H(\mathrm{div},\Omega)}^2+|||u-v_C|||^2) &\le \|f+\operatorname{div} q_{RT}\|_{L^2(\Omega)}^2+\|q_{RT}-\nabla v_C\|_{L^2(\Omega)}^2\\
&= \|\Pi_0 f+\operatorname{div} q_{RT}\|_{L^2(\Omega)}^2+\|\Pi_0 q_{RT}-\nabla v_C\|_{L^2(\Omega)}^2\\
&\quad +\|(1-\Pi_0)f\|_{L^2(\Omega)}^2+\|(1-\Pi_0)q_{RT}\|_{L^2(\Omega)}^2.
\end{aligned}$$

The triangle inequality, Remark 6.2 for $A_0=M_0^{1/2}$ with spectral radius bounded by $\overline{\lambda}^{1/2}$, and $\|F_0\|_{L^2(\Omega)}\le\kappa_1\|(1-\Pi_0)f\|_{L^2(\Omega)}$ from (6.7) result in

$$\begin{aligned}
&c_{\mathrm{LS}}^{-1}(\|p-q_{RT}\|_{H(\mathrm{div},\Omega)}^2+|||u-v_C|||^2)\\
&\quad\le \|\Pi_0 f+\operatorname{div} q_{RT}\|_{L^2(\Omega)}^2+2\|\Pi_0 q_{RT}-\nabla v_C+F_0\|_{L^2(\Omega)}^2+2\|F_0\|_{L^2(\Omega)}^2\\
&\qquad +\|(1-\Pi_0)f\|_{L^2(\Omega)}^2+\|(1-\Pi_0)q_{RT}\|_{L^2(\Omega)}^2\\
&\quad\le \|\Pi_0 f+\operatorname{div} q_{RT}\|_{L^2(\Omega)}^2+2\overline{\lambda}\|M_0^{-1/2}(\Pi_0 q_{RT}-\nabla v_C+F_0)\|_{L^2(\Omega)}^2+2\|F_0\|_{L^2(\Omega)}^2\\
&\qquad +\|(1-\Pi_0)f\|_{L^2(\Omega)}^2+\|(1-\Pi_0)q_{RT}\|_{L^2(\Omega)}^2\\
&\quad\le \max\{1+2\kappa_1^2,2\overline{\lambda}\}\big(LS(f,\mathcal{T};q_{RT},v_C)+\|(1-\Pi_0)f\|_{L^2(\Omega)}^2+\|(1-\Pi_0)q_{RT}\|_{L^2(\Omega)}^2\big).
\end{aligned}$$

The proof of the converse estimate departs from Remark 6.2 in $\|M_0^{-1/2}(\Pi_0 q_{RT}-\nabla v_C+F_0)\|_{L^2(\Omega)}^2\le\underline{\lambda}^{-1}\|\Pi_0 q_{RT}-\nabla v_C+F_0\|_{L^2(\Omega)}^2$ and the triangle inequality to show

$$\begin{aligned}
&LS(f,\mathcal{T};q_{RT},v_C)+\|(1-\Pi_0)f\|_{L^2(\Omega)}^2+\|(1-\Pi_0)q_{RT}\|_{L^2(\Omega)}^2\\
&\quad\le 2\underline{\lambda}^{-1}\|\Pi_0 q_{RT}-\nabla v_C\|_{L^2(\Omega)}^2+2\underline{\lambda}^{-1}\|F_0\|_{L^2(\Omega)}^2+\|\Pi_0 f+\operatorname{div} q_{RT}\|_{L^2(\Omega)}^2\\
&\qquad +\|(1-\Pi_0)f\|_{L^2(\Omega)}^2+\|(1-\Pi_0)q_{RT}\|_{L^2(\Omega)}^2\\
&\quad\le 2\underline{\lambda}^{-1}\|\Pi_0 q_{RT}-\nabla v_C\|_{L^2(\Omega)}^2+\|\Pi_0 f+\operatorname{div} q_{RT}\|_{L^2(\Omega)}^2\\
&\qquad +(1+2\kappa_1^2\underline{\lambda}^{-1})\|(1-\Pi_0)f\|_{L^2(\Omega)}^2+\|(1-\Pi_0)q_{RT}\|_{L^2(\Omega)}^2.
\end{aligned}$$

The abovementioned orthogonalities of $(1-\Pi_0)q_{RT}$ and $(1-\Pi_0)f$ onto $P_0(\mathcal{T})$, $f+\operatorname{div} p=0$, and another triangle inequality with $p=\nabla u$ imply

$$\begin{aligned}
&LS(f,\mathcal{T};q_{RT},v_C)+\|(1-\Pi_0)f\|_{L^2(\Omega)}^2+\|F_0\|_{L^2(\Omega)}^2+\|(1-\Pi_0)q_{RT}\|_{L^2(\Omega)}^2\\
&\quad\le \max\{2\underline{\lambda}^{-1},1+2\kappa_1^2\underline{\lambda}^{-1}\}\big(\|q_{RT}-\nabla v_C\|_{L^2(\Omega)}^2+\|f+\operatorname{div} q_{RT}\|_{L^2(\Omega)}^2\big)\\
&\quad\le 2\max\{2\underline{\lambda}^{-1},1+2\kappa_1^2\underline{\lambda}^{-1}\}\big(\|p-q_{RT}\|_{H(\mathrm{div},\Omega)}^2+|||u-v_C|||^2\big).
\end{aligned}$$

□

Example 6.5 For $f\equiv 0$ and hence $F_0\equiv 0$ from (6.7), the standard least-squares equivalence (6.3) and the estimate $\|(1-\Pi_0)q_{RT}\|_{L^2(\Omega)}\lesssim\|\operatorname{div} q_{RT}\|_{L^2(\Omega)}\le LS(0,\mathcal{T};q_{RT},v_C)$ from the split in Remark 2.11 lead to the equivalence $\|q_{RT}\|_{H(\mathrm{div},\Omega)}^2+|||v_C|||^2\approx LS(0,\mathcal{T};q_{RT},v_C)$. This is the equivalence from Theorem 6.4 without the term $\|(1-\Pi_0)q_{RT}\|_{L^2(\Omega)}$. Nevertheless, the following counterexample shows that for general $f\neq 0$, the term $\|(1-\Pi_0)q_{RT}\|_{L^2(\Omega)}$ in the estimate of Theorem 6.4 cannot be omitted.

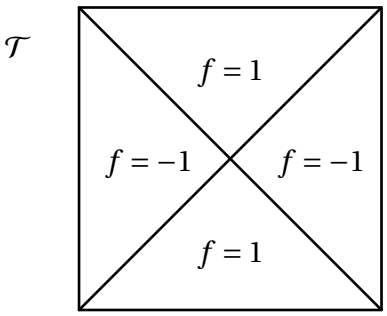

Figure 9: Criss-cross triangulation of the unit square in Example 6.5.

For a class of counterexamples, consider a uniform triangulation $\mathcal{T}$ with $\min_{T\in\mathcal{T}} |T| = \max_{T\in\mathcal{T}} |T|$, and suppose that $|\{T \in \mathcal{T} \mid z \in \mathcal{N}(T)\}|$ an even number for any $z \in \mathcal{N}$, e.g., as in the criss-cross triangulation of Figure 9. Then the choice of $f \in P_0(\mathcal{T})$ such that $f|_T \in \{+1,-1\}$ on $T \in \mathcal{T}$ and $f|_{T_+} = -f|_{T_-}$ on any pair of neighboring triangles $T_\pm \in \mathcal{T}$ that share an edge is possible and assumption (6.7) implies $F_0 = 0$. Let $T_+, T_- \in \mathcal{T}$ with $E = \partial T_+ \cap \partial T_- \in \mathcal{E}(\Omega)$ and ν_E its unit normal vector. Since $|T_+| = |T_-|$ and elementary geometry imply $|\operatorname{conv}\{E, \operatorname{mid}(T_+)\}| = |\operatorname{conv}\{E, \operatorname{mid}(T_-)\}|$, it follows $(\bullet - \operatorname{mid}(T_+)) \cdot \nu_E \equiv \operatorname{dist}(\operatorname{mid}(T_+), E) = \operatorname{dist}(\operatorname{mid}(T_-), E) \equiv -(\bullet - \operatorname{mid}(T_-)) \cdot \nu_E$ along E. Hence, the normal component of $q_{RT} := -f(\bullet - \operatorname{mid}(\mathcal{T}))/n \in RT_0^{NC}(\mathcal{T})$ along edges is continuous, i.e., $[q_{RT} \cdot \nu_E]_E = 0$ for any $E \in \mathcal{E}(\Omega)$ and consequently $q_{RT} \in H(\operatorname{div}, \Omega)$ [BBF13, p. 57]. Then $q_{RT} \in RT_0(\mathcal{T})$ satisfies $\Pi_0 q_{RT} = 0$ and $\operatorname{div} q_{RT} + \Pi_0 f = 0$. Hence, for $v_C = 0$, the right-hand side in Theorem 6.4 without the term $\|(1-\Pi_0)q_{RT}\|_{L^2(\Omega)}$ reads $LS(f, \mathcal{T}; q_{RT}, 0) + \|(1-\Pi_0)f\|^2_{L^2(\Omega)} = 0$. But $f \not\equiv 0$ implies $u \not\equiv 0$ for the solution $(p,u) \in H(\operatorname{div}, \Omega) \times H^1_0(\Omega)$ to the Poisson model problem. Consequently, the left-hand side of Theorem 6.4 is $0 < |||u||| \le \|p - q_{RT}\|^2_{H(\operatorname{div},\Omega)} + |||u - v_C|||^2$ for $v_C = 0$. Consequently, the estimate from Theorem 6.4 without the term $\|(1-\Pi_0)q_{RT}\|_{L^2(\Omega)}$ *cannot* hold in general.

6.4. Global Error Control

Whereas the right-hand side of the estimate in Theorem 6.4 leads to a natural error estimator, the lack of a mesh-size factor in it leads to the severe difficulty to prove axiom (A2). Motivated by the alternative error estimator [CP15] and the estimate of the jump terms in Lemma 3.2 for the reduced mixed methods, this section establishes reliability and efficiency of the estimator σ defined in (6.4)-(6.5) for the generalized least-squares methods.

Lemma 6.6 *Any $V_\mathcal{T} \in H^1(\mathcal{T}; \mathbb{R}^n)$ with the L^2-orthogonality $V_\mathcal{T} \perp (\{q_{RT} \in RT_0(\mathcal{T}) \mid \operatorname{div} q_{RT} = 0\} \oplus \nabla S^1_0(\mathcal{T})) \subset P_0(\mathcal{T}; \mathbb{R}^n)$ satisfies $\Pi_0 V_\mathcal{T} \in \nabla_{NC} CR^1_0(\mathcal{T})$ and*

$$\|V_\mathcal{T}\|^2_{L^2(\Omega)} \lesssim \sum_{T\in\mathcal{T}} |T|^{1/n} \sum_{E\in\mathcal{E}(T)} \|[\Pi_0 V_\mathcal{T}]_E\|^2_{L^2(E)} + \|h_\mathcal{T} \nabla_{NC} V_\mathcal{T}\|^2_{L^2(\Omega)}.$$

If $V_\mathcal{T} \in P_k(\mathcal{T}; \mathbb{R}^n)$ for some $k \in \mathbb{N}_0$, the reverse estimate holds as well.

Proof: Lemma 2.25 shows that the solution $w_{CR} \in CR_0^1(\mathcal{T})$ to

$$(\nabla_{NC} w_{CR}, \nabla_{NC} v_{CR})_{L^2(\Omega)} = (\Pi_0 V_{\mathcal{T}}, \nabla_{NC} v_{CR})_{L^2(\Omega)} \quad \text{for all } v_{CR} \in CR_0^1(\mathcal{T})$$

satisfies $\Pi_0 V_{\mathcal{T}} - \nabla_{NC} w_{CR} \in \{q_{RT} \in RT_0(\mathcal{T}) \mid \operatorname{div} q_{RT} = 0\}$. The orthogonality of $V_{\mathcal{T}}$, and thus $\Pi_0 V_{\mathcal{T}}$ onto $\{q_{RT} \in RT_0(\mathcal{T}) \mid \operatorname{div} q_{RT} = 0\} \subseteq P_0(\mathcal{T};\mathbb{R}^n)$ implies the orthogonality of $\Pi_0 V_{\mathcal{T}} - \nabla_{NC} w_{CR}$ onto this space. Consequently, $\Pi_0 V_{\mathcal{T}} = \nabla_{NC} w_{CR}$ and $\nabla_{NC} w_{CR} \perp \nabla S_0^1(\mathcal{T})$ in $L^2(\Omega)$. Hence, the application of Lemma 3.2 on w_{CR} leads to

$$\|\Pi_0 V_{\mathcal{T}}\|_{L^2(\Omega)}^2 \approx \sum_{T\in\mathcal{T}} |T|^{1/n} \sum_{E\in\mathcal{E}(T)} \|[\Pi_0 V_{\mathcal{T}}]_E\|_{L^2(E)}^2.$$

Since the orthogonality of $(1-\Pi_0) V_{\mathcal{T}}$ onto $\Pi_0 V_{\mathcal{T}}$ shows the split $\|V_{\mathcal{T}}\|_{L^2(\Omega)}^2 = \|\Pi_0 V_{\mathcal{T}}\|_{L^2(\Omega)}^2 + \|(1-\Pi_0) V_{\mathcal{T}}\|_{L^2(\Omega)}^2$, the Poincare inequality from Theorem 2.30 shows $\|V_{\mathcal{T}}\|_{L^2(\Omega)}^2 \lesssim \|\Pi_0 V_{\mathcal{T}}\|_{L^2(\Omega)}^2 + \|h_{\mathcal{T}} \nabla_{NC} V_{\mathcal{T}}\|_{L^2(\Omega)}^2$ and thus, the claimed estimate. The inverse inequality $\|h_{\mathcal{T}} \nabla_{NC} V_{\mathcal{T}}\|_{L^2(\Omega)} \lesssim \|V_{\mathcal{T}}\|_{L^2(\Omega)}$ concludes the proof of the reverse estimate in case $V_{\mathcal{T}} \in P_k(\mathcal{T};\mathbb{R}^n)$. □

Lemma 6.7 *The solution* $(p_{LS}, u_{LS}) \in RT_0(\mathcal{T}) \times S_0^1(\mathcal{T})$ *to the discrete Euler-Lagrange equations* (LS) *satisfies*

$$\begin{aligned} LS(f, \mathcal{T}; p_{LS}, u_{LS}) &\approx \|M_0^{-1}(\Pi_0 p_{LS} - \nabla u_{LS} + F_0)\|_{L^2(\Omega)}^2 \\ &\approx \sum_{T\in\mathcal{T}} |T|^{1/n} \sum_{E\in\mathcal{E}(T)} \|[M_0^{-1}(\Pi_0 p_{LS} - \nabla u_{LS} + F_0)]_E\|_{L^2(E)}^2. \end{aligned}$$

In particular, there exist $c_{\mathrm{rel}}, c_{\mathrm{eff}} \approx 1$ *with*

$$\begin{aligned} c_{\mathrm{rel}}^{-1} \max\{\|M_0^{-1}(\Pi_0 p_{LS} - \nabla u_{LS} + F_0)\|_{L^2(\Omega)}^2, LS(f, \mathcal{T}; p_{LS}, u_{LS})\} \\ \leq \sum_{T\in\mathcal{T}} |T|^{1/n} \sum_{E\in\mathcal{E}(T)} \|[M_0^{-1}(\Pi_0 p_{LS} - \nabla u_{LS} + F_0)]_E\|_{L^2(E)}^2 \\ \leq c_{\mathrm{eff}} \|M_0^{-1}(\Pi_0 p_{LS} - \nabla u_{LS} + F_0)\|_{L^2(\Omega)}^2. \end{aligned}$$

Proof: Set $V_0 := M_0^{-1}(\Pi_0 p_{LS} - \nabla u_{LS} + F_0) \in P_0(\mathcal{T};\mathbb{R}^n)$. The inf-sup stability of the Raviart-Thomas finite element functions [Bra07, p. 151] leads to the existence of $q_{RT} \in RT_0(\mathcal{T})$ with $(\Pi_0 f + \operatorname{div} p_{LS}, \operatorname{div} q_{RT})_{L^2(\Omega)} = \|\Pi_0 f + \operatorname{div} p_{LS}\|_{L^2(\Omega)}^2$ and $\|q_{RT}\|_{H(\operatorname{div},\Omega)} \lesssim \|\Pi_0 f + \operatorname{div} p_{LS}\|_{L^2(\Omega)}$. This, the discrete Euler-Lagrange equations (LS), and the Cauchy inequality imply

$$\begin{aligned} \|\Pi_0 f + \operatorname{div} p_{LS}\|_{L^2(\Omega)}^2 &= (\Pi_0 f + \operatorname{div} p_{LS}, \operatorname{div} q_{RT})_{L^2(\Omega)} = -(V_0, q_{RT})_{L^2(\Omega)} \\ &\lesssim \|V_0\|_{L^2(\Omega)} \|\Pi_0 f + \operatorname{div} p_{LS}\|_{L^2(\Omega)}. \end{aligned}$$

Consequently, Remark 6.2 shows the first of the claimed equivalences,

$$\begin{aligned} LS(f, \mathcal{T}; p_{LS}, u_{LS}) &= \|M_0^{1/2} V_0\|_{L^2(\Omega)}^2 + \|\Pi_0 f + \operatorname{div} p_{LS}\|_{L^2(\Omega)}^2 \\ &\approx \|V_0\|_{L^2(\Omega)}^2 + \|\Pi_0 f + \operatorname{div} p_{LS}\|_{L^2(\Omega)}^2 \approx \|V_0\|_{L^2(\Omega)}^2. \end{aligned}$$

The discrete Euler-Lagrange equations (LS) imply $V_0 \perp \{q_{RT} \in RT_0(\mathcal{T}) \mid \operatorname{div} q_{RT} = 0\} \oplus \nabla S_0^1(\mathcal{T})$. Hence, Lemma 6.6 concludes the proof. □

The application of Lemma 6.7, the equivalence from Theorem 6.4, and $\|(1-\Pi_0)p_{LS}\|^2_{L^2(K)} \approx |K|^{2/n}\|\operatorname{div} p_{LS}\|^2_{L^2(K)}$ for any $K \in \mathcal{T}$ yield the a posteriori error control of the alternative error estimator σ defined in (6.4)-(6.5).

Corollary 6.8 (Reliability and efficiency) It holds $\sigma^2(\mathcal{T}) \approx \|p-p_{LS}\|^2_{H(\operatorname{div},\Omega)} + |||u-u_{LS}|||^2$.□

	M_0	F_0
Primal dPG	$I_{n\times n} + S(\mathcal{T})$	$H_0 f$
Dual dPG	$I_{n\times n}$	0
Primal Mixed dPG	$2I_{n\times n} + S(\mathcal{T})$	$H_0 f$
Ultraweak dPG	$2I_{n\times n} + S(\mathcal{T})$	$H_0 f$

Table 5: Piecewise constant weight functions M_0 and F_0

7. dPG as a Weighted Least-Squares Method

The following section connects the minimal residual formulation (minRes) on p. 20 of four dPG methods to the weighted least-squares method (6.1) for the different weights $M_0 \in P_0(\mathcal{T};\mathbb{S})$ and $F_0 \in P_0(\mathcal{T};\mathbb{R}^n)$ in Table 5. Recall the functions $S(\mathcal{T}) \in P_0(\mathcal{T};\mathbb{S})$, $S(\mathcal{T}) = \Pi_0((\bullet - \mathrm{mid}(\mathcal{T})) \otimes (\bullet - \mathrm{mid}(\mathcal{T})))$ and $s(\mathcal{T}) = \mathrm{tr}\, S(\mathcal{T}) \in P_0(\mathcal{T})$, and the operator $H_0 : L^2(\Omega) \to P_0(\mathcal{T};\mathbb{R}^n)$, $H_0 f = \Pi_0(f(\bullet - \mathrm{mid}(\mathcal{T})))$ from Definition 2.10. Furthermore, the proofs of this section utilize the basis functions $\chi_T \in P_0(\mathcal{T})$ for $T \in \mathcal{T}$ with $\chi_T|_T \equiv 1$ and $\chi_T|_K \equiv 0$ for $K \in \mathcal{T}, K \neq T$.

7.1. Primal dPG Formulation

Consider the primal dPG formulation with the discrete spaces $X_h = S^1_0(\mathcal{T}) \times P_0(\mathcal{E})$, $Y_h = P_1(\mathcal{T})$ and norms and bilinear and linear forms $b : X_h \times Y_h \to \mathbb{R}$ and $F : Y_h \to \mathbb{R}$ from Subsection 4.1.

Theorem 7.1 (Primal dPG is LS) *Any $x_h = (u_C, t_0) \in S^1_0(\mathcal{T}) \times P_0(\mathcal{E})$ and $p_{RT} \in RT_0(\mathcal{T})$ with $\gamma^{\mathcal{T}}_\nu p_{RT} = t_0$ satisfies*

$$\|F - b(x_h, \bullet)\|^2_{Y_h^*} = \|\Pi_0 f + \mathrm{div}\, p_{RT}\|^2_{L^2(\Omega)} + \|(I_{n\times n} + S(\mathcal{T}))^{-1/2}(\Pi_0 p_{RT} - \nabla u_C + H_0 f)\|^2_{L^2(\Omega)}.$$

In particular, if $x_h = (u_{dPG}, t_{dPG}) \in S^1_0(\mathcal{T}) \times P_0(\mathcal{E})$ solves (minRes) *and $p_{LS} \in RT_0(\mathcal{T})$ with $\gamma^{\mathcal{T}}_\nu p_{LS} = t_{dPG}$, then $(p_{LS}, u_{dPG}) \in RT_0(\mathcal{T}) \times S^1_0(\mathcal{T})$ is the unique minimizer of* (6.1) *with $M_0 = I_{n\times n} + S(\mathcal{T})$ and $F_0 = H_0 f$.*

Conversely, for any minimizer $(p_{LS}, u_{LS}) \in RT_0(\mathcal{T}) \times S^1_0(\mathcal{T})$ of (6.1) *with $M_0 = I_{n\times n} + S(\mathcal{T})$ and $F_0 = H_0 f$, $x_h = (u_{LS}, \gamma^{\mathcal{T}}_\nu p_{LS}) \in S^1_0(\mathcal{T}) \times P_0(\mathcal{E})$ minimizes* (minRes).

Proof: Let $v_1 \in P_1(\mathcal{T}) \equiv Y_h$ be the Riesz representation of $F - b(x_h, \bullet) \in Y_h^*$ in the Hilbert space $P_1(\mathcal{T})$, i.e., any $\widetilde{v}_1 \in P_1(\mathcal{T})$ satisfies

$$(v_1, \widetilde{v}_1)_{H^1(\mathcal{T})} = F(\widetilde{v}_1) - b(x_h, \widetilde{v}_1) = (f, \widetilde{v}_1)_{L^2(\Omega)} - a_{NC}(u_C, \widetilde{v}_1) + \langle t_0, \widetilde{v}_1\rangle_{\partial\mathcal{T}}.$$

The substitution of $t_0 = \gamma^{\mathcal{T}}_\nu p_{RT}$ and the integration by parts from Remark 2.23 leads to

$$(v_1, \widetilde{v}_1)_{H^1(\mathcal{T})} = (f + \mathrm{div}\, p_{RT}, \widetilde{v}_1)_{L^2(\Omega)} + (p_{RT} - \nabla u_C, \nabla_{NC}\widetilde{v}_1)_{L^2(\Omega)}.$$

With the identity $\widetilde{v}_1 = \Pi_0 \widetilde{v}_1 + \nabla_{NC} \widetilde{v}_1 \cdot (\bullet - \mathrm{mid}(\mathcal{T}))$, it follows $(f, \widetilde{v}_1)_{L^2(\Omega)} = (\Pi_0 f, \Pi_0 \widetilde{v}_1)_{L^2(\Omega)} + (H_0 f, \nabla_{NC} \widetilde{v}_1)_{L^2(\Omega)}$ and the representation of the scalar product $(\bullet, \bullet)_{H^1(\mathcal{T})}$ on $P_1(\mathcal{T})$ from Remark 2.11 implies

$$\begin{aligned}&(\Pi_0 v_1, \Pi_0 \widetilde{v}_1)_{L^2(\Omega)} + ((I_{n\times n} + S(\mathcal{T}))\nabla_{NC} v_1, \nabla_{NC} \widetilde{v}_1)_{L^2(\Omega)} \\ &\qquad = (\Pi_0 f + \operatorname{div} p_{RT}, \Pi_0 \widetilde{v}_1)_{L^2(\Omega)} + (\Pi_0 p_{RT} - \nabla u_C + H_0 f, \nabla_{NC} \widetilde{v}_1)_{L^2(\Omega)}.\end{aligned}$$

For any $T \in \mathcal{T}$, the choices $\widetilde{v}_1 = \chi_T$ and $\widetilde{v}_1 = \chi_T e_k \cdot (\bullet - \mathrm{mid}(\mathcal{T}))$, $k = 1, \dots, n$, lead to

$$\Pi_0 v_1 = \Pi_0 f + \operatorname{div} p_{RT}, \quad (I_{n\times n} + S(\mathcal{T}))\nabla_{NC} v_1 = \Pi_0 p_{RT} - \nabla u_C + H_0 f.$$

Since the Riesz isomorphism is an isometry, the identity $\|F - b(x_h, \bullet)\|^2_{Y_h^*} = \|v_1\|^2_{H^1(\mathcal{T})} = \|\Pi_0 v_1\|^2_{L^2(\Omega)} + \|(I_{n\times n} + S(\mathcal{T}))^{1/2} \nabla_{NC} v_1\|^2_{L^2(\Omega)}$ from Remark 2.11 concludes the proof of the claimed identity. This proves the second statement, i.e., that the minimization (minRes) of $\|F - b(x_h, \bullet)\|^2_{Y_h^*}$ is equivalent to the minimization of (6.1) with $M_0 = I_{n\times n} + S(\mathcal{T})$ and $F_0 = H_0 f$. □

7.2. Dual dPG Formulation

Recall the spaces $X_h = RT_0(\mathcal{T}) \times P_0(\mathcal{T}) \times S^1_0(\mathcal{E})$, $Y_h = RT_0^{NC}(\mathcal{T}) \times P_0(\mathcal{T})$ and norms and bilinear and linear forms $b : X_h \times Y_h \to \mathbb{R}$ and $F : Y_h \to \mathbb{R}$ of the dual dPG formulation from Subsection 4.2.

Theorem 7.2 *Any $x_h = (p_{RT}, w_0, s_C) \in RT_0(\mathcal{T}) \times P_0(\mathcal{T}) \times S^1_0(\mathcal{E})$ and $u_C \in S^1_0(\mathcal{T})$ with $\gamma_0^{\mathcal{T}} u_C = s_C$ satisfy*

$$\begin{aligned}\|F - b(x_h, \bullet)\|^2_{Y_h^*} = \|\Pi_0 f + \operatorname{div} p_{RT}\|^2_{L^2(\Omega)} + \|\Pi_0 p_{RT} - \nabla u_C\|^2_{L^2(\Omega)} \\ + \|(1 + s(\mathcal{T})/n^2)^{-1/2}(w_0 - \Pi_0 u_C + s(\mathcal{T})/n^2 \operatorname{div} p_{RT})\|^2_{L^2(\Omega)}.\end{aligned}$$

Furthermore, if $x_h = (p_{dPG}, w_{dPG}, s_{dPG}) \in RT_0(\mathcal{T}) \times P_0(\mathcal{T}) \times S^1_0(\mathcal{E})$ solves (minRes) *and $u_{LS} \in S^1_0(\mathcal{T})$ with $\gamma_0^{\mathcal{T}} u_{LS} = s_{dPG}$, then $(p_{dPG}, u_{LS}) \in RT_0(\mathcal{T}) \times S^1_0(\mathcal{T})$ is the unique minimizer of* (6.1) *with $M_0 = I_{n\times n}$ and $F_0 = 0$.*

Conversely, for any minimizer $(p_{LS}, u_{LS}) \in RT_0(\mathcal{T}) \times S^1_0(\mathcal{T})$ of (6.1) *with $M_0 = I_{n\times n}$ and $F_0 = 0$, $x_h = (p_{LS}, w_{dPG}, \gamma_0^{\mathcal{T}} u_{LS}) \in RT_0(\mathcal{T}) \times P_0(\mathcal{T}) \times S^1_0(\mathcal{E})$ with $w_{dPG} = \Pi_0 u_{LS} - s(\mathcal{T}) \operatorname{div} p_{LS}/n^2$ minimizes* (minRes).

Proof: Let $(q_1, v_0) \in RT_0^{NC}(\mathcal{T}) \times P_0(\mathcal{T}) \equiv Y_h$ be the Riesz representation of $F - b(x_h, \bullet) \in Y_h^*$, i.e., any $\widetilde{q}_1 \in RT_0^{NC}(\mathcal{T})$ and $\widetilde{v}_0 \in P_0(\mathcal{T})$ satisfy

$$\begin{aligned}&(q_1, \widetilde{q}_1)_{H(\mathrm{div},NC)} + (v_0, \widetilde{v}_0)_{L^2(\Omega)} = F(\widetilde{q}_1, \widetilde{v}_0) - b(x_h; \widetilde{q}_1, \widetilde{v}_0) \\ &= (\Pi_0 f, \widetilde{v}_0)_{L^2(\Omega)} - (p_{RT}, \widetilde{q}_1)_{L^2(\Omega)} - (w_0, \operatorname{div}_{NC} \widetilde{q}_1)_{L^2(\Omega)} + (\operatorname{div} p_{RT}, \widetilde{v}_0)_{L^2(\Omega)} + \langle \widetilde{q}_1 \cdot \nu, s_C \rangle_{\partial\mathcal{T}}.\end{aligned}$$

An integration by parts from Remark 2.23 with $\gamma_0^{\mathcal{T}} u_C = s_C$ leads to

$$(q_1, \widetilde{q}_1)_{H(\mathrm{div}),NC} + (v_0, \widetilde{v}_0)_{L^2(\Omega)} = (\Pi_0 f + \mathrm{div}\, p_{RT}, \widetilde{v}_0)_{L^2(\Omega)} + (\nabla u_C - p_{RT}, \widetilde{q}_1)_{L^2(\Omega)} + (\Pi_0 u_C - w_0, \mathrm{div}_{NC}\, \widetilde{q}_1)_{L^2(\Omega)}.$$

The representation of the scalar product on $RT_0^{NC}(\mathcal{T})$ from Remark 2.11 results in

$$\begin{aligned}(\Pi_0 q_1, \Pi_0 \widetilde{q}_1)_{L^2(\Omega)} &+ ((1 + s(\mathcal{T})/n^2)\, \mathrm{div}_{NC}\, q_1, \mathrm{div}_{NC}\, \widetilde{q}_1)_{L^2(\Omega)} + (v_0, \widetilde{v}_0)_{L^2(\Omega)} \\ &= (\Pi_0 f + \mathrm{div}\, p_{RT}, \widetilde{v}_0)_{L^2(\Omega)} + (\nabla u_C - \Pi_0 p_{RT}, \Pi_0 \widetilde{q}_1)_{L^2(\Omega)} \\ &\quad + (\Pi_0 u_C - w_0 - s(\mathcal{T})/n^2\, \mathrm{div}\, p_{RT}, \mathrm{div}_{NC}\, \widetilde{q}_1)_{L^2(\Omega)}.\end{aligned}$$

The test functions $\widetilde{q}_1 = \chi_T e_k$ for $k = 1, \dots, n$, $\widetilde{q}_1 = \chi_T(\bullet - \mathrm{mid}(\mathcal{T}))/n$, and $\widetilde{v}_0 = \chi_T$ on any $T \in \mathcal{T}$ lead to

$$\begin{aligned}&\Pi_0 q_1 = \nabla u_C - \Pi_0 p_{RT}, \quad (1 + s(\mathcal{T})/n^2)\, \mathrm{div}_{NC}\, q_1 = \Pi_0 u_C - w_0 - s(\mathcal{T})/n^2\, \mathrm{div}\, p_{RT}, \\ &\quad v_0 = \Pi_0 f + \mathrm{div}\, p_{RT}.\end{aligned}$$

This and $\|(q_1, v_0)\|_{Y_h}^2 = \|\Pi_0 q_1\|_{L^2(\Omega)}^2 + \|(1 + s(\mathcal{T})/n^2)^{1/2}\, \mathrm{div}_{NC}\, q_1\|_{L^2(\Omega)}^2 + \|v_0\|_{L^2(\Omega)}^2$ from Remark 2.11 conclude the proof of the identity for $\|F - b(x_h, \bullet)\|_{Y_h^*}^2$.

Since $S_0^1(\mathcal{E})$ and $S_0^1(\mathcal{T})$ are isomorphic, the minimization (minRes) for $(p_{\mathrm{dPG}}, s_{\mathrm{dPG}}, u_{\mathrm{dPG}}) \in RT_0(\mathcal{T}) \times P_0(\mathcal{T}) \times S_0^1(\mathcal{E})$ is equivalent to the minimization

$$\begin{aligned}(p_{\mathrm{dPG}}, w_{\mathrm{dPG}}, u_{\mathrm{dPG}}) = \operatorname*{arg\,min}_{(p_{RT}, w_0, u_C) \in RT_0(\mathcal{T}) \times P_0(\mathcal{T}) \times S_0^1(\mathcal{T})} &\big(\|\Pi_0 f + \mathrm{div}\, p_{RT}\|_{L^2(\Omega)}^2 + \|\Pi_0 p_{RT} - \nabla u_C\|_{L^2(\Omega)}^2 \\ &+ \|(1 + s(\mathcal{T})/n^2)^{-1/2}(w_0 - \Pi_0 u_C + s(\mathcal{T})/n^2\, \mathrm{div}\, p_{RT})\|_{L^2(\Omega)}^2\big).\end{aligned}$$

The minimization with respect to the component $w_{\mathrm{dPG}} \in P_0(\mathcal{T})$ is local and restricted to $\min_{w_0 \in P_0(\mathcal{T})} \|(1 + s(\mathcal{T})/n^2)^{-1/2}(w_0 - \Pi_0 u_{\mathrm{dPG}} + s(\mathcal{T})/n^2\, \mathrm{div}\, p_{\mathrm{dPG}})\|_{L^2(\Omega)}^2 = 0$. This yields $w_{\mathrm{dPG}} = \Pi_0 u_{\mathrm{dPG}} - s(\mathcal{T})/n^2\, \mathrm{div}\, p_{\mathrm{dPG}}$ and

$$(p_{\mathrm{dPG}}, u_{\mathrm{dPG}}) = \operatorname*{arg\,min}_{(p_{RT}, u_C) \in RT_0(\mathcal{T}) \times S_0^1(\mathcal{T})} \|\Pi_0 f + \mathrm{div}\, p_{RT}\|_{L^2(\Omega)}^2 + \|\Pi_0 p_{RT} - \nabla u_C\|_{L^2(\Omega)}^2.$$

This is the weighted least-squares functional (6.1) with $M_0 = I_{n \times n}$ and $F_0 = 0$. □

7.3. Primal Mixed dPG Formulation

The primal mixed dPG formulation from Subsection 4.3 utilizes the discrete spaces $X_h = P_0(\mathcal{T}; \mathbb{R}^n) \times S_0^1(\mathcal{T}) \times P_0(\mathcal{E})$, $Y_h = P_0(\mathcal{T}; \mathbb{R}^n) \times P_1(\mathcal{T})$ with corresponding norms and a bilinear form $b : X_h \times Y_h \to \mathbb{R}$ and a linear form $F : Y_h \to \mathbb{R}$.

Theorem 7.3 *Any* $x_h = (r_0, u_C, t_0) \in P_0(\mathcal{T};\mathbb{R}^n) \times S^1_0(\mathcal{T}) \times P_0(\mathcal{E})$ *and* $p_{RT} \in RT_0(\mathcal{T})$ *with* $t_0 = \gamma^{\mathcal{T}}_\nu p_{RT}$ *satisfy*

$$\begin{aligned}\|F - b(x_h, \bullet)\|^2_{Y_h^*} &= \|\Pi_0 f + \operatorname{div} p_{RT}\|^2_{L^2(\Omega)} + \|r_0 - \nabla u_C\|^2_{L^2(\Omega)} \\ &\quad + \|(I_{n\times n} + S(\mathcal{T}))^{-1/2}(\Pi_0 p_{RT} - r_0 + H_0 f)\|^2_{L^2(\Omega)}.\end{aligned}$$

Additionally, if $x_h = (r_{dPG}, u_{dPG}, t_{dPG}) \in P_0(\mathcal{T};\mathbb{R}^n) \times S^1_0(\mathcal{T}) \times P_0(\mathcal{E})$ *solves* (minRes) *and* $p_{LS} \in RT_0(\mathcal{T})$ *with* $\gamma^{\mathcal{T}}_\nu p_{LS} = t_{dPG}$, *then* $(p_{LS}, u_{dPG}) \in RT_0(\mathcal{T}) \times S^1_0(\mathcal{T})$ *is the unique minimizer of* (6.1) *with* $M_0 = 2I_{n\times n} + S(\mathcal{T})$ *and* $F_0 = H_0 f$.

Conversely, for any minimizer $(p_{LS}, u_{LS}) \in RT_0(\mathcal{T}) \times S^1_0(\mathcal{T})$ *of* (6.1) *with* $M_0 = 2I_{n\times n} + S(\mathcal{T})$ *and* $F_0 = H_0 f$, $x_h = (r_{dPG}, u_{LS}, \gamma^{\mathcal{T}}_\nu p_{LS}) \in P_0(\mathcal{T};\mathbb{R}^n) \times S^1_0(\mathcal{T}) \times P_0(\mathcal{E})$ *with* $r_{dPG} = \nabla u_{LS} + (2I_{n\times n} + S(\mathcal{T}))^{-1}(\Pi_0 p_{LS} - \nabla u_{LS} + H_0 f)$ *minimizes* (minRes).

Proof: Let $(q_0, v_1) \in P_0(\mathcal{T};\mathbb{R}^n) \times P_1(\mathcal{T}) \equiv Y_h$ be the Riesz representation of $F - b(x_h, \bullet) \in Y_h^*$, i.e., any $\widetilde{q}_0 \in P_0(\mathcal{T};\mathbb{R}^n)$) and $\widetilde{v}_1 \in P_1(\mathcal{T})$ satisfy

$$\begin{aligned}(q_0, \widetilde{q}_0)_{L^2(\Omega)} + (v_1, \widetilde{v}_1)_{H^1(\mathcal{T})} &= F(\widetilde{q}_0, \widetilde{v}_1) - b(x_h; \widetilde{q}_0, \widetilde{v}_1) \\ &= (f, \widetilde{v}_1)_{L^2(\Omega)} - (r_0 - \nabla u_C, \widetilde{q}_0)_{L^2(\Omega)} - (r_0, \nabla_{NC}\widetilde{v}_1)_{L^2(\Omega)} + \langle t_0, \widetilde{v}_1\rangle_{\partial\mathcal{T}}.\end{aligned}$$

The substitution $p_{RT} \in RT_0(\mathcal{T})$ with $\gamma^{\mathcal{T}}_\nu p_{RT} = t_0$ and an integration by parts proves

$$\begin{aligned}(q_0, \widetilde{q}_0)_{L^2(\Omega)} + (v_1, \widetilde{v}_1)_{H^1(\mathcal{T})} &= (f + \operatorname{div} p_{RT}, \widetilde{v}_1)_{L^2(\Omega)} + (\nabla u_C - r_0, \widetilde{q}_0)_{L^2(\Omega)} \\ &\quad + (\Pi_0 p_{RT} - r_0, \nabla_{NC}\widetilde{v}_1)_{L^2(\Omega)}.\end{aligned}$$

The split $\widetilde{v}_1 = \Pi_0\widetilde{v}_1 + \nabla_{NC}\widetilde{v}_1 \cdot (\bullet - \operatorname{mid}(\mathcal{T}))$ and representation of the scalar product in $P_1(\mathcal{T})$ from Remark 2.11 result in

$$\begin{aligned}&(q_0, \widetilde{q}_0)_{L^2(\Omega)} + (\Pi_0 v_1, \Pi_0\widetilde{v}_1)_{L^2(\Omega)} + ((I_{n\times n} + S(\mathcal{T}))\nabla_{NC} v_1, \nabla_{NC}\widetilde{v}_1)_{L^2(\Omega)} \\ &\quad = (\Pi_0 f + \operatorname{div} p_{RT}, \Pi_0\widetilde{v}_1)_{L^2(\Omega)} + (\nabla u_C - r_0, \widetilde{q}_0)_{L^2(\Omega)} + (\Pi_0 p_{RT} - r_0 + H_0 f, \nabla_{NC}\widetilde{v}_1)_{L^2(\Omega)}.\end{aligned}$$

The choices $\widetilde{q}_0 = \chi_T e_k$, $\widetilde{v}_1 = \chi_T e_k \cdot (\bullet - \operatorname{mid}(\mathcal{T}))$, $k = 1, \dots, n$, and $\widetilde{v}_1 = \chi_T$ on any $T \in \mathcal{T}$ show

$$q_0 = \nabla u_C - r_0, \quad (I_{n\times n} + S(\mathcal{T}))\nabla_{NC} v_1 = \Pi_0 p_{RT} - r_0 + H_0 f, \quad \Pi_0 v_1 = \Pi_0 f + \operatorname{div} p_{RT}.$$

Since Remark 2.11 shows $\|(q_0, v_1)\|^2_{Y_h} = \|q_0\|^2_{L^2(\Omega)} + \|\Pi_0 v_1\|^2_{L^2(\Omega)} + \|(I_{n\times n} + S(\mathcal{T}))^{1/2}\nabla_{NC} v_1\|^2_{L^2(\Omega)}$, this conclude the proof of the representation of $\|F - b(x_h, \bullet)\|^2_{Y_h^*} = \|(q_0, v_1)\|^2_{Y_h}$.

The isomorphy between $P_0(\mathcal{T})$ and $RT_0(\mathcal{T})$ from Remark 2.21 shows that minimizing (minRes) for $(r_{\mathrm{dPG}}, u_{\mathrm{dPG}}, t_{\mathrm{dPG}}) \in P_0(\mathcal{T};\mathbb{R}^n) \times S^1_0(\mathcal{T}) \times P_0(\mathcal{E})$ is equivalent to the minimization

$$\begin{aligned}(r_{\mathrm{dPG}}, u_{\mathrm{dPG}}, p_{\mathrm{dPG}}) = \operatorname*{arg\,min}_{(r_0, u_C, p_{RT}) \in P_0(\mathcal{T};\mathbb{R}^n) \times S^1_0(\mathcal{T}) \times RT_0(\mathcal{T})} &\big(\|\Pi_0 f + \operatorname{div} p_{RT}\|^2_{L^2(\Omega)} + \|r_0 - \nabla u_C\|^2_{L^2(\Omega)} \\ &+ \|(I_{n\times n} + S(\mathcal{T}))^{-1/2}(\Pi_0 p_{RT} - r_0 + H_0 f)\|^2_{L^2(\Omega)}\big). \qquad (7.1)\end{aligned}$$

The piecewise minimization for the component $r_0 \in P_0(\mathcal{T};\mathbb{R}^n)$ requires the optimality condition for a piecewise minimization $\min_{x\in\mathbb{R}^n}(|(I_{n\times n}+M)^{-1/2}(A-x)|^2+|x-B|^2)$ with $A,B\in\mathbb{R}^n$ and $M\in\mathbb{R}^{n\times n}$, which reads $(I_{n\times n}+M)^{-1}(x-A)+x-B=0$ and implies

$$x=(2I_{n\times n}+M)^{-1}((I_{n\times n}+M)B+A)=B+(2I_{n\times n}+M)^{-1}(A-B).$$

Hence, $(I_{n\times n}+M)^{-1/2}(A-x)=(I_{n\times n}+M)^{1/2}(x-B)$ and $x-B=(2I_{n\times n}+M)^{-1}(A-B)$ show

$$\min_{x\in\mathbb{R}^n}|(I_{n\times n}+M)^{-1/2}(A-x)|^2+|x-B|^2=|(2I_{n\times n}+M)^{1/2}(x-B)|^2=|(2I_{n\times n}+M)^{-1/2}(A-B)|^2.$$

Consequently, $r_{\mathrm{dPG}}=\nabla u_{\mathrm{dPG}}+(2I_{n\times n}+S(\mathcal{T}))^{-1}(\Pi_0 p_{\mathrm{dPG}}-\nabla u_{\mathrm{dPG}}+H_0 f)\in P_0(\mathcal{T};\mathbb{R}^n)$ minimizes

$$\begin{aligned}\min_{r_0\in P_0(\mathcal{T};\mathbb{R}^n)}\big(\|r_0-\nabla u_{\mathrm{dPG}}\|^2_{L^2(\Omega)}+\|(I_{n\times n}+S(\mathcal{T}))^{-1/2}(\Pi_0 p_{\mathrm{dPG}}-r_0+H_0 f)\|^2_{L^2(\Omega)}\big)\\ =\|(2I_{n\times n}+S(\mathcal{T}))^{-1/2}(\Pi_0 p_{\mathrm{dPG}}-\nabla u_{\mathrm{dPG}}+H_0 f)\|^2_{L^2(\Omega)}.\end{aligned}$$

The minimization (7.1) with this is the minimization of weighted least-squares functional (6.1) with $M_0=2I_{n\times n}+S(\mathcal{T})$ and $F_0=H_0 f$. □

7.4. Ultraweak dPG Formulation

Recall that ultraweak dPG formulation from Subsection 4.4 utilizes the discrete spaces $X_h=P_0(\mathcal{T};\mathbb{R}^n)\times P_0(\mathcal{T})\times P_0(\mathcal{E})\times S^1_0(\mathcal{E})$ and $Y_h=RT_0^{NC}(\mathcal{T})\times P_1(\mathcal{T})$, a bilinear form $b: X_h\times Y_h\to\mathbb{R}$, and a linear form $F: Y_h\to\mathbb{R}$.

Theorem 7.4 *Any $x_h=(r_0,w_0,t_0,s_C)\in P_0(\mathcal{T};\mathbb{R}^n)\times P_0(\mathcal{T})\times P_0(\mathcal{E})\times S^1_0(\mathcal{E})$ and $u_C\in S^1_0(\mathcal{T})$ with $\gamma_0^{\mathcal{T}}u_C=s_C$, $p_{RT}\in RT_0(\mathcal{T})$ with $\gamma_\nu^{\mathcal{T}}p_{RT}=t_0$ satisfy*

$$\begin{aligned}\|F-b(x_h,\bullet)\|^2_{Y_h^*}=\|\Pi_0 f+\operatorname{div}p_{RT}\|^2_{L^2(\Omega)}+\|(I_{n\times n}+S(\mathcal{T}))^{-1/2}(\Pi_0 p_{RT}-r_0+H_0 f)\|^2_{L^2(\Omega)}\\ +\|(1+s(\mathcal{T})/n^2)^{-1/2}(w_0-\Pi_0 u_C)\|^2_{L^2(\Omega)}+\|r_0-\nabla u_C\|^2_{L^2(\Omega)}.\end{aligned}$$

Furthermore, if $x_h=(r_{dPG},w_{dPG},t_{dPG},s_{dPG})\in P_0(\mathcal{T};\mathbb{R}^n)\times P_0(\mathcal{T})\times P_0(\mathcal{E})\times S^1_0(\mathcal{E})$ solves (minRes) *and $u_{LS}\in S^1_0(\mathcal{T})$, $p_{LS}\in RT_0(\mathcal{T})$ with $\gamma_0^{\mathcal{T}}u_{LS}=s_{dPG}$ and $\gamma_\nu^{\mathcal{T}}p_{LS}=t_{dPG}$, then $(p_{LS},u_{LS})\in RT_0(\mathcal{T})\times S^1_0(\mathcal{T})$ is the unique minimizer of* (6.1) *with $M_0=2I_{n\times n}+S(\mathcal{T})$ and $F_0=H_0 f$.*

Conversely, for any minimizer $(p_{LS},u_{LS})\in RT_0(\mathcal{T})\times S^1_0(\mathcal{T})$ of (6.1) *with $M_0=2I_{n\times n}+S(\mathcal{T})$ and $F_0=H_0 f$, $x_h=(r_{dPG},w_{dPG},\gamma_\nu^{\mathcal{T}}p_{RT},\gamma_0^{\mathcal{T}}u_{LS})\in P_0(\mathcal{T};\mathbb{R}^n)\times P_0(\mathcal{T})\times P_0(\mathcal{E})\times S^1_0(\mathcal{E})$ with $r_{dPG}=\nabla u_{LS}+(2I_{n\times n}+S(\mathcal{T}))^{-1}(\Pi_0 p_{LS}-\nabla u_{LS}+H_0 f)$ and $w_{dPG}=\Pi_0 u_{LS}$ minimizes* (minRes).

Proof: Let $(q_1,v_1)\in RT_0^{NC}(\mathcal{T})\times P_1(\mathcal{T})\equiv Y_h$ be the Riesz representation of $F-b(x_h,\bullet)\in Y_h^*$, i.e., any $\widetilde{q}_1\in RT_0^{NC}(\mathcal{T})$ and $\widetilde{v}_1\in P_1(\mathcal{T})$ satisfy

$$\begin{aligned}(q_1,\widetilde{q}_1)_{H(\mathrm{div},NC)}+(v_1,\widetilde{v}_1)_{H^1(\mathcal{T})}&=F(\widetilde{q}_1,\widetilde{v}_1)-b(x_h;\widetilde{q}_1,\widetilde{v}_1)\\ &=(f,\widetilde{v}_1)_{L^2(\Omega)}-(r_0,\widetilde{q}_1)_{L^2(\Omega)}-(r_0,\nabla_{NC}\widetilde{v}_1)_{L^2(\Omega)}\\ &\quad-(w_0,\operatorname{div}_{NC}\widetilde{q}_1)_{L^2(\Omega)}+\langle\widetilde{q}_1\cdot\nu,s_C\rangle_{\partial\mathcal{T}}+\langle t_0,\widetilde{v}_1\rangle_{\partial\mathcal{T}}.\end{aligned}$$

The substitution of $s_C = \gamma_0^{\mathcal{T}} u_C$ and $t_0 = \gamma_v^{\mathcal{T}} p_{RT}$ plus an integration by parts lead to

$$(q_1, \widetilde{q}_1)_{H(\mathrm{div},NC)} + (v_1, \widetilde{v}_1)_{H^1(\mathcal{T})} = (f + \mathrm{div}\, p_{RT}, \widetilde{v}_1)_{L^2(\Omega)} + (\nabla u_C - r_0, \Pi_0 \widetilde{q}_1)_{L^2(\Omega)} + (\Pi_0 p_{RT} - r_0, \nabla_{NC} \widetilde{v}_1)_{L^2(\Omega)} + (\Pi_0 u_C - w_0, \mathrm{div}_{NC}\, \widetilde{q}_1)_{L^2(\Omega)}.$$

The splits $\widetilde{q}_1 = \Pi_0 \widetilde{q}_1 + \mathrm{div}_{NC}\, \widetilde{q}_1(\bullet - \mathrm{mid}(\mathcal{T}))/n$ and $\widetilde{v}_1 = \Pi_0 \widetilde{v}_1 + \nabla_{NC} \widetilde{v}_1 \cdot (\bullet - \mathrm{mid}(\mathcal{T}))$ from Remark 2.11 imply

$$(\Pi_0 q_1, \Pi_0 \widetilde{q}_1)_{L^2(\Omega)} + ((1 + s(\mathcal{T})/n^2)\, \mathrm{div}_{NC}\, q_1, \mathrm{div}_{NC}\, \widetilde{q}_1)_{L^2(\Omega)} = (\nabla u_C - r_0, \Pi_0 \widetilde{q}_1) + (\Pi_0 u_C - w_0, \mathrm{div}_{NC}\, \widetilde{q}_1)_{L^2(\Omega)}$$

and

$$(\Pi_0 v_1, \Pi_0 \widetilde{v}_1)_{L^2(\Omega)} + ((I_{n\times n} + S(\mathcal{T}))\nabla_{NC} v_1, \nabla_{NC} \widetilde{v}_1)_{L^2(\Omega)} = (\Pi_0 f + \mathrm{div}\, p_{RT}, \Pi_0 \widetilde{v}_1)_{L^2(\Omega)} + (\Pi_0 p_{RT} - r_0 + H_0 f, \nabla_{NC} \widetilde{v}_1)_{L^2(\Omega)}.$$

The test functions $\widetilde{q}_1 = \chi_T(\bullet - \mathrm{mid}(\mathcal{T}))/n$, and $\widetilde{q}_1 = \chi_T e_k$ for $k = 1, \dots, n$ on $T \in \mathcal{T}$ lead to

$$(1 + s(\mathcal{T})/n^2)\, \mathrm{div}_{NC}\, q_1 = \Pi_0 u_C - w_0 \quad \text{and} \quad \Pi_0 q_1 = \nabla u_C - r_0.$$

Additionally, the test functions $\widetilde{v}_1 = \chi_T$, and $\widetilde{v}_1 = \chi_T e_k \cdot (\bullet - \mathrm{mid}(T))$ for $k = 1, \dots, n$ on $T \in \mathcal{T}$ lead to

$$(I_{n\times n} + S(\mathcal{T}))\nabla_{NC} v_1 = \Pi_0 p_{RT} - r_0 + H_0 f \quad \text{and} \quad \Pi_0 v_1 = \Pi_0 f + \mathrm{div}\, p_{RT}.$$

This and $\|F - b(x_h, \bullet)\|_{Y_h^*}^2 = \|(q_1, v_1)\|_{Y_h}^2 = \|\Pi_0 q_1\|_{L^2(\Omega)}^2 + \|(1 + s(\mathcal{T})/n^2)^{1/2}\, \mathrm{div}_{NC}\, q_1\|_{L^2(\Omega)}^2 + \|\Pi_0 v_1\|_{L^2(\Omega)}^2 + \|(I_{n\times n} + S(\mathcal{T}))^{1/2}\nabla_{NC} v_1\|_{L^2(\Omega)}$ conclude the proof of the claimed identity.

Since $S_0^1(\mathcal{E})$ and $S_0^1(\mathcal{T})$ as well as $P_0(\mathcal{T})$ and $RT_0(\mathcal{T})$ from Remark 2.21 are isomorphic, the minimization (minRes) for $(r_{\mathrm{dPG}}, w_{\mathrm{dPG}}, t_{\mathrm{dPG}}, s_{\mathrm{dPG}}) \in P_0(\mathcal{T}; \mathbb{R}^n) \times P_0(\mathcal{T}) \times P_0(\mathcal{E}) \times S_0^1(\mathcal{E})$ is equivalent to the minimization

$$(r_{\mathrm{dPG}}, w_{\mathrm{dPG}}, p_{\mathrm{dPG}}, u_{\mathrm{dPG}}) = \operatorname*{argmin}_{(r_0, w_0, p_{RT}, u_C) \in P_0(\mathcal{T};\mathbb{R}^n) \times P_0(\mathcal{T}) \times RT_0(\mathcal{T}) \times S_0^1(\mathcal{T})} \big(\|\Pi_0 f + \mathrm{div}\, p_{RT}\|_{L^2(\Omega)}^2 + \|(I_{n\times n} + S(\mathcal{T}))^{-1/2}(\Pi_0 p_{RT} - r_0 + H_0 f)\|_{L^2(\Omega)}^2 + \|(1 + s(\mathcal{T})/n^2)^{-1/2}(w_0 - \Pi_0 u_C)\|_{L^2(\Omega)}^2 + \|r_0 - \nabla u_C\|_{L^2(\Omega)}^2 \big).$$

The minimization with respect to the component $w_0 \in P_0(\mathcal{T})$ is local and yields $w_{\mathrm{dPG}} = \Pi_0 u_{\mathrm{dPG}}$. The analysis of the piecewise minimization of $\|(I_{n\times n} + S(\mathcal{T}))^{-1/2}(\Pi_0 p_{RT} - r_0 + H_0 f)\|_{L^2(\Omega)}^2 + \|r_0 - \nabla u_C\|_{L^2(\Omega)}^2$ for $r_0 \in P_0(\mathcal{T}; \mathbb{R}^n)$ is analogous to that of the proof of Theorem 7.3 and leads to $r_{\mathrm{dPG}} = \nabla u_{\mathrm{dPG}} + (2I_{n\times n} + S(\mathcal{T}))^{-1}(\Pi_0 p_{\mathrm{dPG}} - \nabla u_{\mathrm{dPG}} + H_0 f)$. It remains the above minimization in form of

$$(p_{\mathrm{dPG}}, u_{\mathrm{dPG}}) = \operatorname*{argmin}_{(p_{RT}, u_C) \in RT_0(\mathcal{T}) \times S_0^1(\mathcal{T})} \|\Pi_0 f + \mathrm{div}\, p_{RT}\|_{L^2(\Omega)}^2 + \|(2I_{n\times n} + S(\mathcal{T}))^{-1/2}(\Pi_0 p_{RT} - \nabla u_C + H_0 f)\|_{L^2(\Omega)}^2.$$

Hence, (minRes) is equivalent to (6.1) with $M_0 = 2I_{n\times n} + S(\mathcal{T})$ and $F_0 = H_0 f$. □

$\mathcal{T}$	$\widehat{\mathcal{T}} \in \mathbb{T}(\mathcal{T})$
(p_{LS}, u_{LS}) solves (LS)	$(\widehat{p}_{LS}, \widehat{u}_{LS})$ solves ($\widehat{\text{LS}}$)
$M_0 \in P_0(\mathcal{T};\mathbb{S})$	$\widehat{M}_0 \in P_0(\widehat{\mathcal{T}};\mathbb{S})$
$F_0 \in P_0(\mathcal{T};\mathbb{R}^n)$	$\widehat{F}_0 \in P_0(\widehat{\mathcal{T}};\mathbb{R}^n)$
$V_0 := M_0^{-1}(\Pi_0 p_{LS} - \nabla u_{LS} + F_0)$	$\widehat{V}_0 := \widehat{M}_0^{-1}(\widehat{\Pi}_0 \widehat{p}_{LS} - \nabla \widehat{u}_{LS} + \widehat{F}_0)$
$W_0 := \Pi_0 p_{LS} - \nabla u_{LS} + F_0$	$\widehat{W}_0 := \widehat{\Pi}_0 \widehat{p}_{LS} - \nabla \widehat{u}_{LS} + \widehat{F}_0$
$\eta(K) := \eta(\mathcal{T}, K), K \in \mathcal{T}$ from (6.4)	$\widehat{\eta}(T) := \eta(\widehat{\mathcal{T}}, T), T \in \widehat{\mathcal{T}}$
$\eta := \eta(\mathcal{T})$,	$\widehat{\eta} := \widehat{\eta}(\widehat{\mathcal{T}})$,
$\mu := \mu(\mathcal{T})$ from (6.5)	$\widehat{\mu} := \mu(\widehat{\mathcal{T}})$,
$h_{\mathcal{T}}, H_{\mathcal{T}}$ mesh-size	$h_{\widehat{\mathcal{T}}}, H_{\widehat{\mathcal{T}}}$ mesh-size
$\mathcal{R} := \mathcal{T} \setminus \widehat{\mathcal{T}}$	
$\delta^2 := \delta^2(\mathcal{T}, \widehat{\mathcal{T}}) := \|\operatorname{div}(p_{LS} - \widehat{p}_{LS})\|^2_{L^2(\Omega)} + \|V_0 - \widehat{V}_0\|^2_{L^2(\Omega)}$ from (8.1)	

Table 6: Standard notation for $\mathcal{T}$ and its refinement $\widehat{\mathcal{T}} \in \mathbb{T}(\mathcal{T})$ for weighted least-squares method

8. Optimal Convergence Rates of Weighted Least-Squares Methods

This section proves optimal convergence rates of the generalized least-squares formulation from Section 6 based the axioms from [CR17] in Subsection 2.4. The axioms (QM) and (A1)-(A3) utilize the notation of Table 6, i.e., a triangulation $\mathcal{T} \in \mathbb{T}$ with a refinement $\widehat{\mathcal{T}} \in \mathbb{T}(\mathcal{T})$ and corresponding weights $M_0 \in P_0(\mathcal{T};\mathbb{S})$, $F_0 \in P_0(\mathcal{T};\mathbb{R}^n)$ on the coarse level and $\widehat{M}_0 \in P_0(\widehat{\mathcal{T}};\mathbb{S})$, $\widehat{F}_0 \in P_0(\widehat{\mathcal{T}};\mathbb{R}^n)$ on the fine level. With the operators $\Pi_0 : L^2(\Omega) \to P_0(\mathcal{T})$, $\widehat{\Pi}_0 : L^2(\Omega) \to P_0(\widehat{\mathcal{T}})$, recall the discrete solution $(p_{LS}, u_{LS}) \in RT_0(\mathcal{T}) \times S^1_0(\mathcal{T})$ to (LS) with respect to $\mathcal{T}$ and the discrete solution $(\widehat{p}_{LS}, \widehat{u}_{LS}) \in RT_0(\widehat{\mathcal{T}}) \times S^1_0(\widehat{\mathcal{T}})$ with respect to $\widehat{\mathcal{T}}$, such that any $(\widehat{q}_{RT}, \widehat{v}_C) \in RT_0(\widehat{\mathcal{T}}) \times S^1_0(\widehat{\mathcal{T}})$ satisfies

$$0 = (\widehat{M}_0^{-1}(\widehat{\Pi}_0 \widehat{p}_{LS} - \nabla \widehat{u}_{LS} + \widehat{F}_0), \widehat{\Pi}_0 \widehat{q}_{RT} - \nabla \widehat{v}_C)_{L^2(\Omega)} + (\widehat{\Pi}_0 f + \operatorname{div} \widehat{p}_{LS}, \operatorname{div} \widehat{q}_{RT})_{L^2(\Omega)}. \quad (\widehat{\text{LS}})$$

Abbreviate $V_0 := M_0^{-1}(\Pi_0 p_{LS} - \nabla u_{LS} + F_0) \in P_0(\mathcal{T};\mathbb{R}^n)$, $W_0 := M_0 V_0 \in P_0(\mathcal{T};\mathbb{R}^n)$ and $\widehat{V}_0 := \widehat{M}_0^{-1}(\widehat{\Pi}_0 \widehat{p}_{LS} - \nabla \widehat{u}_{LS} + \widehat{F}_0) \in P_0(\widehat{\mathcal{T}};\mathbb{R}^n)$, $\widehat{W}_0 := \widehat{M}_0 \widehat{V}_0 \in P_0(\widehat{\mathcal{T}};\mathbb{R}^n)$.

The distance function $\delta := \delta(\mathcal{T}, \widehat{\mathcal{T}})$ is defined as $\delta(\mathcal{T}, \widehat{\mathcal{T}}) := (\delta^2(\mathcal{T}, \widehat{\mathcal{T}}))^{1/2}$ for

$$\delta^2(\mathcal{T}, \widehat{\mathcal{T}}) := \|\operatorname{div}(p_{LS} - \widehat{p}_{LS})\|^2_{L^2(\Omega)} + \|V_0 - \widehat{V}_0\|^2_{L^2(\Omega)}. \quad (8.1)$$

8.1. Quasimonotonicity

Theorem 8.1 (Quasimonotonicity) *There exists a universal constant Λ_{QM} such that any triangulation $\mathcal{T} \in \mathbb{T}$ with refinement $\widehat{\mathcal{T}} \in \mathbb{T}(\mathcal{T})$ satisfies $\sigma(\widehat{\mathcal{T}}) \leq \Lambda_{QM}\sigma(\mathcal{T})$.*

Proof: The reduction $\mu^2(\widehat{\mathcal{T}}) \leq \mu^2(\mathcal{T})$ is based on the L^2-orthogonality of $(1-\widehat{\Pi}_0)f$ onto $P_0(\widehat{\mathcal{T}})$ in the Pythagoras theorem $\|(1-\Pi_0)f\|^2_{L^2(\Omega)} = \|(1-\widehat{\Pi}_0)f\|^2_{L^2(\Omega)} + \|(\widehat{\Pi}_0-\Pi_0)f\|^2_{L^2(\Omega)}$. To show the reduction of $\eta(\widehat{\mathcal{T}})$, Lemma 6.7 with constant c_{eff} proves

$$\eta^2(\widehat{\mathcal{T}}) \leq c_{\mathrm{eff}}\|\widehat{M}_0^{-1}(\widehat{\Pi}_0\widehat{p}_{LS} - \nabla\widehat{u}_{LS} + \widehat{F}_0)\|^2_{L^2(\Omega)} + \|H_{\widehat{\mathcal{T}}}\operatorname{div}\widehat{p}_{LS}\|^2_{L^2(\Omega)}.$$

Remark 6.2, a triangle inequality, and the pointwise estimate $H_{\widehat{\mathcal{T}}} \leq h_{\max}/n^{1/n}$ lead to

$$\begin{aligned}\eta^2(\widehat{\mathcal{T}}) &\leq c_{\mathrm{eff}}\underline{\lambda}^{-1}\|\widehat{M}_0^{-1/2}(\widehat{\Pi}_0\widehat{p}_{LS} - \nabla\widehat{u}_{LS} + \widehat{F}_0)\|^2_{L^2(\Omega)} + 2h^2_{\max}\|\widehat{\Pi}_0 f + \operatorname{div}\widehat{p}_{LS}\|^2_{L^2(\Omega)}/n^{2/n} \\ &\quad + 2\|H_{\widehat{\mathcal{T}}}\widehat{\Pi}_0 f\|^2_{L^2(\Omega)} \\ &\leq \max\{\underline{\lambda}^{-1}c_{\mathrm{eff}}, 2h^2_{\max}/n^{2/n}\}LS(f,\widehat{\mathcal{T}};\widehat{u}_{LS},\widehat{p}_{LS}) + 2\|H_{\widehat{\mathcal{T}}}\widehat{\Pi}_0 f\|^2_{L^2(\Omega)}. \end{aligned} \tag{8.2}$$

Since the solution $(\widehat{p}_{LS},\widehat{u}_{LS}) \in RT_0(\widehat{\mathcal{T}}) \times S^1_0(\widehat{\mathcal{T}})$ to $(\widehat{\mathrm{LS}})$ minimizes $LS(f,\widehat{\mathcal{T}};\bullet)$ and $(p_{LS},u_{LS}) \in RT_0(\mathcal{T}) \times S^1_0(\mathcal{T}) \subseteq RT_0(\widehat{\mathcal{T}}) \times S^1_0(\widehat{\mathcal{T}})$, the triangle inequality results in

$$\begin{aligned}LS(f,\widehat{\mathcal{T}};\widehat{p}_{LS},\widehat{u}_{LS}) &\leq LS(f,\widehat{\mathcal{T}};p_{LS},u_{LS}) \\ &= \|\widehat{M}_0^{-1/2}(\widehat{\Pi}_0 p_{LS} - \nabla u_{LS} + \widehat{F}_0)\|^2_{L^2(\Omega)} + \|\widehat{\Pi}_0 f + \operatorname{div} p_{LS}\|^2_{L^2(\Omega)} \\ &\leq 2\underline{\lambda}^{-1}\overline{\lambda}\|M_0^{-1/2}(\widehat{\Pi}_0 p_{LS} - \nabla u_{LS} + F_0)\|^2_{L^2(\Omega)} + 2\underline{\lambda}^{-1}\|\widehat{F}_0 - F_0\|^2_{L^2(\Omega)} \\ &\quad + \|\widehat{\Pi}_0 f + \operatorname{div} p_{LS}\|^2_{L^2(\Omega)}.\end{aligned}$$

The L^2-orthogonality of $(\widehat{\Pi}_0 - \Pi_0)p_{LS}$ onto $P_0(\mathcal{T})$ leads to

$$\begin{aligned}&\|M_0^{-1/2}(\widehat{\Pi}_0 p_{LS} - \nabla u_{LS} + F_0)\|^2_{L^2(\Omega)} \\ &\quad = \|M_0^{-1/2}(\Pi_0 p_{LS} - \nabla u_{LS} + F_0)\|^2_{L^2(\Omega)} + \|M_0^{-1/2}(\widehat{\Pi}_0 - \Pi_0)p_{LS}\|^2_{L^2(\Omega)} \\ &\quad \leq \|M_0^{-1/2}(\Pi_0 p_{LS} - \nabla u_{LS} + F_0)\|^2_{L^2(\Omega)} + \underline{\lambda}^{-1}\|(1-\Pi_0)p_{LS}\|^2_{L^2(\Omega)}.\end{aligned}$$

Since $\|(\widehat{\Pi}_0 - \Pi_0)f\|^2_{L^2(\Omega)} \leq \mu^2(\mathcal{T})$,

$$\|\widehat{\Pi}_0 f + \operatorname{div} p_{LS}\|^2_{L^2(\Omega)} \leq \|\Pi_0 f + \operatorname{div} p_{LS}\|^2_{L^2(\Omega)} + \mu^2(\mathcal{T}).$$

The triangle inequality, the assumption (6.7), and $\mu^2(\widehat{\mathcal{T}}) \leq \mu^2(\mathcal{T})$ imply

$$\|\widehat{F}_0 - F_0\|^2_{L^2(\Omega)} \leq 4\kappa_1^2\mu^2(\mathcal{T}). \tag{8.3}$$

The previous four displayed estimates and $\|(1-\Pi_0)p_{LS}\|_{L^2(\Omega)} \leq c_{\mathrm{sr}}^{1/n}\|H_{\mathcal{T}}\operatorname{div} p_{LS}\|_{L^2(\Omega)}/(n+1)$ from Remark 2.11 show

$$\begin{aligned}LS(f,\widehat{\mathcal{T}};\widehat{p}_{LS},\widehat{u}_{LS}) &\leq 2\underline{\lambda}^{-1}\overline{\lambda}\|M_0^{-1/2}(\Pi_0 p_{LS} - \nabla u_{LS} + F_0)\|^2_{L^2(\Omega)} \\ &\quad + (1 + 8\kappa_1^2\underline{\lambda}^{-1})\mu^2(\mathcal{T}) + \|\Pi_0 f + \operatorname{div} p_{LS}\|^2_{L^2(\Omega)} \\ &\quad + 2\underline{\lambda}^{-2}\overline{\lambda}c_{\mathrm{sr}}^{2/n}\|H_{\mathcal{T}}\operatorname{div} p_{LS}\|^2_{L^2(\Omega)}/(n+1)^2.\end{aligned} \tag{8.4}$$

The pointwise estimate $H_{\widehat{\mathcal{T}}} \le H_{\mathcal{T}} \le h_{\max}/n^{1/n}$, the theorem of Pythagoras at the beginning of this proof, and the triangle inequality result in

$$\begin{aligned}\|H_{\widehat{\mathcal{T}}}\widehat{\Pi}_0 f\|^2_{L^2(\Omega)} &\le \|H_{\mathcal{T}}\Pi_0 f\|^2_{L^2(\Omega)} + \|H_{\mathcal{T}}(\widehat{\Pi}_0 - \Pi_0)f\|^2_{L^2(\Omega)}\\ &\le 2h^2_{\max}\|\Pi_0 f + \operatorname{div} p_{LS}\|^2_{L^2(\Omega)}/n^{2/n} + 2\|H_{\mathcal{T}}\operatorname{div} p_{LS}\|^2_{L^2(\Omega)} + h^2_{\max}\mu^2(\mathcal{T})/n^{2/n}. \qquad (8.5)\end{aligned}$$

The combination of (8.2) with (8.4)-(8.5) leads to

$$\begin{aligned}\eta^2(\widehat{\mathcal{T}}) \le{}& 2\max\{\underline{\lambda}^{-1}c_{\mathrm{eff}}, 2h^2_{\max}/n^{2/n}\}\underline{\lambda}^{-1}\overline{\lambda}\|M_0^{-1/2}(\Pi_0 p_{LS} - \nabla u_{LS} + F_0)\|^2_{L^2(\Omega)}\\ &+ (4h^2_{\max}/n^{2/n} + \max\{\underline{\lambda}^{-1}c_{\mathrm{eff}}, 2h^2_{\max}/n^{2/n}\})\|\Pi_0 f + \operatorname{div} p_{LS}\|^2_{L^2(\Omega)}\\ &+ (4 + 2\max\{\underline{\lambda}^{-1}c_{\mathrm{eff}}, 2h^2_{\max}/n^{2/n}\}\underline{\lambda}^{-2}\overline{\lambda}c^{2/n}_{\mathrm{sr}}/(n+1)^2)\|H_{\mathcal{T}}\operatorname{div} p_{LS}\|^2_{L^2(\Omega)}\\ &+ (2h^2_{\max}/n^{2/n} + \max\{\underline{\lambda}^{-1}c_{\mathrm{eff}}, 2h^2_{\max}/n^{2/n}\}(1 + 8\kappa_1^2\underline{\lambda}^{-1}))\mu^2(\mathcal{T}).\end{aligned}$$

Hence, Lemma 6.7 concludes the proof with $\Lambda^2_{QM} = \max\{2c_{\mathrm{rel}}c\underline{\lambda}^{-1}\overline{\lambda}, 4c_{\mathrm{rel}}h^2_{\max}/n^{2/n} + c_{\mathrm{rel}}c, 4 + 2c\underline{\lambda}^{-2}\overline{\lambda}c^{2/n}_{\mathrm{sr}}/(n+1)^2, 1 + 2h^2_{\max}/n^{2/n} + c(1 + 8\kappa_1^2\underline{\lambda}^{-1})\}$ for $c = \max\{\underline{\lambda}^{-1}c_{\mathrm{eff}}, 2h^2_{\max}/n^{2/n}\}$. □

8.2. Stability and Reduction

Throughout this subsection, adapt the notation for $\mathcal{T}$ and $\widehat{\mathcal{T}}$ from Table 6 on p. 66. The proofs of Stability and Reduction follow the lines of the proofs for the reduced mixed methods of Subsection 5.1 with the notation at hand.

Theorem 8.2 (Stability) *There exists* $\Lambda_1 \approx 1$ *with*

$$\big|\eta(\mathcal{T}\cap\widehat{\mathcal{T}}) - \widehat{\eta}(\mathcal{T}\cap\widehat{\mathcal{T}})\big| \le \Lambda_1\delta(\mathcal{T},\widehat{\mathcal{T}}). \qquad (A1)$$

Proof: The quantity $\eta(\mathcal{T}\cap\widehat{\mathcal{T}})$ is the Euclidean norm of the vector $v \in \mathbb{R}^m$, $m = (n+2)|\mathcal{T}\cap\widehat{\mathcal{T}}|$, with entries $|T|^{1/n}\|\operatorname{div} p_{LS}\|_{L^2(T)}$, $|T|^{1/(2n)}\|[V_0]_E\|_{L^2(E)}$ for any $T \in \mathcal{T}\cap\widehat{\mathcal{T}}$ and $E \in \mathcal{E}(T)$. In the same way, $\widehat{\eta}(\mathcal{T}\cap\widehat{\mathcal{T}}) = |\widehat{v}|$ for $\widehat{v} \in \mathbb{R}^m$. The reverse triangle inequality in $\mathbb{R}^m$ implies

$$\begin{aligned}|\eta(\mathcal{T}\cap\widehat{\mathcal{T}}) - \widehat{\eta}(\mathcal{T}\cap\widehat{\mathcal{T}})|^2 &\le |v - \widehat{v}|^2\\ &= \sum_{T\in\mathcal{T}\cap\widehat{\mathcal{T}}}\Big(|T|^{1/n}\sum_{E\in\mathcal{E}(T)}(\|[V_0]_E\|_{L^2(E)} - \|[\widehat{V}_0]_E\|_{L^2(E)})^2\\ &\qquad + |T|^{2/n}(\|\operatorname{div} p_{LS}\|_{L^2(T)} - \|\operatorname{div}\widehat{p}_{LS}\|_{L^2(T)})^2\Big).\end{aligned}$$

For any $T \in \mathcal{T}\cap\widehat{\mathcal{T}}$, the reverse triangle inequality in $L^2(T)$ and $n^{1/n}|T|^{1/n} \le h_{\max}$ imply

$$|T|^{2/n}(\|\operatorname{div} p_{LS}\|_{L^2(T)} - \|\operatorname{div}\widehat{p}_{LS}\|_{L^2(T)})^2 \le h^2_{\max}\|\operatorname{div}(p_{LS} - \widehat{p}_{LS})\|^2_{L^2(T)}/n^{2/n}.$$

Like in the proof of (A1) for the reduced mixed method in Theorem 5.1, the reverse triangle inequality in $L^2(E)$ and the discrete jump control [CR17, Lem. 5.2] with constant $c_{\mathrm{jc}} \approx 1$ result in

$$\sum_{T\in\mathcal{T}\cap\widehat{\mathcal{T}}}|T|^{1/n}\sum_{E\in\mathcal{E}(T)}(\|[V_0]_E\|_{L^2(E)} - \|[\widehat{V}_0]_E\|_{L^2(E)})^2 \le c^2_{\mathrm{jc}}\|V_0 - \widehat{V}_0\|^2_{L^2(\Omega)}.$$

This concludes the proof with $\Lambda_1^2 = \max\{h^2_{\max}/n^{2/n}, c^2_{\mathrm{jc}}\}$. □

Theorem 8.3 (Reduction) *There exists* $\Lambda_2 = \Lambda_1 \approx 1$ *with*

$$\widehat{\eta}(\widehat{\mathcal{T}} \setminus \mathcal{T}) - 2^{-1/(2n)}\eta(\mathcal{T} \setminus \widehat{\mathcal{T}}) \leq \Lambda_2 \delta(\mathcal{T}, \widehat{\mathcal{T}}). \tag{A2}$$

Proof: Analogeously to the proof of stability (A1) above, let the vector $\widehat{v} \in \mathbb{R}^m$, $m := (n+2)|\widehat{\mathcal{T}} \setminus \mathcal{T}|$, with, for any $T \in \widehat{\mathcal{T}} \setminus \mathcal{T}$, the $(n+2)$ entries $|T|^{1/n}\|\operatorname{div} \widehat{p}_{LS}\|_{L^2(T)}$ and $|T|^{1/(2n)}\|[\widehat{V}_0]_E\|_{L^2(E)}$ for $E \in \mathcal{E}(T)$ and the vector $v \in \mathbb{R}^m$ with entries $|T|^{1/n}\|\operatorname{div} p_{LS}\|_{L^2(T)}$ and $|T|^{1/(2n)}\|[V_0]_E\|_{L^2(E)}$ for for any $T \in \widehat{\mathcal{T}} \setminus \mathcal{T}$ and $E \in \mathcal{E}(T)$. Then $\widehat{\eta}(\widehat{\mathcal{T}} \setminus \mathcal{T}) = |\widehat{v}|$. For an estimate of $|v|$, $V_0 \in P_0(\mathcal{T})$ shows $[V_0]_{\widehat{E}} \equiv 0$ along any $\widehat{E} \in \bigcup_{T \in \widehat{\mathcal{T}}(K)} \mathcal{E}(T)$ with $\widehat{E} \subseteq \operatorname{int}(K)$ for some $K \in \mathcal{T} \setminus \widehat{\mathcal{T}}$, and $|T| \leq |K|/2$ for $T \in \widehat{\mathcal{T}}(K)$ leads to

$$\begin{aligned}
|v|^2 &= \sum_{K \in \mathcal{T} \setminus \widehat{\mathcal{T}}} \sum_{T \in \widehat{\mathcal{T}}(K)} \Big(|T|^{2/n}\|\operatorname{div} p_{LS}\|^2_{L^2(T)} + |T|^{1/n} \sum_{\widehat{E} \in \mathcal{E}(T)} \|[V_0]_{\widehat{E}}\|^2_{L^2(\widehat{E})} \Big) \\
&\leq \sum_{K \in \mathcal{T} \setminus \widehat{\mathcal{T}}} \Big(|K|^{2/n} 2^{-2/n}\|\operatorname{div} p_{LS}\|^2_{L^2(K)} + |K|^{1/n} 2^{-1/n} \sum_{E \in \mathcal{E}(K)} \|[V_0]_E\|^2_{L^2(E)} \Big) \\
&\leq 2^{-1/n}\eta^2(\mathcal{T} \setminus \widehat{\mathcal{T}}).
\end{aligned}$$

As detailed in the proof of Reduction (A2), Theorem 5.2 for reduced mixed methods, reverse triangle inequalities in $L^2(T)$ and $L^2(E)$, and the discrete jump control of [CR17, Lem. 5.2] on $\widehat{\mathcal{T}}$ prove

$$|\widehat{v} - v| \leq \Lambda_1 \delta(\mathcal{T}, \widehat{\mathcal{T}}).$$

The triangle inequality $|\widehat{v}| \leq |\widehat{v} - v| + |v|$ concludes the proof. □

8.3. Discrete Reliability

This section gives details on a computation for the proof of discrete reliability that is transferred from [CP15] and utilizes the notation of Table 6 on p. 66 for a triangulation $\mathcal{T}$ and its refinement $\widehat{\mathcal{T}} \in \mathbb{T}(\mathcal{T})$. The first aim of this subsection is the proof of the estimate

$$\begin{aligned}
&\|\Pi_0 \operatorname{div}(\widehat{p}_{LS} - p_{LS})\|^2_{L^2(\Omega)} + (\widehat{V}_0 - V_0, \widehat{p}_{LS} - p_{LS} - \nabla(\widehat{u}_{LS} - u_{LS}))_{L^2(\Omega)} \\
&\quad \lesssim \eta(\mathcal{T} \setminus \widehat{\mathcal{T}})(|||u_{LS} - \widehat{u}_{LS}||| + \|p_{LS} - \widehat{p}_{LS}\|_{H(\operatorname{div})}) + \|V_0 - \widehat{V}_0\|_{L^2(\Omega)}\|h_{\mathcal{T}}(1 - \Pi_0)\operatorname{div} \widehat{p}_{LS}\|_{L^2(\Omega)}.
\end{aligned}$$

The proof of this estimate utilizes auxiliary solutions to the lowest-order Raviart-Thomas mixed scheme for the Poisson model problem [Bra07, p. 146] that seeks $p_{RT} \in RT_0(\mathcal{T})$ and $u_0 \in P_0(\mathcal{T})$ with

$$\begin{aligned}
(p_{RT}, q_{RT})_{L^2(\Omega)} + (\operatorname{div} q_{RT}, u_0)_{L^2(\Omega)} &= 0 && \text{for all } q_{RT} \in RT_0(\mathcal{T}), \\
(\operatorname{div} p_{RT}, v_0)_{L^2(\Omega)} &= -(f, v_0)_{L^2(\Omega)} && \text{for all } v_0 \in P_0(\mathcal{T}).
\end{aligned} \tag{8.6}$$

The second equality is equivalent to $\operatorname{div} p_{RT} = -\Pi_0 f$.

Like in [CP15], let $\widehat{q}_M \in RT_0(\widehat{\mathcal{T}})$, $\widehat{q}^{\star}_M \in RT_0(\widehat{\mathcal{T}})$, $q_M \in RT_0(\mathcal{T})$ the Raviart-Thomas parts of the solution to the mixed finite element scheme (8.6) on $\widehat{\mathcal{T}}$, $\widehat{\mathcal{T}}$, $\mathcal{T}$ with right-hand sides $-\operatorname{div}(\widehat{p}_{LS} - p_{LS})$, $-\Pi_0 \operatorname{div}(\widehat{p}_{LS} - p_{LS})$, $-\Pi_0 \operatorname{div}(\widehat{p}_{LS} - p_{LS})$. In particular, $\operatorname{div} \widehat{q}_M = \widehat{\Pi}_0 \operatorname{div}(\widehat{p}_{LS} - p_{LS}) = \operatorname{div}(\widehat{p}_{LS} - p_{LS})$ and $\operatorname{div} \widehat{q}^{\star}_M = \operatorname{div} q_M = \Pi_0 \operatorname{div}(\widehat{p}_{LS} - p_{LS})$.

Lemma 8.4 (Lemma 5.2 from [CP15]) *With* $\widehat{p}_M \coloneqq \widehat{p}_{LS} - p_{LS} - \widehat{q}_M + \widehat{q}_M^\star - q_M \in RT_0(\widehat{\mathcal{T}})$, *any* $v_C \in S^1_0(\mathcal{T})$ *satisfies*

$$\begin{aligned}(\widehat{V}_0 - V_0, \widehat{p}_{LS} - p_{LS} - \nabla(\widehat{u}_{LS} - u_{LS}))_{L^2(\Omega)} + \|\Pi_0 \operatorname{div}(\widehat{p}_{LS} - p_{LS})\|^2_{L^2(\Omega)} \\ = (V_0, \nabla(\widehat{u}_{LS} - u_{LS} - v_C) - \widehat{p}_M)_{L^2(\Omega)} + (V_0 - \widehat{V}_0, \widehat{q}_M^\star - \widehat{q}_M)_{L^2(\Omega)}.\end{aligned}$$

Proof: The test functions $\widehat{q}_{RT} \coloneqq \widehat{p}_{LS} - p_{LS} \in RT_0(\widehat{\mathcal{T}})$ and $\widehat{v}_C \coloneqq \widehat{u}_{LS} - u_{LS} \in S^1_0(\widehat{\mathcal{T}})$ in the discrete Euler-Lagrange equations on the fine level ($\widehat{\mathrm{LS}}$) and the orthogonality of $(1 - \Pi_0)\operatorname{div}(\widehat{p}_{LS} - p_{LS})$ onto $\Pi_0 f + \operatorname{div} p_{LS} \in P_0(\mathcal{T})$ in $L^2(\Omega)$ imply

$$\begin{aligned}(\widehat{V}_0, \widehat{p}_{LS} - p_{LS} - \nabla(\widehat{u}_{LS} - u_{LS}))_{L^2(\Omega)} &= -(\widehat{\Pi}_0 f + \operatorname{div} \widehat{p}_{LS}, \operatorname{div}(\widehat{p}_{LS} - p_{LS}))_{L^2(\Omega)} \\ &= -(\widehat{\Pi}_0 f - \Pi_0 f, \operatorname{div}(\widehat{p}_{LS} - p_{LS}))_{L^2(\Omega)} - (\Pi_0 f + \operatorname{div} p_{LS}, \Pi_0 \operatorname{div}(\widehat{p}_{LS} - p_{LS}))_{L^2(\Omega)} \\ &\quad - \|\operatorname{div}(\widehat{p}_{LS} - p_{LS})\|^2_{L^2(\Omega)}.\end{aligned}$$

The discrete Euler-Lagrange equations (LS) on the coarse level for test functions $q_{RT} \coloneqq q_M \in RT_0(\mathcal{T})$ and any $v_C \in S^1_0(\mathcal{T})$ and $\operatorname{div} q_M = \Pi_0 \operatorname{div}(\widehat{p}_{LS} - p_{LS})$ show $-(\Pi_0 f + \operatorname{div} p_{LS}, \Pi_0 \operatorname{div}(\widehat{p}_{LS} - p_{LS}))_{L^2(\Omega)} = (V_0, q_M - \nabla v_C)_{L^2(\Omega)}$. Hence,

$$\begin{aligned}(\widehat{V}_0 - V_0, \widehat{p}_{LS} - p_{LS} - \nabla(\widehat{u}_{LS} - u_{LS}))_{L^2(\Omega)} + \|\operatorname{div}(\widehat{p}_{LS} - p_{LS})\|^2_{L^2(\Omega)} \\ = (V_0, \nabla(\widehat{u}_{LS} - u_{LS} - v_C) - \widehat{p}_{LS} + p_{LS} + q_M)_{L^2(\Omega)} \\ - (\widehat{\Pi}_0 f - \Pi_0 f, \operatorname{div}(\widehat{p}_{LS} - p_{LS}))_{L^2(\Omega)}.\end{aligned}$$

The splits $-\widehat{p}_{LS} + p_{LS} + q_M = -\widehat{p}_M + \widehat{q}_M^\star - \widehat{q}_M$ and $V_0 = (V_0 - \widehat{V}_0) - \widehat{V}_0$ imply

$$\begin{aligned}(\widehat{V}_0 - V_0, \widehat{p}_{LS} - p_{LS} - \nabla(\widehat{u}_{LS} - u_{LS}))_{L^2(\Omega)} + \|\operatorname{div}(\widehat{p}_{LS} - p_{LS})\|^2_{L^2(\Omega)} \\ = (V_0, \nabla(\widehat{u}_{LS} - u_{LS} - v_C) - \widehat{p}_M)_{L^2(\Omega)} + (V_0 - \widehat{V}_0, \widehat{q}_M^\star - \widehat{q}_M)_{L^2(\Omega)} \\ + (\widehat{V}_0, \widehat{q}_M^\star - \widehat{q}_M)_{L^2(\Omega)} - (\widehat{\Pi}_0 f - \Pi_0 f, \operatorname{div}(\widehat{p}_{LS} - p_{LS}))_{L^2(\Omega)}.\end{aligned}$$

The discrete Euler-Lagrange equations ($\widehat{\mathrm{LS}}$) with the test functions $\widehat{q}_{RT} \coloneqq \widehat{q}_M^\star - \widehat{q}_M \in RT_0(\widehat{\mathcal{T}})$, $\widehat{v}_C \coloneqq 0 \in S^1_0(\widehat{\mathcal{T}})$, $-\operatorname{div}(\widehat{q}_M^\star - \widehat{q}_M) = (1 - \Pi_0)\operatorname{div}(\widehat{p}_{LS} - p_{LS})$, and the orthogonalities of $\widehat{\Pi}_0 f - \Pi_0 f$ and $(1 - \Pi_0)\operatorname{div}(\widehat{p}_{LS} - p_{LS})$ onto $P_0(\mathcal{T})$ prove

$$\begin{aligned}(\widehat{V}_0, \widehat{q}_M^\star - \widehat{q}_M)_{L^2(\Omega)} - (\widehat{\Pi}_0 f - \Pi_0 f, \operatorname{div}(\widehat{p}_{LS} - p_{LS}))_{L^2(\Omega)} \\ = (\widehat{\Pi}_0 f + \operatorname{div} \widehat{p}_{LS}, (1 - \Pi_0)\operatorname{div}(\widehat{p}_{LS} - p_{LS}))_{L^2(\Omega)} - (\widehat{\Pi}_0 f - \Pi_0 f, \operatorname{div}(\widehat{p}_{LS} - p_{LS}))_{L^2(\Omega)} \\ = \|(1 - \Pi_0)\operatorname{div}(\widehat{p}_{LS} - p_{LS})\|^2_{L^2(\Omega)}.\end{aligned}$$

This and the Pythagoras theorem $\|\operatorname{div}(\widehat{p}_{LS} - p_{LS})\|^2_{L^2(\Omega)} = \|\Pi_0 \operatorname{div}(\widehat{p}_{LS} - p_{LS})\|^2_{L^2(\Omega)} + \|(1 - \Pi_0)\operatorname{div}(\widehat{p}_{LS} - p_{LS})\|^2_{L^2(\Omega)}$ conclude the proof. □

The proof of the subsequent lemma is a minor generalization of the proof of [CP15] to the n dimensional case.

Lemma 8.5 (Lemma 5.3 from [CP15]) *The difference $\widehat{q}_M - \widehat{q}_M^\star$ is super-close in that*

$$\|\widehat{q}_M - \widehat{q}_M^\star\|_{L^2(\Omega)} \lesssim \|h_{\mathcal{T}}(1-\Pi_0)\operatorname{div}(\widehat{p}_{LS} - p_{LS})\|_{L^2(\Omega)} = \|h_{\mathcal{T}}(1-\Pi_0)\operatorname{div}\widehat{p}_{LS}\|_{L^2(\Omega)}.$$

Proof: The Pythagoras theorem, the split from Remark 2.11, the pointwise estimate $|(\bullet - \operatorname{mid}(\widehat{T}))/n| \le h_{\mathcal{T}}/(n+1)$, and $\operatorname{div}(\widehat{q}_M - \widehat{q}_M^\star) = (1-\Pi_0)\operatorname{div}(\widehat{p}_{LS} - p_{LS})$ prove

$$\begin{aligned}\|\widehat{q}_M - \widehat{q}_M^\star\|_{L^2(\Omega)}^2 &\le \|h_{\mathcal{T}}\operatorname{div}(\widehat{q}_M - \widehat{q}_M^\star)\|_{L^2(\Omega)}^2/(n+1)^2 + \|\widehat{\Pi}_0(\widehat{q}_M - \widehat{q}_M^\star)\|_{L^2(\Omega)}^2 \\ &= \|h_{\mathcal{T}}(1-\Pi_0)\operatorname{div}(\widehat{p}_{LS} - p_{LS})\|_{L^2(\Omega)}^2/(n+1)^2 + \|\widehat{\Pi}_0(\widehat{q}_M - \widehat{q}_M^\star)\|_{L^2(\Omega)}^2.\end{aligned}$$

For the estimate of the second term, consider the solution $\widehat{v}_{CR} \in CR_0^1(\widehat{\mathcal{T}})$ to $a_{NC}(\widehat{v}_{CR}, \widehat{w}_{CR}) = (\widehat{\Pi}_0(\widehat{q}_M - \widehat{q}_M^\star), \nabla_{NC} w_{CR})_{L^2(\Omega)}$ for all $\widehat{w}_{CR} \in CR_0^1(\widehat{\mathcal{T}})$. Then $\widehat{p}_{RT} := \widehat{\Pi}_0(\widehat{q}_M - \widehat{q}_M^\star) - \nabla_{NC}\widehat{v}_{CR} \in P_0(\widehat{\mathcal{T}}) \subset RT_0^{NC}(\widehat{\mathcal{T}})$ and Lemma 2.25 shows $\widehat{p}_{RT} \in RT_0(\widehat{\mathcal{T}})$ with $\operatorname{div}\widehat{p}_{RT} = 0$. Consequently, the first equation of the mixed system 8.6 and Lemma 2.25 show that $0 = (\widehat{q}_M - \widehat{q}_M^\star, \widehat{p}_{RT})_{L^2(\Omega)} = (\widehat{\Pi}_0(\widehat{q}_M - \widehat{q}_M^\star) - \nabla_{NC}\widehat{v}_{CR}, \widehat{p}_{RT})_{L^2(\Omega)} = \|\widehat{p}_{RT}\|_{L^2(\Omega)}^2$. Hence, $\widehat{\Pi}_0(\widehat{q}_M - \widehat{q}_M^\star) = \nabla_{NC}\widehat{v}_{CR}$ and an integration by parts prove

$$\|\widehat{\Pi}_0(\widehat{q}_M - \widehat{q}_M^\star)\|_{L^2(\Omega)}^2 = (\widehat{q}_M - \widehat{q}_M^\star, \nabla_{NC}\widehat{v}_{CR})_{L^2(\Omega)} = -(\operatorname{div}(\widehat{q}_M - \widehat{q}_M^\star), \widehat{v}_{CR})_{L^2(\Omega)}.$$

This, $\operatorname{div}(\widehat{q}_M - \widehat{q}_M^\star) = (1-\Pi_0)\operatorname{div}(\widehat{p}_{LS} - p_{LS})$, and the discrete Poincaré inequality from Theorem 2.30 result in

$$\begin{aligned}\|\widehat{\Pi}_0(\widehat{q}_M - \widehat{q}_M^\star)\|_{L^2(\Omega)}^2 &= -(h_{\mathcal{T}}(1-\Pi_0)\operatorname{div}(\widehat{p}_{LS} - p_{LS}), h_{\mathcal{T}}^{-1}(1-\Pi_0)\widehat{v}_{CR})_{L^2(\Omega)} \\ &\le c_{\mathrm{dP}}\|h_{\mathcal{T}}(1-\Pi_0)\operatorname{div}(\widehat{p}_{LS} - p_{LS})\|_{L^2(\Omega)}|||\widehat{v}_{CR}|||_{NC}.\end{aligned}$$

Since $|||\widehat{v}_{CR}|||_{NC} = \|\widehat{\Pi}_0(\widehat{q}_M - \widehat{q}_M^\star)\|_{L^2(\Omega)}$, this and $(1-\Pi_0)\operatorname{div} p_{LS} = 0$ conclude the proof. □

Lemma 8.6 (Lemma 5.4 from [CP15]) *There exists $v_C^* \in S_0^1(\mathcal{T})$ that satisfies*

$$(V_0, \nabla(\widehat{u}_{LS} - u_{LS} - v_C^*))_{L^2(\Omega)} \lesssim \eta(\mathcal{T}\setminus\widehat{\mathcal{T}})|||\widehat{u}_{LS} - u_{LS}|||.$$

Proof: Following the proof of Lemma 5.4 from [CP15], consider $\widehat{u}_C := \widehat{u}_{LS} - u_{LS} \in S_0^1(\widehat{\mathcal{T}})$ and its Scott-Zhang quasi-interpolation $v_C^* = J_{\mathrm{dQI}}\widehat{v}_C \in S_0^1(\mathcal{T})$ from Theorem 2.38. Like shown in detail in the proof of Lemma 3.7 for the reduced method, i.e., with some $\nabla_{NC}v_{CR}$ instead of V_0, a piecewise integration by parts, $\widehat{u}_C - J_{\mathrm{dQI}}\widehat{u}_C = 0$ along any $E = \partial T_+ \cap \partial T_- \in \mathcal{E}(\Omega)$ with $T_+ \in \mathcal{T}\cap\widehat{\mathcal{T}}$ or $T_- \in \mathcal{T}\cap\widehat{\mathcal{T}}$, and the discrete trace inequality prove

$$(V_0, \widehat{u}_C - J_{\mathrm{dQI}}\widehat{u}_C)_{L^2(\Omega)} \lesssim \Big(\sum_{T\in\mathcal{T}\setminus\widehat{\mathcal{T}}} |T|^{1/n} \sum_{E\in\mathcal{E}(T)} \|[V_0]_E\cdot\nu_E\|_{L^2(E)}^2\Big)^{1/2} \|h_{\mathcal{T}}^{-1}(\widehat{u}_C - J_{\mathrm{dQI}}\widehat{u}_C)\|_{L^2(\Omega)}.$$

The approximation property $\|h_{\mathcal{T}}^{-1}(\widehat{u}_C - J_{\mathrm{dQI}}\widehat{u}_C)\|_{L^2(\Omega)}/c_{\mathrm{dQI}} \le |||\widehat{u}_C||| = |||\widehat{u}_{LS} - u_{LS}|||$ from Theorem 2.38 and $\sum_{T\in\mathcal{T}\setminus\widehat{\mathcal{T}}} |T|^{1/n}\sum_{E\in\mathcal{E}(T)}\|[V_0]_E\cdot\nu_E\|_{L^2(E)}^2 \le \eta^2(\mathcal{T}\setminus\widehat{\mathcal{T}})$ conclude the proof. □

The proof of the subsequent lemma differs from the proof in [CP15], which utilizes a discrete Helmholtz decomposition and is therefore restricted to $n = 2$. In contrast to that, the following proof employs the discrete quasi-interpolation for Crouzeix-Raviart functions from Theorem 2.39 and holds for any space dimension.

Lemma 8.7 (Lemma 5.5 from [CP15]) *With $\widehat{p}_M \in RT_0(\widehat{\mathcal{T}})$ from Lemma 8.4, it holds*

$$-(V_0, \widehat{p}_M)_{L^2(\Omega)} \lesssim \eta(\mathcal{T} \setminus \widehat{\mathcal{T}}) \|\widehat{p}_{LS} - p_{LS}\|_{H(\mathrm{div})}.$$

Proof: Since the discrete Euler-Lagrange equations (LS) show that V_0 is orthogonal to $\{q_{RT} \in RT_0(\mathcal{T}) \mid \operatorname{div} q_{RT} = 0\}$, Lemma 6.6 implies the existence of $v_{CR} \in CR^1_0(\mathcal{T})$ with $V_0 = \nabla_{NC} v_{CR}$. Since $\operatorname{div} \widehat{p}_M = \operatorname{div}(\widehat{p}_{LS} - p_{LS} - \widehat{q}_M + \widehat{q}^\star_M - q_M) = (1 - \widehat{\Pi}_0) \operatorname{div}(\widehat{p}_{LS} - p_{LS}) = 0$, the integration by parts from Lemma 2.25 with $J_{\mathrm{dCR}} v_{CR} \in CR^1_0(\widehat{\mathcal{T}})$ from Theorem 2.39 and $\widehat{p}_M \in RT_0(\widehat{\mathcal{T}})$ lead to $(\nabla_{NC} J_{\mathrm{dCR}} v_{CR}, \widehat{p}_M)_{L^2(\Omega)} = 0$. Hence, the Cauchy inequality and the error estimate from Theorem 2.39 prove

$$-(V_0, \widehat{p}_M)_{L^2(\Omega)} = -(\nabla_{NC}(v_{CR} - J_{\mathrm{dCR}} v_{CR}), \widehat{p}_M)_{L^2(\Omega)} \lesssim \eta(\mathcal{T} \setminus \widehat{\mathcal{T}}) \|\widehat{p}_M\|_{L^2(\Omega)}.$$

The triangle inequality implies $\|\widehat{p}_M\|_{L^2(\Omega)} \le \|\widehat{p}_{LS} - p_{LS}\|_{L^2(\Omega)} + \|\widehat{q}_M - \widehat{q}^\star_M\|_{L^2(\Omega)} + \|q_M\|_{L^2(\Omega)}$. The super-closeness of Lemma 8.5 proves $\|\widehat{q}_M - \widehat{q}^\star_M\|_{L^2(\Omega)} \le h_{\max} \|\operatorname{div}(\widehat{p}_{LS} - p_{LS})\|_{L^2(\Omega)}$. The stability [Bra07, p. 151] of the mixed scheme (8.6) shows $\|q_M\|_{L^2(\Omega)} \lesssim \|\Pi_0 \operatorname{div}(\widehat{p}_{LS} - p_{LS})\|_{L^2(\Omega)} \le \|\operatorname{div}(\widehat{p}_{LS} - p_{LS})\|_{L^2(\Omega)}$. Hence, $\|\widehat{p}_M\|_{L^2(\Omega)} \lesssim \|\widehat{p}_{LS} - p_{LS}\|_{H(\mathrm{div})}$ concludes the proof. □

Lemmas 8.4–8.7 imply the following assertion.

Corollary 8.8 It holds

$$\begin{aligned}\|\Pi_0 \operatorname{div}(\widehat{p}_{LS} - p_{LS})\|^2_{L^2(\Omega)} &+ (\widehat{V}_0 - V_0, \widehat{p}_{LS} - p_{LS} - \nabla(\widehat{u}_{LS} - u_{LS}))_{L^2(\Omega)} \\ &\lesssim \eta(\mathcal{T} \setminus \widehat{\mathcal{T}}) (|||\widehat{u}_{LS} - u_{LS}||| + \|\widehat{p}_{LS} - p_{LS}\|_{H(\mathrm{div})}) \\ &\quad + \|\widehat{V}_0 - V_0\|_{L^2(\Omega)} \|h_{\mathcal{T}} (1 - \Pi_0) \operatorname{div} \widehat{p}_{LS}\|_{L^2(\Omega)}.\end{aligned}$$ □

The remaining part of this section is devoted to the proof of discrete reliability following ideas of [CP15] with the extra difficulty caused by the fact that M_0 and $\widehat{M}_0$ are different. This requires a careful analysis of the spectral radius $\varrho(\bullet)$ of different powers of M_0 and $\widehat{M}_0$.

Theorem 8.9 *Let $\mathcal{T} \in \mathbb{T}$ with refinement $\widehat{\mathcal{T}} \in \mathbb{T}(\mathcal{T})$, vector fields $X \in P_0(\mathcal{T}; \mathbb{R}^n)$, $\widehat{X} \in P_0(\widehat{\mathcal{T}}; \mathbb{R}^n)$, and let $A_0 \in P_0(\mathcal{T}; \mathbb{S})$, $\widehat{A}_0 \in P_0(\widehat{\mathcal{T}}; \mathbb{S})$ be piecewise SPD. Set the minimal and maximal eigenvalues*

$$\underline{\varrho} := \min_{T \in \mathcal{T}} \lambda_{\min}(A_0|_T) \quad \text{and} \quad \overline{\varrho} := \max_{T \in \mathcal{T}} \varrho(A_0|_T)$$

and $\varrho(\widehat{A}_0, A_0) := \|\varrho(\widehat{A}_0 - A_0)\|_{L^\infty(\Omega)} = \max_{T \in \widehat{\mathcal{T}}} |\varrho(A_0|_T - \widehat{A}_0|_T)|$. Then it holds

$$\begin{aligned}&\|\widehat{A}_0 \widehat{X} - A_0 X\|^2_{L^2(\Omega)} \le 2\overline{\varrho}(\widehat{A}_0 \widehat{X} - A_0 X, \widehat{X} - X)_{L^2(\Omega)} + \overline{\varrho}^2 \underline{\varrho}^{-2} \varrho(\widehat{A}_0, A_0)^2 \|\widehat{X}\|^2_{L^2(\Omega)} \text{ and} \\ &\|\widehat{A}_0 \widehat{X} - A_0 X\|^2_{L^2(\Omega)} \le 4\overline{\varrho}^2 \|\widehat{X} - X\|^2_{L^2(\Omega)} + 2\overline{\varrho}^2 \underline{\varrho}^{-2} \varrho(\widehat{A}_0, A_0)^2 \|\widehat{X}\|^2_{L^2(\Omega)}.\end{aligned}$$

Proof: Like explained in Remark 6.2, $\max_{T\in\mathcal{T}}\varrho(A_0^{1/2}|_T)\le\overline{\varrho}^{1/2}$, the pointwise symmetry of A_0^{-1}, and the Cauchy inequality yield

$$\begin{aligned}\|\widehat{A}_0\widehat{X}-A_0X\|_{L^2(\Omega)}^2/\overline{\varrho}&\le\|A_0^{-1/2}(\widehat{A}_0\widehat{X}-A_0X)\|_{L^2(\Omega)}^2\\&=(A_0^{-1}(\widehat{A}_0\widehat{X}-A_0X),\widehat{A}_0\widehat{X}-A_0X)_{L^2(\Omega)}\\&=(\widehat{X}-X,\widehat{A}_0\widehat{X}-A_0X)_{L^2(\Omega)}\\&\quad-((I_{n\times n}-A_0^{-1}\widehat{A}_0)\widehat{X},\widehat{A}_0\widehat{X}-A_0X)_{L^2(\Omega)}\\&\le(\widehat{A}_0\widehat{X}-A_0X,\widehat{X}-X)_{L^2(\Omega)}\\&\quad+\|(I_{n\times n}-A_0^{-1}\widehat{A}_0)\widehat{X}\|_{L^2(\Omega)}\|\widehat{A}_0\widehat{X}-A_0X\|_{L^2(\Omega)}.\end{aligned}$$

The estimates $\|(I_{n\times n}-A_0^{-1}\widehat{A}_0)\widehat{X}\|_{L^2(\Omega)}=\|A_0^{-1}(A_0-\widehat{A}_0)\widehat{X}\|_{L^2(\Omega)}\le\underline{\varrho}^{-1}\|(A_0-\widehat{A}_0)\widehat{X}\|_{L^2(\Omega)}$ and $\|(A_0-\widehat{A}_0)\widehat{X}\|_{L^2(\Omega)}\le\varrho(\widehat{A}_0,A_0)\|\widehat{X}\|_{L^2(\Omega)}$ plus the Young inequality from Theorem 2.32 with $\lambda=1$ show

$$\begin{aligned}\|\widehat{A}_0\widehat{X}-A_0X\|_{L^2(\Omega)}^2&\le\overline{\varrho}(\widehat{A}_0\widehat{X}-A_0X,\widehat{X}-X)_{L^2(\Omega)}\\&\quad+\overline{\varrho}^2\underline{\varrho}^{-2}\varrho(\widehat{A}_0,A_0)^2\|\widehat{X}\|_{L^2(\Omega)}^2/2+\|\widehat{A}_0\widehat{X}-A_0X\|_{L^2(\Omega)}^2/2.\end{aligned}$$

The absorption of $\|\widehat{A}_0\widehat{X}-A_0X\|_{L^2(\Omega)}^2/2$ into the left-hand side concludes the proof of the first assertion. The second follows from the Cauchy and the Young inequality. □

Theorem 8.10 (Discrete reliability) *There exists $\Lambda_3=\widehat{\Lambda}_3\approx1$ such that any $\mathcal{T}$ with admissible refinement $\widehat{\mathcal{T}}$ satisfies*

$$\delta^2(\mathcal{T},\widehat{\mathcal{T}})\le\Lambda_3(\eta^2(\mathcal{T}\setminus\widehat{\mathcal{T}})+\mu^2)+\widehat{\Lambda}_3\eta^2(\widehat{\mathcal{T}}).\tag{A3}$$

Proof: *Step 1. Split of the left-hand side.* The theorem of Pythagoras $\|\operatorname{div}(\widehat{p}_{LS}-p_{LS})\|_{L^2(\Omega)}^2=\|\Pi_0(\operatorname{div}(\widehat{p}_{LS}-p_{LS}))\|_{L^2(\Omega)}^2+\|(1-\Pi_0)(\operatorname{div}(\widehat{p}_{LS}-p_{LS}))\|_{L^2(\Omega)}^2$ and $(1-\Pi_0)\operatorname{div}p_{LS}=0$ lead to

$$\delta^2(\mathcal{T},\widehat{\mathcal{T}})=\|(1-\Pi_0)\operatorname{div}\widehat{p}_{LS}\|_{L^2(\Omega)}^2+\|\Pi_0\operatorname{div}(\widehat{p}_{LS}-p_{LS})\|_{L^2(\Omega)}^2+\|\widehat{V}_0-V_0\|_{L^2(\Omega)}^2.$$

Step 2. Estimate of the first term. A triangle inequality, $\|\widehat{\Pi}_0f-\Pi_0f\|_{L^2(\Omega)}\le\mu$ as in the beginning of the proof of Theorem 8.1, and Lemma 6.7 lead to

$$\begin{aligned}\|(1-\Pi_0)\operatorname{div}\widehat{p}_{LS}\|_{L^2(\Omega)}&=\|(1-\Pi_0)(\Pi_0f+\operatorname{div}\widehat{p}_{LS})\|_{L^2(\Omega)}\le\|\Pi_0f+\operatorname{div}\widehat{p}_{LS}\|_{L^2(\Omega)}\\&\le\|\widehat{\Pi}_0f-\Pi_0f\|_{L^2(\Omega)}+\|\widehat{\Pi}_0f+\operatorname{div}\widehat{p}_{LS}\|_{L^2(\Omega)}\\&\le\mu+(LS(f,\widehat{\mathcal{T}};\widehat{p}_{LS},\widehat{u}_{LS}))^{1/2}\le\mu+c_{\mathrm{rel}}^{1/2}\widehat{\eta}.\end{aligned}$$

Step 3. Estimate of the second and third term. Theorem 8.9 with $A_0=M_0^{-1}$, $\widehat{A}_0=\widehat{M}_0^{-1}$, $X=W_0=\Pi_0p_{LS}-\nabla u_{LS}+F_0$, and $\widehat{X}=\widehat{W}_0=\widehat{\Pi}_0\widehat{p}_{LS}-\nabla\widehat{u}_{LS}+\widehat{F}_0$ implies

$$\|\widehat{V}_0-V_0\|_{L^2(\Omega)}^2=\|\widehat{M}_0^{-1}\widehat{W}_0-M_0^{-1}W_0\|_{L^2(\Omega)}^2\le2\underline{\lambda}^{-1}(\widehat{V}_0-V_0,\widehat{W}_0-W_0)_{L^2(\Omega)}+C_1\|\widehat{W}_0\|_{L^2(\Omega)}^2$$

for $C_1 = 2\underline{\lambda}^{-2}\overline{\lambda}^2\varrho(\widehat{M}_0^{-1}, M_0^{-1})^2 \le 8\underline{\lambda}^{-4}\overline{\lambda}^2$ with a triangle inequality in the last estimate. The orthogonality $V_0 - \widehat{V}_0 \perp (1-\Pi_0)p_{LS}$ in $L^2(T)$ for any $T \in \mathcal{T} \cap \widehat{\mathcal{T}}$ shows

$$\begin{aligned}(\widehat{V}_0 - V_0, \widehat{W}_0 - W_0)_{L^2(\Omega)} &= (\widehat{V}_0 - V_0, \widehat{\Pi}_0\widehat{p}_{LS} - \Pi_0 p_{LS} - \nabla(\widehat{u}_{LS} - u_{LS}) + \widehat{F}_0 - F_0)_{L^2(\Omega)} \\ &= (\widehat{V}_0 - V_0, \widehat{p}_{LS} - p_{LS} - \nabla(\widehat{u}_{LS} - u_{LS}))_{L^2(\Omega)} + (\widehat{V}_0 - V_0, (1-\Pi_0)p_{LS})_{L^2(\mathcal{T}\setminus\widehat{\mathcal{T}})} \\ &\quad + (\widehat{V}_0 - V_0, \widehat{F}_0 - F_0)_{L^2(\Omega)}.\end{aligned}$$

Remark 6.2 and Lemma 6.7 lead to

$$\|\widehat{W}_0\|^2_{L^2(\Omega)} = \|\widehat{M}_0\widehat{V}_0\|^2_{L^2(\Omega)} \le \overline{\lambda}^2\|\widehat{V}_0\|^2_{L^2(\Omega)} \le c_{\mathrm{rel}}\overline{\lambda}^2\widehat{\eta}^2.$$

The last three displayed estimates, $C_2 = \max\{2\underline{\lambda}^{-1}, 1\}$ and Corollary 8.8 with constant $C_3 \approx 1$ show

$$\begin{aligned}\|\Pi_0\operatorname{div}(\widehat{p}_{LS} - p_{LS})\|^2_{L^2(\Omega)} + \|\widehat{V}_0 - V_0\|^2_{L^2(\Omega)} &\le C_1 c_{\mathrm{rel}}\overline{\lambda}^2\widehat{\eta}^2 \\ &\quad + C_2(\widehat{V}_0 - V_0, (1-\Pi_0)p_{LS})_{L^2(\mathcal{T}\setminus\widehat{\mathcal{T}})} + C_2(\widehat{V}_0 - V_0, \widehat{F}_0 - F_0)_{L^2(\Omega)} \\ &\quad + C_2C_3\eta(\mathcal{T}\setminus\widehat{\mathcal{T}})(|||\widehat{u}_{LS} - u_{LS}||| + \|\widehat{p}_{LS} - p_{LS}\|_{H(\mathrm{div})}) \\ &\quad + C_2C_3\|\widehat{V}_0 - V_0\|_{L^2(\Omega)}\|h_{\mathcal{T}}(1-\Pi_0)\operatorname{div}\widehat{p}_{LS}\|_{L^2(\Omega)}.\end{aligned}$$

Step 4. The Cauchy inequality, $\|(1-\Pi_0)p_{LS}\|_{L^2(\mathcal{T}\setminus\widehat{\mathcal{T}})} \le c_{\mathrm{sr}}^{1/n}\eta(\mathcal{T}\setminus\widehat{\mathcal{T}})/(n+1)$, $\|\widehat{F}_0 - F_0\|_{L^2(\Omega)} \le 2\kappa_1\mu$ like in (8.3), Step 2, and the Young inequality from Theorem 2.32 with $\lambda = 1$ imply that $C_4 = C_2\max\{c_{\mathrm{sr}}^{1/n}/(n+1), 2\kappa_1 + h_{\max}C_3, h_{\max}C_3c_{\mathrm{rel}}^{1/2}\}$ satisfies

$$\begin{aligned}&C_2(\widehat{V}_0 - V_0, (1-\Pi_0)p_{LS})_{L^2(\mathcal{T}\setminus\widehat{\mathcal{T}})} + C_2(\widehat{V}_0 - V_0, \widehat{F}_0 - F_0)_{L^2(\Omega)} \\ &\qquad + C_2C_3\|\widehat{V}_0 - V_0\|_{L^2(\Omega)}\|h_{\mathcal{T}}(1-\Pi_0)\operatorname{div}\widehat{p}_{LS}\|_{L^2(\Omega)} \\ &\quad \le C_4\|\widehat{V}_0 - V_0\|_{L^2(\Omega)}(\eta(\mathcal{T}\setminus\widehat{\mathcal{T}}) + \mu + \widehat{\eta}) \\ &\quad \le \|\widehat{V}_0 - V_0\|_{L^2(\Omega)}/2 + 3C_4^2(\mu^2 + \widehat{\eta}^2 + \eta^2(\mathcal{T}\setminus\widehat{\mathcal{T}}))/2.\end{aligned}$$

Step 5. Combination of Steps 1–4. The previous steps show

$$\begin{aligned}\delta^2(\mathcal{T},\widehat{\mathcal{T}}) &\le (2 + 3C_4^2/2)\mu^2 + (2c_{\mathrm{rel}} + C_1c_{\mathrm{rel}}\overline{\lambda}^2 + 3C_4^2/2)\widehat{\eta}^2 + 3C_4^2\eta(\mathcal{T}\setminus\widehat{\mathcal{T}})/2 \\ &\quad + \|\widehat{V}_0 - V_0\|^2_{L^2(\Omega)}/2 + C_2C_3\eta(\mathcal{T}\setminus\widehat{\mathcal{T}})\big(|||\widehat{u}_{LS} - u_{LS}||| + \|\widehat{p}_{LS} - p_{LS}\|_{H(\mathrm{div})}\big).\end{aligned}$$

The absorption of $\|V_0 - \widehat{V}_0\|^2_{L^2(\Omega)} \le \delta^2(\mathcal{T},\widehat{\mathcal{T}})$ into the left-hand shows that $C_5 = 2\max\{2 + 3C_4^2/2, 2c_{\mathrm{rel}} + C_1c_{\mathrm{rel}}\overline{\lambda}^2 + 3C_4^2/2, C_2C_3\}$ satisfies

$$\delta^2(\mathcal{T},\widehat{\mathcal{T}}) \le C_5\big(\mu^2 + \widehat{\eta}^2 + \eta^2(\mathcal{T}\setminus\widehat{\mathcal{T}}) + \eta(\mathcal{T}\setminus\widehat{\mathcal{T}})(|||u_{LS} - \widehat{u}_{LS}||| + \|p_{LS} - \widehat{p}_{LS}\|_{H(\mathrm{div})})\big). \quad (8.7)$$

Step 6. Estimation of $|||u_{LS} - \widehat{u}_{LS}||| + \|p_{LS} - \widehat{p}_{LS}\|_{H(\mathrm{div})}$. The equivalence (6.3) on p. 53 for the standard least-squares functional, the orthogonality $(1-\widehat{\Pi}_0)$ onto $P_0(\widehat{\mathcal{T}})$, and the split

$\widehat{p}_{LS} - p_{LS} = \widehat{\Pi}_0(\widehat{p}_{LS} - p_{LS}) + \operatorname{div}(\widehat{p}_{LS} - p_{LS})(\bullet - \operatorname{mid}(\mathcal{T}))/n$ from Remark 2.11 in $\|(1-\widehat{\Pi}_0)(\widehat{p}_{LS} - p_{LS})\|_{L^2(\Omega)} \le h_{\max}\|\operatorname{div}(\widehat{p}_{LS} - p_{LS})\|_{L^2(\Omega)}/(n+1)$ result in

$$\begin{aligned}
\big(|||\widehat{u}_{LS} - u_{LS}||| + \|\widehat{p}_{LS} - p_{LS}\|_{H(\operatorname{div})}\big)/(2c_{\mathrm{LS}})^{1/2} \\
&\le \|\operatorname{div}(\widehat{p}_{LS} - p_{LS})\|_{L^2(\Omega)} + \|\widehat{p}_{LS} - p_{LS} - \nabla(\widehat{u}_{LS} - u_{LS})\|_{L^2(\Omega)} \\
&\le (1 + h_{\max}/(n+1))\|\operatorname{div}(\widehat{p}_{LS} - p_{LS})\|_{L^2(\Omega)} \\
&\quad + \|\widehat{\Pi}_0(\widehat{p}_{LS} - p_{LS}) - \nabla(\widehat{u}_{LS} - u_{LS})\|_{L^2(\Omega)} \\
&\le (1 + h_{\max}/(n+1))\|\operatorname{div}(\widehat{p}_{LS} - p_{LS})\|_{L^2(\Omega)} + \|(\Pi_0 - \widehat{\Pi}_0)p_{LS}\|_{L^2(\Omega)} \\
&\quad + \|\widehat{W}_0 - W_0\|_{L^2(\Omega)} + \|\widehat{F}_0 - F_0\|_{L^2(\Omega)}. \qquad (8.8)
\end{aligned}$$

Since $(\Pi_0 - \widehat{\Pi}_0)p_{LS} = 0$ on $\mathcal{T} \cap \widehat{\mathcal{T}}$ and Lemma 2.24 implies $\Pi_0 = \widehat{\Pi}_0 \circ \Pi_0$, it follows

$$\|(\Pi_0 - \widehat{\Pi}_0)p_{LS}\|_{L^2(\Omega)} \le \|(1 - \Pi_0)p_{LS}\|_{L^2(\mathcal{T} \setminus \widehat{\mathcal{T}})} \le c_{\mathrm{sr}}^{1/n}\eta(\mathcal{T} \setminus \widehat{\mathcal{T}})/(n+1).$$

The second part of Theorem 8.9 with $X = V_0$, $\widehat{X} = \widehat{V}_0$, $A_0 = M_0$, and $\widehat{A}_0 = \widehat{M}_0$ shows

$$\begin{aligned}
\|\widehat{W}_0 - W_0\|_{L^2(\Omega)}^2 &\le 4\overline{\lambda}^2\|\widehat{V}_0 - V_0\|_{L^2(\Omega)}^2 + 8\overline{\lambda}^4\underline{\lambda}^{-2}\|\widehat{V}_0\|_{L^2(\Omega)}^2 \\
&\le 4\overline{\lambda}^2\|\widehat{V}_0 - V_0\|_{L^2(\Omega)}^2 + 8c_{\mathrm{rel}}\overline{\lambda}^4\underline{\lambda}^{-2}\widehat{\eta}^2.
\end{aligned}$$

This, (8.8), and the Cauchy inequality in $\mathbb{R}^2$ show that $C_6 = (2c_{\mathrm{LS}})^{1/2}((1 + h_{\max}/(n+1))^2 + 4\overline{\lambda}^2)^{1/2}$ satisfies

$$\begin{aligned}
&|||u_{LS} - \widehat{u}_{LS}||| + \|p_{LS} - \widehat{p}_{LS}\|_{H(\operatorname{div})} \\
&\quad \le C_6\delta(\mathcal{T}, \widehat{\mathcal{T}}) + (2c_{\mathrm{LS}})^{1/2}c_{\mathrm{sr}}^{1/n}\eta(\mathcal{T} \setminus \widehat{\mathcal{T}})/(n+1) + (2c_{\mathrm{LS}})^{1/2}((8c_{\mathrm{rel}})^{1/2}\overline{\lambda}^2\underline{\lambda}^{-1}\widehat{\eta} + 2\kappa_1\mu).
\end{aligned}$$

The constant $C_7 = \max\{C_5^2C_6^2/2 + C_5(2c_{\mathrm{LS}})^{1/2}c_{\mathrm{sr}}^{1/n}/(n+1) + C_5^2, 8c_{\mathrm{LS}}c_{\mathrm{rel}}\overline{\lambda}^4\underline{\lambda}^{-2}, 4c_{\mathrm{LS}}\kappa_1^2\}$ and several Young inequalities result in

$$\begin{aligned}
&C_5\eta(\mathcal{T} \setminus \widehat{\mathcal{T}})(|||u_{LS} - \widehat{u}_{LS}||| + \|p_{LS} - \widehat{p}_{LS}\|_{H(\operatorname{div})}) \\
&\qquad \le \delta^2(\mathcal{T}, \widehat{\mathcal{T}})/2 + C_7(\eta^2(\mathcal{T} \setminus \widehat{\mathcal{T}}) + \widehat{\eta}^2 + \mu^2). \qquad (8.9)
\end{aligned}$$

Step 7. Finish of the proof. The combination of (8.7) with (8.9) in the last two steps and the absorption of $\delta^2(\mathcal{T}, \widehat{\mathcal{T}})/2$ conclude the proof with $\Lambda_3 = 2(C_5 + C_7)$. □

8.4. Quasiorthogonality

The proof of quasiorthogonality with parameter $\varepsilon > 0$ relies on the two following lemmas. As for the reduced mixed methods, axiom (A4) follows for a sufficiently small parameter ε.

Lemma 8.11 *Given any $\mathcal{T} \in \mathbb{T}$ with a refinement $\widehat{\mathcal{T}} \in \mathbb{T}(\mathcal{T})$, the quantities of Table 6 on p. 66 satisfy*

$$\begin{aligned}\delta^2(\mathcal{T},\widehat{\mathcal{T}}) \lesssim\ & LS(f,\mathcal{T};p_{LS},u_{LS}) - LS(f,\widehat{\mathcal{T}};\widehat{p}_{LS},\widehat{u}_{LS}) \\ & + \|(1-\Pi_0)f\|^2_{L^2(\Omega)} - \|(1-\widehat{\Pi}_0)f\|^2_{L^2(\Omega)} \\ & + 2(\widehat{V}_0,(1-\widehat{M}_0^{1/2}M_0^{-1/2})W_0)_{L^2(\Omega)} + 2(\widehat{V}_0,\widehat{F}_0-F_0)_{L^2(\Omega)} \\ & + 2(\widehat{V}_0,(1-\Pi_0)p_{LS})_{L^2(\mathcal{T}\setminus\widehat{\mathcal{T}})} + \varrho(\widehat{M}_0^{-1/2},M_0^{-1/2})^2\|\widehat{V}_0\|^2_{L^2(\Omega)}.\end{aligned}$$

Proof: The second part of Theorem 8.9 with $X = M_0^{1/2}V_0$, $A_0 = M_0^{-1/2}$, $\widehat{X} = \widehat{M}_0^{1/2}\widehat{V}_0$, and $\widehat{A}_0 = \widehat{M}_0^{-1/2}$ and Remark 6.2 show that

$$\begin{aligned}\|V_0-\widehat{V}_0\|^2_{L^2(\Omega)} &\le 4\underline{\lambda}^{-1}\|M_0^{1/2}V_0-\widehat{M}_0^{1/2}\widehat{V}_0\|^2_{L^2(\Omega)} + 2\overline{\lambda}\underline{\lambda}^{-1}\varrho(\widehat{M}_0^{-1/2},M_0^{-1/2})^2\|\widehat{M}_0^{1/2}\widehat{V}_0\|^2_{L^2(\Omega)} \\ &\le 4\underline{\lambda}^{-1}\|M_0^{1/2}V_0-\widehat{M}_0^{1/2}\widehat{V}_0\|^2_{L^2(\Omega)} + 2\overline{\lambda}^2\underline{\lambda}^{-1}\varrho(\widehat{M}_0^{-1/2},M_0^{-1/2})^2\|\widehat{V}_0\|^2_{L^2(\Omega)}.\end{aligned}$$

Hence, $C_8 = \max\{1, 4\underline{\lambda}^{-1}, 2\overline{\lambda}^2\underline{\lambda}^{-1}\}$ satisfies

$$\delta^2(\mathcal{T},\widehat{\mathcal{T}})/C_8 \le \|\operatorname{div}(\widehat{p}_{LS}-p_{LS})\|^2_{L^2(\Omega)} + \|M_0^{1/2}V_0-\widehat{M}_0^{1/2}\widehat{V}_0\|^2_{L^2(\Omega)} + \varrho(\widehat{M}_0^{-1/2},M_0^{-1/2})^2\|\widehat{V}_0\|^2_{L^2(\Omega)}.$$

It remains to analyse the sum $\|\operatorname{div}(\widehat{p}_{LS}-p_{LS})\|^2_{L^2(\Omega)} + \|M_0^{1/2}V_0-\widehat{M}_0^{1/2}\widehat{V}_0\|^2_{L^2(\Omega)}$. With the orthogonality of $(1-\Pi_0)f$ onto $\Pi_0 f + \operatorname{div} p_{LS} \in P_0(\mathcal{T})$, the weighted least-squares functional on the coarse level reads

$$\begin{aligned}LS(f,\mathcal{T};p_{LS},u_{LS}) &= \|\Pi_0 f + \operatorname{div} p_{LS}\|^2_{L^2(\Omega)} + \|M_0^{1/2}V_0\|^2_{L^2(\Omega)} \\ &= \|f+\operatorname{div} p_{LS}\|^2_{L^2(\Omega)} - \|(1-\Pi_0)f\|^2_{L^2(\Omega)} + \|M_0^{1/2}V_0\|^2_{L^2(\Omega)}\end{aligned}$$

This and the analog identity for $(\widehat{p}_{LS},\widehat{u}_{LS}) \in RT_0(\widehat{\mathcal{T}}) \times S^1_0(\widehat{\mathcal{T}})$ on the fine level $\widehat{\mathcal{T}}$ lead to

$$\begin{aligned}LS(f,\mathcal{T};p_{LS},u_{LS}) - LS(f,\widehat{\mathcal{T}};\widehat{p}_{LS},\widehat{u}_{LS}) &= \|f+\operatorname{div} p_{LS}\|^2_{L^2(\Omega)} - \|f+\operatorname{div}\widehat{p}_{LS}\|^2_{L^2(\Omega)} \\ &\quad + \|(1-\widehat{\Pi}_0)f\|^2_{L^2(\Omega)} - \|(1-\Pi_0)f\|^2_{L^2(\Omega)} + \|M_0^{1/2}V_0\|^2_{L^2(\Omega)} - \|\widehat{M}_0^{1/2}\widehat{V}_0\|^2_{L^2(\Omega)}.\end{aligned}$$

The identities

$$\begin{aligned}\|f+\operatorname{div} p_{LS}\|^2_{L^2(\Omega)} &= \|f+\operatorname{div}\widehat{p}_{LS}\|^2_{L^2(\Omega)} + \|\operatorname{div}(p_{LS}-\widehat{p}_{LS})\|^2_{L^2(\Omega)} \\ &\qquad + 2(f+\operatorname{div}\widehat{p}_{LS},\operatorname{div}(p_{LS}-\widehat{p}_{LS}))_{L^2(\Omega)} \text{ and} \\ \|M_0^{1/2}V_0\|^2_{L^2(\Omega)} &= \|\widehat{M}_0^{1/2}\widehat{V}_0\|^2_{L^2(\Omega)} + \|M_0^{1/2}V_0-\widehat{M}_0^{1/2}\widehat{V}_0\|^2_{L^2(\Omega)} \\ &\qquad + 2(\widehat{M}_0^{1/2}\widehat{V}_0, M_0^{1/2}V_0-\widehat{M}_0^{1/2}\widehat{V}_0)_{L^2(\Omega)}\end{aligned}$$

prove

$$\begin{aligned}LS(f,\mathcal{T};p_{LS},u_{LS}) - LS(f,\widehat{\mathcal{T}};\widehat{p}_{LS},\widehat{u}_{LS}) &+ \|(1-\Pi_0)f\|^2_{L^2(\Omega)} - \|(1-\widehat{\Pi}_0)f\|^2_{L^2(\Omega)} \\ &- \|\operatorname{div}(\widehat{p}_{LS}-p_{LS})\|^2_{L^2(\Omega)} - \|M_0^{1/2}V_0-\widehat{M}_0^{1/2}\widehat{V}_0\|^2_{L^2(\Omega)} \\ &= 2\big((f+\operatorname{div}\widehat{p}_{LS},\operatorname{div}(p_{LS}-\widehat{p}_{LS}))_{L^2(\Omega)} \\ &\qquad + (\widehat{M}_0^{1/2}\widehat{V}_0, M_0^{1/2}V_0-\widehat{M}_0^{1/2}\widehat{V}_0)_{L^2(\Omega)}\big).\end{aligned}$$

The pointwise symmetry of $\widehat{M}_0^{1/2}$ and the discrete Euler-Lagrange equations ($\widehat{\mathrm{LS}}$) on the fine level with test functions $\widehat{q}_{RT} \coloneqq p_{LS} - \widehat{p}_{LS} \in RT_0(\widehat{\mathcal{T}})$ and $\widehat{v}_C \coloneqq u_{LS} - \widehat{u}_{LS} \in S^1_0(\widehat{\mathcal{T}})$ prove

$$\begin{aligned}
&(f + \operatorname{div} \widehat{p}_{LS}, \operatorname{div}(p_{LS} - \widehat{p}_{LS}))_{L^2(\Omega)} + (\widehat{M}_0^{1/2} \widehat{V}_0, M_0^{1/2} V_0 - \widehat{M}_0^{1/2} \widehat{V}_0)_{L^2(\Omega)} \\
&\qquad = (f + \operatorname{div} \widehat{p}_{LS}, \operatorname{div}(p_{LS} - \widehat{p}_{LS}))_{L^2(\Omega)} + (\widehat{V}_0, \widehat{M}_0^{1/2} M_0^{1/2} V_0 - \widehat{W}_0)_{L^2(\Omega)} \\
&\qquad = (\widehat{V}_0, \widehat{\Pi}_0(\widehat{p}_{LS} - p_{LS}) - \nabla(\widehat{u}_{LS} - u_{LS}) + \widehat{M}_0^{1/2} M_0^{1/2} V_0 - \widehat{W}_0)_{L^2(\Omega)} \\
&\qquad = (\widehat{V}_0, \widehat{M}_0^{1/2} M_0^{1/2} V_0 - \widehat{\Pi}_0 p_{LS} + \nabla u_{LS} - \widehat{F}_0)_{L^2(\Omega)}.
\end{aligned}$$

Since $V_0 = M_0^{-1} W_0$ and $(\Pi_0 - \widehat{\Pi}_0) p_{LS} = 0$ on $\mathcal{T} \cap \widehat{\mathcal{T}}$, this equals

$$\begin{aligned}
&(\widehat{V}_0, \widehat{M}_0^{1/2} M_0^{-1/2} W_0 - \Pi_0 p_{LS} + \nabla u_{LS} - F_0)_{L^2(\Omega)} + (\widehat{V}_0, (\Pi_0 - \widehat{\Pi}_0) p_{LS})_{L^2(\Omega)} + (\widehat{V}_0, F_0 - \widehat{F}_0)_{L^2(\Omega)} \\
&\quad = (\widehat{V}_0, (\widehat{M}_0^{1/2} M_0^{-1/2} - 1) W_0)_{L^2(\Omega)} - (\widehat{V}_0, (1 - \Pi_0) p_{LS})_{L^2(\mathcal{T} \setminus \widehat{\mathcal{T}})} - (\widehat{V}_0, \widehat{F}_0 - F_0)_{L^2(\Omega)}.
\end{aligned}$$

The previous three identities result in

$$\begin{aligned}
&\| \operatorname{div}(\widehat{p}_{LS} - p_{LS}) \|^2_{L^2(\Omega)} + \| M_0^{1/2} V_0 - \widehat{M}_0^{1/2} \widehat{V}_0 \|^2_{L^2(\Omega)} \\
&\quad = LS(f, \mathcal{T}; p_{LS}, u_{LS}) - LS(f, \widehat{\mathcal{T}}; \widehat{p}_{LS}, \widehat{u}_{LS}) + \| (1 - \Pi_0) f \|^2_{L^2(\Omega)} - \| (1 - \widehat{\Pi}_0) f \|^2_{L^2(\Omega)} \\
&\qquad - 2(\widehat{V}_0, (\widehat{M}_0^{1/2} M_0^{-1/2} - 1) W_0)_{L^2(\Omega)} + 2(\widehat{V}_0, \widehat{F}_0 - F_0)_{L^2(\Omega)} \\
&\qquad + 2(\widehat{V}_0, (1 - \Pi_0) p_{LS})_{L^2(\mathcal{T} \setminus \widehat{\mathcal{T}})}.
\end{aligned}$$

This concludes the proof. □

In the remainder of this section, let $\mathcal{T}_0, \mathcal{T}_1, \mathcal{T}_2, \dots$ denote the outcome of the adaptive algorithm with respective weights $M_k = M_0^{\mathcal{T}_k} \in P_0(\mathcal{T}_k; \mathbb{S})$, $F_k = F_0^{\mathcal{T}_k} \in P_0(\mathcal{T}_k; \mathbb{R}^n)$, projections $\Pi_k : L^2(\Omega) \to P_0(\mathcal{T}_k)$ and discrete solutions $(p_k, u_k) \in RT_0(\mathcal{T}_k) \times S^1_0(\mathcal{T}_k)$ to (LS) on $\mathcal{T}_k$, and denote the corresponding quantities $W_k = \Pi_k p_k - \nabla u_k + F_k$, $V_k = M_k^{-1} W_k$, $\eta_k \coloneqq \eta(\mathcal{T}_k)$, $\mu_k \coloneqq \mu(\mathcal{T}_k)$, $\sigma_k \coloneqq \sigma(\mathcal{T}_k)$, $h_k = h_{\mathcal{T}_k}$, $H_k = H_{\mathcal{T}_k}$.

Lemma 8.12 *Any $\ell, m \in \mathbb{N}_0$, and the output $(\mathcal{T}_k)_{k \in \mathbb{N}_0}$ of the AFEM algorithm satisfy*

$$\sum_{k=\ell}^{\ell+m} \| (1 - \Pi_k) p_k \|^2_{L^2(\mathcal{T}_k \setminus \mathcal{T}_{k+1})} \lesssim \sigma_\ell^2 + h_{\max}^2 \sum_{k=\ell}^{\ell+m} \sigma_k^2.$$

Proof: The split from Remark 2.11, the triangle inequality, and the pointwise estimate $h_k \le c_{\mathrm{sr}}^{1/n} H_k$ prove

$$\begin{aligned}
n \| (1 - \Pi_k) p_k \|_{L^2(\mathcal{T}_k \setminus \mathcal{T}_{k+1})} &\le \| h_k \operatorname{div} p_k \|_{L^2(\mathcal{T}_k \setminus \mathcal{T}_{k+1})} \\
&\le \| h_k (\operatorname{div} p_k + \Pi_k f) \|_{L^2(\mathcal{T}_k \setminus \mathcal{T}_{k+1})} + \| h_k f \|_{L^2(\mathcal{T}_k \setminus \mathcal{T}_{k+1})} \\
&\le h_{\max} LS(f, \mathcal{T}_k; p_k, u_k)^{1/2} + c_{\mathrm{sr}}^{1/n} \| H_k f \|_{L^2(\mathcal{T}_k \setminus \mathcal{T}_{k+1})}.
\end{aligned}$$

An elementary calculation like in [CFPP14, Prop. 5.3] reveals that

$$\| H_k f \|^2_{L^2(\mathcal{T}_k \setminus \mathcal{T}_{k+1})} (1 - 2^{-2/n}) \le \| H_k f \|^2_{L^2(\Omega)} - \| H_{k+1} f \|^2_{L^2(\Omega)}.$$

This and a telescoping sum show that

$$n^2 \sum_{k=\ell}^{\ell+m} \|(1-\Pi_k)p_k\|^2_{L^2(\mathcal{T}_k\setminus\mathcal{T}_{k+1})} \le 2h_{\max}^2 \sum_{k=\ell}^{\ell+m} LS(f,\mathcal{T}_k;p_k,u_k) + 2(1-2^{-2/n})^{-1} c_{\mathrm{sr}}^{2/n} \|H_\ell f\|^2_{L^2(\Omega)}.$$

The triangle inequality, the pointwise estimate $H_\ell \le h_{\max} n^{-1/n}$ and the reliability of $\|\operatorname{div} p_\ell + \Pi_\ell f\|^2_{L^2(\Omega)}$ from Lemma 6.7 result in

$$\begin{aligned}
\|H_\ell f\|^2_{L^2(\Omega)} &\le 3h_{\max}^2 n^{-2/n}\mu_\ell^2 + 3h_{\max}^2 n^{-2/n}\|\Pi_\ell f + \operatorname{div} p_\ell\|^2_{L^2(\Omega)} + 3\|H_\ell \operatorname{div} p_\ell\|^2_{L^2(\Omega)} \\
&\le 3h_{\max}^2 n^{-2/n}\mu_\ell^2 + 3\max\{h_{\max}^2 n^{-2/n} c_{\mathrm{rel}}, 1\}\eta_\ell^2 \\
&\le 3\max\{h_{\max}^2 n^{-2/n}, h_{\max}^2 n^{-2/n} c_{\mathrm{rel}}, 1\}\sigma_\ell^2.
\end{aligned}$$

Hence, $C_9 = \max\{2c_{\mathrm{rel}}, 6(1-2^{-2/n})^{-1} c_{\mathrm{sr}}^{2/n} h_{\max}^2 n^{-2/n}, 6(1-2^{-2/n})^{-1} c_{\mathrm{sr}}^{2/n} h_{\max}^2 n^{-2/n} c_{\mathrm{rel}}, 6(1-2^{-2/n})^{-1} c_{\mathrm{sr}}^{2/n}\}/n^2$, and the conclusion $LS(f,\mathcal{T}_k;p_k,u_k) \le c_{\mathrm{rel}}\eta_k^2 \le c_{\mathrm{rel}}\sigma_k^2$ from Lemma 6.7 imply

$$\sum_{k=\ell}^{\ell+m} \|(1-\Pi_k)p_k\|^2_{L^2(\mathcal{T}_k\setminus\mathcal{T}_{k+1})}/C_9 \le h_{\max}^2 \sum_{k=\ell}^{\ell+m} \sigma_k^2 + \sigma_\ell^2. \qquad \square$$

Theorem 8.13 (Quasiorthogonality with $\varepsilon > 0$) *For any $\varepsilon > 0$, there exist $\Lambda_4(\varepsilon), c(\varepsilon) \approx 1$ such that for $h_{\max} \le c(\varepsilon)$ sufficiently small (i.e., $\mathcal{T}_0 \in \mathbb{T}(c(\varepsilon))$), any $\ell, m \in \mathbb{N}_0$, and the output $(\mathcal{T}_k)_{k\in\mathbb{N}_0}$ of Algorithm 2 satisfy*

$$\sum_{k=\ell}^{\ell+m} \delta^2(\mathcal{T}_k,\mathcal{T}_{k+1}) \le \Lambda_4(\varepsilon)\sigma^2(\mathcal{T}_\ell) + \varepsilon \sum_{k=\ell}^{\ell+m} \sigma^2(\mathcal{T}_k). \tag{A4$_\varepsilon$}$$

Proof: With the notation $\varrho_{\ell,\ell+m} := \max_{k=\ell,\dots,\ell+m} \varrho(M_{k+1}^{-1/2}, M_k^{-1/2})$, the sum of the estimate from Lemma 8.11 with constant C_8 over the levels and two telescoping sums lead to

$$\begin{aligned}
C_8^{-1} \sum_{k=\ell}^{\ell+m} \delta^2(\mathcal{T}_k,\mathcal{T}_{k+1}) &\le LS(f,\mathcal{T}_\ell;p_\ell,u_\ell) + \|(1-\Pi_\ell)f\|^2_{L^2(\Omega)} \\
&\quad + 2\sum_{k=\ell}^{\ell+m} (V_{k+1}, (1-M_{k+1}^{1/2}M_k^{-1/2})W_k)_{L^2(\Omega)} + 2\sum_{k=\ell}^{\ell+m} (V_{k+1}, F_{k+1}-F_k)_{L^2(\Omega)} \\
&\quad + 2\sum_{k=\ell}^{\ell+m} (V_{k+1}, (1-\Pi_k)p_k)_{L^2(\mathcal{T}_k\setminus\mathcal{T}_{k+1})} + \varrho_{\ell,\ell+m}^2 \sum_{k=\ell}^{\ell+m} \|V_{k+1}\|^2_{L^2(\Omega)}.
\end{aligned}$$

The Cauchy inequality, the weighted Young inequality from Theorem 2.32 with $\lambda > 0$ for the term $(V_{k+1}, (1-\Pi_k)p_k)_{L^2(\mathcal{T}_k\setminus\mathcal{T}_{k+1})}$, and Lemma 6.7 and the quasimonotonicity from Theorem 8.1 in the estimate $\|V_{k+1}\|_{L^2(\Omega)} \le c_{\mathrm{rel}}^{1/2}\sigma_{k+1} \le c_{\mathrm{rel}}^{1/2}\Lambda_{QM}\sigma_k$ show

$$\begin{aligned}
C_8^{-1} \sum_{k=\ell}^{\ell+m} \delta^2(\mathcal{T}_k,\mathcal{T}_{k+1}) &\le LS(f,\mathcal{T}_\ell;p_\ell,u_\ell) + \|(1-\Pi_\ell)f\|^2_{L^2(\Omega)} \\
&\quad + 2c_{\mathrm{rel}}^{1/2}\Lambda_{QM} \sum_{k=\ell}^{\ell+m} \sigma_k \big(\|(M_{k+1}^{1/2}(M_{k+1}^{-1/2}-M_k^{-1/2})W_k\|_{L^2(\Omega)} + \|F_{k+1}-F_k\|_{L^2(\Omega)} \big) \\
&\quad + \lambda^{-1} \sum_{k=\ell}^{\ell+m} \|(1-\Pi_k)p_k\|^2_{L^2(\mathcal{T}_k\setminus\mathcal{T}_{k+1})} + c_{\mathrm{rel}}\Lambda_{QM}^2(\lambda + \varrho_{\ell,\ell+m}^2) \sum_{k=\ell}^{\ell+m} \sigma_k^2.
\end{aligned}$$

Remark 6.2 and Lemma 6.7 yield

$$\|(M_{k+1}^{1/2}(M_{k+1}^{-1/2}-M_k^{-1/2})W_k\|_{L^2(\Omega)} \le \overline{\lambda}^{3/2}\varrho_{\ell,\ell+m}\|V_k\|_{L^2(\Omega)} \le c_{\mathrm{rel}}^{1/2}\overline{\lambda}^{3/2}\varrho_{\ell,\ell+m}\eta_k.$$

Assumption (6.7) like in (8.3) implies $\|F_{k+1}-F_k\|_{L^2(\Omega)} \le 2\kappa(\mathcal{T}_k)\mu_k \le 2\kappa_{\ell,\ell+m}\mu_k$ for $\kappa_{\ell,\ell+m} := \max_{k=\ell,\dots,\ell+m}\kappa(\mathcal{T}_k)$. Hence, the Cauchy inequality in $\mathbb{R}^2$ proves

$$\|(M_{k+1}^{1/2}(M_{k+1}^{-1/2}-M_k^{-1/2})W_k\|_{L^2(\Omega)} + \|F_{k+1}-F_k\|_{L^2(\Omega)} \le (c_{\mathrm{rel}}^{1/2}\overline{\lambda}^{3/2}\varrho_{\ell,\ell+m} + 2\kappa_{\ell,\ell+m})\sigma_k.$$

Altogether, Lemma 8.12 with the constant C_9, and the definition of $\tilde{\varepsilon} = C_{10}(\varrho_{\ell,\ell+m}+\kappa_{\ell,\ell+m}+\lambda^{-1}h_{\max}^2+\lambda+\varrho_{\ell,\ell+m}^2)$ with $C_{10} = \max\{2c_{\mathrm{rel}}\Lambda_{QM}\overline{\lambda}^{3/2}, 4c_{\mathrm{rel}}^{1/2}\Lambda_{QM}, C_9, c_{\mathrm{rel}}\Lambda_{QM}^2\}$ show

$$C_8^{-1}\sum_{k=\ell}^{\ell+m}\delta^2(\mathcal{T}_k,\mathcal{T}_{k+1}) \le LS(f,\mathcal{T}_\ell;p_\ell,u_\ell) + \|(1-\Pi_\ell)f\|_{L^2(\Omega)}^2 + \lambda^{-1}C_9\sigma_\ell^2 + \tilde{\varepsilon}\sum_{k=\ell}^{\ell+m}\sigma_k^2.$$

Consider $\delta>0$ from condition (6.8) on the weights for $\min\{\varepsilon/(5C_8C_{10}),1\}$, i.e., such that $\mathcal{T}_0\in\mathbb{T}(\delta)$ implies $\kappa_{\ell,\ell+m}<\varepsilon/(5C_8C_{10})$ and $\varrho_{\ell,\ell+m}^2<\varrho_{\ell,\ell+m}<\varepsilon/(5C_8C_{10})$. The choice of $\lambda<\varepsilon/(5C_8C_{10})$ and $c(\varepsilon)=\min\{\delta,(\varepsilon\lambda/(5C_8C_{10}))^{1/2}\}$ implies $\lambda^{-1}h_{\max}^2<\varepsilon/(5C_8C_{10})$ for $\mathcal{T}_0\in\mathbb{T}(c(\varepsilon))$. Hence, $\mathcal{T}_0\in\mathbb{T}(c(\varepsilon))$ implies

$$C_8\tilde{\varepsilon} < C_8C_{10}(\varepsilon/(5C_8C_{10})+\varepsilon/(5C_8C_{10})+\varepsilon/(5C_8C_{10})+\varepsilon/(5C_8C_{10})+\varepsilon/(5C_8C_{10})) = \varepsilon.$$

This and $LS(f,\mathcal{T}_\ell;p_\ell,u_\ell)\le c_{\mathrm{rel}}\eta_\ell^2$ from Lemma 6.7 conclude the proof with constant $\Lambda_4(\varepsilon) := C_8(\max\{c_{\mathrm{rel}},1\}+\lambda^{-1}C_9)$. □

8.5. Optimal Convergence Rates

This subsection deduces the optimal convergence rates from the results of this chapter for sufficiently small initial mesh-size $h_{\max}$.

Theorem 8.14 (Optimal rates) *There exists $h_0>0$ such that for $\max_{\mathcal{T}\in\mathbb{T}}h_{\mathcal{T}}\le h_0$ and sufficiently small bulk parameter θ, the output $(\mathcal{T}_k)_{k=1,2,\dots}$ of the AFEM algorithm with corresponding quantities $\sigma_k := \sigma(\mathcal{T}_k)$ and any $s>0$ satisfy*

$$\sup_{\ell\in\mathbb{N}_0}(1+|\mathcal{T}_\ell|-|\mathcal{T}_0|)^s\sigma_\ell \approx \sup_{N\in\mathbb{N}_0}(1+N)^s\min\{\sigma(\mathcal{T})\,|\,\mathcal{T}\in\mathbb{T}\text{ with }|\mathcal{T}|-|\mathcal{T}_0|\le N\}.$$

Proof: Theorems 8.2, 8.3, 8.10, and 8.1 imply (A1)–(A3) and (QM) from [CR17]. The proof of quasimonotonicity $\mu(\widehat{\mathcal{T}})\le\mu(\mathcal{T})$ in axiom (B1) is included in Theorem 8.1, and the axiom (B1) as a property of the data approximation algorithm `approx` is proved in [CR17, §5.2] for the case of mixed finite element methods, that utilizes the same μ as the weighted least-squares methods of this thesis and thus transfers directly. For $\varepsilon_0 := (1-\varrho_{12})/\Lambda_{12}$ from [CR17, Thm 3.1] with ϱ_{12}, Λ_{12} depending on the bulk-parameter $\theta<\theta_0 := (1+\Lambda_1^2\Lambda_3)^{-1}$, Λ_1, Λ_2, and $\varrho_2 := 2^{-1/(2n)}$, the choice of $\mathcal{T}_0\in\mathbb{T}(c(\varepsilon_0))$ with $c(\varepsilon_0)$ from Theorem 8.13 implies quasiorthogonality $(\mathrm{A4})_{\varepsilon_0}$ with ε_0. Hence, [CR17, Thm 3.1] shows (A4):=$(\mathrm{A4})_0$ and [CR17, Thm 2.1] for the adaptive algorithm with separate marking and proves optimal convergence rates. □

9. Numerical Experiments

This section presents selected numerical experiments in $2d$ for the reduced mixed methods and weighted least-squares methods analysed in this thesis and compares them exemplarily with the primal and the ultraweak dPG method as the least and most complex of the four dPG methods introduced in this thesis. All methods were implemented in MATLAB based on the software package [AFEM], details in Appendix A, and the experiments were conducted on a server with MATLAB version 8.2.0.701 (MATLAB2013b). Although the analysis of this thesis restricts to homogeneous Dirichlet boundary conditions, the implementation is able to cope with inhomogeneous Dirichlet and Neumann boundary conditions. The calculation of local system matrices was done in parallel on 8 kernels. The implementation employs the MATLAB backslash operator \ for the solution of the system of equations. The adaptive experiments for the reduced mixed method utilize collective marking from Algorithm 1 with the error estimator η_R from (3.1). If not stated otherwise, the adaptive experiments for the weighted least-squares utilize Algorithm 2 with separate marking and η_{LS} and μ from (6.4)-(6.5).

The convergence history plots in this thesis utilize a log-log scale. In the majority of the plots, same or comparable quantities (estimator η, different parts of the error, or data approximation μ if applicable) are plotted in same colors independent of the method or the refinement strategy. The plots utilize markers to distinguish between the methods (triangles for the reduced mixed method, squares for the weighted least-squares method, and diamonds for the primal or ultraweak dPG method). In all plots comparing uniform with adaptive refinement strategies, solid lines and markers stand for uniform refinement, whereas dashed lines and hatched markers indicate adaptive refinement.

9.1. Setup of Comparison with dPG Methods

Based on the equivalences of Sections 4 and 7, the numerical experiments of this thesis compare the reduced mixed method and the weighted least-squares method with a certain choice of parameters to the corresponding dPG methods as explained below. Although the theory of this thesis utilizes the nonconforming energy norm $|||\cdot|||_{NC}$ for the space $CR^1_0(\mathcal{T})$ in the reduced mixed method, the numerical experiments display the equivalent norm $\|\cdot\|_{H^1(\mathcal{T})}$ for better comparison with the corresponding dPG methods. The legends of the plots of the numerical experiments of this thesis utilize the notation η standing for $\eta \in \{\eta_R, \eta_{LS}, \eta_{\mathrm{dPG}}\}$ depending on the respective method. Analogously, $u_C \in \{u_R, u_{LS}, u_{\mathrm{dPG}}\}$, $p_{RT} \in \{p_{LS}, p_{\mathrm{dPG}}\}$, and $v_1 \in \{v_R, v_{\mathrm{dPG}}\}$ for the variables below.

Primal dPG method. The choice of parameters $\alpha = 1$, $Q = \mathrm{id}$ for the reduced mixed method from Table 4 on p. 36 and $M_0 = I_{2\times 2} + S(\mathcal{T})$, $F_0 = H_0 f$ from Table 5 on p. 60 correspond to the primal dPG method. Let $(u_{\mathrm{dPG}}, t_{\mathrm{dPG}}, v_{\mathrm{dPG}}) \in S^1_0(\mathcal{T}) \times P_0(\mathcal{E}) \times P_1(\mathcal{T})$ be the solution to the primal dPG method, $(v_R, u_R) \in CR^1_0(\mathcal{T}) \times S^1_0(\mathcal{T})$ be the solution to the reduced mixed method, and $(p_{LS}, u_{LS}) \in RT_0(\mathcal{T}) \times S^1_0(\mathcal{T})$ be the solution to the weighted least-squares method

with these parameters. Then Theorems 4.1 and 7.1 state that $u_{\mathrm{dPG}} = u_R = u_{LS}$, $v_{\mathrm{dPG}} = v_R$ and $p_{\mathrm{dPG}} = p_{LS}$ for the unique extension $p_{\mathrm{dPG}} \in RT_0(\mathcal{T})$ of t_{dPG} with $\gamma_v^{\mathcal{T}} p_{\mathrm{dPG}} = t_{\mathrm{dPG}}$ from Remark 2.21.

The error of the normal traces $\|\gamma_v^{\mathcal{T}}(\nabla u) - t_{\mathrm{dPG}}\|_{H^{-1/2}(\partial\mathcal{T})}$ in the minimal extension norm from Definition 2.20 is approximated in the code by its upper bound $\|\nabla u - p_{\mathrm{dPG}}\|_{H(\mathrm{div},\Omega)}$.

The experiments for the primal dPG method employ Algorithm 1 with the built-in error estimator $\eta_{\mathrm{dPG}}^2(K) = \|v_1\|_{H^1(K)}^2 + h_K^2 \|f\|_{L^2(K)}^2$ for $K \in \mathcal{T}$ from Theorem 2.16 and Remark 2.17.

Ultraweak dPG method. Subsections 4.4 and 7.4 show that reduced mixed method with parameters $\alpha = 0.5$ and $Q = \mathrm{id}$, as well as the weighted least-squares method with $M_0 = 2I_{2\times 2} + S(\mathcal{T})$ and $F_0 = H_0 f$ are equivalent to the ultraweak dPG method. For the ultraweak dPG method with solution $(r_{\mathrm{dPG}}, w_{\mathrm{dPG}}, t_{\mathrm{dPG}}, s_{\mathrm{dPG}}, q_{\mathrm{dPG}}, v_{\mathrm{dPG}}) \in P_0(\mathcal{T};\mathbb{R}^n) \times P_0(\mathcal{T}) \times P_0(\mathcal{E}) \times S_0^1(\mathcal{E}) \times RT_0^{NC}(\mathcal{T}) \times P_1(\mathcal{T})$, the corresponding reduced mixed method with solution $(v_R, u_R) \in CR_0^1(\mathcal{T}) \times S_0^1(\mathcal{T})$, and the equivalent weighted least-squares method with solution $(p_{LS}, u_{LS}) \in RT_0(\mathcal{T}) \times S_0^1(\mathcal{T})$, Theorems 4.4 and 7.4 reveal $v_{\mathrm{dPG}} = v_R/2$, $p_{\mathrm{dPG}} = p_{LS}$, and $u_{\mathrm{dPG}} = u_R = u_{LS}$ for the unique extensions $p_{\mathrm{dPG}} \in RT_0(\mathcal{T})$ of t_{dPG} with $\gamma_v^{\mathcal{T}} p_{\mathrm{dPG}} = t_{\mathrm{dPG}}$ and $u_{\mathrm{dPG}} \in S_0^1(\mathcal{T})$ to $s_{\mathrm{dPG}} \in S_0^1(\mathcal{E})$ with $\gamma_0^{\mathcal{T}} u_{\mathrm{dPG}} = s_{\mathrm{dPG}}$.

The minimal extension norm $\|\gamma_v^{\mathcal{T}} u - s_{\mathrm{dPG}}\|_{H^{1/2}(\partial\mathcal{T})}$ is approximated in the computation by its upper bound $|||u - u_{\mathrm{dPG}}|||$.

Theorem 2.16 and Remark 2.17 reveal the built-in error estimator for the ultraweak dPG method, which reads $\eta_{\mathrm{dPG}}^2(K) = \|v_{\mathrm{dPG}}\|_{H^1(K)}^2 + \|q_{\mathrm{dPG}}\|_{H(\mathrm{div},T)}^2 + h_{\max}^2 \|f\|_{L^2(K)}^2$ for $K \in \mathcal{T}$.

9.2. Square Domain with Exact Solution

The numerical examples of this subsection consider the unit square $\Omega = (0,1)^2$ with homogeneous Dirichlet boundary conditions $u_D = 0$ on $\Gamma_D = \partial\Omega$ of the exact solution $u(x,y) = x(x-1)y(y-1)$. The corresponding right-hand side reads $f(x,y) = -2(x(x-1) + y(y-1))$.

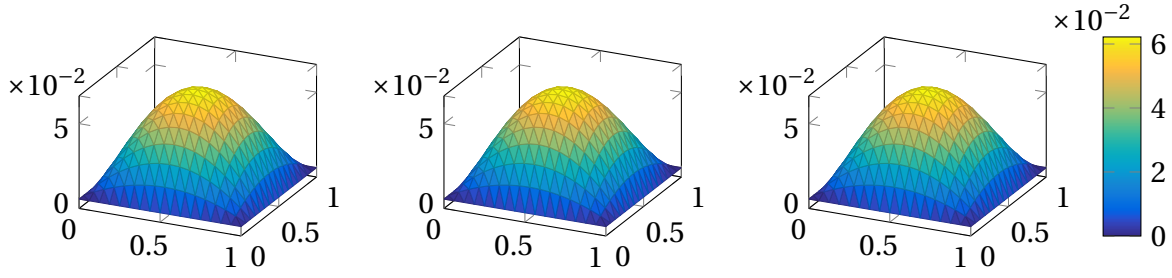

u_R, 961 ndof $\quad$ u_{LS}, 1025 ndof $\quad$ u_{dPG}, 2561 ndof

Figure 10: Solution plots of respective parts in $S_0^1(\mathcal{T})$ on uniformly refined triangulation with 512 triangles of square domain from Subsection 9.2.

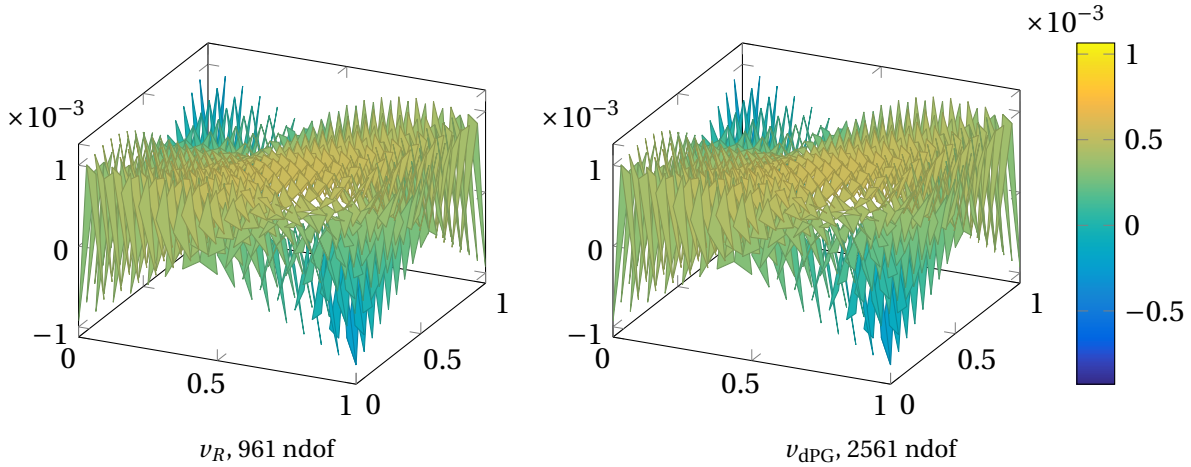

v_R, 961 ndof v_{dPG}, 2561 ndof

Figure 11: Solution plots of respective parts in $P_1(\mathcal{T})$ on uniformly refined triangulation with 512 triangles of square domain from Subsection 9.2.

The first examples compare the primal dPG method with its equivalent reduced mixed method and weighted least-squares method as described in the preceding subsection. The piecewise affine, globally continuous parts of the three solutions are displayed in Figure 10, the piecewise affine approximations of the residuals in Figure 11 on a uniformly refined triangulation. They match visually as expected from the theory.

Figure 12 shows the comparison of the three methods corresponding to the primal dPG method. All adaptive algorithms utilize $\theta = 0.5$, additionally $\kappa = 0.3$, $\varrho = 0.1$ in Algorithm 2 for the weighted least-squares method. All three methods show the expected optimal convergence rate of $1/2$ for uniform as well as adaptive refinement. The estimators for the reduced mixed method and the weighted least-squares method coincide. This is in accordance with the theory, since the proof of Theorem 7.1 reveals that the estimator (6.4) for the weighted least-squares method can be written as $\eta_{LS}^2(K) = |K|^{2/n}\|\Pi_0(f - v_R)\|_{L^2(K)}^2 + |K|^{1/n}\sum_{E\in\mathcal{E}(K)}\|[\nabla_{NC} v_R]_E\|_{L^2(E)}^2$ for any $K \in \mathcal{T}$, which is equivalent to the estimator η_R up to a midpoint quadrature in the volume term.

The convergence history plot of Figure 13 exhibits the parts of the errors for the primal dPG method and its equivalent reduced mixed method. For the reduced mixed method, the total error is split into roughly equal parts of $\|v_R\|_{H^1(\mathcal{T})}$ and $|||u - u_R|||$. The total error of the primal dPG method is dominated by the error of the normal traces $\|\nabla u - p_{\mathrm{dPG}}\|_{H(\mathrm{div},\Omega)}$ and coincides with the error estimator η_{dPG}. Although it is visible that on the same level and thus, the same mesh, the primal dPG method has a larger number of degrees of freedom, the values of $\|v_R\|_{H^1(\mathcal{T})}$ and $\|v_{\mathrm{dPG}}\|_{H^1(\mathcal{T})}$, and of $|||u - u_R|||$ and $|||u - u_{\mathrm{dPG}}|||$ coincide, as expected from the equivalence of the two methods proved in Subsection 4.1. Accordingly, the total error for the primal dPG method is significantly higher than that of the reduced mixed method.

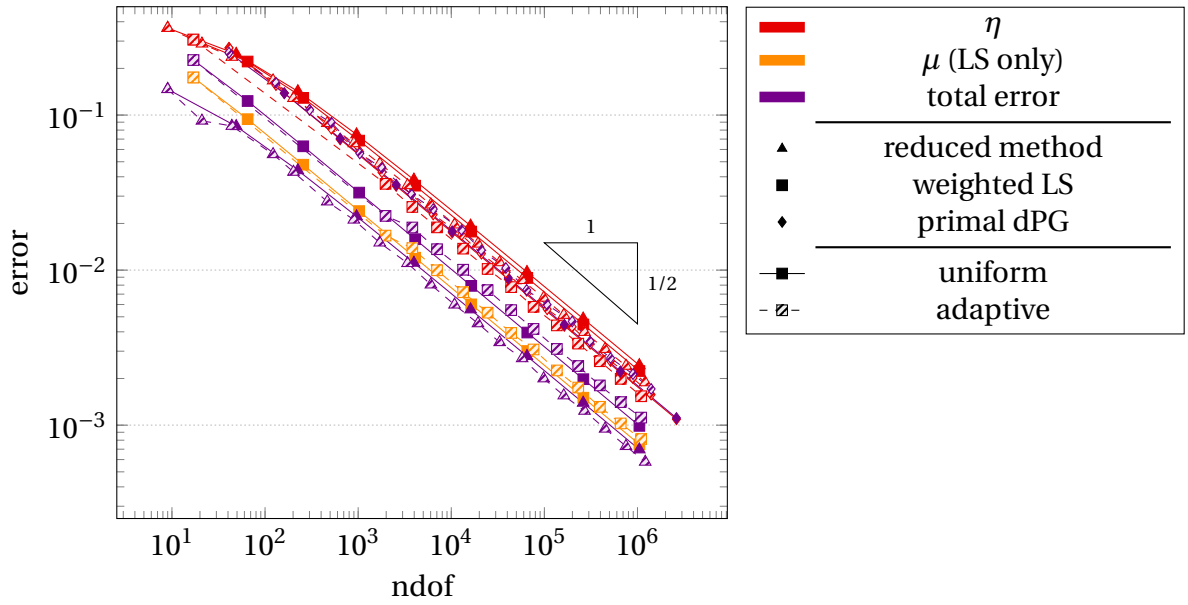

Figure 12: Comparison of methods equivalent to primal dPG for uniform and adaptive refinement of square domain from Subsection 9.2.

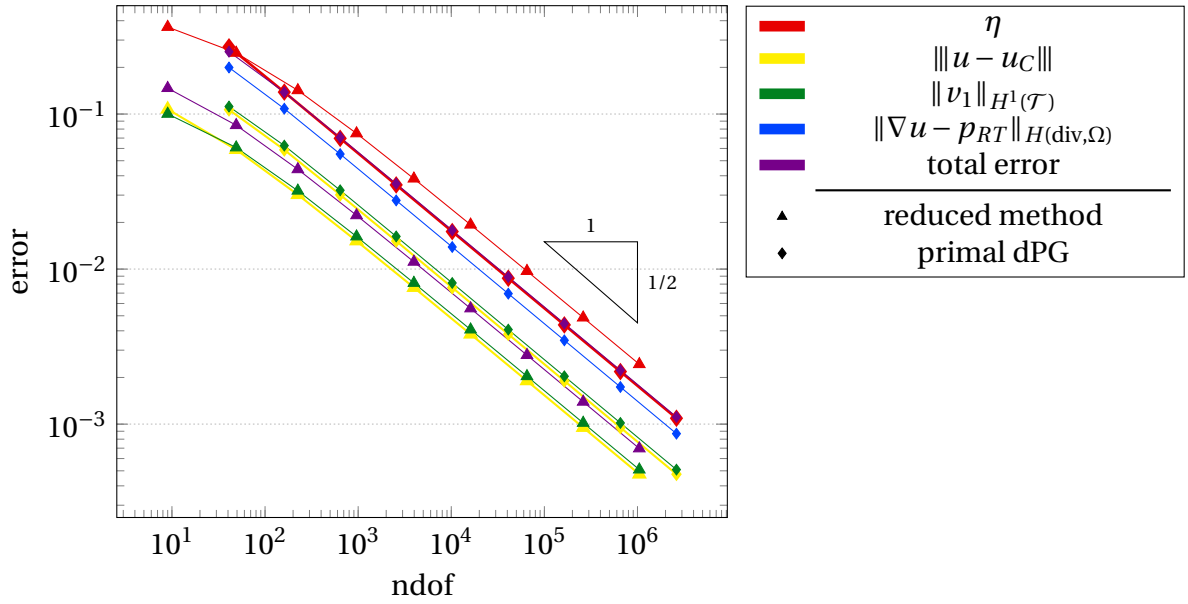

Figure 13: Parts of error for primal dPG and equivalent reduced mixed method for uniform refinement of square domain from Subsection 9.2.

The convergence history for the ultraweak dPG method and its equivalent reduced mixed method from Subsection 9.1 is displayed in Figure 15. The parameters for adaptive refinement read $\theta = 0.5$ and $\kappa = 0.3$, $\varrho = 0.1$ for the weighted least-squares method. The figure shows that the errors and estimators of all three methods converge with optimal

rate 1/2 for uniform and adaptive refinement. The error estimator and error of the adaptive ultraweak dPG method suffer from a preasymptotic range. Since undisplayed experiments with alternative estimator $\eta^2_{\mathrm{dPG}}(K) = \|v_{\mathrm{dPG}}\|^2_{H^1(K)} + \|q_{\mathrm{dPG}}\|^2_{H(\mathrm{div},T)}$ for $K \in \mathcal{T}$ do not share this preasymptotic behavior, an overestimation in the data approximation error estimate $\|F \circ (1-\Pi)\|_{Y^*} \lesssim h_{\max}\|f\|_{L^2(\Omega)}$ is a possible explanation for this. In the log-log plot at hand, the estimators of the weighted least-squares and the reduced mixed method differ by $0.3 \approx \log 2$. This translates to a multiplicative factor of 2 confirmed by the theory of Subsections 4.4 and 7.4, where $v_{\mathrm{dPG}} = v_R/2$, and the argumentation for Figure 12 above.

Figure 14 shows adaptively refined triangulations of these experiments for all three methods. Since the solution has no singularities and therefore even uniform refinement leads to the optimal convergence rate, also the adaptive algorithms lead to almost uniformly refined triangulations.

Similar to Figure 13 for the primal dPG method, Figure 16 displays some parts of the error for the ultraweak dPG method compared to its equivalent weighted least-squares method. For the ultraweak dPG method, undisplayed plots show that the error parts $\|u - w_{\mathrm{dPG}}\|_{L^2(\Omega)}$, $\|v_{\mathrm{dPG}}\|_{H^1(\mathcal{T})}$, and $\|q_{\mathrm{dPG}}\|_{H(\mathrm{div},NC)}$ coincide with the error $|||u - u_{\mathrm{dPG}}|||$ and are therefore not plotted for clarity in display. Like for the primal dPG method in Figure 13, the total error of the ultraweak dPG method is dominated by $\|\nabla u - p_{\mathrm{dPG}}\|_{H(\mathrm{div},\Omega)}$. The smallest part of the error is $\|\nabla u - r_{\mathrm{dPG}}\|_{L^2(\Omega)}$, and the total error is roughly equal to the error estimator η_{dPG}. For equal levels, hence meshes, the ultraweak dPG method utilizes significantly more degrees of freedom than the weighted LS method, but the equivalence of the extensions of $(p_{\mathrm{dPG}}, u_{\mathrm{dPG}})$ and (p_{LS}, u_{LS}) is confirmed in the convergence history plots by the equality of the errors $\|\nabla u - p_{\mathrm{dPG}}\|_{H(\mathrm{div},\Omega)}$ and $\|\nabla u - p_{LS}\|_{H(\mathrm{div},\Omega)}$, and of $|||u - u_{\mathrm{dPG}}|||$ and $|||u - u_{LS}|||$.

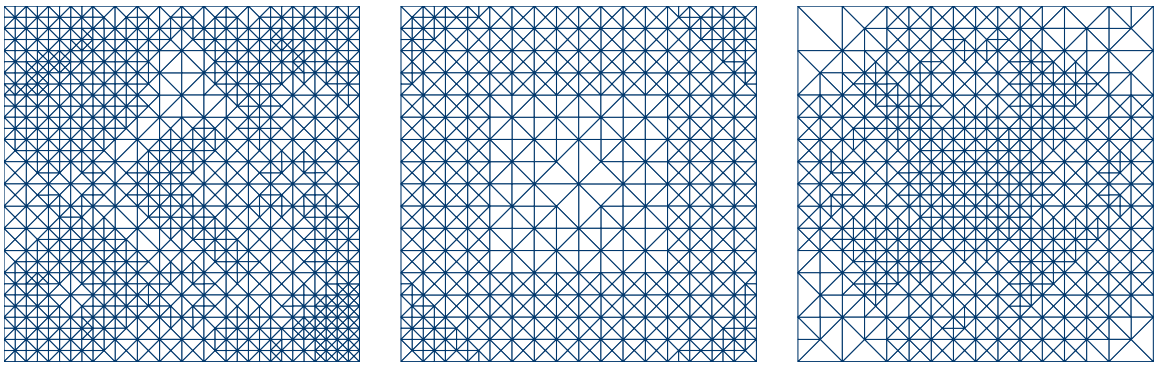

reduced mixed method (1746 triangles, 3391 ndof)

weighted LS method (984 triangles, 1969 ndof)

ultraweak dPG method (1220 triangles, 13421 ndof)

Figure 14: Adaptively refined triangulations of square domain from Subsection 9.2.

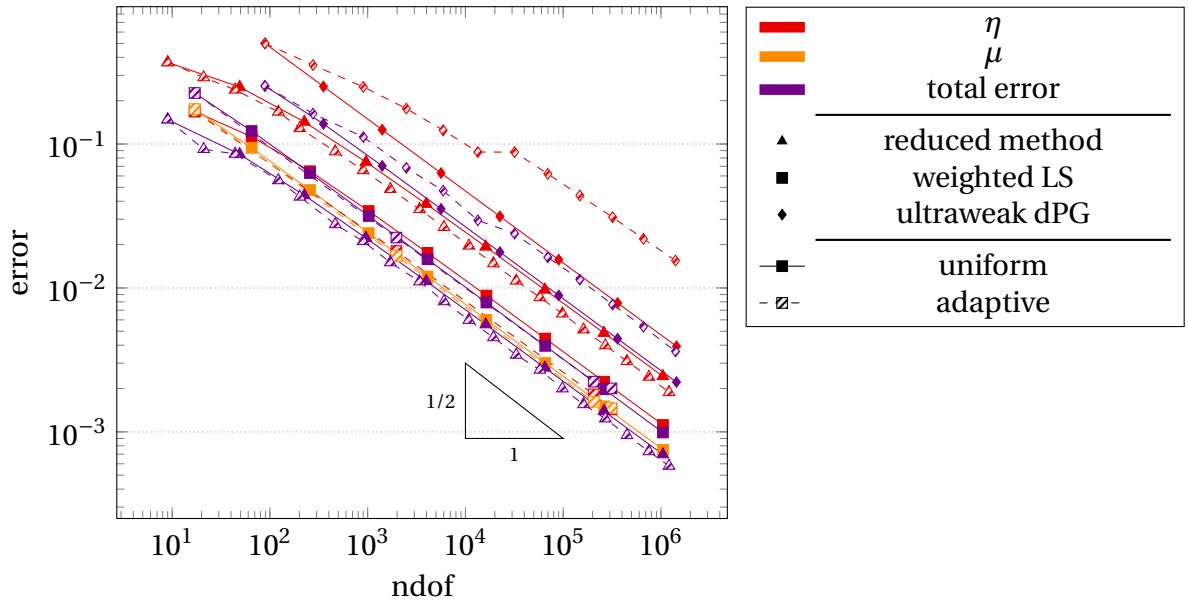

Figure 15: Comparison of methods equivalent to ultraweak dPG for uniform and adaptive refinement of square domain from Subsection 9.2.

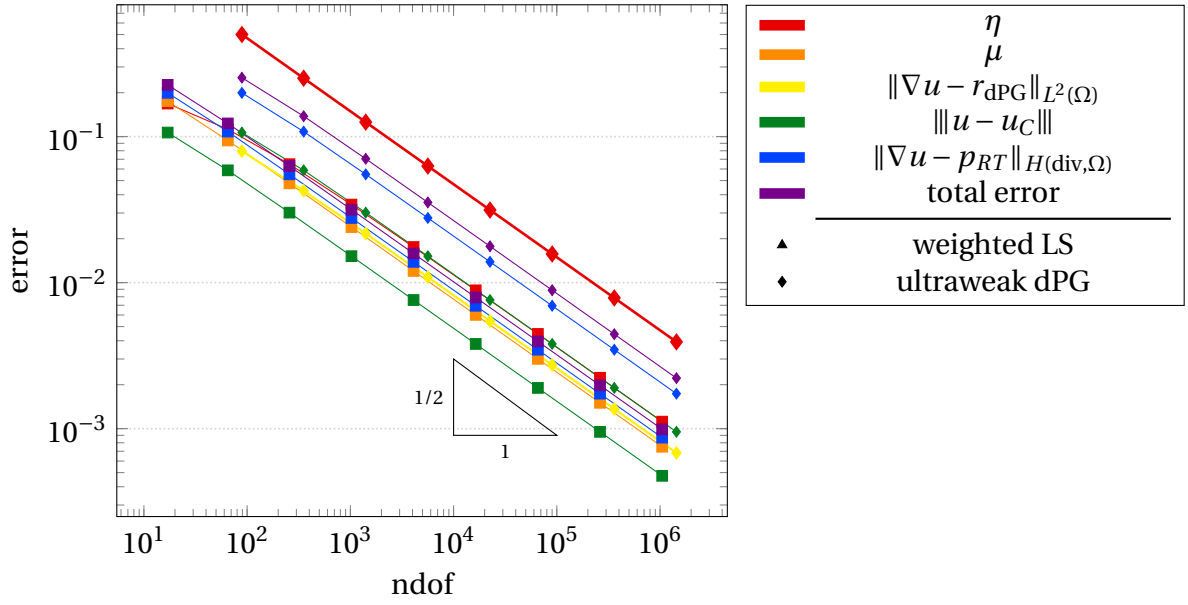

Figure 16: Parts of error for ultraweak dPG and equivalent weighted LS method for uniform refinement of square domain from Subsection 9.2.

9.3. Waterfall Example

The Waterfall example [CGHW14, §4.2] considers the unit square $\Omega = (0,1)^2$ with homogeneous Dirichlet boundary conditions $u_D = 0$ on $\Gamma_D = \partial\Omega$, where the exact solution

$$u(x,y) = x(x-1)y(y-1)e^{(-100(x-1/2)^2-(y-117)^2/10000)}$$

specifies the right-hand side $f := -\Delta u$, visualized in Figure 17.

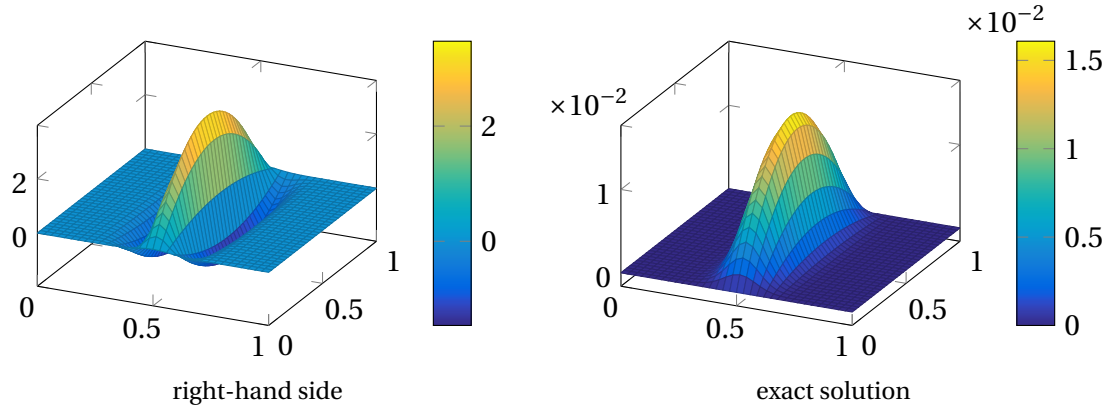

Figure 17: Right-hand side f and exact solution u for Waterfall example of Subsection 9.3.

The first experiments consider the ultraweak dPG method and its corresponding reduced mixed and weighted least-squares method with parameters described in Subsection 9.1. Figure 18 shows the piecewise affine, globally continuous parts u_R, u_{LS}, and u_{dPG} of the three solutions. Figures 19–23 show the remaining parts of the three solution including postprocessed quantities for the reduced mixed and the weighted least-squares method, where Figures 20-22 visualize vector fields in quiver plots. In detail, the variables $(r_R, w_R, t_R, q_R) \in P_0(\mathcal{T};\mathbb{R}^n) \times P_0(\mathcal{T}) \times P_0(\mathcal{E}) \times RT_0^{NC}(\mathcal{T})$ are calculated from $(v_R, u_R) \in CR_0^1(\mathcal{T}) \times S_0^1(\mathcal{T})$ according to Theorem 4.4 for the reduced mixed method, and the variables $(r_{LS}, w_{LS}, q_{LS}, v_{LS}) \in P_0(\mathcal{T};\mathbb{R}^n) \times P_0(\mathcal{T}) \times RT_0^{NC}(\mathcal{T}) \times P_1(\mathcal{T})$ are calculated from $(p_{LS}, u_{LS}) \in RT_0(\mathcal{T}) \times S_0^1(\mathcal{T})$ for the weighted least-squares method with Theorem 7.4. The figures confirm the theory in that the postprocessed quantities coincide with the terms calculated directly with the ultraweak dPG method, with a scaling with factor 2 for v_R as expected.

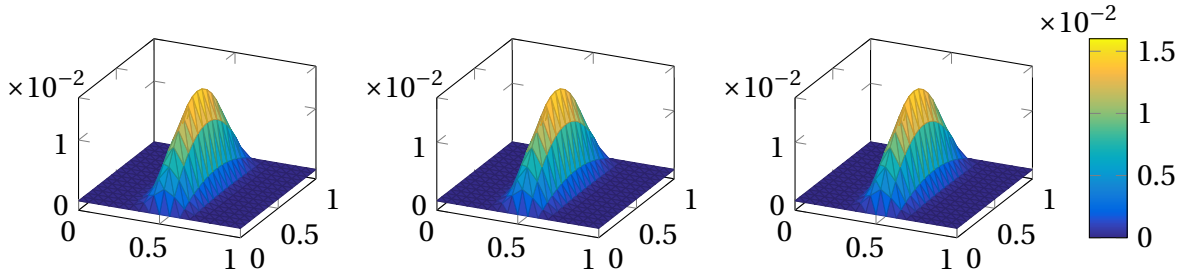

u_R, 961 ndof u_{LS}, 1025 ndof u_{dPG}, 5633 ndof

Figure 18: Solution plots of respective parts in $S^1_0(\mathcal{T})$ on uniformly refined triangulation with 512 triangles of Waterfall example from Subsection 9.3.

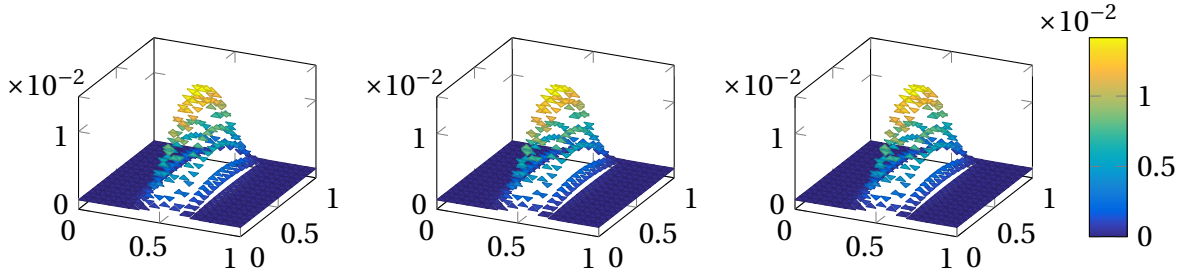

w_R, 961 ndof w_{LS}, 1025 ndof w_{dPG}, 5633 ndof

Figure 19: Solution plots of respective parts in $P_0(\mathcal{T})$.

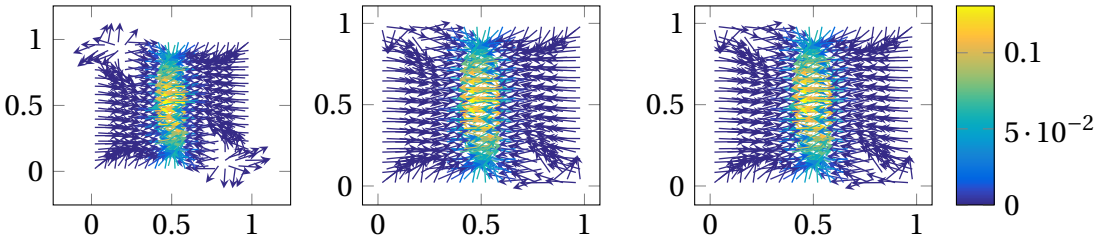

r_R, 961 ndof r_{LS}, 1025 ndof r_{dPG}, 5633 ndof

Figure 20: Solution plots of respective parts in $P_0(\mathcal{T};\mathbb{R}^2)$.

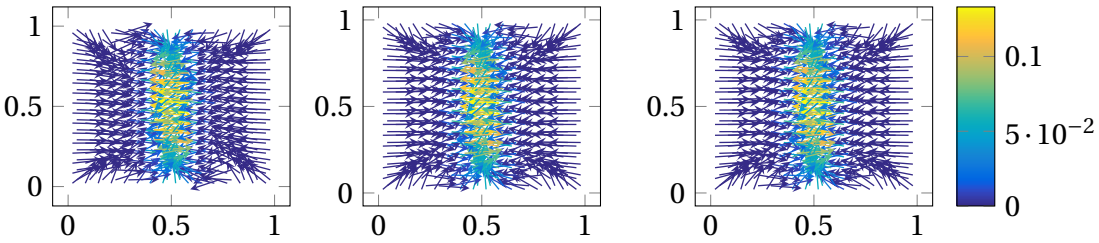

p_R, 961 ndof p_{LS}, 1025 ndof p_{dPG}, 5633 ndof

Figure 21: Solution plots of respective parts in $RT_0(\mathcal{T})$, where $p_R \in RT_0(\mathcal{T})$ is the unique extension to $t_R \in P_0(\mathcal{E})$.

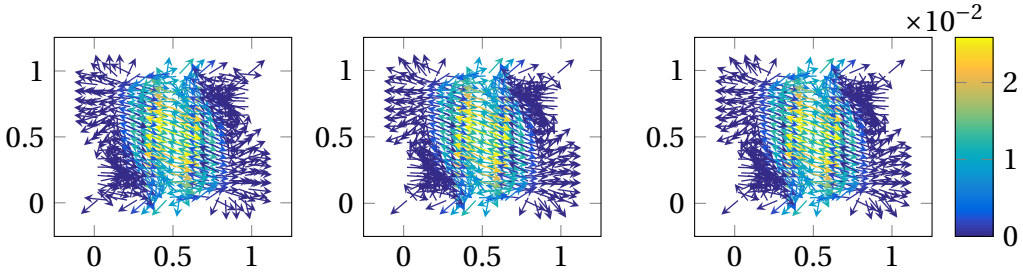

q_R, 961 ndof q_{LS}, 1025 ndof q_{dPG}, 5633 ndof

Figure 22: Solution plots of respective parts in $RT_0^{NC}(\mathcal{T})$.

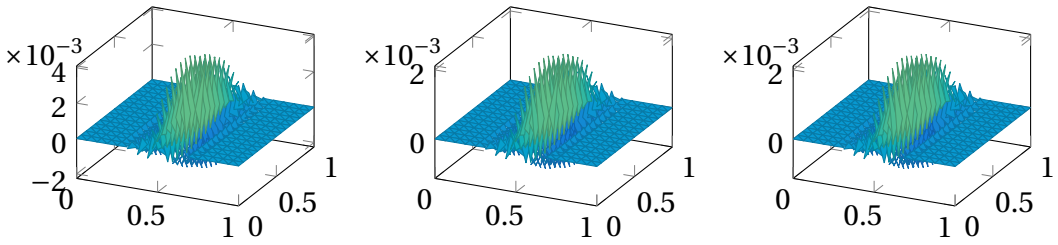

v_R, 961 ndof v_{LS}, 1025 ndof v_{dPG}, 5633 ndof

Figure 23: Solution plots of respective parts in $P_1(\mathcal{T})$.

Figure 24 displays the convergence history plot of errors, estimators and data approximation for the reduced mixed and the weighted least-squares methods corresponding the the dual dPG method. In particular, the choice of parameters is $Q = \Pi_0$, $\alpha = 1$ from Table 4 on p. 36, and $M_0 = I_{2\times 2}$, $F_0 = 0$ from Table 5 on p. 60. All quantities of both methods converge with optimal rate 1/2 for uniform and adaptive refinement, but the steep slope of the right-hand side f, which needs to be resolved by the mesh, leads to a preasymptotic range for all methods. Indeed, the triangulations in Figure 25 generated by adaptive refinement show a refinement towards the parts of the domain with high oscillatory right-hand side.

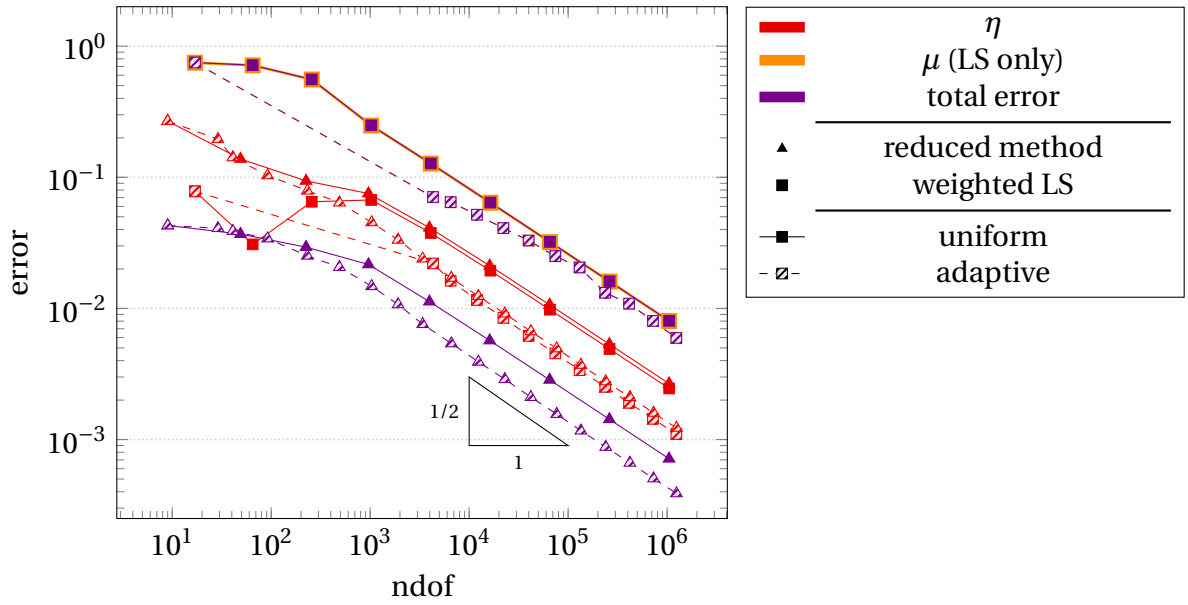

Figure 24: Comparison of methods equivalent to dual dPG for uniform and adaptive refinement of Waterfall example from Subsection 9.3.

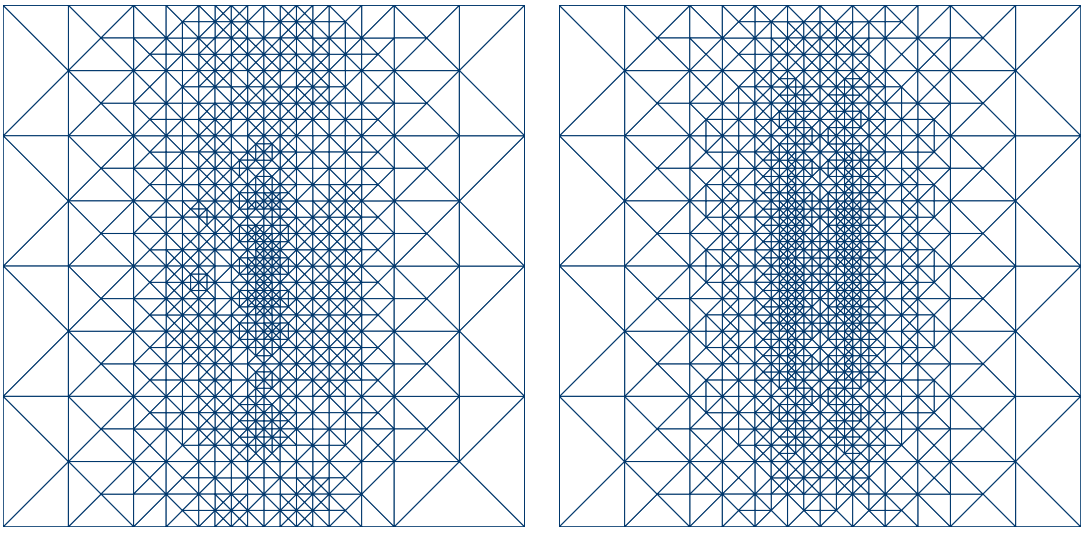

reduced mixed method (1715 triangles, 3392 ndof)

weighted LS method (2156 triangles, 4313 ndof)

Figure 25: Adaptively refined triangulations of methods equivalent to dual dPG for Waterfall example from Subsection 9.3.

Figure 26 investigates the influence of the parameter α and local projection Q on the total errors of the reduced mixed method. Several of the proofs of the theory on reduced mixed methods, e.g., the a priori result in Theorem 3.1, rely on the estimate $\alpha \leq 1$. This would suggest a strong influence of the constants in the proof of large parameter α. Nevertheless, the

difference in the behavior between small and large α is minimal and only in a preasymptotic range. This is true also for the two different choices of $Q = \mathrm{id}$ and $Q = \Pi_0$.

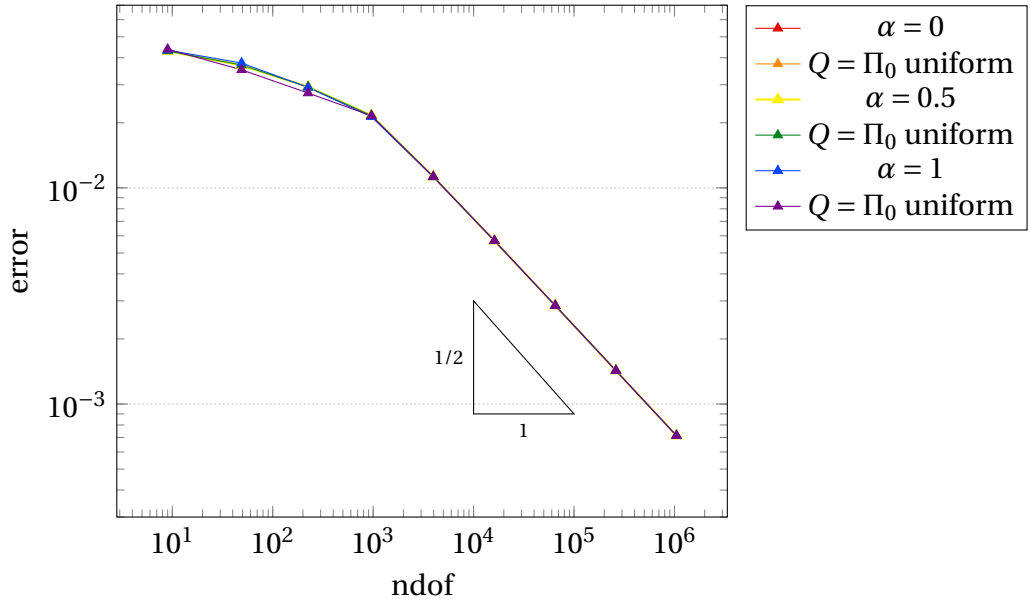

Figure 26: Waterfall example, influence of α on total errors.

9.4. L-Shaped Domain with Exact Solution

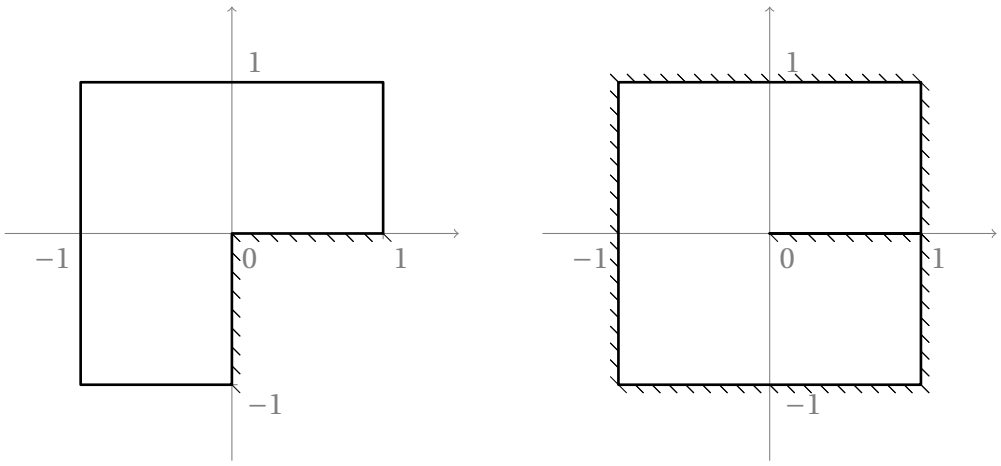

Figure 27: L-shaped domain from Subsection 9.4 and slit domain from Subsection 9.5. Hatched lines indicate Dirichlet boundary.

The subsection describes numerical experiments on the L-shaped domain $(-1,1)^2 \setminus ([0,1] \times [-1,0])$ from Figure 27 with Dirichlet boundary $\Gamma_D = ([0,1] \times \{0\}) \cup (\{0\} \times [-1,0])$, Neumann boundary $\Gamma_N = \partial\Omega \setminus \Gamma_N$ and right-hand side $f \equiv 0$. The boundary conditions $u_D = 0$ and $g := \nabla u \cdot \nu$ derive from the exact solution $u(r,\varphi) = r^{2/3}\sin(2\varphi/3)$ given in polar coordinates $(r,\varphi) \in (0,\infty) \times (0,2\pi)$. Throughout the plots of this subsection, $\mu = 0$ is not displayed and separate marking parameters κ, ϱ are not needed.

Figure 28 shows triangulations with roughly 1500 triangles generated by the adaptive algorithms of the reduced mixed method and the weighted least-squares method for the parameters of the primal dPG method as in Subsection 9.1 with $\theta = 0.5$. As expected, the adaptive algorithms refine locally towards the reentrant corner $(0,0)$ of the domain, where the exact solution has a singularity. Although equivalence of the three methods and therefore of the three estimators was proven only globally, these numerical experiments show that local refinement in the respective adaptive algorithms is similar, as the triangulations are qualitatively equal.

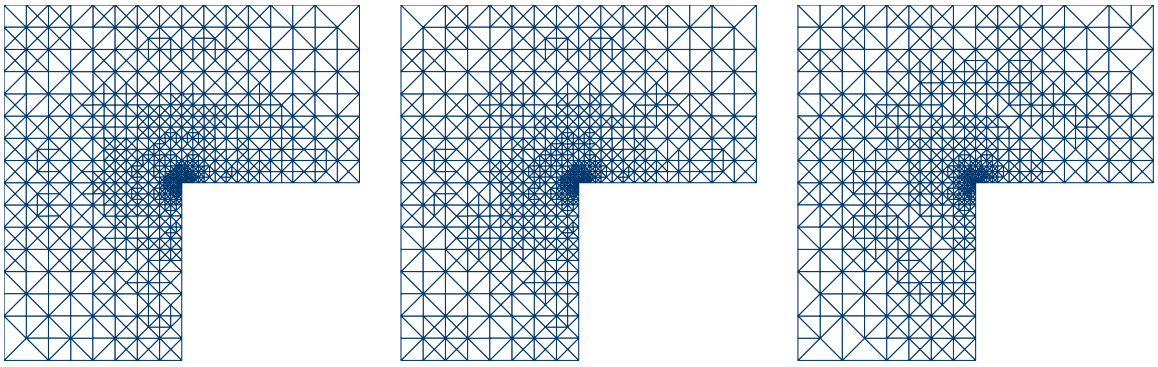

reduced mixed method (1529 triangles, 3065 ndof)

weighted LS method (1542 triangles, 3084 ndof)

primal dPG method (1313 triangles, 6565 ndof)

Figure 28: Adaptively refined triangulations of L-shaped domain from Subsection 9.4.

The piecewise affine parts of the solutions to the ultraweak dPG method and its equivalent reduced mixed and weighted least-squares method are displayed in Figures 29 and 30. As expected, the globally continuous variables u_R, u_{LS} and u_{dPG} coincide for the three methods. The discontinuous parts v_R and v_{dPG} are qualitatively equal, but scale with a factor of 2.

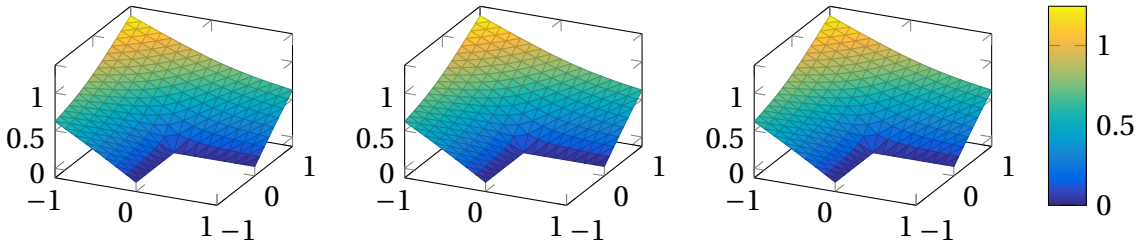

u_R, 800 ndof u_{LS}, 768 ndof u_{dPG}, 4224 ndof

Figure 29: Solution plots of respective parts in $S^1_0(\mathcal{T})$ on uniformly refined triangulation with 384 triangles of square domain from Subsection 9.4.

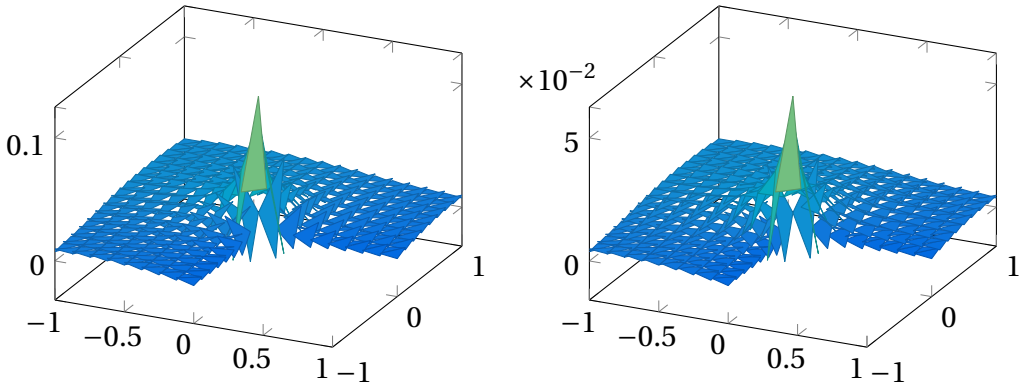

v_R, 800 ndof v_{dPG}, 4224 ndof

Figure 30: Solution plots of respective parts in $P_1(\mathcal{T})$ on uniformly refined triangulation with 384 triangles of square domain from Subsection 9.4.

Figure 31 displays the convergence history plot for the three equivalent methods corresponding to the primal dPG method, whereas Figure 32 contains the convergence history plot for the three equivalent methods corresponding to the ultraweak dPG method. Both plots show that the singularity at the reentrant corner $(0,0)$ leads to the suboptimal convergence rate $1/3$ for the uniform refinement strategy for the errors and estimators. However, all three adaptive refinement strategies in both plots recover the optimal convergence rate of $1/2$. The figures also show that the built-in error estimator of the dPG methods, i.e., the residual in the discrete dual norm, is not asymptotically exact like for the example of Subsection 9.2 and like recently observed for least-squares methods in [CS18].

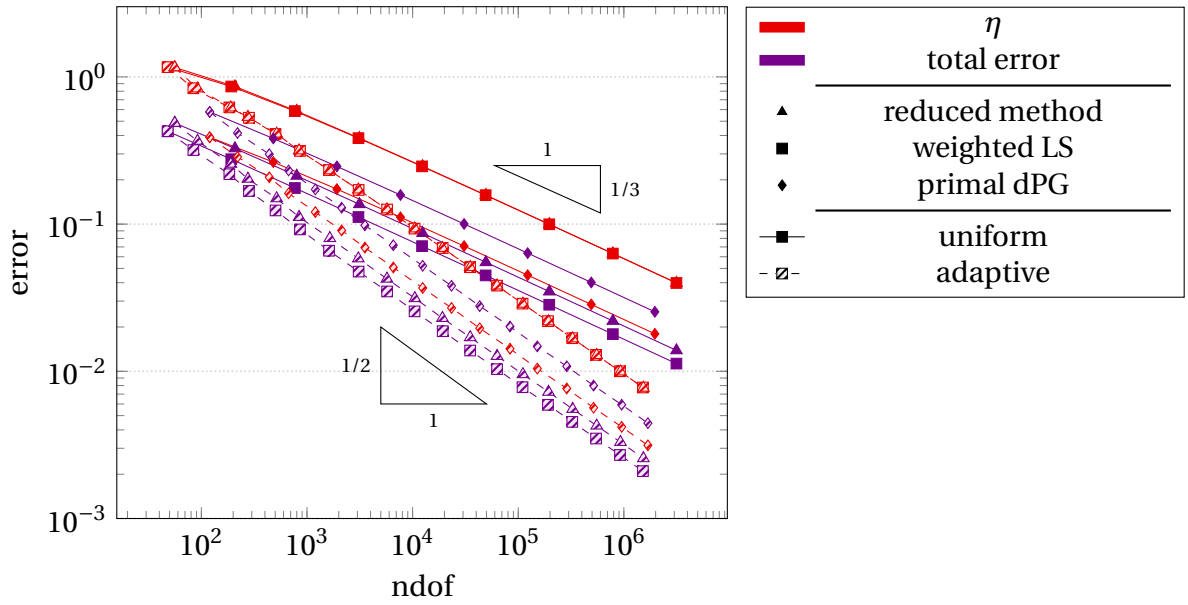

Figure 31: Comparison of methods equivalent to primal dPG for uniform and adaptive refinement of L-shaped domain from Subsection 9.4.

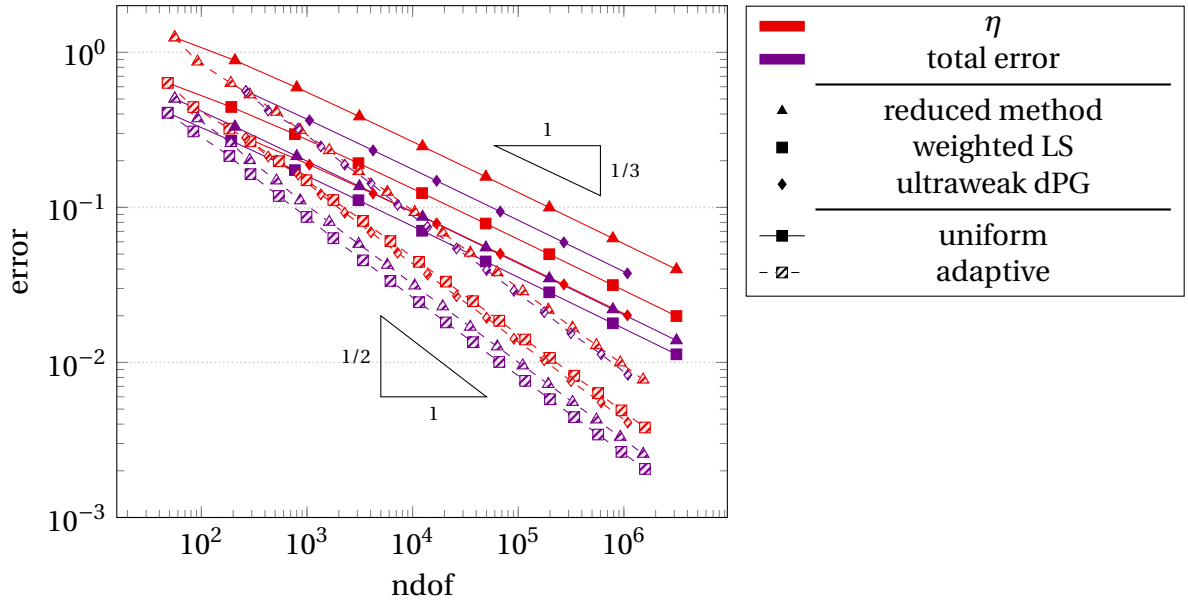

Figure 32: Comparison of methods equivalent to ultraweak dPG for uniform and adaptive refinement of L-shaped domain from Subsection 9.4.

The estimated condition numbers with respect to the maximum absolute column sum norm of the respective system matrices for uniform and adaptive refinement in the primal dPG method and the corresponding reduced mixed and weighted least-squares method are displayed in Figure 33. Those for the ultraweak dPG method and equivalent reduced mixed

and weighted least-squares methods are shown in Figure 34. In both plots, the condition numbers for uniform refinement diverge with a rate of about 1, which translates to $O(h^{-2})$ similar to standard lowest-order methods [BS08, p. 261] with uniform refinement. The condition numbers for the reduced mixed method with adaptive refinement also diverge with rate 1, a behavior which is observed for the Courant- and Crouzeix-Raviart-FEM in the weak formulation (1.3) and analysed for Courant-FEM in [BS89; BS08] for the spectral condition number. Since the reduced mixed method combines these two finite element methods, this is a possible explanation for a rate of 1 even for adaptive refinement. Nevertheless, the rate of divergence of roughly 2 of condition numbers for weighted least-squares and dPG methods with adaptive refinement is worse than that of uniform refinement. This observation is common also for other methods and other types of adaptive refinement, e.g., in [HKMP17] in the context of isogeometric analysis, and bases on the estimate of the condition number by $O(h_{\min}^{-2})$ [SF08, Thm. 5.1].

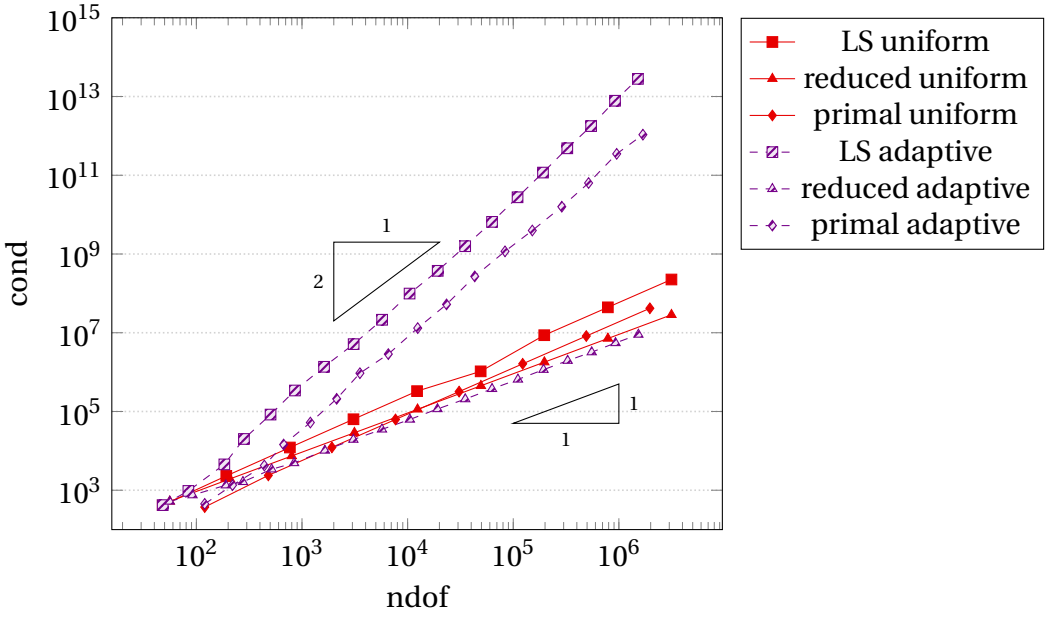

Figure 33: Condition numbers of methods equivalent to primal dPG for uniform and adaptive refinement of L-shaped domain from Subsection 9.4.

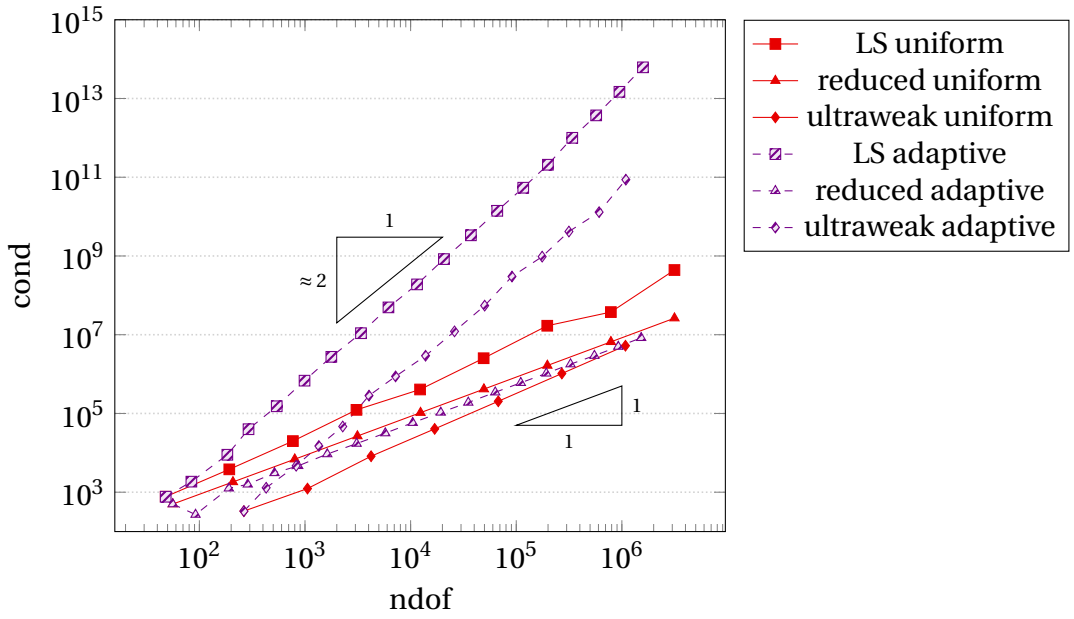

Figure 34: Condition numbers of methods equivalent to ultraweak dPG for uniform and adaptive refinement of L-shaped domain from Subsection 9.4.

The remaining part of this subsection analyses CPU times spent for assembling and solving the linear system of equations displayed in several tables measured with the MATLAB functions `tic` and `toc`. Cells with "–" indicate that solution of the respective method on this level was not possible due to lack of memory.

Tables 7 and 8 show these times for the primal dPG method and the equivalent reduced mixed and weighted least-squares methods for uniform refinement. Table 7 shows that whereas the number of degrees of freedom on equal triangulations is considerably higher for the primal dPG method than for the reduced mixed and the weighted least-squares method, the times for assembling the system matrix are of the same order of magnitude. Starting from level 5, the reduced mixed and the primal dPG method take a similar, significantly lower time to assemble the system matrix than the weighted least-squares method. Although all three methods are equivalent in theory, the solution of the linear system for the primal dPG method needs longer time than that of the reduced mixed method as shown in Table 8. The solution of the weighted least-squares method is the fastest of all three. However, the primal dPG method calculates a variable more than the other two methods, $t_{\mathrm{dPG}} \in P_0(\mathcal{E})$ when compared with the reduced mixed method from Theorem 4.4 and $v_{\mathrm{dPG}} \in P_1(\mathcal{T})$ in relation to the weighted least-squares method from Theorem 7.4. Indeed, when additionally taking into account the time for postprocessing to calculate the additional variables based on Theorems 4.4 and 7.4, displayed in column "total" with the sum of times for solving and postprocessing, the reduced mixed method takes longer than the primal dPG method. Then again, the solving and postprocessing step in the weighted least-squares method takes less time than solving the system of equations for the primal dPG method. This is because the proof of Theorem 4.4 reveals that the postprocessing step of the reduced

mixed method involves an inversion of the bilinear form $\langle \bullet, \bullet \rangle_{\partial \mathcal{T}}$, i.e., a global problem. In contrast to that, the postprocessing for the weighted least-squares method from Theorem 7.4 consists of a local calculation of the piecewise affine function v_{dPG}, which can be done in parallel. Undisplayed results show that the postprocessed quantities indeed coincide with the quantities directly calculated with the ultraweak dPG method and confirm the theory.

ndof			assemble		
R	LS	dPG	R	LS	dPG
$5.60 \cdot 10^{1}$	$4.80 \cdot 10^{1}$	$1.20 \cdot 10^{2}$	$2.20 \cdot 10^{-1}$	$2.59 \cdot 10^{-1}$	$3.94 \cdot 10^{-2}$
$2.08 \cdot 10^{2}$	$1.92 \cdot 10^{2}$	$4.80 \cdot 10^{2}$	$2.31 \cdot 10^{-1}$	$2.91 \cdot 10^{-1}$	$4.52 \cdot 10^{-2}$
$8.00 \cdot 10^{2}$	$7.68 \cdot 10^{2}$	$1.92 \cdot 10^{3}$	$2.45 \cdot 10^{-1}$	$2.75 \cdot 10^{-1}$	$5.65 \cdot 10^{-2}$
$3.14 \cdot 10^{3}$	$3.07 \cdot 10^{3}$	$7.68 \cdot 10^{3}$	$2.64 \cdot 10^{-1}$	$3.41 \cdot 10^{-1}$	$8.78 \cdot 10^{-2}$
$1.24 \cdot 10^{4}$	$1.23 \cdot 10^{4}$	$3.07 \cdot 10^{4}$	$3.60 \cdot 10^{-1}$	$5.91 \cdot 10^{-1}$	$2.19 \cdot 10^{-1}$
$4.94 \cdot 10^{4}$	$4.92 \cdot 10^{4}$	$1.23 \cdot 10^{5}$	$8.80 \cdot 10^{-1}$	$1.73 \cdot 10^{0}$	$8.09 \cdot 10^{-1}$
$1.97 \cdot 10^{5}$	$1.97 \cdot 10^{5}$	$4.92 \cdot 10^{5}$	$3.26 \cdot 10^{0}$	$6.67 \cdot 10^{0}$	$3.14 \cdot 10^{0}$
$7.87 \cdot 10^{5}$	$7.86 \cdot 10^{5}$	$1.97 \cdot 10^{6}$	$1.29 \cdot 10^{1}$	$2.64 \cdot 10^{1}$	$1.24 \cdot 10^{1}$
$3.15 \cdot 10^{6}$	$3.15 \cdot 10^{6}$	–	$5.27 \cdot 10^{1}$	$1.04 \cdot 10^{2}$	–

Table 7: CPU times for assembly of methods equivalent to primal dPG for uniform refinement.

ndof			solve			total	
R	LS	dPG	R	LS	dPG	R	LS
$5.60 \cdot 10^{1}$	$4.80 \cdot 10^{1}$	$1.20 \cdot 10^{2}$	$1.90 \cdot 10^{-4}$	$1.81 \cdot 10^{-4}$	$3.39 \cdot 10^{-4}$	$3.70 \cdot 10^{-2}$	$3.62 \cdot 10^{-2}$
$2.08 \cdot 10^{2}$	$1.92 \cdot 10^{2}$	$4.80 \cdot 10^{2}$	$6.71 \cdot 10^{-4}$	$3.72 \cdot 10^{-4}$	$1.34 \cdot 10^{-3}$	$4.28 \cdot 10^{-2}$	$4.23 \cdot 10^{-2}$
$8.00 \cdot 10^{2}$	$7.68 \cdot 10^{2}$	$1.92 \cdot 10^{3}$	$2.88 \cdot 10^{-3}$	$1.45 \cdot 10^{-3}$	$5.69 \cdot 10^{-3}$	$5.53 \cdot 10^{-2}$	$5.16 \cdot 10^{-2}$
$3.14 \cdot 10^{3}$	$3.07 \cdot 10^{3}$	$7.68 \cdot 10^{3}$	$1.86 \cdot 10^{-2}$	$7.79 \cdot 10^{-3}$	$2.62 \cdot 10^{-2}$	$9.98 \cdot 10^{-2}$	$7.98 \cdot 10^{-2}$
$1.24 \cdot 10^{4}$	$1.23 \cdot 10^{4}$	$3.07 \cdot 10^{4}$	$1.24 \cdot 10^{-1}$	$3.65 \cdot 10^{-2}$	$1.57 \cdot 10^{-1}$	$3.30 \cdot 10^{-1}$	$3.00 \cdot 10^{-1}$
$4.94 \cdot 10^{4}$	$4.92 \cdot 10^{4}$	$1.23 \cdot 10^{5}$	$9.61 \cdot 10^{-1}$	$2.04 \cdot 10^{-1}$	$7.50 \cdot 10^{-1}$	$1.71 \cdot 10^{0}$	$8.63 \cdot 10^{-1}$
$1.97 \cdot 10^{5}$	$1.97 \cdot 10^{5}$	$4.92 \cdot 10^{5}$	$7.36 \cdot 10^{0}$	$9.04 \cdot 10^{-1}$	$3.91 \cdot 10^{0}$	$1.02 \cdot 10^{1}$	$3.37 \cdot 10^{0}$
$7.87 \cdot 10^{5}$	$7.86 \cdot 10^{5}$	$1.97 \cdot 10^{6}$	$6.92 \cdot 10^{1}$	$4.61 \cdot 10^{0}$	$2.27 \cdot 10^{1}$	$8.26 \cdot 10^{1}$	$1.44 \cdot 10^{1}$
$3.15 \cdot 10^{6}$	$3.15 \cdot 10^{6}$	–	$5.51 \cdot 10^{2}$	$2.20 \cdot 10^{1}$	–	$6.28 \cdot 10^{2}$	$6.08 \cdot 10^{1}$

Table 8: CPU times for solving and postprocessing of methods equivalent to primal dPG for uniform refinement.

Analogously to the preceding two tables, the CPU times for assembly and solution of the ultraweak dPG method and respective reduced mixed and weighted least-squares methods are collected in tables Tables 9 and 10. Whereas the number of degrees of freedom for the reduced mixed and the weighted least-squares methods equal those of the case for the primal dPG from before, the ultraweak dPG method calculates additional variables and

therefore has an even higher number of degrees of freedom than the primal dPG method on the same triangulation. Indeed, the time for assembling the linear system of equations is slightly higher, but still of the same order of magnitude. As expected, the solution also takes longer for the ultraweak dPG method compared to the primal dPG method. On the contrary, the smaller times for solving the reduced mixed and the weighted least-squares methods do not depend on the choice of parameters corresponding to either the primal or the ultraweak dPG method.

When also considering the time for postprocessing for calculating the extra variables provided by the ultraweak dPG method, in contrast to the primal case, the reduced mixed method is competitive, in particular for higher levels, where the solution of the ultraweak dPG method was not possible due to memory issues. Again, the postprocessing step of the weighted least-squares method is the fastest of all due to parallelization.

ndof			assemble		
R	LS	dPG	R	LS	dPG
$5.60 \cdot 10^{1}$	$4.80 \cdot 10^{1}$	$2.64 \cdot 10^{2}$	$4.17 \cdot 10^{-1}$	$4.92 \cdot 10^{-1}$	$9.47 \cdot 10^{-2}$
$2.08 \cdot 10^{2}$	$1.92 \cdot 10^{2}$	$1.06 \cdot 10^{3}$	$2.43 \cdot 10^{-1}$	$2.83 \cdot 10^{-1}$	$4.38 \cdot 10^{-2}$
$8.00 \cdot 10^{2}$	$7.68 \cdot 10^{2}$	$4.22 \cdot 10^{3}$	$2.70 \cdot 10^{-1}$	$4.54 \cdot 10^{-1}$	$6.11 \cdot 10^{-2}$
$3.14 \cdot 10^{3}$	$3.07 \cdot 10^{3}$	$1.69 \cdot 10^{4}$	$3.84 \cdot 10^{-1}$	$4.40 \cdot 10^{-1}$	$1.16 \cdot 10^{-1}$
$1.24 \cdot 10^{4}$	$1.23 \cdot 10^{4}$	$6.76 \cdot 10^{4}$	$5.10 \cdot 10^{-1}$	$7.76 \cdot 10^{-1}$	$3.55 \cdot 10^{-1}$
$4.94 \cdot 10^{4}$	$4.92 \cdot 10^{4}$	$2.70 \cdot 10^{5}$	$1.08 \cdot 10^{0}$	$1.85 \cdot 10^{0}$	$1.31 \cdot 10^{0}$
$1.97 \cdot 10^{5}$	$1.97 \cdot 10^{5}$	$1.08 \cdot 10^{6}$	$4.43 \cdot 10^{0}$	$6.36 \cdot 10^{0}$	$5.27 \cdot 10^{0}$
$7.87 \cdot 10^{5}$	$7.86 \cdot 10^{5}$	–	$1.31 \cdot 10^{1}$	$2.58 \cdot 10^{1}$	–
$3.15 \cdot 10^{6}$	$3.15 \cdot 10^{6}$	–	$5.22 \cdot 10^{1}$	$1.03 \cdot 10^{2}$	–

Table 9: CPU times for assembly of methods equivalent to ultraweak dPG for uniform refinement.

ndof			solve			total	
R	LS	dPG	R	LS	dPG	R	LS
$5.60\cdot10^{1}$	$4.80\cdot10^{1}$	$2.64\cdot10^{2}$	$1.93\cdot10^{-2}$	$1.88\cdot10^{-4}$	$6.80\cdot10^{-4}$	$8.26\cdot10^{-2}$	$5.09\cdot10^{-2}$
$2.08\cdot10^{2}$	$1.92\cdot10^{2}$	$1.06\cdot10^{3}$	$6.81\cdot10^{-4}$	$3.67\cdot10^{-4}$	$2.81\cdot10^{-3}$	$5.92\cdot10^{-2}$	$4.14\cdot10^{-2}$
$8.00\cdot10^{2}$	$7.68\cdot10^{2}$	$4.22\cdot10^{3}$	$1.71\cdot10^{-2}$	$1.49\cdot10^{-3}$	$1.30\cdot10^{-2}$	$8.28\cdot10^{-2}$	$6.14\cdot10^{-2}$
$3.14\cdot10^{3}$	$3.07\cdot10^{3}$	$1.69\cdot10^{4}$	$1.76\cdot10^{-2}$	$4.69\cdot10^{-2}$	$6.64\cdot10^{-2}$	$1.30\cdot10^{-1}$	$1.50\cdot10^{-1}$
$1.24\cdot10^{4}$	$1.23\cdot10^{4}$	$6.76\cdot10^{4}$	$1.54\cdot10^{-1}$	$3.50\cdot10^{-1}$	$3.49\cdot10^{-1}$	$4.69\cdot10^{-1}$	$6.69\cdot10^{-1}$
$4.94\cdot10^{4}$	$4.92\cdot10^{4}$	$2.70\cdot10^{5}$	$1.06\cdot10^{0}$	$4.77\cdot10^{-1}$	$2.12\cdot10^{0}$	$2.02\cdot10^{0}$	$1.45\cdot10^{0}$
$1.97\cdot10^{5}$	$1.97\cdot10^{5}$	$1.08\cdot10^{6}$	$1.05\cdot10^{1}$	$2.52\cdot10^{0}$	$1.33\cdot10^{1}$	$1.41\cdot10^{1}$	$5.99\cdot10^{0}$
$7.87\cdot10^{5}$	$7.86\cdot10^{5}$	–	$6.96\cdot10^{1}$	$6.00\cdot10^{0}$	–	$8.47\cdot10^{1}$	$1.95\cdot10^{1}$
$3.15\cdot10^{6}$	$3.15\cdot10^{6}$	–	$7.52\cdot10^{2}$	$2.35\cdot10^{1}$	–	$8.36\cdot10^{2}$	$7.70\cdot10^{1}$

Table 10: CPU times for solving and postprocessing of methods equivalent to ultraweak dPG for uniform refinement.

9.5. Slit Domain with Exact Solution

The slit domain displayed in Figure 27 reads $\Omega = (-1,1)^2 \setminus ([0,1] \times \{0\})$ and can be seen as a degenerated version of the L-shaped domain from Subsection 9.4 with interior angle 2π at the tip $O \coloneqq (0,0)$ of the slit. To appropriately model a possible discontinuity along $(0,1) \times \{0\}$, the initial triangulation contains the point $(1,0)$ twice, once as P_a coming from above, and once as P_b coming from below. The Neumann boundary Γ_N consists of the upper part of the slit, i.e., $\Gamma_N = \overline{OP_a}$. The Dirichlet boundary contains the lower part of the slit and the remaining boundary, i.e., $\Gamma_D = \overline{OP_b} \cup \partial((-1,1)^2)$. The respective boundary conditions stem from the exact solution given in polar coordinates by $u(r,\varphi) = r^{1/4}\sin(\varphi/4)$. The right-hand side $f \equiv 0$, thus $\mu = 0$ and the choice of the separate marking parameters κ, ϱ is not necessary.

The experiments of this subsection concern the reduced mixed method and the weighted least-squares method with the parameters for the primal dPG method. Figure 35 diplays the solutions of the piecewise affine, globally continuous parts of both solutions with clearly visible jump, hence singularity, at the tip of the slit. Accordingly, the adaptively refined triangulations in Figure 36 are refined towards his tip.

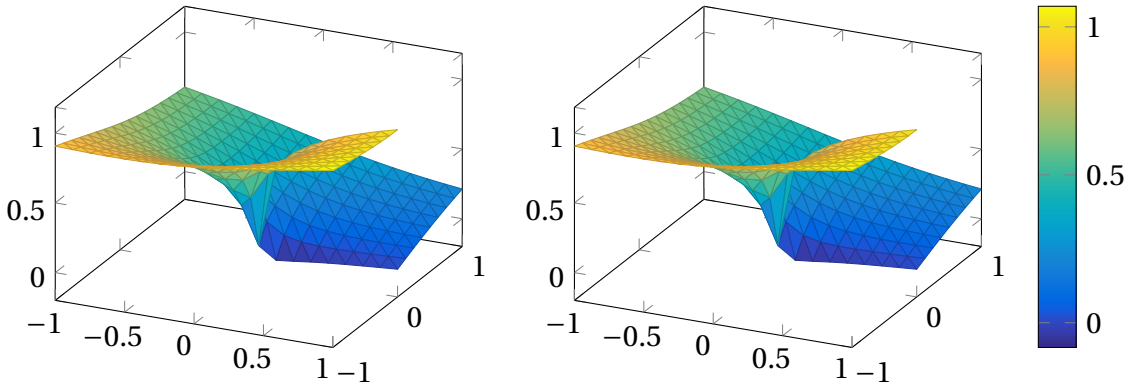

reduced mixed method, 960 ndof

weighted LS method, 1024 ndof

Figure 35: Solution plots of respective parts in $S^1_0(\mathcal{T})$ on uniformly refined triangulation with 512 triangles of slit domain from Subsection 9.5.

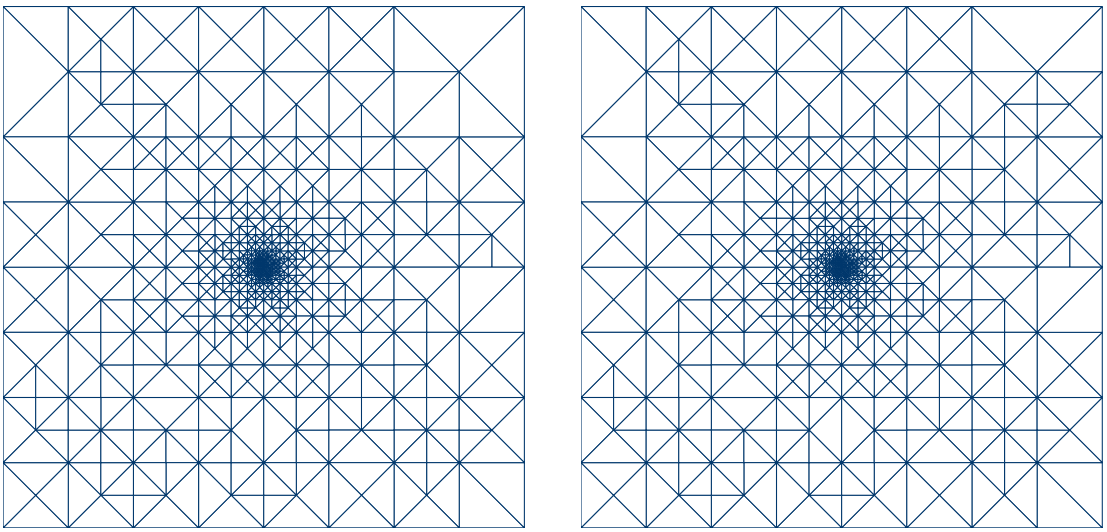

reduced mixed method (1479 triangles, 2921 ndof)

weighted LS method (1484 triangles, 2968 ndof)

Figure 36: Adaptively refined triangulations of slit domain from Subsection 9.5.

The convergence history plots exhibited in Figure 37 show the suboptimal convergence rate of 1/8 for errors and estimators of the reduced mixed and the weighted least-squares method. However, the adaptive algorithms with $\theta = 0.5$ recover the optimal convergence rate of 1/2.

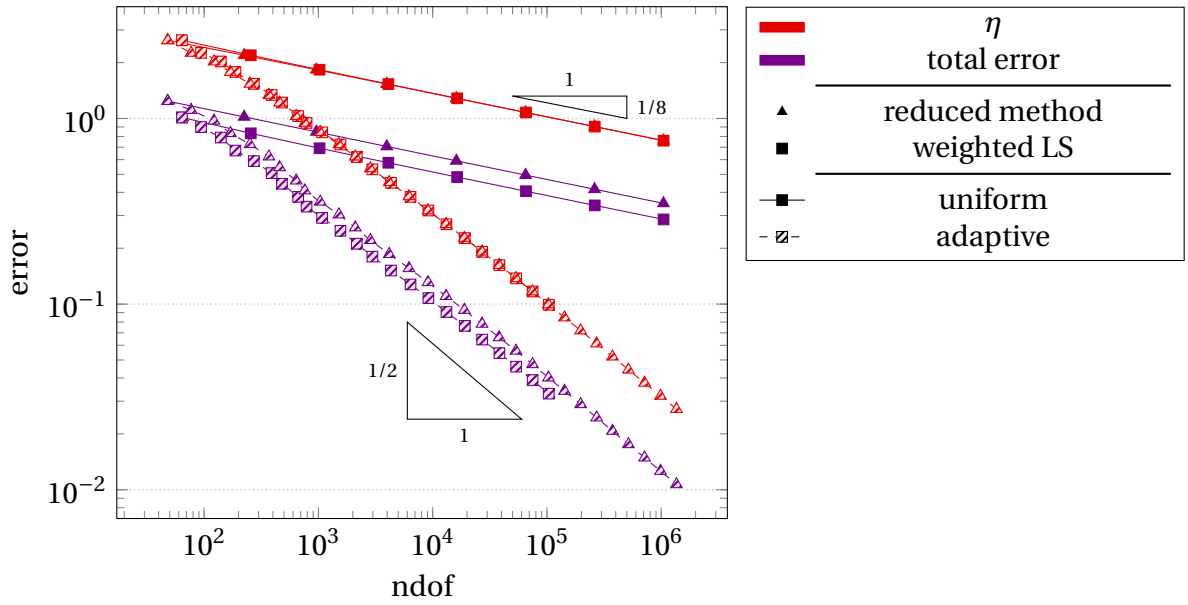

Figure 37: Comparison of methods equivalent to primal dPG for uniform and adaptive refinement of slit domain from Subsection 9.5.

Figure 38 examines the influence of the bulk parameter θ on the errors of the adaptive reduced mixed method, where $\theta = 1$ stands for uniform refinement. It shows that even for a large bulk parameter of 0.9, the method converges with the optimal rate of $1/2$, but for $\theta \geq 0.6$, there is a preasymptotic range. The smaller the bulk parameter, the more solutions of the system of equations are needed for reaching a certain number of degrees of freedom. Hence, the choice of $\theta = 0.5$ with a balance of these phenomena in all the experiments is justified.

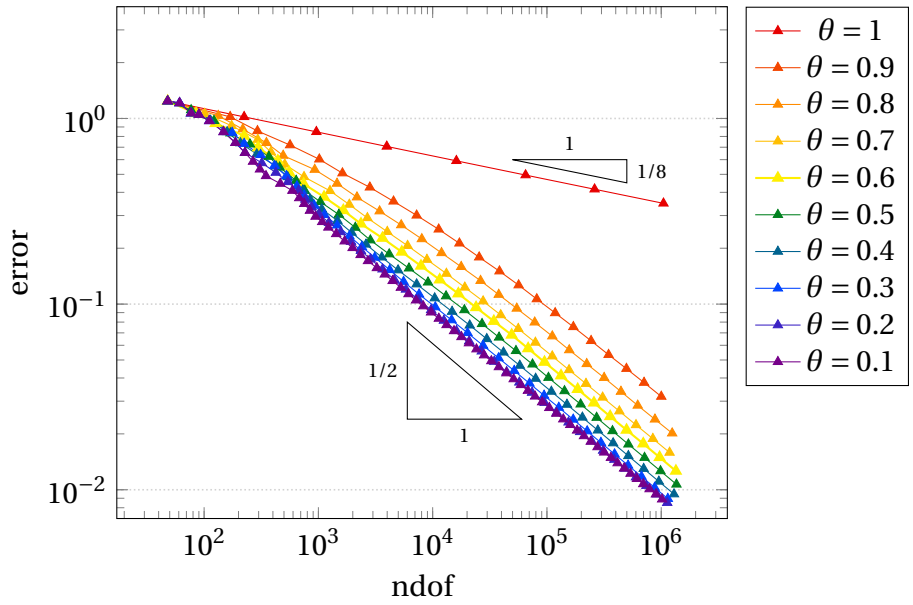

Figure 38: Influence of bulk parameter θ on error of reduced mixed method on slit domain of Subsection 9.5.

Similar to Figure 38, Figure 39 shows the errors of the adaptive weighted least-squares method for different bulk parameters. The behavior is similar to that of the reduced mixed method, with optimal convergence rates for $\theta \leq 0.9$ and no preasymptotics for $\theta \leq 0.6$. However, the smaller the bulk parameter, the earlier the computations are aborted. An explanation for this is the behavior of condition numbers displayed in Figure 40. As observed for the L-shaped domain in Figures 33 and 34, the rate of divergence for the condition numbers depends on the type of refinement. Indeed, the smaller θ, the higher the rate of divergence for the condition number, a behavior that is not observed for the reduced mixed method.

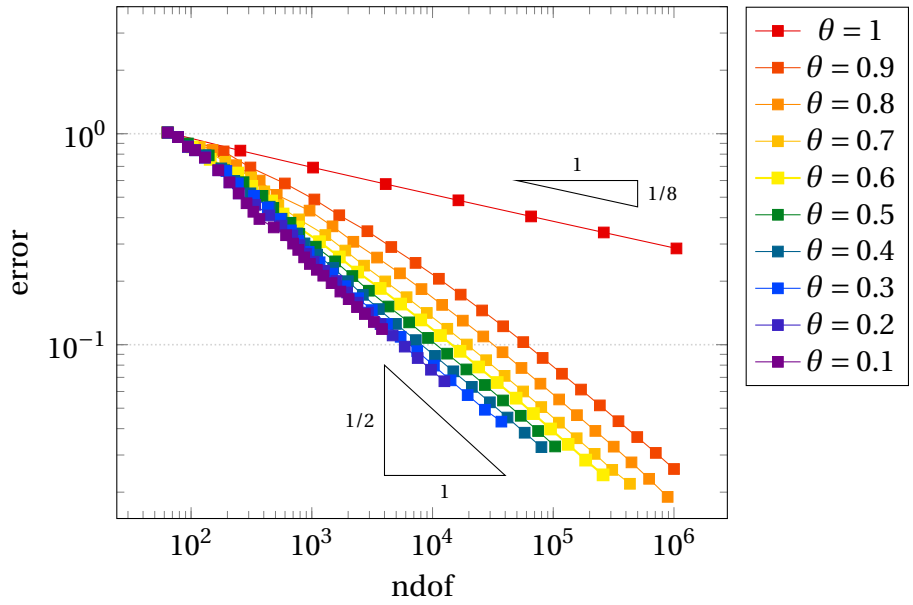

Figure 39: Influence of bulk parameter θ on errors of weighted least-squares method on slit domain of Subsection 9.5.

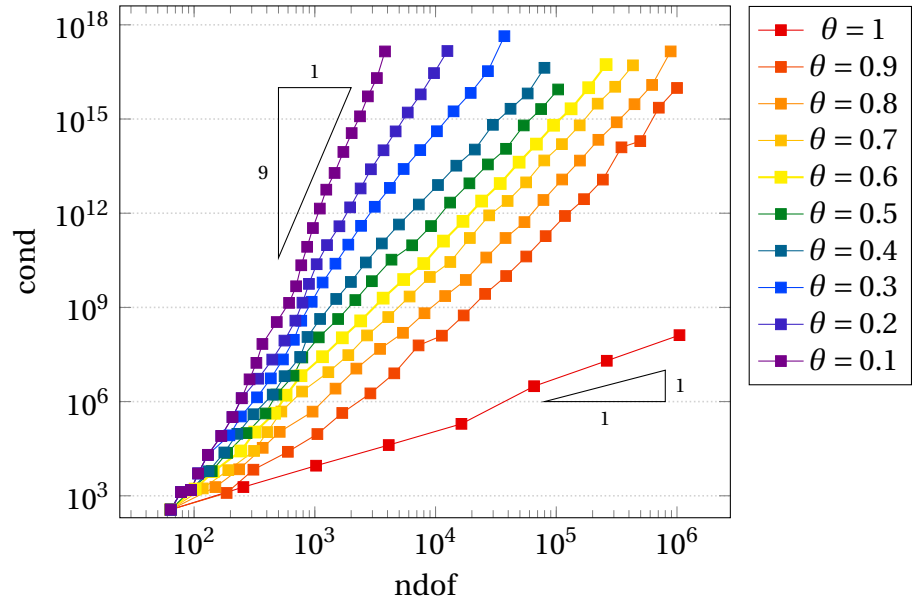

Figure 40: Influence of bulk parameter θ on condition numbers of weighted least-squares method on slit domain of Subsection 9.5.

9.6. L-Shaped Domain with Point Load

This subsection describes a probem with no known exact solution on the L-shaped domain $(-1,1)^2 \setminus ([0,1] \times [-1,0])$ with homogeneous Dirichlet boundary conditions $u_D = 0$ on $\Gamma_D = \partial\Omega$. The right-hand side is given as a point load on a small square $\omega = (0.5-\varepsilon, 0.5+\varepsilon)^2$ around $(0.5, 0.5)$ for $\varepsilon = 2^{-5}$ and reads $f = 1$ on ω and $f = 0$ on $\Omega \setminus \omega$ as visualized in Figure 41.

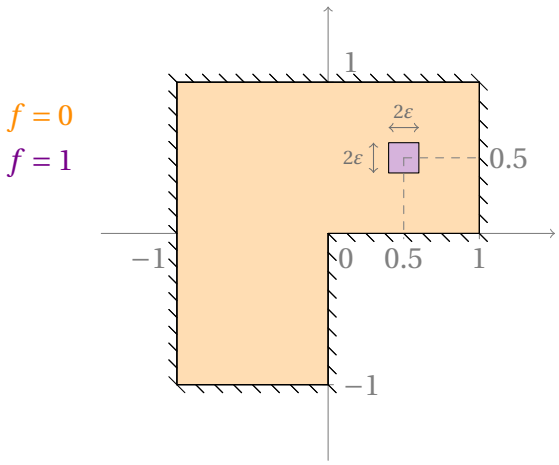

Figure 41: L-shaped domain with point load from Subsection 9.6.

The piecewise affine, globally continuous parts of the primal dPG and equivalent reduced mixed and weighted least-squares methods are displayed in Figure 42 and show a singularity at the point load $(0.5, 0.5)$. The adaptive algorithms with $\theta = 0.5$ and $\kappa = 0.3$, $\varrho = 0.1$ refine towards this point as shown in Figure 43, although the triangulation generated by the adaptive weighted least-squares method is closer to uniform than the other two. Figure 43 also displays the adaptively generated triangulation for the weighted LS method with collective marking from Algorithm 1, which resembles that of the weighted LS method with separate marking.

The convergence history plots of these three methods are shown in Figure 44. The error estimators of all three methods converge with optimal rate $1/2$ for adaptive refinement, and with a rate of almost $1/2$ for uniform refinement. However, all methods need a number of refinement steps to resolve the point load, which leads to a preasymptotic range. The adaptive algorithms lead to a significantly faster decay in this preasymptotic range compared to the uniform refinement.

For the weighted least-squares method, this is examined in more detail in Figure 45. It shows the full error estimators σ and the data approximation μ for uniform refinement and for adaptive refinement with separate marking and collective marking. The uniform and collective marking strategies suffer from a large preasymptotic range, which a separate marking strategy with appropriate choice of parameters can overcome faster.

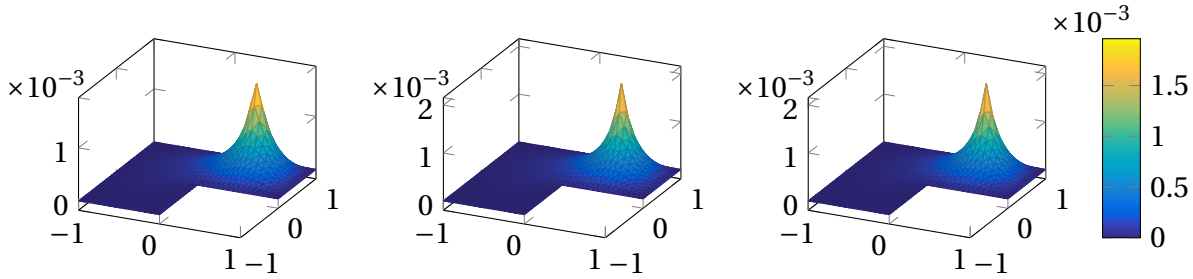

u_R, 2945 ndof u_{LS}, 3073 ndof u_{dPG}, 7681 ndof

Figure 42: Solution plots of respective parts in $S_0^1(\mathcal{T})$ on uniformly refined triangulation with 1536 triangles of L-shaped domain with point load from Subsection 9.6.

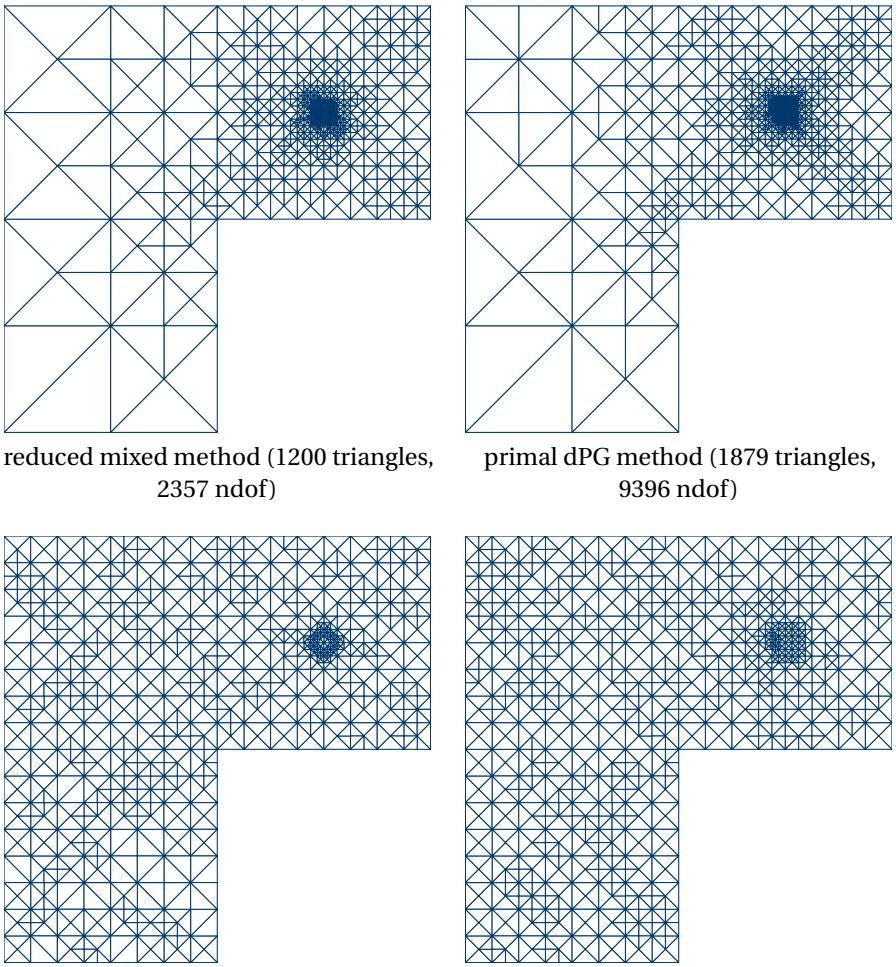

reduced mixed method (1200 triangles, 2357 ndof)

primal dPG method (1879 triangles, 9396 ndof)

weighted LS method with separate marking (1166 triangles, 2333 ndof)

weighted LS method with collective marking (1304 triangles, 2609 ndof)

Figure 43: Adaptively refined triangulations of primal dPG and equivalent method on L-shaped domain with point load from Subsection 9.6.

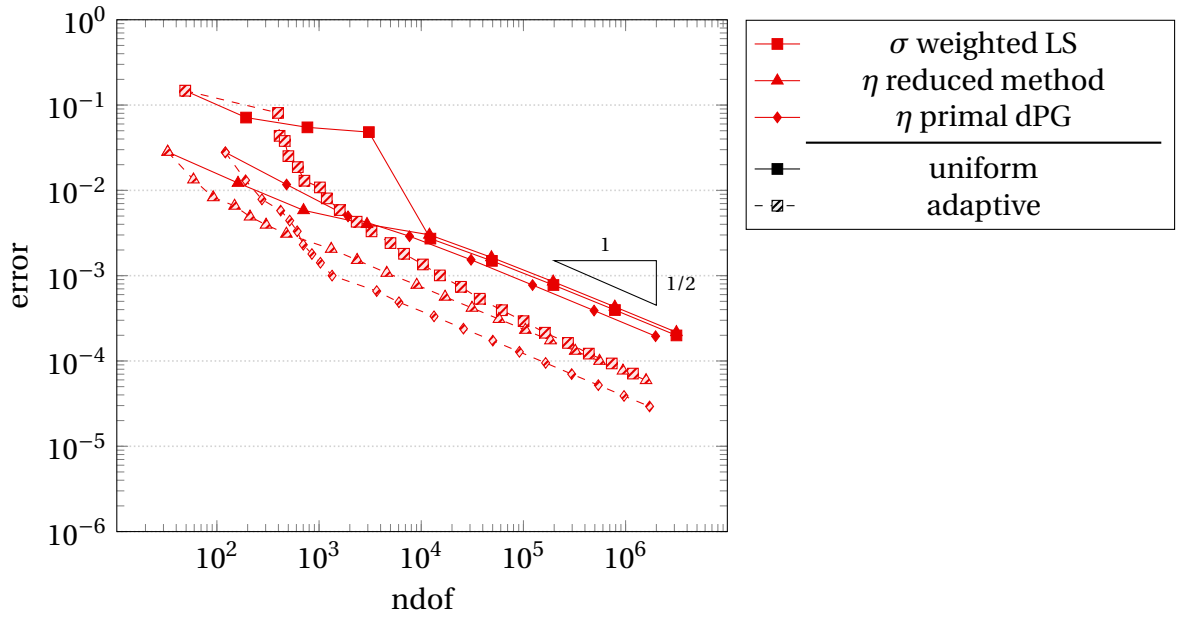

Figure 44: Comparison of methods equivalent to primal dPG for uniform and adaptive refinement of L-shaped domain with point load from Subsection 9.6.

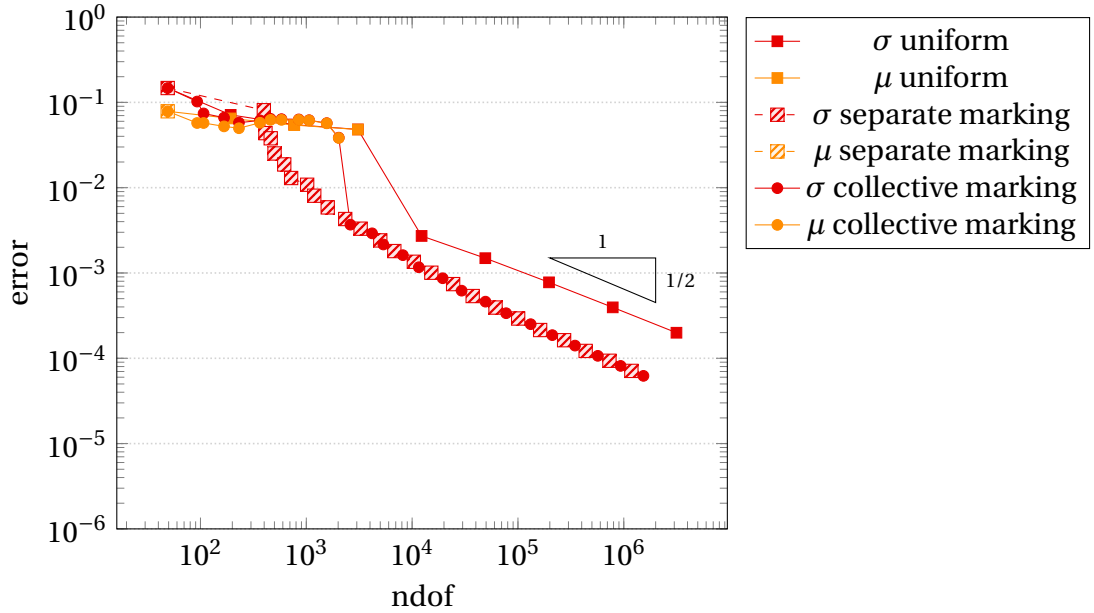

Figure 45: Different refinement types of weighted least-squares method on L-shaped domain with point load from Subsection 9.6.

The remainder of this subsection considers the L-shaped problem with a reversed point load $\widetilde{f} := 1 - f$, i.e., $\widetilde{f} = 0$ on ω and $\widetilde{f} = 1$ on $\Omega \setminus \omega$. The piecewise affine, globally continuous parts of the solutions of the primal dPG method and equivalent weighted LS and reduced

mixed methods on uniform triangulations are displayed in Figure 46 and are similar to those for a constant right-hand side 1 shown in Figures 2-4 of Section 1 including the singularity at the re-entrant corner.

The convergence history plot of Figure 47 shows that all three methods converge with the suboptimal rate of $2/5$ for uniform refinement. The adaptive algorithms with parameters $\theta = 0.5$ and $\kappa = 0.01$, $\varrho = 0.1$ for the weighted LS methods recover the optimal convergence rate of $1/2$. Similar to Figure 45, Figure 48 compares the estimators σ and μ for three refinement strategies for the weighted LS method. The estimator σ for the collective marking strategy shows the optimal convergence rate of $1/2$. The separate marking strategy reduces the data approximation term μ to almost zero after the first two levels of the adaptive algorithm. The reduction of σ in those two steps is smaller than the reduction of σ for the collective marking strategy. However, the adaptive algorithms are asymptotically equal. Figure 49 shows adaptively refined triangulations of the primal dPG and the reduced mixed method next to the weighted LS method with collective and separate marking. All four methods refine towards the re-entrant corner, but the weighted LS method with separate marking strategy is the only one that additionally refines towards the pertubation of the right-hand side around $(0.5, 0.5)$.

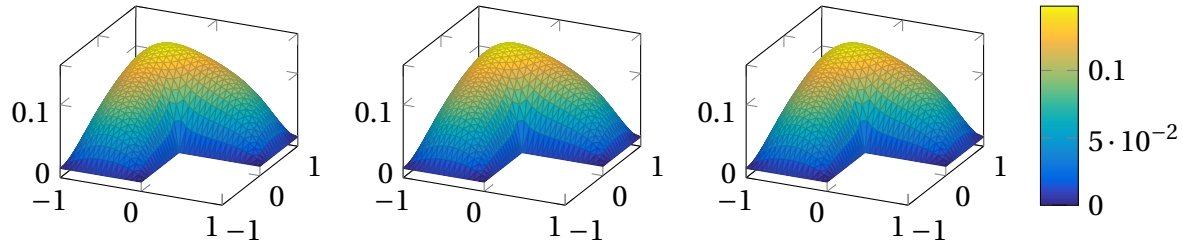

u_R, 2945 ndof u_{LS}, 3073 ndof u_{dPG}, 7681 ndof

Figure 46: Solution plots of respective parts in $S^1_0(\mathcal{T})$ on uniformly refined triangulation with 1536 triangles of L-shaped domain with point load from Subsection 9.6.

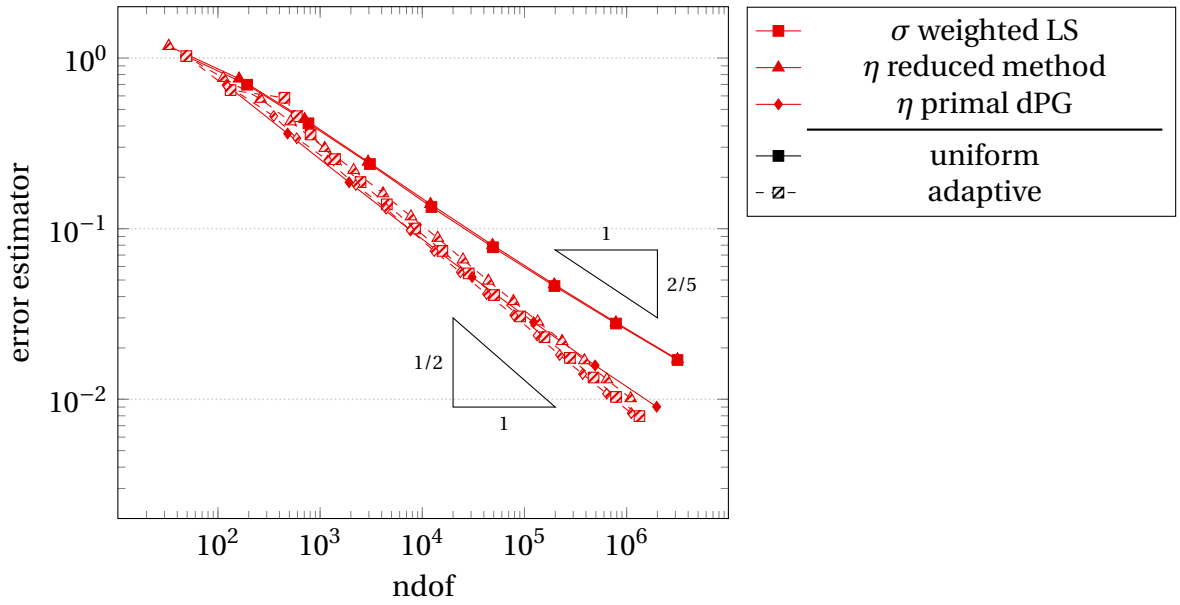

Figure 47: Comparison of methods equivalent to primal dPG for uniform and adaptive refinement of L-shaped domain with reversed point load from Subsection 9.6.

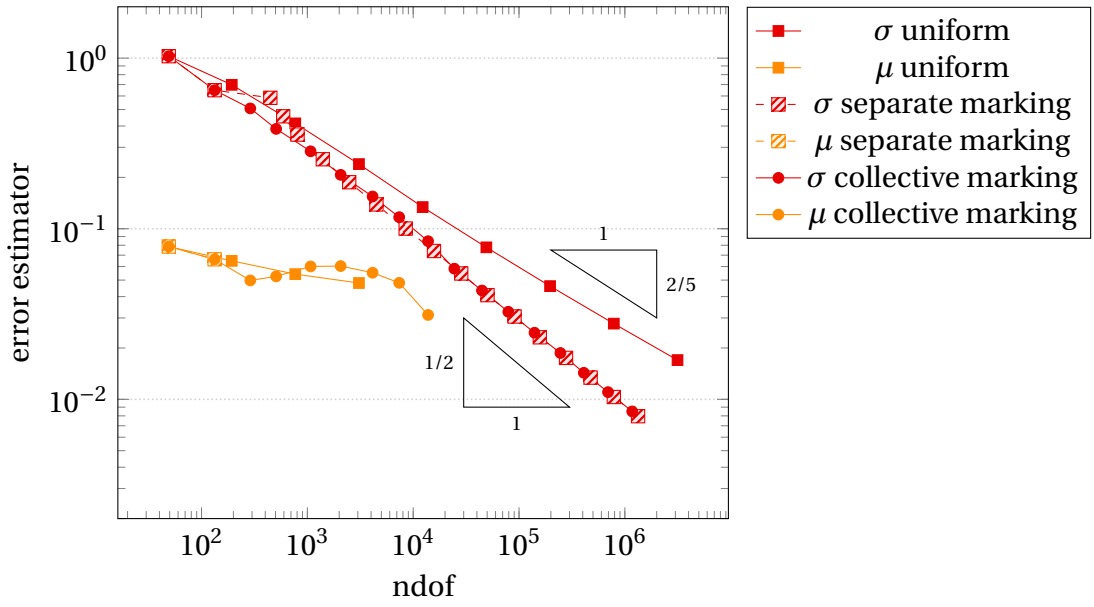

Figure 48: Different refinement types of weighted least-squares method on L-shaped domain with reversed point load from Subsection 9.6.

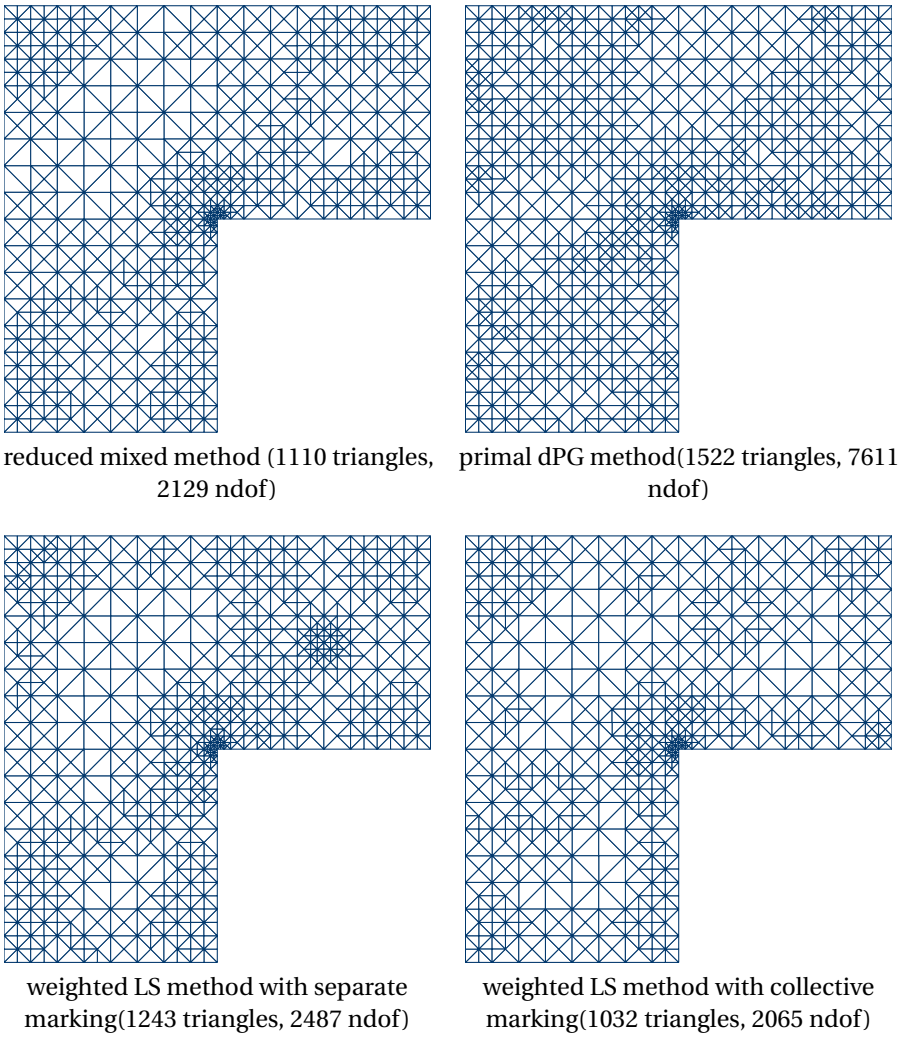

Figure 49: Adaptively refined triangulations of primal dPG and equivalent method on L-shaped domain with reversed point load from Subsection 9.6.

9.7. Discussion of Experiments

All numerical experiments for the reduced mixed, the weighted least-squares and the primal and ultraweak dPG method confirm the optimal convergence rates of the adaptive algorithms and their superiority to the uniform refinement strategies. Although the theory of the preceding sections proves rate-optimality only for a sufficiently small initial mesh-size, all experiments show convergence even for coarse initial triangulations. Preasymptotic behavior occurs only for highly oscillating right-hand sides that need to be resolved by the triangulation first. The theoretically predicted equivalences of certain parts of the solutions to the different methods are observed in solution plots and convergence history plots.

Concerning differences between the methods, the most severe drawback of the weighted

least-squares method is its ill conditioning. In contrast to the reduced mixed and the dPG methods, the divergence rate depends heavily on the choice of bulk parameter, so that for small bulk parameters, solution is only possible up to an unsatisfactory number of degrees of freedom. Additionally, the choice of the parameters κ and ϱ for the separate marking algorithm is not trivial, and experience when conducting the experiments was that time spent in the data approximation step was many times higher than the actual solution of the method, which makes the separate marking algorithm slow. However, the solution of the weighted least-squares system is slightly faster than that of the reduced mixed system, which is still faster than any of the dPG methods. For the ultraweak dPG method, solution and postprocessing of the corresponding reduced mixed and weighted least-squares method takes less time than solving the dPG method itself.

Which of the three methodologies is preferred highly depends on the situation at hand. Even if all solution variables of the dPG methods are needed, which might not always be the case, the equivalent reduced mixed or weighted least-squares methods including postprocessing of the extra variables are superior in terms of computation times. However, since the weighted least-squares method is badly conditioned for adaptive refinement with small bulk parameters, the choice of the reduced mixed method is advised here. All in all, the reduced mixed method seems to be the most convenient of the three methods when seen over all examples. It posesses a stable rate of condition numbers even for adaptive refinement, is faster than the dPG methods and almost as fast as the weighted least-squares method, or even faster when taking into account the long time for the refinement step in separate marking, and there is no need to investigate suitable separate marking parameters.

10. Conclusion and Outlook

This thesis analyses optimal convergence rates for sufficiently fine initial triangulations for two different non-standard finite element methods, the reduced mixed and the weighted least-squares method. As a consequence of the shown equivalence of four lowest-order dPG methods with these two methods, optimal convergence rates of these methods follow in two separate ways. Interestingly enough, one of the equivalent adaptive methods enforces a separate marking strategy, whereas the other one does not. The numerical experiments confirm the rate-optimality and equivalence of the three methodologies and show that the calculation with the reduced mixed and the weighted least-squares methods is superior to the direct calculation with the dPG methods, whereas overall, the reduced mixed method is advantageous in terms of conditioning.

The proofs of optimal convergence rates for both methods rely on a sufficiently fine initial triangulation, but the experiments show convergence already starting from a coarse initial triangulation. Up to now, it is unclear, how to omit this condition on the initial mesh-size. The crucial point in both methods in achieving that will be the proof of quasi-orthogonality with ε without a dependence of ε on the mesh-size.

This thesis approaches the proofs of optimal convergence rates of dPG methods through a construction of equivalent error estimators, a similar strategy to that of least-squares methods. Nevertheless, many publications and the experiments from the preceding section show the convergence of the natural adaptive dPG methods employing the built-in error estimator. The proof of optimal convergence rates of this natural adaptive dPG algorithm is an open problem, even in the context of the more extensively studied least-squares methods, where there is only a result on plain convergence [CPB17].

Although some numerical experiments of this thesis suggest that the asymptotic behavior of the weighted LS method with collective marking resembles that of separate marking, it is yet unclear how to prove rate-optimality of the weighted LS method with collective marking.

As mentioned in the introduction, a lot of applications of the dPG method utilize higher-order polynomials or augmented order in the test space, since the construction of a Fortin operator to prove well-posedness is then local. The proofs of this thesis heavily rely on the lowest-order case and it is not immediately clear how to transfer the arguments. It is left for future research to derive methods equivalent to higher-order dPG methods to prove optimal convergence rates by construction of an alternative error estimator.

Of course, the presented analysis on the Poisson model problem should just be the kick-off to move on to more relevant applications of the dPG methodology. The applications [CH16; CP18] for linear elasticity and the Stokes problem as well as the nonlinear model problem in [CBHW18] utilize lowest-order dPG methods similar to those presented here and may therefore relate to the proofs of this thesis in a more direct way than others. However, a first investigation on linear elasticity suggests that there are severe differences in the resulting reduced mixed system and the weighted least-squares functional that make the proofs of this thesis not directly accessible and require an additional thorough analysis in the future.

References

[ABH18] G. Acosta, J. P. Borthagaray, and N. Heuer. “Finite element approximations of the nonhomogeneous fractional Dirichlet problem”. In: *IMA J. Numer. Anal.* (2018). Published Online. DOI: 10.1093/imanum/dry023.

[AFEM] *AFEM software package and documentation*. Humboldt-Universität zu Berlin. Carstensen, C. and Numerical Analysis Group.

[Alt16] H. W. Alt. *Linear functional analysis*. Springer, London, 2016. DOI: 10.1007/978-1-4471-7280-2.

[BBF13] D. Boffi, F. Brezzi, and M. Fortin. *Mixed finite element methods and applications*. Springer, Heidelberg, 2013. DOI: 10.1007/978-3-642-36519-5.

[BDD04] P. Binev, W. Dahmen, and R. DeVore. “Adaptive Finite Element Methods with convergence rates”. In: *Numer. Math.* 97.2 (2004), pp. 219–268. DOI: 10.1007/s00211-003-0492-7.

[BDGQ12] J. Bramwell, L. Demkowicz, J. Gopalakrishnan, and W. Qiu. “A locking-free hp DPG method for linear elasticity with symmetric stresses”. In: *Numer. Math.* 122.4 (2012), pp. 671–707. DOI: 10.1007/s00211-012-0476-6.

[BDS18] D. Broersen, W. Dahmen, and R. P. Stevenson. “On the stability of DPG formulations of transport equations”. In: *Math. Comp.* 87.311 (2018), pp. 1051–1082. DOI: 10.1090/mcom/3242.

[BG09] P. B. Bochev and M. D. Gunzburger. *Least-squares finite element methods*. Springer, New York, 2009. DOI: 10.1007/b13382.

[BGH14] T. Bouma, J. Gopalakrishnan, and A. Harb. “Convergence rates of the DPG method with reduced test space degree”. In: *Comput. Math. Appl.* 68.11 (2014), pp. 1550–1561. DOI: 10.1016/j.camwa.2014.08.004.

[BR78] I. Babuška and W. C. Rheinboldt. “Error estimates for adaptive finite element computations”. In: *SIAM J. Numer. Anal.* 15.4 (1978), pp. 736–754. DOI: 10.1137/0715049.

[BR81] I. Babuška and W. C. Rheinboldt. “A posteriori error analysis of finite element solutions for one-dimensional problems”. In: *SIAM J. Numer. Anal.* 18.3 (1981), pp. 565–589. DOI: 10.1137/0718036.

[Bra07] D. Braess. *Finite elements*. Cambridge University Press, 2007. DOI: 10.1017/CBO9780511618635.

[BS08] S. C. Brenner and L. R. Scott. *The mathematical theory of finite element methods*. Springer, New York, 2008. DOI: 10.1007/978-0-387-75934-0.

[BS14] D. Broersen and R. Stevenson. “A robust Petrov-Galerkin discretisation of convection-diffusion equations”. In: *Comput. Math. Appl.* 68.11 (2014), pp. 1605–1618. DOI: 10.1016/j.camwa.2014.06.019.

[BS15] D. Broersen and R. P. Stevenson. “A Petrov-Galerkin discretization with optimal test space of a mild-weak formulation of convection-diffusion equations in mixed form”. In: *IMA J. Numer. Anal.* 35.1 (2015), pp. 39–73. DOI: 10.1093/imanum/dru003.

[BS89] R. E. Bank and L. R. Scott. “On the conditioning of finite element equations with highly refined meshes”. In: *SIAM J. Numer. Anal.* 26.6 (1989), pp. 1383–1394. DOI: 10.1137/0726080.

[BV84] I. Babuška and M. Vogelius. “Feedback and adaptive finite element solution of one-dimensional boundary value problems”. In: *Numer. Math.* 44.1 (1984), pp. 75–102. DOI: 10.1007/BF01389757.

[CBHW18] C. Carstensen, P. Bringmann, F. Hellwig, and P. Wriggers. “Nonlinear discontinuous Petrov–Galerkin methods”. In: *Numer. Math.* 139.3 (2018), pp. 529–561. DOI: 10.1007/s00211-018-0947-5.

[CBJ02] C. Carstensen, S. Bartels, and S. Jansche. “A posteriori error estimates for nonconforming finite element methods”. In: *Numer. Math.* 92.2 (2002), pp. 233–256.

[CDG14] C. Carstensen, L. Demkowicz, and J. Gopalakrishnan. “A Posteriori Error Control for DPG Methods”. In: *SIAM J. Numer. Anal.* 52.3 (2014), pp. 1335–1353. DOI: 10.1137/130924913.

[CDG16] C. Carstensen, L. Demkowicz, and J. Gopalakrishnan. “Breaking spaces and forms for the DPG method and applications including Maxwell equations”. In: *Comput. Math. Appl.* 72.3 (2016), pp. 494–522. DOI: 10.1016/j.camwa.2016.05.004.

[CDM14] J. Chan, L. Demkowicz, and R. Moser. “A DPG method for steady viscous compressible flow”. In: *Comput. & Fluids* 98 (2014), pp. 69–90. DOI: 10.1016/j.compfluid.2014.02.024.

[CDW12] A. Cohen, W. Dahmen, and G. Welper. “Adaptivity and variational stabilization for convection-diffusion equations”. In: *ESAIM Math. Model. Numer. Anal.* 46.5 (2012), pp. 1247–1273. DOI: 10.1051/m2an/2012003.

[CEHL12] C. Carstensen, M. Eigel, R. Hoppe, and C. Löbhard. “A review of unified a posteriori finite element error control”. In: *Numer. Math. Theory Methods Appl.* 5.4 (2012), pp. 509–558. DOI: 10.4208/nmtma.2011.m1032.

[CEQ14] J. Chan, J. A. Evans, and W. Qiu. “A dual Petrov-Galerkin finite element method for the convection-diffusion equation”. In: *Comput. Math. Appl.* 68.11 (2014), pp. 1513–1529. DOI: 10.1016/j.camwa.2014.07.008.

[CFPP14] C. Carstensen, M. Feischl, M. Page, and D. Praetorius. “Axioms of adaptivity”. In: *Comput. Math. Appl.* 67.6 (2014), pp. 1195–1253. DOI: 10.1016/j.camwa.2013.12.003.

[CGHW14] C. Carstensen, D. Gallistl, F. Hellwig, and L. Weggler. “Low-order dPG-FEM for an elliptic PDE”. In: *Comput. Math. Appl.* 68.11 (2014), pp. 1503–1512. DOI: 10.1016/j.camwa.2014.09.013.

[CGS13] C. Carstensen, D. Gallistl, and M. Schedensack. “Discrete reliability for Crouzeix-Raviart FEMs”. In: *SIAM J. Numer. Anal.* 51.5 (2013), pp. 2935–2955. DOI: 10.1137/130915856.

[CH16] C. Carstensen and F. Hellwig. “Low-order discontinuous Petrov-Galerkin finite element methods for linear elasticity”. In: *SIAM J. Numer. Anal.* 54.6 (2016), pp. 3388–3410. DOI: 10.1137/15M1032582.

[CH18a] C. Carstensen and F. Hellwig. “Constants in Discrete Poincaré and Friedrichs Inequalities and Discrete Quasi-Interpolation”. In: *Comput. Methods Appl. Math.* 18.3 (2018), pp. 433–450. DOI: 10.1515/cmam-2017-0044.

[CH18b] C. Carstensen and F. Hellwig. “Optimal convergence rates for adaptive lowest-order discontinuous Petrov-Galerkin schemes”. In: *SIAM J. Numer. Anal.* 56.2 (2018), pp. 1091–1111. DOI: 10.1137/17M1146671.

[CHBD14] J. Chan, N. Heuer, T. Bui-Thanh, and L. Demkowicz. “A robust DPG method for convection-dominated diffusion problems II: adjoint boundary conditions and mesh-dependent test norms”. In: *Comput. Math. Appl.* 67.4 (2014), pp. 771–795. DOI: 10.1016/j.camwa.2013.06.010.

[Cia02] P. G. Ciarlet. *The finite element method for elliptic problems*. Reprint of the 1978 original [North-Holland, Amsterdam; MR0520174 (58 #25001)]. SIAM, Philadelphia, 2002. DOI: 10.1137/1.9780898719208.

[CKNS08] J. M. Cascon, C. Kreuzer, R. H. Nochetto, and K. G. Siebert. “Quasi-optimal convergence rate for an adaptive finite element method”. In: *SIAM J. Numer. Anal.* 46.5 (2008), pp. 2524–2550. DOI: 10.1137/07069047X.

[Cou43] R. Courant. “Variational methods for the solution of problems of equilibrium and vibrations”. In: *Bull. Amer. Math. Soc.* 49 (1943), pp. 1–23. DOI: 10.1090/S0002-9904-1943-07818-4.

[CP15] C. Carstensen and E.-J. Park. “Convergence and optimality of adaptive Least Squares Finite Element Methods”. In: *SIAM J. Numer. Anal.* 53 (2015), pp. 43–62. DOI: 10.1137/130949634.

[CP18] C. Carstensen and S. Puttkammer. “A low-order discontinuous Petrov–Galerkin method for the Stokes equations”. In: *Numer. Math.* 140.1 (2018), pp. 1–34. DOI: 10.1007/s00211-018-0965-3.

[CPB17] C. Carstensen, E. J. Park, and P. Bringmann. “Convergence of natural adaptive least squares FEMs”. In: *Numer. Math.* 136.4 (2017), pp. 1097–1115. DOI: 10.1007/s00211-017-0866-x.

[CR17] C. Carstensen and H. Rabus. “Axioms of Adaptivity with Separate Marking for Data Resolution”. In: *SIAM J. Numer. Anal.* 55.6 (2017), pp. 2644–2665. DOI: 10.1137/16M1068050.

[CR73] M. Crouzeix and P.-A. Raviart. “Conforming and nonconforming finite element methods for solving the stationary Stokes equations. I”. In: *Rev. Française Automat. Informat. Recherche Opérationnelle Sér. Rouge* 7.R-3 (1973), pp. 33–75.

[CS18] C. Carstensen and J. Storn. “Asymptotic Exactness of the Least-Squares Finite Element Residual”. In: *SIAM J. Numer. Anal.* 56.4 (2018), pp. 2008–2028. DOI: 10.1137/17M1125972.

[DE12] D. A. Di Pietro and A. Ern. *Mathematical aspects of discontinuous Galerkin methods*. Springer, Heidelberg, 2012. DOI: 10.1007/978-3-642-22980-0.

[DG10] L. Demkowicz and J. Gopalakrishnan. “A class of discontinuous Petrov-Galerkin methods. Part I: the transport equation”. In: *Comput. Methods Appl. Mech. Engrg.* 199.23-24 (2010), pp. 1558–1572. DOI: 10.1016/j.cma.2010.01.003.

[DG11a] L. Demkowicz and J. Gopalakrishnan. “A class of discontinuous Petrov-Galerkin methods. II. Optimal test functions”. In: *Numer. Methods Partial Differential Equations* 27.1 (2011), pp. 70–105. DOI: 10.1002/num.20640.

[DG11b] L. Demkowicz and J. Gopalakrishnan. “Analysis of the DPG method for the Poisson equation”. In: *SIAM J. Numer. Anal.* 49.5 (2011), pp. 1788–1809. DOI: 10.1137/100809799.

[DG13] L. Demkowicz and J. Gopalakrishnan. “A primal DPG method without a first-order reformulation”. In: *Comput. Math. Appl.* 66.6 (2013), pp. 1058–1064. DOI: 10.1016/j.camwa.2013.06.029.

[DGMZ12] L. Demkowicz, J. Gopalakrishnan, I. Muga, and J. Zitelli. “Wavenumber explicit analysis of a DPG method for the multidimensional Helmholtz equation”. In: *Comput. Methods Appl. Mech. Engrg.* 213-216 (2012), pp. 126–138. DOI: 10.1016/j.cma.2011.11.024.

[DGN12] L. Demkowicz, J. Gopalakrishnan, and A. H. Niemi. “A class of discontinuous Petrov-Galerkin methods. Part III: Adaptivity”. In: *Appl. Numer. Math.* 62.4 (2012), pp. 396–427. DOI: 10.1016/j.apnum.2011.09.002.

[DGNS17] L. Demkowicz, J. Gopalakrishnan, S. Nagaraj, and P. Sepúlveda. “A spacetime DPG method for the Schrödinger equation”. In: *SIAM J. Numer. Anal.* 55.4 (2017), pp. 1740–1759. DOI: 10.1137/16M1099765.

[DH13] L. Demkowicz and N. Heuer. “Robust DPG method for convection-dominated diffusion problems”. In: *SIAM J. Numer. Anal.* 51.5 (2013), pp. 2514–2537. DOI: 10.1137/120862065.

[DL13] L. Demkowicz and J. Li. “Numerical simulations of cloaking problems using a DPG method”. In: *Comput. Mech.* 51.5 (2013), pp. 661–672. DOI: 10.1007/s00466-012-0744-4.

[Dör96] W. Dörfler. “A convergent adaptive algorithm for Poisson’s equation”. In: *SIAM J. Numer. Anal.* 33.3 (1996), pp. 1106–1124. DOI: 10.1137/0733054.

[EFHK17] V. J. Ervin, T. Führer, N. Heuer, and M. Karkulik. “DPG method with optimal test functions for a fractional advection diffusion equation”. In: *J. Sci. Comput.* 72.2 (2017), pp. 568–585. DOI: 10.1007/s10915-017-0369-z.

[Eva10] L. C. Evans. *Partial differential equations*. American Mathematical Society, Providence, 2010. DOI: 10.1090/gsm/019.

[FDW17] F. Fuentes, L. Demkowicz, and A. Wilder. “Using a DPG method to validate DMA experimental calibration of viscoelastic materials”. In: *Comput. Methods Appl. Mech. Engrg.* 325 (2017), pp. 748–765. DOI: 10.1016/j.cma.2017.07.012.

[FH17] T. Führer and N. Heuer. “Robust coupling of DPG and BEM for a singularly perturbed transmission problem”. In: *Comput. Math. Appl.* 74.8 (2017), pp. 1940–1954. DOI: 10.1016/j.camwa.2016.09.016.

[FHK17] T. Führer, N. Heuer, and M. Karkulik. “On the coupling of DPG and BEM”. In: *Math. Comp.* 86.307 (2017), pp. 2261–2284. DOI: 10.1090/mcom/3170.

[FHK18] T. Führer, N. Heuer, and M. Karkulik. “An ultraweak formulation of the Kirchhoff–Love plate bending model and DPG approximation”. In: *Math. Comp.* (2018). DOI: 10.1090/mcom/3381.

[FHKR17] T. Führer, N. Heuer, M. Karkulik, and R. Rodríguez. “Combining the DPG Method with Finite Elements”. In: *Comput. Methods Appl. Math.* (2017). Published Online. DOI: 10.1515/cmam-2017-0041.

[FHS17a] T. Führer, N. Heuer, and J. Sen Gupta. “A time-stepping DPG scheme for the heat equation”. In: *Comput. Methods Appl. Math.* 17.2 (2017), pp. 237–252. DOI: 10.1515/cmam-2016-0037.

[FHS17b] T. Führer, N. Heuer, and E. P. Stephan. “On the DPG method for Signorini problems”. In: *IMA J. Numer. Anal.* (2017). Published Online. DOI: 10.1093/imanum/drx048.

[FKDL17] F. Fuentes, B. Keith, L. Demkowicz, and P. Le Tallec. “Coupled variational formulations of linear elasticity and the DPG methodology”. In: *J. Comput. Phys.* 348 (2017), pp. 715–731. DOI: 10.1016/j.jcp.2017.07.051.

[Füh18] T. Führer. “Superconvergence in a DPG method for an ultra-weak formulation”. In: *Comput. Math. Appl.* 75.5 (2018), pp. 1705–1718. DOI: 10.1016/j.camwa.2017.11.029.

[Gal14] D. Gallistl. “Adaptive finite element computation of eigenvalues”. PhD thesis. Humboldt-Universität zu Berlin, Mathematisch-Naturwissenschaftliche Fakultät II, 2014. DOI: 10.18452/17002.

[GMO14] J. Gopalakrishnan, I. Muga, and N. Olivares. “Dispersive and dissipative errors in the DPG method with scaled norms for Helmholtz equation”. In: *SIAM J. Sci. Comput.* 36.1 (2014), A20–A39. DOI: 10.1137/130918186.

[GQ14] J. Gopalakrishnan and W. Qiu. “An analysis of the practical DPG method”. In: *Math. Comp.* 83.286 (2014), pp. 537–552. DOI: 10.1090/S0025-5718-2013-02721-4.

[Gri11] P. Grisvard. *Elliptic problems in nonsmooth domains*. Reprint of the 1985 original [MR0775683]. SIAM, Philadelphia, 2011. DOI: 10.1137/1.9781611972030.ch1.

[HK15] N. Heuer and M. Karkulik. "DPG method with optimal test functions for a transmission problem". In: *Comput. Math. Appl.* 70.5 (2015), pp. 1070–1081. DOI: 10.1016/j.camwa.2015.06.032.

[HK17a] N. Heuer and M. Karkulik. "A robust DPG method for singularly perturbed reaction-diffusion problems". In: *SIAM J. Numer. Anal.* 55.3 (2017), pp. 1218–1242. DOI: 10.1137/15M1041304.

[HK17b] N. Heuer and M. Karkulik. "Discontinuous Petrov–Galerkin boundary elements". In: *Numer. Math.* 135.4 (2017), pp. 1011–1043. DOI: 10.1007/s00211-016-0824-z.

[HKMP17] P. Hennig, M. Kästner, P. Morgenstern, and D. Peterseim. "Adaptive mesh refinement strategies in isogeometric analysis—a computational comparison". In: *Comput. Methods Appl. Mech. Engrg.* 316 (2017), pp. 424–448. DOI: 10.1016/j.cma.2016.07.029.

[HKS14] N. Heuer, M. Karkulik, and F.-J. Sayas. "Note on discontinuous trace approximation in the practical DPG method". In: *Comput. Math. Appl.* 68.11 (2014), pp. 1562–1568. DOI: 10.1016/j.camwa.2014.07.006.

[HP14] N. Heuer and F. Pinochet. "Ultra-weak formulation of a hypersingular integral equation on polygons and DPG method with optimal test functions". In: *SIAM J. Numer. Anal.* 52.6 (2014), pp. 2703–2721. DOI: 10.1137/130920538.

[KFD16] B. Keith, F. Fuentes, and L. Demkowicz. "The DPG methodology applied to different variational formulations of linear elasticity". In: *Comput. Methods Appl. Mech. Engrg.* 309 (2016), pp. 579–609. DOI: 10.1016/j.cma.2016.05.034.

[KKRE+17] B. Keith, P. Knechtges, N. V. Roberts, S. Elgeti, M. Behr, and L. Demkowicz. "An ultraweak DPG method for viscoelastic fluids". In: *J. Non-Newton. Fluid Mech.* 247 (2017), pp. 107–122. DOI: 10.1016/j.jnnfm.2017.06.006.

[LS10] R. S. Laugesen and B. A. Siudeja. "Minimizing Neumann fundamental tones of triangles: an optimal Poincaré inequality". In: *J. Differential Equations* 249.1 (2010), pp. 118–135. DOI: 10.1016/j.jde.2010.02.020.

[Mar85] L. D. Marini. "An Inexpensive Method for the Evaluation of the Solution of the Lowest Order Raviart-Thomas Mixed Method". In: *SIAM J. Numer. Anal.* 22.3 (1985), pp. 493–496.

[Mey00] C. D. Meyer. *Matrix Analysis and Applied Linear Algebra*. SIAM, Philadelphia, 2000. DOI: 10.1137/1.9780898719512.

[Mit89] W. F. Mitchell. "A comparison of adaptive refinement techniques for elliptic problems". In: *ACM Trans. Math. Software* 15.4 (1989), pp. 326–347. DOI: 10.1145/76909.76912.

[MNS00] P. Morin, R. H. Nochetto, and K. G. Siebert. “Data oscillation and convergence of adaptive FEM”. In: *SIAM J. Numer. Anal.* 38.2 (2000), pp. 466–488. DOI: 10.1137/S0036142999360044.

[MZ17] I. Muga and K. G. van der Zee. *Discretization of Linear Problems in Banach Spaces: Residual Minimization, Nonlinear Petrov-Galerkin, and Monotone Mixed Methods*. 2017. arXiv: 1511.04400.

[NSV09] R. H. Nochetto, K. G. Siebert, and A. Veeser. “Theory of adaptive finite element methods: An introduction”. In: *Multiscale, Nonlinear and Adaptive Approximation*. Berlin, Heidelberg: Springer, 2009. DOI: 10.1007/978-3-642-03413-8.

[PD17] S. Petrides and L. F. Demkowicz. “An adaptive DPG method for high frequency time-harmonic wave propagation problems”. In: *Comput. Math. Appl.* 74.8 (2017), pp. 1999–2017. DOI: 10.1016/j.camwa.2017.06.044.

[Rab14] H. Rabus. “On the quasi-optimal convergence of adaptive nonconforming finite element methods in three examples”. PhD thesis. Humboldt-Universität zu Berlin, Mathematisch-Naturwissenschaftliche Fakultät II, 2014. DOI: 10.18452/16970.

[RBD14] N. V. Roberts, T. Bui-Thanh, and L. Demkowicz. “The DPG method for the Stokes problem”. In: *Comput. Math. Appl.* 67.4 (2014), pp. 966–995. DOI: 10.1016/j.camwa.2013.12.015.

[RDM15] N. V. Roberts, L. Demkowicz, and R. Moser. “A discontinuous Petrov–Galerkin methodology for adaptive solutions to the incompressible Navier–Stokes equations”. In: *J. Comput. Phys.* 301 (2015), pp. 456–483. DOI: 10.1016/j.jcp.2015.07.014.

[RT77] P. A. Raviart and J. M. Thomas. “A mixed finite element method for 2-nd order elliptic problems”. In: *Mathematical Aspects of Finite Element Methods*. Ed. by I. Galligani and E. Magenes. Berlin, Heidelberg: Springer, 1977, pp. 292–315. DOI: 10.1007/BFb0064470.

[SF08] G. Strang and G. Fix. *An analysis of the finite element method*. Second. Wellesley-Cambridge Press, Wellesley, 2008.

[Ste07] R. Stevenson. “Optimality of a standard adaptive finite element method”. In: *Found. Comput. Math.* 7.2 (2007), pp. 245–269. DOI: 10.1007/s10208-005-0183-0.

[Ste08] R. Stevenson. “The completion of locally refined simplicial partitions created by bisection”. In: *Math. Comp.* 77.261 (2008), pp. 227–241. DOI: 10.1090/S0025-5718-07-01959-X.

[Tem77] R. Temam. *Navier-Stokes equations. Theory and numerical analysis*. North-Holland Publishing Co., Amsterdam-New York-Oxford, 1977.

[Tra97] C. T. Traxler. “An algorithm for adaptive mesh refinement in n dimensions”. In: *Computing* 59.2 (1997), pp. 115–137. DOI: 10.1007/BF02684475.

[Ver96] R. Verfürth. *A Review of A Posteriori Error Estimation and Adaptive Mesh-Refinement Techniques*. Wiley-Teubner, Chichester, Stuttgart, 1996.

[ZMDG+11] J. Zitelli, I. Muga, L. Demkowicz, J. Gopalakrishnan, D. Pardo, and V. M. Calo. "A class of discontinuous Petrov-Galerkin methods. Part IV: the optimal test norm and time-harmonic wave propagation in 1D". In: *J. Comput. Phys.* 230.7 (2011), pp. 2406–2432. DOI: 10.1016/j.jcp.2010.12.001.

List of Tables

List of Figures

A. Remarks on the Implementation

This appendix gives some details on the code utilized for the numerical experiments of Section 9. The main contribution of the enclosed software is the implementation of four finite element methods – the reduced mixed and the weighted least-squares methods with different parameters, the primal dPG method, and the ultraweak dPG method. The implementation is embedded into the software package [AFEM] and utilizes its framework for marking and refining. Each method consists of a solver and functions for computing error estimator and errors. Furthermore, there are main functions, one for the reduced mixed method, one for the weighted LS method and one for the dPG methods. The data approximation algorithm and related methods for the separate marking algorithm are original or slightly modified functions from [Rab14]. The software was tested under MATLAB versions 8.2.0.701 (MATLAB 2013b) and 9.0.0.341360 (MATLAB R2016a). The directory structure of the software is shown below in order to give an overview of its functionality. Functions written exclusively for this thesis are marked in green, functions from [Rab14] in purple.

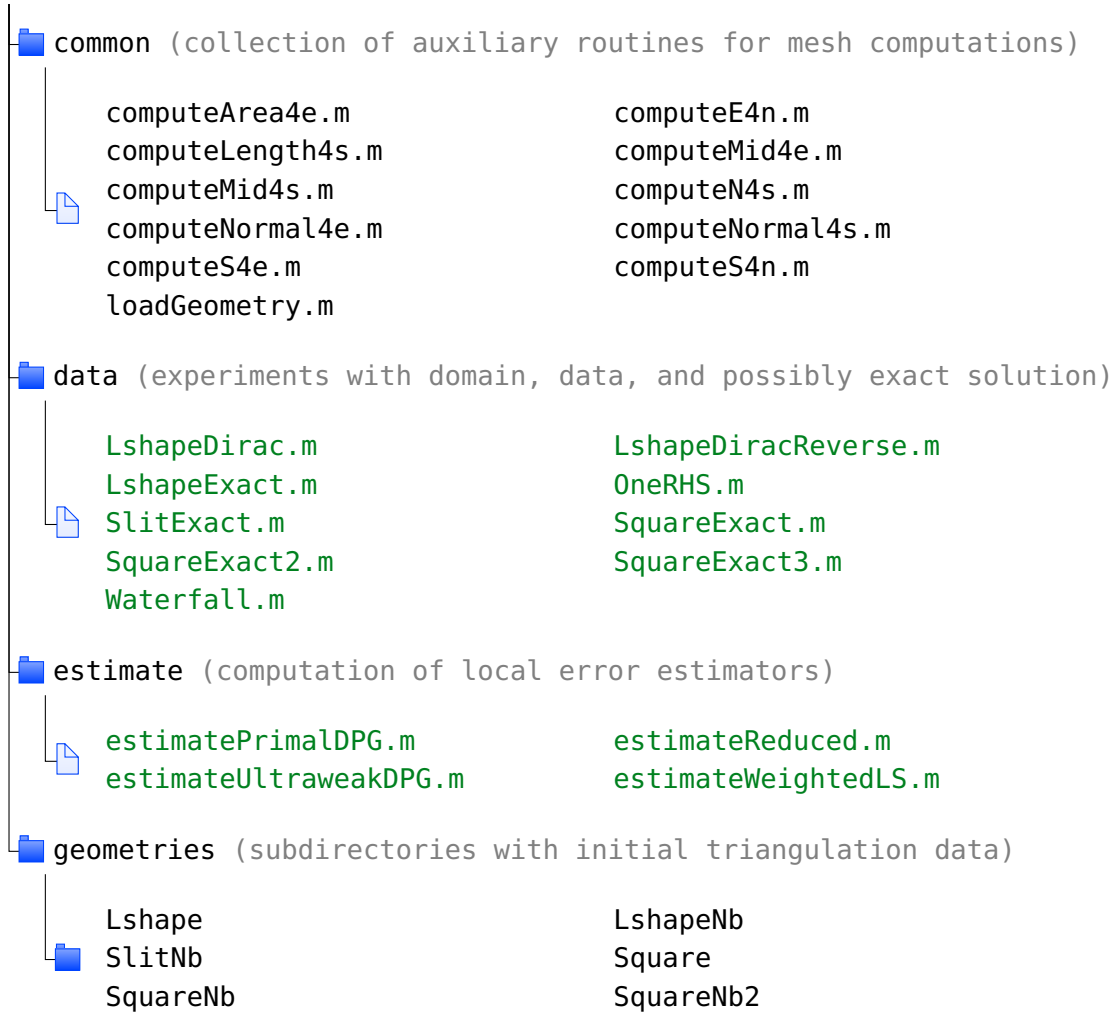

```
integrate (computation of errors, weights and weighted integrals)
    calculateApproximationRHS.m     calculateF0.m
    calculateL2Product.m            calculateM0.m
    error4ePrimalDPG.m              error4eReduced.m
    error4eUltraweakDPG.m           error4eWeightedLS.m
    integrate.m
mark (collective marking and approx algorithm)
    approx.m                        markBulk.m
output (directory for output of experiments)
plot (plot routines for convergence history and solutions)
    plotConvergenceColor.m          plotCR.m
    plotP04e.m                      plotP1.m
    plotTriangulation.m
refine (functions for refinement)
    closure.m                       completion.m
    overlay.m                       refineBi3GB_irregular.m
    refineBi3GB.m                   refineRGB.m
    refineUniformRed.m
solve (solvers for four methods)
    solveDPGPrimal.m                solveDPGUltraweak.m
    solveReducedFormulation.m       solveWeightedLSFormulation.m
afemDPG.m (main function for the two dPG methods)
afemReduced.m (main function for reduced mixed method)
afemWeightedLS.m (main function for weighted LS method)
conductExperimentsDPG.m (execute dPG experiments)
conductExperimentsLS.m (execute weighted LS experiments)
conductExperimentsReduced.m (execute reduced mixed experiments)
```

To reproduce the numerical experiments of Section 9 of this thesis, run the functions `conductExperimentsDPG(minNrDoF)`, `conductExperimentsLS(minNrDoF)`, and `conductExperimentsReduced(minNrDoF)` with `minNrDoF=1000000` or another value suit-

able for the available computational power and memory. The folder `\data\` contains the files with the experiments, i.e., the choice of the domain with Dirichlet and Neumann boundary and its initial triangulation, the right-hand side f, and the boundary data. If it is known, the file includes also the exact solution and its gradient. Table 11 displays the available problems and references their discussion in this thesis.

file	description of problem
`LshapeDirac.m`	L-shaped domain with point load from Subsection 9.6
`LshapeDiracReverse.m`	L-shaped domain with reversed point load from Subsection 9.6
`LshapeExact.m`	L-shaped domain with exact solution from Subsection 9.4
`OneRHS.m`	L-shaped domain with constant right-hand side 1 from Introduction
`SlitExact.m`	Slit domain with exact solution from Subsection 9.5
`SquareExact.m`	Unit square with exact solution from Subsection 9.2
`SquareExact2.m`	Unit square with Dirichlet and Neumann boundary and exact solution
`SquareExact3.m`	Unit square with Dirichlet and Neumann boundary and exact solution
`Waterfall.m`	Waterfall example from Subsection 9.3

Table 11: Overview of examples.

The remainder of this appendix briefly describes the operating of the software. For a description of single steps of the algorithms, the reader is referred directly to the commentary in the code.

A.1. Primal and Ultraweak dPG Method

Experiments with the primal and ultraweak dPG method are started with the function

```
afemDPG(example,method,theta,minNrDoF)
```

This routine runs the adaptive finite element loop for one experiment with one dPG method and saves the output (numbers of degrees of freedom, values of error estimators and errors, for coarse triangulations also the triangulation data and discrete solutions) as data files in an accordingly named subfolder of `\output\`. Table 12 displays the input variables and their options.

variable	description	options
`example`	numerical example (domain, data) to be calculated	any filename from directory `\data\`, e.g., `'SquareExact'`
`method`	dPG method to be used	`'primal'`, `'ultraweak'`
`theta`	bulk parameter θ for adaptive refinement	$0 < \theta \leq 1$, $\theta = 1$ for uniform refinement
`minNrDoF`	break after this number of degrees of freedom is reached	> 0

Table 12: Input variables of function `afemDPG`.

Depending on the parameter `method`, `afemDPG` calls either the solver `solveDPGPrimal` or `solveDPGUltraweak`. A description of the input variables of these solvers can be found in Table 13, of output variables in Tables 14 and 15.

The implementation considers bases $\{\Phi_1, \dots, \Phi_m\}$ of X_h and $\{\Psi_1, \dots, \Psi_\ell\}$ of Y_h consisting of standard basis functions of the respective spaces. The assembly of the stiffness matrix $S = (b(\Phi_j, \Psi_k))_{kj} \in \mathbb{R}^{\ell \times m}$ and norm matrix $M = (\langle \Phi_j, \Phi_k \rangle)_{kj} \in \mathbb{R}^{\ell \times \ell}$ needed for these solvers is a simpler case of the more involved lowest-order ultraweak dPG method for linear elasticity explained in detail in the supplementary material to [CH16]. Both matrices are split into blocks corresponding to the respective parts of the solutions.

Consider the coefficient vectors $x \in \mathbb{R}^m$ and $y \in \mathbb{R}^\ell$ of the discrete solution $(x_h, y_h) \in X_h \times Y_h$ to the mixed dPG system (M) on p. 20, and the right-hand side vector $b = (F(\Psi_j))_j \in \mathbb{R}^\ell$. Then the system of equations resulting from (M) and employed in the solvers reads

$$\begin{bmatrix} M & S \\ S^\top & 0 \end{bmatrix} \begin{bmatrix} y \\ x \end{bmatrix} = \begin{bmatrix} b \\ 0 \end{bmatrix}.$$

The boundary conditions are incorporated into the right-hand side of the system of equations via a split in the variables `u` (for Dirichlet boundary data) and `t` (for Neumann boundary data).

variable	description	type
`c4n`	coordinates of nodes of triangulation $\mathcal{T}$	$\mathbb{R}^{\lvert\mathcal{N}\rvert \times 2}$
`n4e`	nodes of elements in $\mathcal{T}$	$\mathbb{R}^{\lvert\mathcal{T}\rvert \times 3}$
`n4sDb`	Dirichlet boundary edges	$\mathbb{R}^{\lvert\mathcal{E}(\Gamma_D)\rvert \times 2}$
`n4sNb`	Neumann boundary edges	$\mathbb{R}^{\lvert\mathcal{E}(\Gamma_N)\rvert \times 2}$
`f`	right-hand side function	function handle
`u4Db`	Dirichlet boundary data	function handle
`g`	Neumann boundary data	function handle

Table 13: Input variables of all solvers.

variable	description	type
u	coefficient vector of $u_C \in S_0^1(\mathcal{T})$	$\mathbb{R}^{\lvert\mathcal{N}\rvert}$
t	coefficient vector of $t_0 \in P_0(\mathcal{E})$	$\mathbb{R}^{\lvert\mathcal{E}\rvert}$
v	coefficient vector of $v_1 \in P_1(\mathcal{T})$	$\mathbb{R}^{3\lvert\mathcal{T}\rvert}$
nrDoF	number of degrees of freedom (size of system matrix)	$\mathbb{N}$
data	time for assembly, time for solution, and condition number of system of equations collected in vector	$\mathbb{R}^3$

Table 14: Output variables of `solveDPGPrimal`.

variable	description	type
r	coefficient vector of $r_0 \in P_0(\mathcal{T};\mathbb{R}^2)$	$\mathbb{R}^{2\lvert\mathcal{T}\rvert}$
w	coefficient vector of $w_0 \in P_0(\mathcal{T})$	$\mathbb{R}^{\lvert\mathcal{T}\rvert}$
t	coefficient vector of $t_0 \in P_0(\mathcal{E})$	$\mathbb{R}^{\lvert\mathcal{E}\rvert}$
u	coefficient vector of $s_C \in S_0^1(\mathcal{E})$	$\mathbb{R}^{\lvert\mathcal{N}\rvert}$
q	coefficient vector of $q_1 \in RT_0^{NC}(\mathcal{T})$	$\mathbb{R}^{3\lvert\mathcal{T}\rvert}$
v	coefficient vector of $v_1 \in P_1(\mathcal{T})$	$\mathbb{R}^{3\lvert\mathcal{T}\rvert}$
nrDoF	number of degrees of freedom (size of system matrix)	$\mathbb{N}$
data	time for assembly, time for solution, and condition number of system of equations collected in vector	$\mathbb{R}^3$

Table 15: Output variables of `solveDPGUltraweak`.

After the solution of the discrete problems, the local error estimators of the two methods are calculated with calls of `estimatePrimalDPG(c4n,n4e,f,v)` or `estimateUltraweakDPG (c4n,n4e,f,q,v)`. The errors with respect to the components $v_1 \in P_1(\mathcal{T})$, and in case of the ultraweak dPG method additionally that of $q_1 \in RT_0^{NC}(\mathcal{T})$, are a by-product in the calculation of the error estimator. Therefore, the computation of these error components is not contained in the routines `error4ePrimalDPG(c4n,n4e,f,graduExact,u,t)` and `error4eUltraweakDPG(c4n,n4e,f,uExact,graduExact,r,w,t,u)`. The output of these four functions consists of different vectors in $\mathbb{R}^{\lvert\mathcal{T}\rvert}$ named `eta4e`, `error4eR`, `error4eW`, `error4eT`, `error4eU`, `error4eQ`, and `error4eV` containing the respective local error estimators or errors on each element of the triangulation.

A.2. Reduced Mixed Methods

Similar as described for the dPG methods, the function `afemReduced(example,alpha,Q, compare,theta,minNrDoF)` runs the adaptive finite element loop for one experiment with the reduced mixed method and saves the output in `\output\`. The input parameters are listed in Table 16.

variable	description	options
`example`	numerical example (domain, data) to be calculated	any filename from directory `\data\`, e.g., `'SquareExact'`
`alpha`	parameter from reduced mixed method	$0 \leq \alpha \leq 1$
`Q`	local projection from reduced mixed method	`'identity'` for $Q = \mathrm{id}$, `'piZero'` for $Q = \Pi_0$
`compare`	choose if equivalent dPG method shall be solved and saved on triangulations from the loop	1 if comparison is wanted, 0 if not
`theta`	bulk parameter θ for adaptive refinement	$0 < \theta \leq 1$, $\theta = 1$ for uniform refinement
`minNrDoF`	break after this number of degrees of freedom is reached	> 0

Table 16: Input variables of function `afemReduced`.

The function `solveReducedFormulation(c4n,n4e,n4sDb,n4sNb,f,u4Db,g,alpha,Q)` takes input variables of the dPG solvers in Table 13, and additionally, the variables `alpha` and `Q` described in Table 12. Table 17 shows its output. The function includes a post-processing in case of a choice of parameters corresponding to the primal or ultraweak dPG method. In order to assemble the stiffness matrix, the solver calls `[Clocal,bRHS] = calculateL2Product(c4n,n4e,f,Q)` to compute the local stiffness matrices $C_{\mathrm{local}}(T) = ((Q\Psi_j, \Psi_k)_{L^2(T)})_{kj} \in \mathbb{R}^3$ for the local edge-oriented basis $\{\Psi_1, \Psi_2, \Psi_3\}$ of $P_1(T)$ and local right-hand side vectors $b_{\mathrm{RHS}}(T) = ((Q\Psi_j, f)_{L^2(T)})_j \in \mathbb{R}^3$. An inclusion of further choices of Q would require a modification of this function only. The computation of the other local terms of the reduced mixed formulation and the assembly of the global stiffness matrix are standard.

Whereas the Dirichlet boundary data is incorporated into the right-hand side via a split of the variable `u`, the Neumann boundary is included by adding the term $\int_{\Gamma_N} g\, w_{CR}\, \mathrm{d}s$ to the right-hand side of the first equation of (R), where $g \in H^{1/2}(\partial\Omega)$ are the Neumann boundary data.

variable	description	type
`v`	coefficient vector of $v_{CR} \in CR^1_0(\mathcal{T})$	$\mathbb{R}^{\lvert\mathcal{E}\rvert}$
`u`	coefficient vector of $u_C \in S^1_0(\mathcal{T})$	$\mathbb{R}^{\lvert\mathcal{N}\rvert}$
`nrDoF`	number of degrees of freedom (size of system matrix)	$\mathbb{N}$
`data`	time for assembly, time for solution, time for postprocessing, and condition number of system of equations collected in vector	$\mathbb{R}^4$

Table 17: Output variables of `solveReducedFormulation`.

The functions `eta4e = estimateReduced(c4n,n4e,f,alpha,Q,v)` and `[error4eTotal, error4eU,error4eV] = error4eReduced(c4n,n4e,graduExact,u,v)` compute the local error estimators, and local components of the error for problems with known exact solution.

A.3. Weighted Least-Squares Methods

The structure of the implementation is analogous to that of the dPG and reduced mixed method. The main function

```
afemWeightedLS(example,tag_M0,tag_F0,compare,theta,kappa,rho,minNrDoF)
```

with input parameters from Table 18 contains the adaptive finite element loop and saves the computed data. In contrast to the adaptive algorithm with collective marking employed for the previous methods, the weighted LS method utilizes separate marking, which leads to two different cases in the marking step.

variable	description	options
`example`	numerical example (domain, data) to be calculated	any filename from directory `\data\`, e.g., `'SquareExact'`
`tag_M0`	matrix valued weight from weighted LS method	`'identity'` for $M_0 = I_{2\times 2}$, `'identitySZero'` for $M_0 = I_{2\times 2} + S(\mathcal{T})$, `'twoidentitySZero'` for $M_0 = 2I_{2\times 2} + S(\mathcal{T})$
`tag_F0`	vector field from weighted LS method	`'zero'` for $F_0 = 0$, `'H0'` for $F_0 = H_0 f$
`compare`	choose if equivalent dPG method shall be solved and saved on triangulations from the loop	1 if comparison is wanted, 0 if not
`theta`	bulk parameter θ for adaptive refinement	$0 < \theta \leq 1$, $\theta = 1$ for uniform refinement
`kappa`	parameter κ for separate marking	$0 < \kappa$
`rho`	parameter ϱ, for `approx` algorithm	$0 < \varrho < 1$
`minNrDoF`	break after this number of degrees of freedom is reached	> 0

Table 18: Input variables of function `afemWeightedLS`.

In addition to the input variables from Table 13, the solver `solveWeightedLSFormulation (c4n,n4e,n4sDb,n4sNb,f,u4Db,g,M,F)` needs the variables `tag_M0` and `tag_F0` for the calls of `localMatrices = calculateM0(c4n,n4e,tag_M0)` and `localOszillations = calculateF0(c4n,n4e,tag_F0,f)` to compute M_0 and F_0 locally. Other choices of M_0 and F_0 than treated in this thesis may be implemented in these two functions. The assembly of the local and global stiffness matrices is a slight adjustment of the assembly of standard least-squares finite elements with a one-point quadrature in the term $(M_0^{-1}\Pi_0 p_{LS}, \Pi_0 q_{RT})_{L^2(\Omega)}$ of the discrete Euler-Lagrange equations (LS) and these weights. Table 19 displays the output of the solver. Similar to the reduced mixed method, this function postprocesses the extra dPG variables for the appropriate weights.

The right-hand side contains the Dirichlet boundary condition in a split of `u` and the Neumann boundary condition in a split of `p`.

variable	description	type
`p`	coefficient vector of $p_{LS} \in RT_0(\mathcal{T})$	$\mathbb{R}^{\lvert\mathcal{E}\rvert}$
`u`	coefficient vector of $u_{LS} \in S_0^1(\mathcal{T})$	$\mathbb{R}^{\lvert\mathcal{N}\rvert}$
`nrDoF`	number of degrees of freedom (size of system matrix)	$\mathbb{N}$
`data`	time for assembly, time for solution, time for postprocessing, and condition number of system of equations collected in vector	$\mathbb{R}^4$

Table 19: Output variables of `solveWeightedLSFormulation`.

The local error estimators are computed in `eta4e = estimateWeightedLS(c4n,n4e,f, tag_M0,tag_F0,u,p)` and the components of the error in `[error4eTotal,error4eU,error4eP] = error4eWeightedLS(c4n,n4e,f,graduExact,u,p)`.